

**Preliminary Economic Assessment
for the Bandeira Lithium Project,
Minas Gerais State, Brazil**

Developed by GE21 Ltda. on behalf of:

Lithium Ionic Corp.

Effective Date: August 30th, 2023

Issue Date: November 30th, 2023

Qualified Person: Carlos José Evangelista Silva – MSc (Geo), MAIG

Qualified Person: Branca H. A. Abrantes – BSc (Geog), MAIG

Qualified Person: Guilherme Gomides Ferreira – BSc (Min Eng), MAIG

Qualified Person: Paulo Bergman – BSc (Min Eng), FAusIMM

Peer Reviewer: Porfírio Cabaleiro Rodriguez – BSc (Min Eng), FAIG

| | | | |
|-----------------------|----------------------------------|--------------------------|-------------------------|
| Authors: | Carlos José Evangelista Silva | Geologist | MSc (Geo), MAIG |
| | Branca Horta de Almeida Abrantes | Environmental Specialist | BSc (Geog), MAIG |
| | Guilherme Gomides Ferreira | Mining Engineer | BSc (Mine Eng), MAIG |
| | Paulo Bergman | Mining Engineer | BSc (Mine Eng), FAusIMM |
| Peer Reviewer: | Porfírio Cabaleiro Rodriguez | Mining Engineer | BSc (Min Eng), FAIG |

| | |
|-------------------------|---|
| Effective Date: | August 30 th , 2023 |
| Issue Date: | November 30 th , 2023 |
| GE21 Project N°: | 230602 |
| Version: | Final |
| Work Directory: | S:\Projetos\MGLIT-Empreendimento\230602-PEA-Itinga\23_Relatorio |
| Print Date: | November 30 th , 2023 |
| Copies: | Lithium Ionic Corp. (1) |
| | GE21 Consultoria Mineral Ltda. (1) |

Change Control

| Version | Description | Authors | Date |
|---------|-------------|---------|------|
| | | | |
| | | | |
| | | | |

| | |
|--|--|
| <i>Original document signed and sealed.</i> | <i>Original document signed and sealed.</i> |
| Carlos José Evangelista Silva MSc (Geo), MAIG | Branca Horta de Almeida Abrantes BSc (Geog), MAIG |

| | |
|---|---|
| <i>Original document signed and sealed.</i> | <i>Original document signed and sealed.</i> |
| Guilherme Gomides Ferreira BSc (Min Eng), MAIG | Paulo Bergman BSc (Min Eng), FAusIMM |

Date and Signature

This Report, entitled "Preliminary Economic Assessment for the Bandeira Lithium Project, Minas Gerais State, Brazil", was prepared on behalf of Lithium Ionic Corp. by Carlos José Evangelista Silva, Branca Horta de Almeida Abrantes, Guilherme Gomides Ferreira and Paulo Bergman.

Dated at Belo Horizonte, Brazil, on November 30th, 2023.

Original document signed and sealed.

Carlos José Evangelista Silva, MSc (Geo), MAIG

Original document signed and sealed.

Branca Horta de Almeida Abrantes, BSc (Geog), MAIG

Original document signed and sealed.

Guilherme Gomides Ferreira, BSc (Min Eng.), MAIG

Original document signed and sealed.

Paulo Bergman, BSc (Min Eng), FAusIMM

IMPORTANT NOTICE

This Report was prepared following the requirements of the Canadian 'NI 43-101 Standards of Disclosure for Mineral Projects (CIM NI43-101) by GE21 Consultoria Mineral Ltda. ('GE21') on behalf of Lithium Ionic Corp. GE21 elaborated this technical report incorporating the information prepared by Lithium Ionic Corp. presented in the "Preliminary Economic Assessment and Technical Report for the Itinga Mine" and in the "Independent Technical Report for the Itinga Project, Brazil-2022".

The quality of information, conclusions, and estimates contained herein is consistent with the level of effort involved in the report authors' services, based on i) information available at the time of preparation, ii) data supplied by outside sources, and iii) the assumptions, conditions, and qualifications set forth in this report.

This report is intended for use by Lithium Ionic Corp. subject to terms and conditions of its individual contracts with the report authors and to the relevant securities legislation.

The contract permits Lithium Ionic Corp. to file this report as a technical report with Canadian securities regulatory authorities pursuant to the Canadian Securities Administrators' National Instrument 43-101, Standards of Disclosure for Mineral Projects, Companion Policy 43-101CP and form 43-101F1 (collectively, "NI 43-101").

Except for the purposes legislated under provincial securities law, any other uses of this report by any third party are at that party's sole risk.

The responsibility for this disclosure remains with Lithium Ionic Corp. The user of this document should ensure that this is the most recent technical report for the property as it is not valid if a new technical report has been issued.

GE21 is under no obligation to update this Technical Report, except as may be agreed to between Lithium Ionic Corp. and GE21 by contract from time to time.

The user of this document should ensure that this is the most recent Technical Report for the property as it is not valid if a new Technical Report has been issued.

Currency is expressed in U.S. dollars and metric units are used, unless otherwise stated.

INDEX

| | | |
|----------|---|-----------|
| 1 | EXECUTIVE SUMMARY | 18 |
| 1.1 | INTRODUCTION AND TERMS OF REFERENCE | 18 |
| 1.2 | RELIANCE ON OTHER EXPERTS | 19 |
| 1.3 | PROPERTY DESCRIPTION AND LOCATION | 19 |
| 1.4 | ACCESSIBILITY, CLIMATE, LOCAL RESOURCES, INFRASTRUCTURE AND PHYSIOGRAPHY | 19 |
| 1.5 | HISTORY | 19 |
| 1.6 | GEOLOGICAL SETTING AND MINERALIZATION | 19 |
| 1.7 | DEPOSIT TYPES | 20 |
| 1.8 | EXPLORATION | 20 |
| 1.9 | DRILLING | 20 |
| 1.10 | SAMPLE PREPARATION, ANALYSIS AND SECURITY | 20 |
| 1.11 | DATA VERIFICATION..... | 21 |
| 1.12 | MINERAL PROCESSING AND METALLURGICAL TESTING..... | 21 |
| 1.13 | MINERAL RESOURCES ESTIMATES | 21 |
| 1.14 | MINERAL RESERVES ESTIMATES..... | 22 |
| 1.15 | MINING METHODS | 22 |
| 1.16 | RECOVERY METHODS..... | 24 |
| 1.17 | PROJECT INFRASTRUCTURE..... | 25 |
| 1.18 | MARKET STUDIES AND CONTRACTS..... | 26 |
| 1.19 | ENVIRONMENTAL STUDIES, PERMITS, AND SOCIAL OR COMMUNITY IMPACTS..... | 28 |
| 1.20 | CAPITAL AND OPERATING COSTS | 29 |
| 1.21 | ECONOMIC ANALYSIS | 30 |
| 1.22 | ADJACENT PROPERTIES | 31 |
| 1.23 | INTERPRETATION AND CONCLUSIONS | 31 |
| 1.24 | RECOMMENDATIONS | 33 |
| 2 | INTRODUCTION AND TERMS OF REFERENCE | 35 |
| 2.1 | Qualifications, Experience, and Independence..... | 36 |
| 2.2 | Effective Date | 37 |
| 2.3 | Units of Measure..... | 37 |
| 3 | RELIANCE ON OTHER EXPERTS | 38 |
| 4 | PROPERTY DESCRIPTION AND LOCATION..... | 39 |
| 4.1 | Location..... | 39 |
| 4.2 | Mineral Tenure | 40 |
| 4.3 | Mineral Tenure Status | 41 |
| 4.4 | Property Surface Rights..... | 44 |
| 4.5 | Permits and Authorization | 46 |
| 4.6 | Environmental Considerations | 46 |
| 4.7 | Other Significant Factors and Risks | 46 |
| 5 | ACCESSIBILITY, CLIMATE, LOCAL RESOURCES, INFRASTRUCTURE AND PHYSIOGRAPHY. 47 | |
| 5.1 | Accessibility..... | 47 |
| 5.2 | Climate..... | 47 |

| | | |
|--------|--|------------|
| 5.3 | Local Resources and Infrastructure..... | 47 |
| 5.4 | Physiography | 47 |
| 6 | HISTORY | |
| 6.1 | Historical Exploration..... | 48 |
| 6.2 | Historical Mineral Resource Estimates..... | 48 |
| 7 | GEOLOGICAL SETTING AND MINERALIZATION | 50 |
| 7.1 | Regional Lithium History and Geology..... | 51 |
| 7.1.1 | <i>Pegmatites</i> | <i>54</i> |
| 7.2 | Structural Geology..... | 60 |
| 7.3 | Local Geology | 65 |
| 7.4 | Mineralization Model..... | 67 |
| 8 | DEPOSIT TYPES..... | 78 |
| 9 | EXPLORATION | 79 |
| 9.1 | Chip Rock Sampling | 79 |
| 9.2 | Soil Sampling Program | 79 |
| 9.3 | Trench Program | 80 |
| 9.4 | Structural Analysis | 83 |
| 9.5 | Geophysical Surveys..... | 85 |
| 10 | DRILLING | |
| 10.1 | Lithium Ionic Drilling Campaigns | 90 |
| 10.2 | Drill Type | 90 |
| 10.3 | Lithium Ionic Drilling Campaigns | 90 |
| 10.4 | Drill Collar Monuments..... | 90 |
| 10.5 | Drillhole Surveying | 90 |
| 10.6 | Core Orientation..... | 91 |
| 10.7 | Drill Core Chain custody | 91 |
| 10.8 | Core Logging Procedures..... | 91 |
| 10.9 | Ore Drilling Intercepts | 95 |
| 10.1 | QP's Comments | 100 |
| 11 | SAMPLE PREPARATION, ANALYSIS AND SECURITY | 101 |
| 11.1 | Sampling..... | 101 |
| 11.2 | Sample Preparation, Security and Custody Chain of Custody..... | 102 |
| 11.3 | Density Measurements..... | 102 |
| 11.4 | Sample Analysis | 103 |
| 11.5 | Quality Assurance and Quality Control (QAQC) | 103 |
| 11.5.1 | <i>Preparation Blank – Coarse Blank</i> | <i>104</i> |
| 11.5.2 | <i>Analytical Blank – Fine Blank.....</i> | <i>105</i> |
| 11.5.3 | <i>Certified/Standard Reference Material – CRM/SRM</i> | <i>106</i> |
| 11.5.4 | <i>Crushed Duplicates.....</i> | <i>108</i> |
| 11.5.5 | <i>Pulverized duplicates</i> | <i>109</i> |
| 11.5.6 | <i>Check Assay</i> | <i>110</i> |
| 11.6 | QP Opinion | 111 |

| | |
|--|------------|
| 12 DATA VERIFICATION | 112 |
| 12.1 QP Verification | 112 |
| 13 MINERAL PROCESSING AND METALLURGICAL TESTING | 122 |
| 13.1 Mineralogical Characterization | 122 |
| 13.2 Chemical Analysis of the Mineralized Material..... | 123 |
| 13.3 Metallurgical Tests..... | 123 |
| 13.3.1 Dense Media Separation..... | 123 |
| 13.3.2 Ore Sorter | 131 |
| 14 MINERAL RESOURCE ESTIMATES | 136 |
| 14.1 Drilling Database..... | 136 |
| 14.2 Geological Modeling..... | 137 |
| 14.1 Geostatistical Structural Analysis..... | 140 |
| 14.1.1 Regularization of samples | 140 |
| 14.1.2 Exploratory Data Analysis (EDA) | 140 |
| 14.1.3 Variographic Analysis..... | 142 |
| 14.2 Block Model..... | 145 |
| 14.3 Grade Estimation | 145 |
| 14.4 Estimation Validation | 146 |
| 14.5 Density..... | 146 |
| 14.6 Classification of Mineral Resources | 152 |
| 15 MINERAL RESERVES ESTIMATES | 155 |
| 16 MINING METHODS | 156 |
| 16.1 Mine Design..... | 156 |
| 16.1.1 Mining Method Selection..... | 157 |
| 16.1.2 Geotechnical Analysis..... | 159 |
| 16.1.3 Underground Stope Optimization | 160 |
| 16.2 Mining Operation | 169 |
| 16.3 Mining Scheduling | 170 |
| 16.4 Mining Equipment..... | 180 |
| 16.4.1 Rock Types Properties..... | 181 |
| 16.4.2 Assumptions..... | 181 |
| 16.4.3 Operations | 183 |
| 16.4.4 Work Shifts..... | 183 |
| 16.4.5 Opening and Maintenance of Roads and Accesses..... | 183 |
| 16.4.6 Drilling and Blasting | 184 |
| 16.4.7 Explosives Supply | 187 |
| 16.4.8 Labour Mining | 187 |
| 17 RECOVERY METHODS | 188 |
| 17.1 Process Description | 188 |
| 17.1.1 Description of the Processing Plant | 188 |
| 18 PROJECT INFRASTRUCTURE | 191 |
| 18.1 Site Facilities | 191 |

| | | |
|--------|--|-----|
| 18.2 | Waste Dump | 195 |
| 18.3 | Tailings Dump | 195 |
| 18.4 | Electrical Power Supply | 195 |
| 18.5 | Water Supply | 196 |
| 18.6 | Security | 196 |
| 19 | MARKET STUDIES AND CONTRACTS | 197 |
| 19.1 | Projected Demand for Lithium Compounds (LCE) | 197 |
| 19.2 | Projected Supply of Lithium Compounds (LCE) | 202 |
| 19.3 | Projected Price of LCE and Spodumene | 203 |
| 19.4 | Contracts | 205 |
| 20 | ENVIRONMENTAL STUDIES, PERMITS, AND SOCIAL OR COMMUNITY IMPACTS | 206 |
| 21 | CAPITAL AND OPERATING COSTS | 207 |
| 21.1 | Capital Costs | 207 |
| 21.2 | Operating Costs | 208 |
| 22 | ECONOMIC ANALYSIS | 209 |
| 22.1 | Taxes..... | 209 |
| 22.1.1 | <i>Discounted Cash Flow</i> | 209 |
| 22.2 | Sensitivity Analysis | 212 |
| 23 | ADJACENT PROPERTIES..... | 213 |
| 24 | OTHER RELEVANT DATA AND INFORMATION | 215 |
| 25 | INTERPRETATION AND CONCLUSIONS..... | 216 |
| 25.1 | Geology and Mineral Resources | 216 |
| 25.2 | Mining Study | 217 |
| 26 | RECOMMENDATIONS..... | 218 |
| 26.1 | Work Required to Increase Confidence in the Resource | 218 |
| 26.1.1 | <i>Geology and Mineral Resource Estimate</i> | 218 |
| 26.1.2 | <i>Mining and Infrastructure Studies</i> | 218 |
| 26.1.3 | <i>Environmental Studies, Permitting and Social/Community Impact</i> | 219 |
| 27 | REFERENCES..... | 220 |

LIST OF TABLES

| | |
|---|-----|
| Table 1.1: Bandeira Drill Holes Summary..... | 20 |
| Table 1.2: Bandeira Mineral Resource Estimates (Base Case Cut-off Grade of 0.5 % Li ₂ O)..... | 22 |
| Table 1.3: Bandeira’s Project Production Profile..... | 23 |
| Table 1.4: Bandeira’s Project Capital Costs..... | 29 |
| Table 1.5: Bandeira Project PEA Summary..... | 30 |
| Table 1.6 Planned Budget Recommendations..... | 34 |
| Table 2.1: Presents the QPs Matrix of Responsibility..... | 37 |
| Table 4.1: Lithium Ionic Land Tenure Information..... | 44 |
| Table 4.2: Acquisition Status..... | 45 |
| Table 4.3: Surface Owners..... | 45 |
| Table 6.1: Itinga Property; Bandeira and Outro Lado Deposits In-Pit and Underground (below-pit) Mineral Resource Estimate, June 24, 2023..... | 48 |
| Table 7.1: Main features of the orogenic igneous supersuites of the Araçuaí Orogen (simplified from Pedrosa-Soares et al. 2023)..... | 56 |
| Table 7.2: Features of the Main Pegmatite Districts of the Eastern Brazilian Pegmatite Province..... | 58 |
| Table 9.1: Summary of the Trenches Executed in the Bandeira Deposit..... | 81 |
| Table 10.1: Bandeira Drill Holes..... | 90 |
| Table 10.2: Bandeira Drill Holes..... | 93 |
| Table 10.3: Bandeira Drill Collars..... | 94 |
| Table 10.4: Mineralized Intercepts by Bandeira Drill Holes..... | 96 |
| Table 10.5: Mineralized Intercepts by Bandeira Drill Holes..... | 97 |
| Table 11.1: QAQC Program Summary..... | 104 |
| Table 13.1: Lithium Minerals Found in Pegmatite Rocks..... | 122 |
| Table 13.2: Mineralogical Analysis of the Bandeira Project (Visual Modal)..... | 123 |
| Table 13.3: Average Chemical Analysis of Mineralized Intervals from Bandeira Cores (Typology = PegLi)..... | 123 |
| Table 13.4: Properties and Applications of Sensor-based Classification (Revuelta, 2018; Wotruba and Harbeck, 2012)..... | 133 |
| Table 13.5: Pre-Concentration Ore Sorter Results for -31.5 +19mm..... | 135 |
| Table 13.6: Pre-Concentration Ore Sorter Results for -19 +9.5mm..... | 135 |
| Table 14.1: Variographic Parameters..... | 142 |
| Table 14.2: Block Model Dimensions..... | 145 |
| Table 14.3: Block Model Variables Summary..... | 145 |
| Table 14.4: Kriging Parameters..... | 146 |
| Table 14.5: Density Values..... | 147 |
| Table 14.6: Bandeira Mineral Resource Estimates (<i>base case cut-off grade of 0.5 % Li₂O</i>) – October 11, 2023..... | 153 |
| Table 16.1: Dimensions of pillar - room and pillar..... | 157 |
| Table 16.2: Dimensions of panels and columns - Sublevel Stopping..... | 158 |
| Table 16.3: MSO Parameters..... | 161 |
| Table 16.4: Advancement meterage for each structure..... | 164 |
| Table 16.5: First Pass Parameters..... | 168 |
| Table 16.6: Production Profile..... | 168 |

| | |
|--|-----|
| Table 16.7: Development structures metrics..... | 170 |
| Table 16.8: Bandeira Mining Assumptions EPS – Reference..... | 171 |
| Table 16.9: Mining Scheduling Results..... | 179 |
| Table 16.10: Equipment Utilization, Availability, and Performance Factors..... | 181 |
| Table 16.11: Schedule of Primary Equipment for Room and Pillar..... | 181 |
| Table 16.12: Schedule of Primary Equipment for Sublevel Stopping..... | 182 |
| Table 16.13: Preliminary plan for underground gallery development blasting..... | 184 |
| Table 16.14: Drilling productivity data for development..... | 185 |
| Table 16.15: Data for hole properties and charge per hole..... | 185 |
| Table 16.16: Table of explosives used for detonations..... | 185 |
| Table 16.17: Explosive charge used for advance blasting..... | 185 |
| Table 16.18: Characteristics of hole loading by explosive..... | 186 |
| Table 16.19: Development blasting productivity..... | 186 |
| Table 16.20: Development blasting productivity..... | 187 |
| Table 17.1: Lithium minerals found in pegmatite rocks..... | 188 |
| Table 19.1 Conversion Units at Different Stages of Development..... | 199 |
| Table 19.2 Presents the Main Batteries Available in the Market for Different Sectors..... | 201 |
| Table 21.1 Total CAPEX Estimated..... | 207 |
| Table 21.2 OPEX Mining Unitary Costs..... | 208 |
| Table 21.3 Summary Project OPEX..... | 208 |
| Table 22.1 Discounted Cash Flow for the Project – Page 1..... | 210 |
| Table 22.2 Discounted Cash Flow for the Project – Page 2..... | 211 |
| Table 22.3: Simplified Discounted Cash Flow Results (Post-Tax)..... | 212 |
| Table 25.1: Bandeira Mineral Resource Estimates (<i>base case cut-off grade of 0.5 % Li₂O</i>)..... | 216 |
| Table 26.1 Planned Budget recommendations..... | 219 |

LIST OF FIGURES

| | |
|--|----|
| Figure 1.1: PEA Mine Plan and Schedule with Li ₂ O%..... | 24 |
| Figure 1.2: Block Diagram for the Bandeira Process Flowsheet..... | 25 |
| Figure 1.3: Proposed Project Layout and Infrastructure..... | 26 |
| Figure 1.4 Lithium Asset Transactions from 2012 to 2022..... | 27 |
| Figure 1.5 – Li ₂ O SPO 5.5% Price Curve during the next 30 years | 28 |
| Figure 1.6 – Li ₂ O SPO 3% Price Curve during the next 30 Years..... | 28 |
| Figure 1.7: Post-Tax NPV8% Price Sensitivity Analysis. | 31 |
| Figure 4.1: Project Localization..... | 39 |
| Figure 4.2: Lithium Ionic Tenements Map..... | 42 |
| Figure 4.3: Bandeira Project Tenements Map..... | 43 |
| Figure 4.4: Bandeira Project Surface Rights Map..... | 46 |
| Figure 7.1: Simplified geologic map of the Araçuaí Orogen (modified from Pedrosa-Soares et al., 2020), | 52 |
| Figure 7.2: Distributions of U-Pb ages for detrital zircon grains from metamorphosed sedimentary and volcanic rocks (Figure from Pedrosa-Soares et al., 2023). | 55 |
| Figure 7.3: Araçuaí Orogen – Eastern Brazilian Pegmatite Province..... | 57 |
| Figure 7.4: Geological map of the Araçuaí Pegmatite District..... | 61 |
| Figure 7.5: Photos from outcrops and a drill core showing structures of the deformation events D ₁ and D ₂ on the Salinas Formation in the Araçuaí Pegmatite District..... | 63 |
| Figure 7.6: Geological Map of the Bandeira Deposit..... | 65 |
| Figure 7.7: Schists of the Salinas Formation observed in the Bandeira Deposit..... | 66 |
| Figure 7.8: Spodumene-Rich Pegmatites observed in the Bandeira Deposit..... | 67 |
| Figure 7.9: Location of the Bandeira deposit in relation to the CBL's Cachoeira mine and the Sigma's Barreiro deposit (cf. Corporate Presentation, Lithium Ionic Corporation, March 2023..... | 68 |
| Figure 7.10: The Cachoeira mine in the mid 1970's..... | 69 |
| Figure 7.11: Map of the Cachoeira Pegmatite Group in CBL's mine area (adapted and updated from Romeiro, 1998). | 70 |
| Figure 7.12: 13 Photos from spodumene-rich pegmatites (SRP) in the Cachoeira underground mine (CBL). | 71 |
| Figure 7.13: Photos from underground galleries of an old digging for gem prospecting (Garimpo in Brazilian Portuguese), | 72 |
| Figure 7.14: Spodumene Pegmatites interpretations..... | 73 |
| Figure 7.15: Photos from host rocks of spodumene-rich orebodies in the Bandeira deposit..... | 74 |
| Figure 7.16: Drill core samples from spodumene-rich orebodies and their host rocks in the Bandeira deposit (photos by Geologist Fabiana Guimarães). | 76 |
| Figure 7.17: Characterization illustrated summary for a typical spodumene-rich pegmatite (SRP) of the Bandeira deposit, based on intercept with 6,75 m thick and 1.99 wt% Li ₂ O..... | 77 |
| Figure 9.1: Chip Rock Map in the Bandeira Deposit emphasizing the Distribution of Each Collected Sample [Li (ppm)] and the Regions where the Pegmatites are Exposed on the Surface..... | 79 |
| Figure 9.2: Soil Geochemical Map of the Bandeira Deposit. The Remarkable NE-SW Anomalous Trend is coincident with the Direction of the Spodumene-Rich Pegmatites..... | 80 |
| Figure 9.3: Trench Map of the Bandeira Deposit. Twenty-two trenches were executed, preferably in the soil anomalous region. Most of them intercepted pegmatites..... | 82 |
| Figure 9.4: Trenches..... | 83 |

Figure 9.5: Structural Map of the Bandeira Target emphasizing the Distribution of the Mapped Structures. 84

Figure 9.6: a) fractured biotite-schist in the Bandeira area (UTM: 189,232 / 8,141,577); b) scheme emphasizing the interpreted structures in the same outcrop (a): regional ductile foliation (schistosity S_1) and spaced brittle structures possibly related to conjugated system (F_1 , with moderate dip to southeast; and F_2 , subvertical)..... 85

Figure 9.7: Location of the Lines and Measuring Stations of the Chargeability and Resistivity data of Area 1 and Area 2 of the Lithium Project..... 86

Figure 9.8: Depth Model of the Chargeability (Top Panel) and the Actual Resistivity (Bottom Panel) of Line 2 of Area 1. 86

Figure 9.9: Depth Model of the Actual Chargeability (Top Panel) and the Actual Resistivity (Bottom Panel) of Line 3 of Area 1..... 87

Figure 9.10: Depth Model Chargeability (Top Panel) and Resistivity (Bottom Panel) of Line 3 Area 2. 87

Figure 9.11: Depth Model Chargeability (Top Panel) and Resistivity (Bottom Panel) of Line 4 Area 2. 88

Figure 9.12: Conceptual Geological Model from Geophysics Data..... 89

Figure 10.1: Lithium Ionic Drill Holes and Trenches..... 92

Figure 10.2: Horizontal Projection of Bandeira Drilling Holes with Mineralized Intercepts. 98

Figure 10.3: Oblique View of Drill Holes with Mineralized Intercepts. 99

Figure 11.1: QAQC Program..... 104

Figure 11.2: Blank Control Chart – ITAK QG-01..... 105

Figure 11.3: Blank Control Chart – ITAK QF-15..... 106

Figure 11.4: Blank Control Chart – ITAK QF-16..... 106

Figure 11.5: Standard Reference Material Chart – ITAK 1100. 107

Figure 11.6: Standard Reference Material Chart – ITAK 1101. 107

Figure 11.7: Standard Reference Material Chart – OREAS 750. 108

Figure 11.8: Standard Reference Material Chart – OREAS 752..... 108

Figure 11.9: Crushed Duplicates Control Chart. 109

Figure 11.10: Pulverized Duplicates Control Chart. 110

Figure 11.11: Check Assay Control Chart..... 111

Figure 12.1: Collar Moments and Trench on Lithium Ionic Bandeira Property..... 113

Figure 12.2: Drilling Ring and Survey Equipment on Lithium Ionic Bandeira Property..... 114

Figure 12.3: Lithium Ionic Core Shed Storage House in Araçuaí..... 115

Figure 12.4: Cores Boxes Storage in Lithium Ionic Core Shed..... 116

Figure 12.5: Lithium Ionic Staff Working in Logs and Sampling Procedures..... 117

Figure 12.6: Lithium Ionic Density Procedures and QAQC Standards Stock..... 118

Figure 12.7: Lithium Ionic Data Base System Interface..... 119

Figure 12.8: Lithium Ionic Drilling Files Storage..... 120

Figure 12.9: Lithium Ionic Bandeira Property Spodumene Pegmatites Interceptes..... 121

Figure 13.1: Schematic Representation of Dense Medium Drum. 124

Figure 13.2: Schematic Representation of Cone. 125

Figure 13.3: Schematic Representation of a Dense Medium Cyclone..... 125

Figure 13.4: Schematic Representation of the Dynawhirlpool. 126

Figure 13.5: Flowchart of the Sample Preparation Procedure and HLS Test. 127

Figure 13.6: Particle Size Distribution of the 12.5mm Crushing Product..... 128

| | |
|--|-----|
| Figure 13.7: Chemical Composition of the Bandeira Sample..... | 128 |
| Figure 13.8: HLS Test Flowchart. | 129 |
| Figure 13.9: Result of chemical analysis of Li ₂ O and Fe by HLS test step..... | 129 |
| Figure 13.10: Recovery and Li ₂ O Content in the HLS. | 129 |
| Figure 13.11: Sepro's Sample Preparation and Testing Flowchart. | 130 |
| Figure 13.12: Result of Chemical Analysis Feed Sepro Tests. | 130 |
| Figure 13.13: Sepro Test Results. | 131 |
| Figure 13.14: Result of chemical analysis of Li ₂ O and Fe by condition of the HLS and DMS tests. | 131 |
| Figure 13.15: Schematic Representation of the Sensor-based Sorter (VERAS, 2018)..... | 132 |
| Figure 13.16: XRT Sorter Cascade Sorting Flowchart. | 134 |
| Figure 14.1: Drillhole Location Map. | 137 |
| Figure 14.2: Assay Composites Classified by Li ₂ O > 0.3% Grade Limit in Pegmatites Veins. | 138 |
| Figure 14.3: Assays Composites within the Li ₂ O > 0.3% limit in pegmatites veins grouped by separated lenses and dykes. | 138 |
| Figure 14.4: Spodumene grade shells modeled with assays composites Li ₂ O > 0.3 % - horizontal view plan (left side) and section view (right view plan). | 139 |
| Figure 14.5: Spodumene grades shells model - assays composites Li ₂ O > 0.3 % - section view. | 139 |
| Figure 14.6: Weathering zone model - horizontal view plan (left side) and section view (right view plan). | 140 |
| Figure 14.7: Bandeira Assays Interval Length Statistics. | 140 |
| Figure 14.8: Li ₂ O (%) Spodumene Pegmatites Veins Model Statistics – Boxplots (left side) and Statistics Table (right side). | 141 |
| Figure 14.9: Variographic Model – Domains Set NW..... | 143 |
| Figure 14.10: Variographic Ellipsoid – Domains Set NW. | 143 |
| Figure 14.11: Variographic Model – Domains Set SE..... | 144 |
| Figure 14.12: Variographic Ellipsoid – Domains set SE..... | 144 |
| Figure 14.13: Estimation Validation - NN Check to Li ₂ O. | 148 |
| Figure 14.14: Estimation Validation - NN Check to Density. | 149 |
| Figure 14.15: Estimation Validation - SwathPlot Li ₂ O..... | 150 |
| Figure 14.16: Estimation Validation - SwathPlot Denstiy. | 151 |
| Figure 14.17: Resource Classification with RPEE – Horizontal view. | 154 |
| Figure 14.18: Resource Classification with RPEE – Oblique view. | 154 |
| Figure 16.1: Proposed Project Layout and Infrastructure..... | 156 |
| Figure 16.2: Dimensions of the Stopes cross-sections. | 159 |
| Figure 16.3: Schematic drawing of the room-and-pillar mining method. | 160 |
| Figure 16.4: Room and Pillar solids generated. | 162 |
| Figure 16.5: Sublevel Stopping solids generated..... | 163 |
| Figure 16.6: Mine design with all the development structures | 165 |
| Figure 16.7: The mineralized body is fixed to the development structures - Room and pilar. | 166 |
| Figure 16.8: The mineralized body is fixed to the development structures - Sublevel Stopping. | 167 |
| Figure 16.9: Plan view (left) and cross-sectional view (right) of the mining scheduling for year 1..... | 172 |
| Figure 16.10: Plan view (left) and cross-sectional view (right) of the mining scheduling for year 2..... | 173 |
| Figure 16.11: Plan view (left) and cross-sectional view (right) of the mining scheduling for year 3..... | 174 |
| Figure 16.12: Plan view (left) and cross-sectional view (right) of the mining scheduling for year 5..... | 175 |
| Figure 16.13: Plan view (left) and cross-sectional view (right) of the mining scheduling for year 10..... | 176 |

Figure 16.14: Plan view (left) and cross-sectional view (right) of the mining scheduling for year 15..... 177

Figure 16.15: Plan view (left) and cross-sectional view (right) of the mining scheduling for year 20..... 178

Figure 16.16: Mine Plan and Schedule with Li₂O%..... 180

Figure 16.17: Blasting holes per cross-sectional area of each development activity. 184

Figure 16.18: Scheme of fan drilling, both ascending and descending, in the stopes..... 186

Figure 17.1: Process flowchart..... 189

Figure 18.1: Bandeira Project Location..... 192

Figure 18.2: Proposed Project Layout and Infrastructure..... 193

Figure 18.3 Master Plan - Bandeira Project 194

Figure 19.1 Map indicating countries with the largest resources..... 198

Figure 19.2 Lithium supply chain from mineral resource to product..... 198

Figure 19.3 Strategic Growth Plan for Cell and Battery Manufacturing Companies..... 200

Figure 19.4 Lithium Asset Transactions from 2012 to 2022. 203

Figure 19.5 Lithium carbonate price curve in China over the last five years; value of CNY 217,500/t of Li₂CO₃ = US\$ 29,795/t of Li₂CO₃ on August 28, 2023. 204

Figure 19.6 – Li₂O SPO 5.5% Price Curve during the next 30 years 204

Figure 19.7 – Li₂O SPO 3% Price Curve during the next 30 years..... 205

Figure 22.1 Sensitivity Analysis 212

Figure 23.1 Mining Right MGLIT 832.439/2009 (in red) and in the Surrounding Areas CBL and Sigma. . 214

UNITS, SYMBOLS AND ABBREVIATIONS

| Name | Abbreviation |
|---|-------------------|
| Australian Institute of Geoscientists | AIG |
| Average Transportation Distances | ATDs |
| Bandeira Room and Pillar | BRP |
| Bandeira Sublevel | BSL |
| Brazilian Institute of Geography, and Statistics | IBGE |
| Brazilian Lithium Company | CBL |
| Build Your Dreams | BYD |
| Canadian Institute of Mining, Metallurgy and Petroleum | CIM |
| Canadian National Instrument 43-101 | NI 43-101 |
| Capital Expenditures | CAPEX |
| Celsius degree | °C |
| Centimeter(s) | cm |
| Certified Reference Materials | CRM |
| Compound Annual Growth Rate | CAGR |
| Contemporary Amperex Technology Co., Ltd. | CATL |
| Cubic meter(s) | m ³ |
| Dense Medium Separation | DMS |
| Diamond Drill Holes | DDH |
| Direct Lithium Extraction | DLE |
| Discounted Cash Flow | DCF |
| Eastern Brazilian Pegmatite Province | EBPP |
| Electric Vehicles | EVs |
| Electromagnetic | EM |
| End of Period | EOP |
| Environmental Control Plan | PCA |
| Environmental Impact Assessment | EIA |
| Exploration Authorization | EA |
| Exploratory Data Analysis | EDA |
| Fellow Australian Institute of Geoscientists | FAIG |
| Financial Compensation for the Exploration of Mineral Resources | CFEM |
| GE21 Consultoria Mineral Ltda. | GE21 |
| General and Administrative | G&A |
| Global Positioning System | GPS |
| Gram(s) per cubic centimeter(s) | g/cm ³ |
| Heavy Liquid Separation | HLS |
| Hectare | ha |
| High Pressure | HP |
| High Temperature | HT |
| Independent Technical Report | ITR |
| Induced Polarization | IP |
| Infrared | IR |
| Intermediate Pressure | IP |
| Intermediate Temperature | IT |
| Intermediate Waste Storage | I.W.S. |
| Internal Rate of Return | IRR |
| International Organization for Standardization | IOS |
| Kilometer(s) | km |

| | |
|--|--------|
| Kilotons (metric) | kt |
| Life of Mine | LOM |
| Lithium Carbonate Equivalent | LCE |
| Lithium-Cesium-Tantalum | LCT |
| Load Haul Dump | LHD |
| Low Pressure | LP |
| Low Temperature | LT |
| Measured and Indicated | M&I |
| Medium Pressure | MP |
| Medium Temperature | MT |
| Metric tons per year | Mtpy |
| Member Australian Institute of Geoscientists | MAIG |
| Meters per hour(s) | m/h |
| Meter(s) | m |
| MGLIT Empreendimentos Ltda. | MGLIT |
| Millions of Years | Ma |
| Microsoft | MS |
| Millimeter(s) | mm |
| Mineable Stope Optimization | MSO |
| Mineral Resources Estimates | MRE |
| National Mining Agency | ANM |
| Near infrared | NIR |
| Neolit Minerals Participações Ltda | Neolit |
| Net Present Value | NPV |
| Niobium-Yttrium-Fluorine | NYF |
| North | N |
| North-northwest | NNW |
| Operating Expenditures | OPEX |
| Operation License | OL |
| Ordinary Kriging | OK |
| Particle Size Analysis | PSA |
| Parts per million | ppm |
| Percent(age) | % |
| Pressure | P |
| Philosophy Doctor | PhD |
| Photometric | PM |
| Inch | " |
| Independent Technical Report | ITR |
| Installation License | LI |
| International Energy Agency | IEA |
| Portable Document Format | PDF |
| Preliminary License | LP |
| Preliminary Economic Assessment | PEA |
| Qualified Person (as defined in NI 43-101) | QP |
| Quality Assurance / Quality Control | QA/QC |
| Radiometric | RM |
| Reasonable Prospect for Eventual Economic Extraction | RPEEE |
| Resistivity | RES |
| Rock Mass Rating | RMR |
| Rock Quality Designation | RQD |

| | |
|---|------------------|
| Run-of-Mine | ROM |
| Selling, General & Administrative Expense | SG&A |
| SGS Geological Services | SGS |
| Standard Reference Materials | SRM |
| South | S |
| Sub-Level Retreat | SLR |
| Spodumene Concentrate at 3% | SC3 |
| Spodumene Concentrate at 5.5% | SC5.5 |
| Spodumene-quartz Intergrowth | SQUI |
| Spodumene-rich Pegmatites | SRP |
| Square kilometer(s) | km ² |
| Standard Operational Procedures | SOP |
| System of Units | SI |
| Temperature | T |
| Three-dimensional | 3D |
| Ton(s) (metric) | t |
| Tons per cubic meter | t/m ³ |
| Tons per hour | tph |
| TSX Venture Exchange | TSXV |
| Two-dimensional | 2D |
| United States Dollars | US\$ |
| Universal Transverse Mercator | UTM |
| West | W |
| X-ray Fluorescence | XRF |
| X-ray Transmission | XRT |
| Year | y |

1 EXECUTIVE SUMMARY

Lithium Ionic Corp. is a Canadian mining company exploring and developing its lithium properties in Brazil. Its flagship Itinga and Salinas projects cover 14,182 ha in the northeastern part of Minas Gerais state, a mining-friendly jurisdiction that is quickly emerging as a world-class hard-rock lithium district.

The Bandeira Project is situated in the same region as CBL's Cachoeira lithium mine, which has produced lithium for +30 years, as well as Sigma Lithium Corp.'s Grota do Cirilo project, which hosts the largest hard-rock lithium deposit in the Americas.

1.1 INTRODUCTION AND TERMS OF REFERENCE

GE21 Consultoria Mineral Ltda. ("GE21") was engaged by Lithium Ionic Corp. to prepare an Independent Technical Report ("ITR") containing a NI 43-101 Technical Report (The "Report") on Lithium Ionic's Bandeira deposit located in Minas Gerais State, Brazil (Project).

This Report titled "Preliminary Economic Assessment for the Bandeira Lithium Project, Minas Gerais State, Brazil" outlines all relevant data about the Bandeira Project (The "Project"). They are technical information and data related to the drilling program and the status of the current Lithium Mineral Resources contained in the spodumene-bearing pegmatites.

Qualified Persons

The Technical information has been reviewed and approved by Independent Qualified Persons as defined in NI 43-101, Carlos José Evangelista Silva (MAIG Membership Number 7868) for the MRE, and Guilherme Gomides Ferreira (MAIG Membership Number: 7586) for the PEA, both from GE21.

GE21 is an independent mineral consulting firm based in Brazil formed by a team of professionals accredited by the Australian Institute of Geoscientists ("AIG") as Qualified Persons ("QP") for declaration of Mineral Resources and Mineral Reserves in accordance with National Instrument 43-101 – Standards of Disclosure for Mineral Projects ("NI 43-101").

The independent QP responsible for this report's content on issues related to Mineral Resources is Carlos José Evangelista Silva (MAIG, M.Sc.), a Geologist, who has at least 17 years of experience in the mineral industry, including lithium mining companies.

The independent QP responsible for this report's content on issues related to Mineable Resources estimation and economic analysis is Guilherme Gomides Ferreira (MAIG, B.Sc.), a Mining Engineer and Manager Engineer of GE21 Consultoria Mineral, who has at least 17 years of experience in mining projects.

The independent QP responsible for this report's content on issues related to Mineral Processing and Metallurgical Tests, and Recovery Methods is Paulo Bergman (FAusIMM, B.Sc.), a Mining Engineer of GE21 Consultoria Mineral, who has at least 43 years of experience in mining projects.

The Qualified Person responsible for the environmental assessment carried out in the Preliminary Economic Assessment level is the expert Branca Horta de Almeida Abrantes (MAIG, B.Sc.). Branca has 19 years of experience in the environmental sector.

Porfirio Cabaleiro Rodriguez (FAIG, B.Sc.) is the reviewer of this technical report. Mr. Rodriguez has at least 45 years of experience in all aspects of mining project evaluation, from initial exploration to bankable feasibility studies. He is a senior mining engineer and managing director of GE21 Mineral Consulting.

1.2 RELIANCE ON OTHER EXPERTS

The authors have not independently verified ownership or mineral title beyond the information that Lithium Ionic has provided. The Property description presented in this Report is not intended to represent a legal or any other opinion as to title.

Verification of information concerning Property status and ownership, which are presented in Item 4 below, has been provided to the Author by Carlos H C Costa, VP Exploration for Lithium Ionic by way of an Email on July 14, 2023. The Authors only preliminarily reviewed the land tenure and has not independently verified the legal status or ownership of the Property or any underlying agreements or obligations attached to ownership of the Property. However, the Authors have no reason to doubt that the title situation is other than what is presented in this technical report (Item 4).

The Authors are not qualified to express any legal opinion concerning Property titles or current ownership.

1.3 PROPERTY DESCRIPTION AND LOCATION

The Bandeira Project (The “Project”) covers 175 hectares within Lithium Ionic’s large land package of 14,182 hectares and is located between the towns of Araçuaí and Itinga within Brazil’s “Lithium Valley” - a hard rock lithium district that is quickly emerging as an important global lithium producer.

1.4 ACCESSIBILITY, CLIMATE, LOCAL RESOURCES, INFRASTRUCTURE AND PHYSIOGRAPHY

The Project is situated in the northeastern region of Minas Gerais State, Brazil, within the Jequitinhonha Valley, approximately 600 kilometers northeast of Belo Horizonte. Lithium Ionic fully owns the property. It is conveniently located about 75 kilometers south of the town of Salinas, with a population of approximately 42,000, and roughly 25 kilometers east of the town of Araçuaí, with a population of approximately 40,000. Access to the project is facilitated by well-maintained public and private roads, thanks to its proximity to National Roads 251 and 116.

The Project remains accessible year-round through a network of main and secondary service roads. National routes BR 116 and 262 provides access to the Port of Vitória in the State of Espírito Santo, located approximately 850 kilometers from the project site. This port offers potential export opportunities for any spodumene production from the project. Additionally, national roads BR 116 and BR 415 connect to the Ilhéus Port in the Bahia State, which is situated about 540 kilometers from the project and serves as an alternative shipping port option.

1.5 HISTORY

The Bandeira site and all other Mineral Tenures haven’t had drilling activity before 2022.

1.6 GEOLOGICAL SETTING AND MINERALIZATION

The Bandeira Project lies in the Middle Jequitinhonha River valley, northeastern Minas Gerais State, currently known as the Lithium Valley of Brazil. The region is part of the Eastern Brazilian Pegmatite Province (EBPP), one of the largest pegmatitic provinces around the world with 150,000 km² (cf. synthesis in Pedrosa-Soares et al., 2011). The EBPP is an outcome of magmatic and tectonic-metamorphic events that formed the Araçuaí Orogen from the Early Ediacaran (ca. 630 Ma) to the Late Cambrian (ca. 490 Ma). The significant EBPP pegmatite populations found within the Araçuaí Orogen have been grouped into twelve pegmatite districts (Pedrosa-Soares et al., 2011, 2023) that include residual pegmatites (representing late silicate melts released by fractional crystallization of parent granites) and/or anatectic pegmatites (formed directly from partial melting of country rocks).

The Itinga Pegmatite Field includes the spodumene mines and deposits of CBL (Companhia Brasileira de Lítio) and Sigma Lithium, as well as Lithium Ionic’s properties of its Bandeira Project,

such as the Bandeira spodumene deposit. The lithium ore bodies exploited in the CBL’s underground mine, since the early 1990’s, display a closely spaced swarm of relatively narrow (6 m thick on average) but long (up to 700 m along strike) non-zoned spodumene-rich pegmatites (SRP) with on average 25 vol% of disseminated spodumene (Romeiro and Pedrosa-Soares, 2005). In the Sigma Lithium properties, where several large spodumene-rich pegmatites are found (e.g., Barreiro, Murial, Xuxa; Delboni Jr. et al., 2023), an open pit mine is currently being developed on the Xuxa SRP deposit (15 m thick x 1800 m long x 500 m down dip open).

1.7 DEPOSIT TYPES

According to the most accepted petrologic-metallogenetic classification of pegmatites, published by Cerný (1991) and updated by Cerný and Ercit (2005) and Cerný et al. (2012), all the spodumene-rich pegmatites found within the Bandeira deposit, as well as in the whole Cachoeira Pegmatite Group, belong to the rare element class, Li subclass, and albite-spodumene type.

Although generally included in the LCT (Lithium-Cesium-Tantalum) family, the non- to poorly zoned spodumene-rich pegmatites (SRP) found in the Bandeira deposit, as well as all the orebodies mined in CBL’s Cachoeira Mine since the 1990’s, the Xuxa and other spodumene-rich deposits of Sigma Lithium (Sá, 1977; Delboni et al., 2023), and the Outro Lado deposit of Lithium Ionic, are rather poor both in Ta and Cs when compared with the complex zoned LCT pegmatites.

1.8 EXPLORATION

Trench sampling program, rock chip sampling programs, structural mapping and geophysical surveys were completed on the Property. A total of 22 trenches were completed in 2023 at the Bandeira target by Lithium Ionic totaling 1,401 m. Field work included rock samples in the field and a preliminary field mapping of visible outcrops.

Some basic field data such as outcrop attitude (strike and dip), foliation and cleavage which located several occurrences of spodumene never previously known or reported. Since this initial discovery, Lithium Ionic rapidly advanced the Project with drill testing of the target(s) and the pegmatite system.

1.9 DRILLING

All drilling activities conducted within the Bandeira Property until August 2023 have been incorporated into the Mineral Resource estimation process. It is important to note that any drill holes completed in 2023 after this date, as well as pending sample assay results, have not been considered in the present resource statement Table 1.1.

Table 1.1: Bandeira Drill Holes Summary.

| Drill Type | Year | Number Drill | Length (m) |
|------------|-------|--------------|------------|
| DDH | 2022 | 52 | 5,930 |
| | 2023 | 130 | 33,749 |
| | Total | 182 | 39,679 |

1.10 SAMPLE PREPARATION, ANALYSIS AND SECURITY

Sample intervals in the mineralized zones are defined based on a 1.0m support. Mineralized samples must have a minimum length of 1.0m and a maximum length of 1.5m. In some specific situations, samples shorter than 1.0m can be generated.

Drill core samples are prepared and analyzed by an independent commercial laboratory (SGS Geosol). The SGS Geosol facility is ISO 9001, ISO 14001, and ISO 17025 certified. The sample shipment was delivered to the SGS Geosol facility in Vespasiano, Minas Gerais, Brazil, via a parcel transport company.

All samples received at SGS Geosol were inventoried and weighted before processing. Samples were dried at 105°C, crushed to 75% passing a 3 mm sieve, homogenized, split (Jones riffle splitter), and pulverized (250 to 300 g of sample) in a steel mill to 95% passing 150 mesh.

Samples are prepared from NQ diameter drill cores (47.6mm core diameter). The sampling procedures described in this section reflect the current Standard Operational Procedures (SOP) in use by Lithium Ionic.

The sample batch composition includes 5 Quality Control Samples for every 30 regular samples. The Quality Control composition of the batches is described next:

- a) Coarse (Preparation) and Fine (Analytical) Blanks: 6% of the batch, or two blanks per batch, one of each type.
- b) Standards: 6% of the batch, or two standards per batch.
- c) Crushed Duplicates: 3% of the batch, or 1 sample per batch.
- d) Pulverized Duplicates: 3% of the batch, or 1 sample per batch.

Lithium Ionic has submitted Check Assay batches for analysis at the ALS Laboratory in Vancouver, British Columbia, Canada. This procedure is used to verify the reliability of the primary laboratory results by crosschecking it with a secondary reference laboratory.

The Qualified Person thinks that the sampling, sample preparation, security and analysis performed by Lithium Ionic and hired companies are suited for a Mineral Resource Estimation study. Quality Assurance procedures follow the industry's best practices, and Quality Control results are within industry standards, attesting to the quality of the Database information.

1.11 DATA VERIFICATION

Mr. Carlos José E. Silva, an independent QP for Geology Exploration and Mineral Resource Estimate, carried out a site visit on the Bandeira Project between 13 and 14 of September 2023. Lithium Ionic allowed unlimited access to the Company's facilities during this time.

All verified procedures related to sampling management, storage, logging, sample preparation and assay were checked, and it is considered inside acceptance limits and in compliance with mineral industry practices. Rock-type descriptions fit with the checked mineralization style.

1.12 MINERAL PROCESSING AND METALLURGICAL TESTING

The ROM from the Bandeira Project's underground mine consists of pegmatite mineralized with minerals such as spodumene, albite, quartz, muscovite, K-feldspar, cookeite, and minor amounts of petalite. The technological characterization of this material to define the process flowchart for size reduction, classification, and concentration by dense media was carried out using 2" (50.8 mm) diameter drill samples.

The technological characterization was carried out through chemical and mineralogical analyses, physical tests to determine hardness, particle size distribution in crushing tests, level of abrasiveness and metallurgical tests to understand the response of the material when subjected to the simulation of the industrial process of concentrating the mineral, spodumene.

1.13 MINERAL RESOURCES ESTIMATES

The PEA is based on an updated MRE for the Bandeira Project summarized in Table 1.2. The Bandeira MRE contains Measured and Indicated ("M&I") Resources of 13.72Mt grading 1.40% Li₂O, containing 474,892 tonnes of Lithium Carbonate Equivalent ("LCE"), the benchmark equivalent raw material used in the lithium industry, in addition to Inferred Resources of 15.79Mt grading 1.34% Li₂O, or 523,118 tonnes of LCE.

The updated MRE for Bandeira is based on 182 diamond drill holes conducted on the Bandeira property until August 30, 2023. This compares to drill data from 120 holes in the previous MRE for Bandeira announced on June 27, 2023. This additional drilling significantly expanded the MRE, with the tonnes in the Indicated category increasing by 196% compared to the previous Estimate.

Table 1.2: Bandeira Mineral Resource Estimates (Base Case Cut-off Grade of 0.5 % Li₂O).

| Category | Resource (Mt) | Grade (% Li ₂ O) | Contained LCE (t) |
|-----------------------------|---------------|-----------------------------|-------------------|
| Measured | 2.00 | 1.40 | 69,226 |
| Indicated | 11.72 | 1.40 | 405,666 |
| Measured + Indicated | 13.72 | 1.40 | 474,892 |
| Inferred | 15.79 | 1.34 | 523,118 |

Notes related to the Mineral Resource Estimate:

1. The spodumene pegmatite domains were modeled using composites with Li₂O grades greater than 0.3%.
2. The Mineral Resource Estimates were prepared in accordance with the CIM Standards, and the CIM Guidelines, using geostatistical and/or classical methods, plus economic and mining parameters appropriate to the deposit.
3. Mineral Resources are not Ore Reserves and are not demonstrably economically recoverable.
4. Grades reported using Dry Density.
5. The effective date of the MRE is October 11, 2023.
6. The QP responsible for the Mineral Resources is geologist Carlos José Evangelista da Silva (MAIG #7868).
7. The MRE numbers provided have been rounded to the estimate relative precision. Values cannot be added due to rounding.
8. The MRE is delimited by Lithium Ionic Bandeira Target Claims (ANM).
9. The MRE was estimated using Ordinary Kriging in (12 x 12 x 4) m blocks.
10. The MRE Report Table was produced in Leapfrog Geo Software.
11. The reported MRE only contains Fresh Rock Domains.
12. The MRE was restricted by grade shell, simulating a UG method, using 0.5% Li₂O cut-off.

1.14 MINERAL RESERVES ESTIMATES

No Mineral Reserves have been estimated for the Project.

1.15 MINING METHODS

The Bandeira Project will have dual underground mining operations. The primary orebodies, accounting for approximately 90% of the deposit, are proposed to be extracted using a bottom-up “sublevel stoping” method (Bandeira Sublevel Mine, “BSL mine”). Simultaneously, the secondary southeast orebody, comprising approximately 1.8 million tonnes, is expected to be mined using “room-and-pillar” method (Bandeira Room and Pillar, “BRP mine”).

The BSL mine has been planned with two declines, extending along a NE/SW mineralized trend spanning 1.0 km. It is divided into 12 panels, each measuring 55 meters, and consists of two sublevels.

The BRP mine features a single panel with approximate dimensions of 380 meters in length, 330 meters in width, and 10 meters in height. Access to the ore chamber will be provided through five

cross-cuts originating from the southern decline. Once fully operational, the BSL and BRP mines are expected to achieve a combined production of approximately 1.3 million tonnes per annum.

The Table 1.3 present the Bandeira's Project Production Profile and Figure 1.1 shows the annual plant feed along with Li₂O grade.

Table 1.3: Bandeira's Project Production Profile.

| Total Project Life (LOM) | 20 years |
|--|--------------------------------------|
| Room and Pilar LOM Production (Diluted) | 1.8 Mt @ 1.05% Li ₂ O |
| Sub Level LOM Production (Diluted) | 21.1 Mt @ 1.25% Li ₂ O |
| Total LOM Production (Diluted) | 22.9 Mt @ 1,23Li₂O |
| Nominal Plant Capacity | 1.3 Mtpa |
| Average Plant Throughput | 1.26 Mtpa |
| Run-of-Mine Underground Mining Dilution | 16.8% |
| Waste Generation Average from Year 0 to 20 | 439 ktpa |
| SPO average Annual Production @ 5,5% Li ₂ O from Years 1 to 18 | 187 ktpa |
| SPO average Annual Production @ 3,0% Li ₂ O from Years 1 to 18 | 56 ktpa |
| SPO average Annual Production @ 5.5% Li ₂ O Equivalent from Years 1 to 18 | 218 ktpa |
| SPO 5,5% Li ₂ O Metallurgical Recovery | 67.0% |
| SPO 3,0% Li ₂ O Metallurgical Recovery | 10.7% |
| SPO 5,5% Li ₂ O Mass Recovery | 15.2% |
| SPO 3,0% Li ₂ O Mass Recovery | 4.5% |

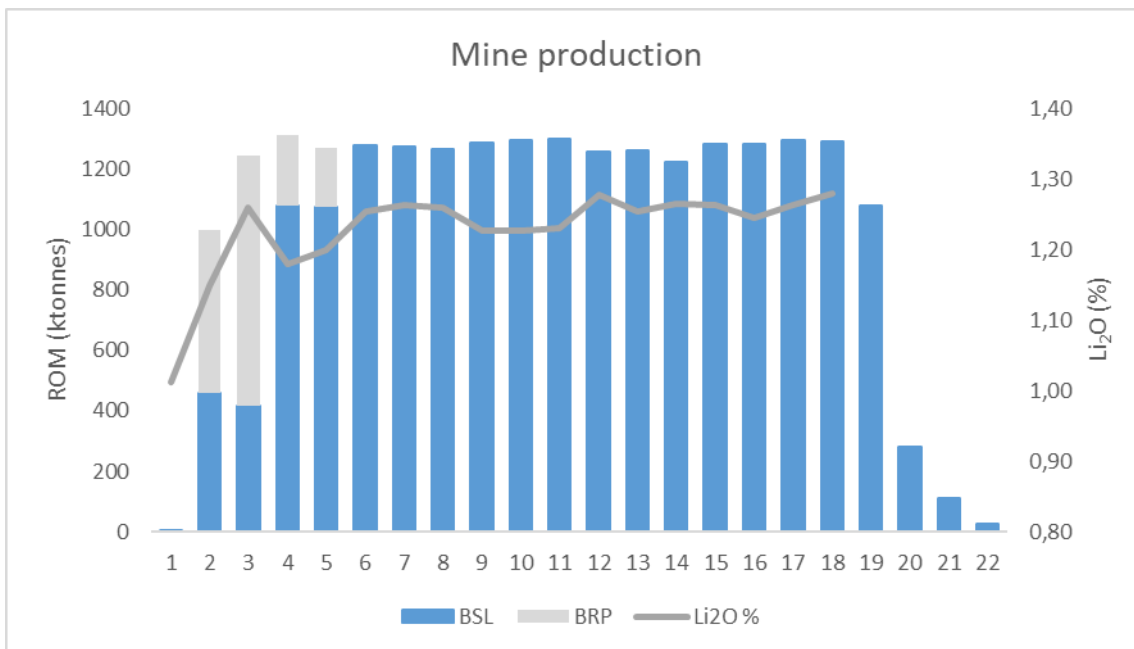


Figure 1.1: PEA Mine Plan and Schedule with Li₂O%.

1.16 RECOVERY METHODS

The mineral processing flowsheet is structured around a two-stage crushing circuit (comprising a Jaw crusher and Gyratory Cone crusher), ore size classification, the implementation of an ore sorter for coarse and medium materials, and the utilization of DMS (Dense Media Separation) for coarse and medium materials. Additionally, fines are subjected to gravity concentration with spirals. For a visual representation of the process the Figure 1.2 show the specific design criteria for mineral processing.

The underground mine is anticipated to yield ROM with an average Li₂O grade of 1.23% over the Life of Mine (LOM), accounting for dilution at 16.8%. The ore sorting process will effectively purify the ore by removing undesirable dilution and non-lithium-bearing minerals like albite, feldspar, and quartz. This enrichment process will improve the lithium oxide grade to approximately 1.50%, ensuring a higher feed for the DMS I and II units. Based on the preliminary testwork program, Li₂O recovery is projected to reach 67%, with an additional 10.7% achieved through gravity concentration in the fines fraction.

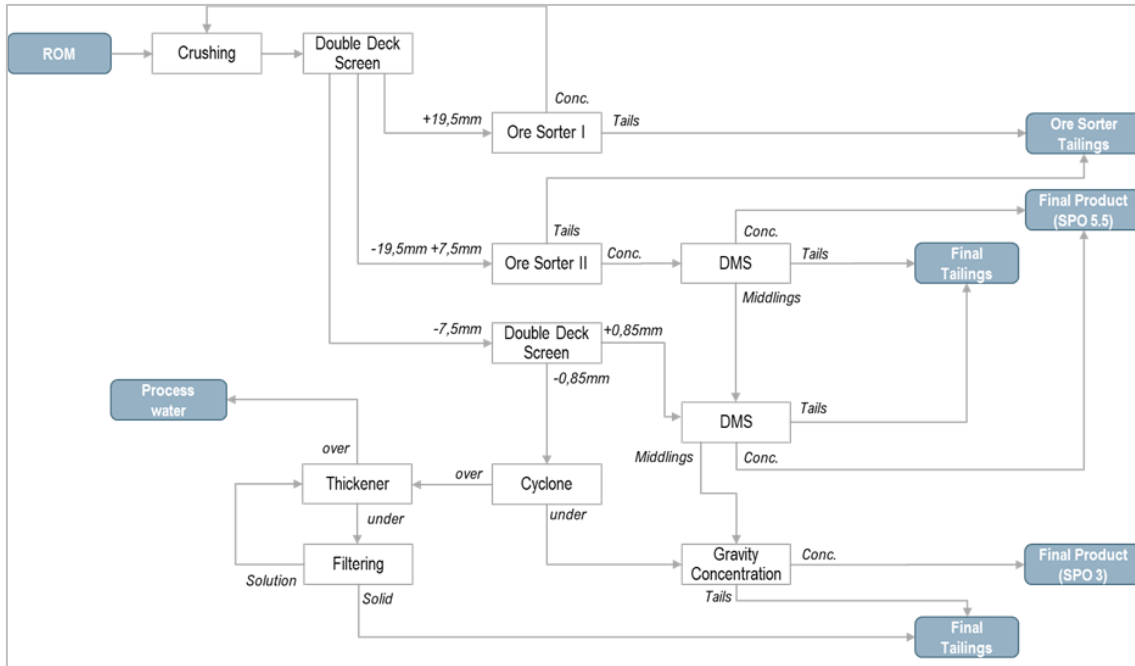


Figure 1.2: Block Diagram for the Bandeira Process Flowsheet.

1.17 PROJECT INFRASTRUCTURE

The location alternatives for the installation of the spodumene mineral concentration unit are closely tied to the mineral deposit location. The structures required for mineral beneficiation should be installed adjacent to the mining areas, increasing the synergy between mine and plant operations.

The administrative facilities (gatehouse, cafeteria, central office, infirmary, and firehouse) will be located on the left bank of the Piauí River, while the operational area (crushing unit, ore sorter, DMS, laboratory, maintenance, mine office) will be on the right side. The project layout is illustrated in Figure 1.3.

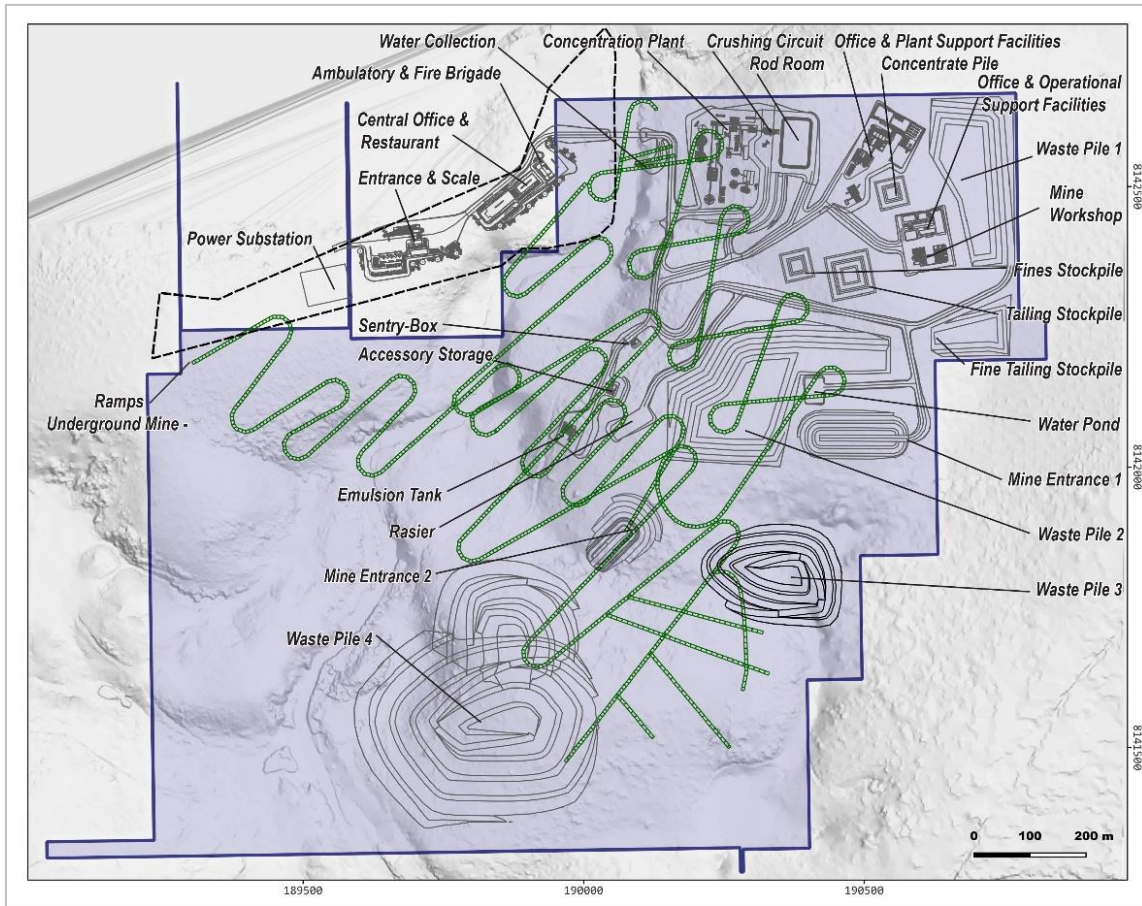


Figure 1.3: Proposed Project Layout and Infrastructure.

The beneficiation plant, which includes the unit operations of crushing, pre-concentration, dense medium separation, filtration, and thickening, is indicated in item 1. Areas 2, 3, and 4 are designated for the construction of the laboratory, intermediate waste storage (I.W.S.), warehouse, vehicle wash station, vehicle workshop, tire repair shop, industrial workshop, mine office, I.W.S., and fuel station.

1.18 MARKET STUDIES AND CONTRACTS

Since the Stockholm Conference in June 1972, the world has been calling for greater attention to environmental issues. However, at that time, there were no efficient tools to address the growth of the global industry and the negative impact of greenhouse gas emissions, particularly carbon dioxide.

Based on Environmental, Social and Governance (ESG) protocols, the demand for renewable energy have increased over the last three years at an annual rate exceeding 25% and the mineral that will help this energy transition is lithium. The supply of spodumene concentrate recorded a lower offer than the demand in the years 2021 and 2022. This fact is substantiated by China's initiation of imports of fine ore, a fraction smaller than 0.5mm, which is rejected at the DMS unit. The supply of spodumene is expected to increase by approximately 250,000 tons in 2023 with the start-up of concentration units in Brazil, Zimbabwe, and Australia.

Figure 1.4 presents the lithium mineral asset transactions that occurred from 2012 to 2022, indicating a pressure on supply with the potential for an excess of lithium compounds within a 5 to 10-year timeframe.

| Buyer | Seller | Property | Negotiation value (\$M) |
|--|--|--------------------------------|-------------------------|
| Chengdu Tianqi Industry Group Co. Ltd. | SQM Chile SA | Salar de Atacama, Mt Holland | 4066,2 |
| Rio Tinto Group | Sentient Equity Partners | Rincon Mining Pty Ltd. | 825,0 |
| Chengdu Tianqi Industry Group Co. Ltd. | Greenbushes Lithium | Greenbushes | 803,3 |
| Zijin Mining Group Co. Ltd. | Neo Lithium Corp. | Neo Lithium Corp. | 765,3 |
| Zijin Mining Group Co. Ltd. | Neo Lithium Corp. | Tres Quebradas | 765,0 |
| Zijin Mining Group Co. Ltd. | Dunan Holding Group Co. Ltd. | Lakkor Tso Salt Lake | 741,1 |
| Sibanye Stillwater Ltd. | ioneer Ltd. | Rhyolite Ridge | 490,0 |
| Lithium Americas Corp. | Millennial Lithium Corp. | Millennial Lithium Corp. | 400,0 |
| Zhejiang Huayou Cobalt Co. Ltd. | Prospect Resources Ltd. | Arcadia | 342,9 |
| Contemporary Amperex Technology Ltd. | Millennial Lithium Corp. | Cauchari East, Pastos Grandes | 298,2 |
| Ganfeng Lithium Co. Ltd. | Bacanora Lithium Plc | Sonora and Zinnwald | 259,3 |
| Suzhou CATH Energy Technologies Ltd. | AVZ Minerals Ltd. | Manono | 240,0 |
| Sinomine Resource Group Co. Ltd. | Undisclosed sellers | Bikita Minerals Ltd. | 192,4 |
| Sayona Mining Ltd. | Lithium Royalty Corp.; GUOAO Lithium Ltd. | Moblan | 87,5 |
| Zhejiang Huayou Cobalt Co. Ltd. | Private investors | Arcadia | 44,2 |
| Lithium Power Intrnational Ltd. | Minera Salar Blanco SPA | Minera Salar Blanco SPA | 41,2 |
| Jiangxi Ganfeng Lithium Co. Ltd. | Reed Industrial Minerals Pty Ltd | Mount Marion | 27,2 |
| Jilin Jien Nickel Industry Co. Ltd. | Quebec Lithium Mine | Quebec | 23,6 |
| Lithium Ionic | Diversos | Diversos | 23,0 |
| Lithium Power Intrnational Ltd. | Bearing Lithium Corp. | Bearing Lithium Corp. | 20,1 |
| Jiangxi Ganfeng Lithium Co. Ltd. | Reed Industrial Minerals Pty Ltd | Mount Marion | 19,5 |
| Ganfeng Lithium Corp. | International Lithium Corp. | Mariana project | 13,2 |
| American Lithium Corp. | Undisclosed sellers | Crescent Dunes | 5,4 |
| Kodal Minerals PLC | Gorutumu Mining SARL; Triumvirat Mining Co. SARL | Bougouni | 1,2 |
| Spearmint Resources Inc. | Undisclosed sellers | Green Clay | 0,4 |
| Mineral Resources Ltd. | New Age Metals Inc. | Lithium Project | 0,3 |
| Jiangxi Ganfeng Lithium Co. Ltd. | International Lithium Corp. | Mavis | 0,2 |
| Green Technology Metals Ltd. | Solstice Gold Corp. | Lithium exploration properties | 0,1 |
| Mineral Resources Ltd. | Albemarle Corp. | Wodgina | N.A. |

Figure 1.4 Lithium Asset Transactions from 2012 to 2022.

Source: S&P Global Market Intelligence.

Energy Trend forecasts an excess supply of LCE around 85,000 tons in 2023. This trend is expected to persist in the coming years to accommodate the production expansion of Sigma Lithium in Brazil, with a production forecast of 760,000 tons of concentrate starting from 2025. From 2027 onwards, the market should again return to a balance in the supply and demand for spodumene and LCE.

Projected Price of LCE and Spodumene

The selling price used for SPO 5.5% was based on a projection based on price history of Li₂O, in accordance with market practices. It predicts an oscillation of the price during the next 10 years, stabilizing at the current price level. Figure 1.5 shows the SPO 5.5% price curve for the next 30 years.

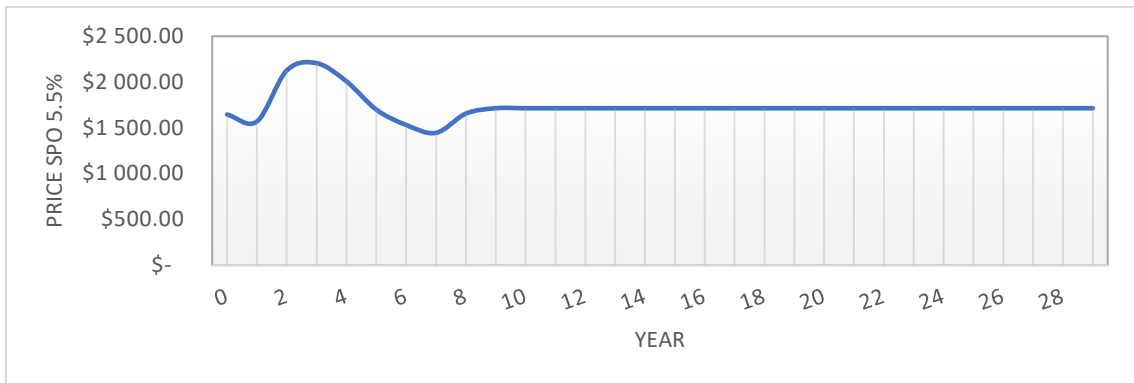


Figure 1.5 – Li₂O SPO 5.5% Price Curve during the next 30 years

The same method was applied for the projection of SPO 3% which was based on price history of Li₂O 3%, in accordance with market practices. It predicts an oscillation of the price during the next 10 years, stabilizing at the current price level. Figure 1.6 shows the SPO 3% price curve for the next 30 years.

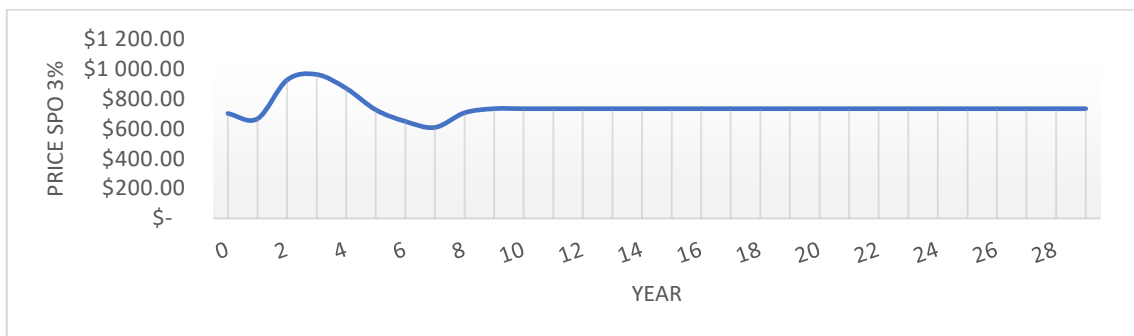


Figure 1.6 – Li₂O SPO 3% Price Curve during the next 30 Years Contracts

MGLIT and Lithium Ionic Corp. have not yet signed contracts for the sale of spodumene concentrate or contracts for the construction of the Project.

1.19 ENVIRONMENTAL STUDIES, PERMITS, AND SOCIAL OR COMMUNITY IMPACTS

For mineral extraction activities, environmental studies, permits, and social or community impacts it is mandatory in Brazil and must be carried out in accordance with Federal Decree No. 99,274/90, which regulates Federal Law No. 6,938/81, which, in turn, establishes the National Environmental Policy.

Within the scope of environmental licensing, in addition to complying with applicable legislation at the Federal, State and Municipal levels, relevant environmental aspects are analyzed — such as water and effluents, flora and fauna, noise, natural, cultural, historical and archaeological heritage, environment, education, indigenous lands and quilombola and traditional populations —, and also analyzed the manifestations of the intervening bodies, including the City Hall, attesting to the project's compliance with municipal legislation on land use and occupation.

For mining activities, it is also necessary for the entrepreneur to prove that he holds the right to explore the intended mineral substance, which is granted by the National Mining Agency, considering that the mineral resources are property of the Union under the terms of art. 20, IX of the Federal Constitution of 1988.

The National Environmental Council through resolution CONAMA 237/97 has established a three-stage licensing process for mining projects in Brazil:

Issuance of a Preliminary License (LP) at the planning stage of development. Obtaining an LP requires approval by the relevant Environmental Authority of the project Environment Impact Assessment and Report (EIA-RIMA) and plan for the recovery of degraded areas (PRAD).

Issuance of an Installation License (LI), which authorizes construction according to specifications contained in the approved Environmental Impact Assessment (EIA) or Environmental Assessment (EA), as well as the Environmental Control Plan (PCA).

Issuance of the Operation License (LO). The LO is required to mine, process, and sell mineral substances, and is granted once the Environmental Authority has inspected the site and verified that construction was completed in keeping with all the requirements of the LI, and that the environmental control measures and other conditions of the LI have been satisfactorily implemented.

In Minas Gerais State the environmental licensing or permitting is responsibility of Secretaria de Estado de Meio-Ambiente e Desenv. Sustentável - SEMAD. Which is the institution that regulates, approves, and issues environmental licenses (LP, LI and LO).

All licenses are required before production can begin.

1.20 CAPITAL AND OPERATING COSTS

The capital expenses estimated for the Bandeira Project is based on the design of the engineering project, which contemplates an underground mining operation operated by MGLit itself.

Bandeira Project mining costs consist of acquisition of equipment's, pre-production investments and the first year of the underground project development.

The Total Mining Capex estimated is US\$ 72.5M.

The mineral processing is based on the quotation of fixed plant, structured around a two-stage crushing circuit, ore size classification, the implementation of an ore sorter for coarse and medium materials, and the utilization of DMS (Dense Media Separation) for coarse and medium materials. The capacity is based on a production of 1.3Mt of Li₂O. The Total Plant Capex estimated is US\$ 80.5M.

The Economic Assessment Estimates a Capital Sustaining of US\$ 118M applied from the third year of the Project.

The Capital Expenses forecast other costs such as engineering, environmental and infrastructures resulting in a Total Capex estimated is about US\$ 351M. The detailed pricing is presented on the Table 1.4 below:

Table 1.4: Bandeira's Project Capital Costs.

| Project Capital Costs | |
|---|----------------|
| Mine (Development + Equipment's + Pre-Production) | \$72.5 million |
| Plant | \$80.5 million |
| Environmental | \$2.9 million |
| Engineering Services | \$20.0 million |
| General Infrastructure & Others | \$10.3 million |
| Contingency (25%) | \$46.6 million |

| | |
|---|------------------|
| Total Capital Cost Estimate | \$232.8 million |
| SUDENE Incentive tax benefit over first 10 years | 75% |
| Operating Costs (OPEX) | |
| Operating costs (based on ore processed) | \$61/t ore |
| Mining | \$45/ t ore |
| Processing + Tailings handling | \$12/ t ore |
| SG&A | \$4/t ore |
| Operating costs (based on SPO 5.5 concentrate produced) | \$349/t SPO 5.5E |
| Mining | \$258/t SPO 5.5E |
| Processing + Tailings handling | \$68/t SPO 5.5E |
| SG&A | \$23/t SPO 5.5E |
| Transportation costs to customer destination <i>(Mine in Itinga - Araçuaí to Shanghai Port, China)</i> | \$120/t SPO |

1.21 ECONOMIC ANALYSIS

A Discounted Cash Flow (DCF) analysis was developed for the Bandeira Project based on the economic-financial parameters, the results of the mine scheduling and the premises of evaluating the material mined.

The Project base case estimates a Net Present Value of US\$ 1.6 billion post-tax, at a Discount Rate of 8% per year. Table 1.5 presents the Bandeira Project PEA Summary and Figure 1.7 shows the Sensitivity Analysis.

Table 1.5: Bandeira Project PEA Summary.

| Project Economics | |
|--|---------------|
| Post - Tax NPV ₈ | \$1.6 billion |
| Post - Tax IRR | 121% |
| Pre - Tax NPV ₈ | \$2.3 billion |
| Pre - Tax IRR | 163% |
| Annual Revenue – Average | \$337 million |
| Annual Free Cash Flow -Average | \$243 million |
| Payback | 14 months |
| Economic Assumptions & Parameters | |
| SPO 5.5% Li ₂ O Price, CIF China | \$1,859/t |
| SPO 3.0% Li ₂ O Price, CIF China | \$865/t |
| Exchange rate | US\$5.00 /R\$ |
| Discount Rate | 8% |

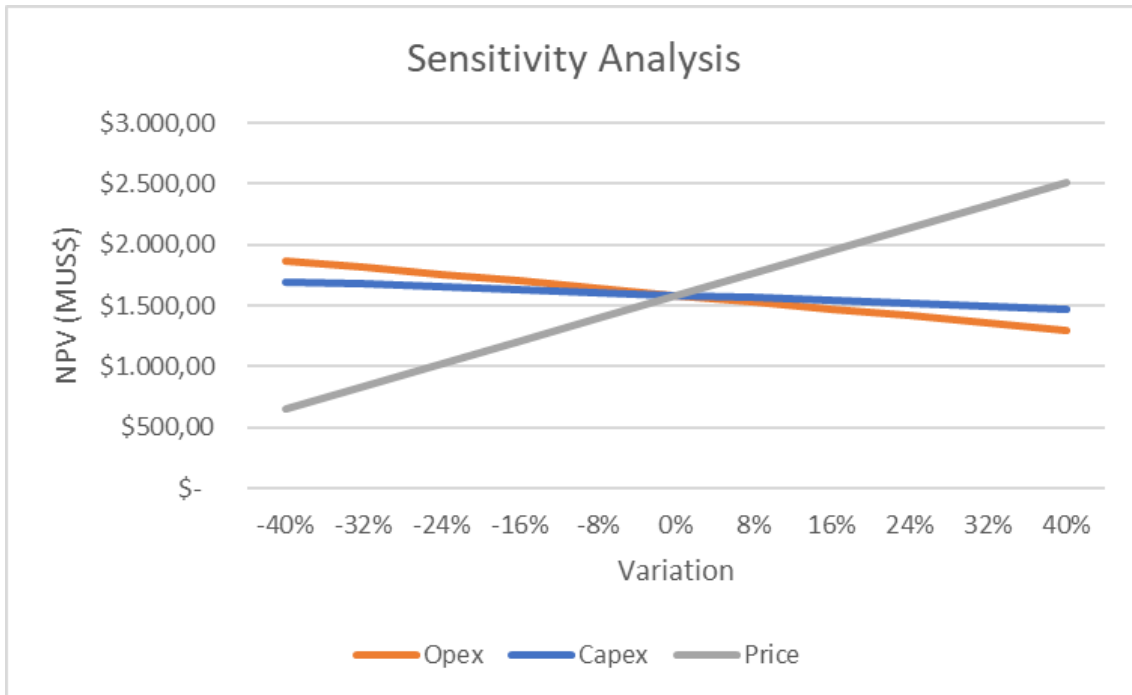


Figure 1.7: Post-Tax NPV8% Price Sensitivity Analysis.

1.22 ADJACENT PROPERTIES

The Itinga Pegmatite Field includes the spodumene mines and deposits of CBL (Companhia Brasileira de Lítio) and Sigma Lithium.

The Lithium ore bodies exploited in the CBL's underground mine, since the early 1990's, display a closely spaced swarm of relatively narrow (6 m thick on average) but long (up to 700 m along strike) non-zoned spodumene-rich pegmatites (SRP) with on average 25 vol% of disseminated coarse-grained spodumene (Romeiro and Pedrosa-Soares, 2005).

In the Sigma Lithium properties, where several large spodumene-rich pegmatites are found (e.g., Barreiro, Murial, Xuxa; Delboni Jr. et al., 2023), an open pit mine is currently being developed on the Xuxa SRP deposit (15 m thick x 1800 m long x 500 m downdip open).

1.23 INTERPRETATION AND CONCLUSIONS

Mineral Resources were estimated and limited to the areas outlined using the Mining Rights polygonal that comprise the Bandeira Property and the reasonable possibility of economic extraction (Reasonable Prospect for Eventual Economic Extraction - RPEEE) was applied.

The Bandeira database contains 4,876 assay intervals covering 4,592 meters, comprising 164 assays from trenches totaling 157 meters and 4,712 assay intervals from drill holes totaling 4,434 meters.

A set of solid grade shells for estimation domains was created using a 0.3% Li₂O (%) threshold. These interpretations were then transformed into a series of implicit 3D models, aligned with the dominant strike directions of 235° and 140°. Additionally, weathering modeling was performed, taking into account the information provided in the logs. The model was built from implicit modelling using the Leapfrog 2023.1 software.

The Ordinary Kriging (OK) estimation method was used on the Li₂O% and density variables based on the results of the structural analysis conducted in this work.

The criterion for classifying the resource was based on criteria:

- e) The Measured Mineral Resource classification had as a reference the 50 meters of the Average Euclidean distance to sample (AvgD) used in ordinary kriging estimation with a minimum of five composites in at least three different drill holes.
- f) The Indicated Mineral Resource classification had as a reference the 100 meters of the Average Euclidean distance to sample (AvgD) used in ordinary kriging with a minimum of five composites in at least three different drill holes.
- g) The Inferred Mineral Resource classification is all remaining estimated blocks.

The PEA is based on an updated MRE for the Bandeira Project summarized in Table 1.2. The Bandeira MRE contains Measured and Indicated (“M&I”) Resources of 13.72Mt grading 1.40% Li₂O, containing 474,892 tonnes of Lithium Carbonate Equivalent (“LCE”), the benchmark equivalent raw material used in the lithium industry, in addition to Inferred Resources of 15.79Mt grading 1.34% Li₂O, or 523,118 tonnes of LCE.

The updated MRE for Bandeira is based on 182 diamond drill holes conducted on the Bandeira property until August 30, 2023. This compares to drill data from 120 holes in the previous MRE for Bandeira announced on June 27, 2023. This additional drilling significantly expanded the MRE, with the tonnage in the Indicated category increasing by 196% compared to the previous Estimate.

The Bandeira Project have potential for dual underground mining operations. The primary orebodies, accounting for approximately 90% of the deposit, are proposed to be extracted using a bottom-up “sublevel stoping” method (Bandeira Sublevel Mine, “BSL mine”) comprising 21.1Mt @1.25% Li₂O. Simultaneously, the secondary southeast orebody, comprising approximately 1.8Mt @1.05% Li₂O, is expected to be mined using “room-and-pillar” technique (Bandeira Room and Pillar, “BRP mine”).

The BSL mine has been planned with two declines, extending along a NE/SW mineralized trend spanning 1.0 km. It is divided into 12 panels, each measuring 55 meters, and consists of two sublevels.

The BRP mine features a single panel with approximate dimensions of 380 meters in length, 330 meters in width, and 10 meters in height. Access to the ore chamber will be provided through five cross-cuts originating from the southern decline.

The mineral processing is based on the fixed plant, structured around a two-stage crushing circuit, ore size classification, the implementation of an ore sorter for coarse and medium materials, and the utilization of DMS (Dense Media Separation) for coarse and medium materials.

The PEA Study resulted in an underground mine scenario processing 1.3Mtpa of ore over a 20 year mining life, with an average LOM annual production of 217,700t of high-quality spodumene concentrate at 5.5% Li₂O (“SC5.5”) equivalent (187,230 tpa SC5.5, in addition to 56,860 tpa of spodumene tails concentrate at 3% Li₂O, or “SC3”) after ramp up in the year 03.

The economics results of Bandeira PEA present Post-tax Net Present Value (“NPV”) 8% of \$1.6 billion, Post-tax Internal Rate of Return (“IRR”) of 121% and After-tax payback of 14 months. The Total capital expenditure (“CAPEX”) of \$233 million (including a 25% contingency), Pre-tax annual average free cash flow of \$243 million.

Mineral Resources that are not Mineral Reserves do not have demonstrated economic viability. The estimate of Mineral Resources may be materially affected by environmental, permitting, legal, title, socio-political, marketing, or other relevant issues.

1.24 RECOMMENDATIONS

Based on the positive nature of this PEA the primary recommendation is to continue the development of the Project through additional detailed investigations and higher confidence engineering studies. The aim being to complete a higher confidence engineering study as the next major project milestone.

The following recommendations are made with respect to future work on the Property. This work will be required for upgrading Bandeira's resources to Indicated and Measured category, and to advance next stage detailed engineering and economic studies. These are listed as separate phases, as increasing the confidence of the resources to Indicated or Measured category will be required prior to economic studies.

GE21 proposes the following recommendations for the continuous improvement of the Mineral Resource estimate:

- h) A 50x50m infill drilling program in domain of the indicate resource classification where will focus on resource delineation improvement.
- i) A 100x100m infill drilling program in domain of the inferred resource classification where will focus on resource delineation improvement.
- j) A density campaign to measure the density of drill holes cores by drying the samples in an oven, as well as waterproofing them. Compare the results with the methodology used in the current project procedure to check whether there is a bias in the results.
- k) Conduct an on-site density survey in the weathered zone.
- l) An updated mineral resource assessment is currently underway through the ongoing infill drilling programme.
- m) Detail Geotechnical analysis including a geotechnical oriented diamond drilling campaign and logging, including sampling collecting for tensile, compressive and shear strength tests.
- n) Perform supplementary geotechnical investigations of planned infrastructure sites including at waste pile areas; supplementary geochemical tests (ARD); large-scale waste rock and tailings co-disposal stockpile field test.
- o) To implement the hydrological and hydrogeological studies for the next phases of the project.

For the next stage, GE21 recommends the following trade-offs to be undertaken:

- p) It is suggested to conduct an underground dilution study to verify the suitability of the assumed dilution rate.
- q) Study the depth-specific moisture content of the material to ensure compliance with standards.
- r) Carry out a ventilation system study within the underground mining to ensure compliance with required standards for air quality, temperature, and airflow.
- s) To conduct a quotation for mining equipment including a full services contract for corrective and preventive maintenance services, including the supply of parts.

Environmental Studies, Permitting and Social/Community Impact:

- t) MGLIT will need to initiate the EIA process, by engaging with the appropriate federal and provincial authorities and engage in the process. Commencement and completion of the required permitting process will be dependent on timing and outcome of the EIA.

The Table 1.6 estimate a budget for the implementation of the recommendations.

Table 1.6 Planned Budget Recommendations.

| Recommended work | | Details | Estimated cost (US\$) |
|---|--|--|-----------------------|
| Additional work to upgrade to Indicated and Measured category | A 50x50m Infill Drilling Program | | ~\$50,000 |
| | A 100x100m Infill Drilling Program in domain of the Inferred Resource Classification | | ~\$3,000,000 |
| | A Density Campaign | | ~\$15,000 |
| | On-site Density Survey | | ~\$15,000 |
| | Updated Mineral Resources | Interpretation Modelling Reporting | ~\$60,000 |
| | Total Estimated Costs | | |
| Work to advance next stage higher level engineering study | Detail Geotechnical Analysis | | ~\$500,000 |
| | Perform Supplementary Geotechnical Investigations | | ~\$350,000 |
| | Environmental Studies | Commence baseline studies, stakeholder engagement, preliminary work for ESIA | ~\$500,000 |
| | Geotechnical Study | Drilling, sampling, analysis, and reporting | ~\$300,000 |
| | Hydrogeology and hydrology studies | Drilling, data gathering, modelling | ~\$1,000,000 |
| | Mining Studies (PFS) | | ~\$450,000 |
| | Infrastructure Studies | | ~\$160,000 |
| | Total Estimated Costs | | |
| GRAND TOTAL | | | ~\$6,400,000 |

2 INTRODUCTION AND TERMS OF REFERENCE

GE21 Consultoria Mineral Ltda. (“GE21”) was engaged by Lithium Ionic Corp. to prepare an Independent Technical Report (“ITR”) containing a NI 43-101 Technical Report (The “Report”) on Lithium Ionic’s Bandeira deposit located in Minas Gerais State, Brazil (“Project”). This report titled “Bandeira Project, Minas Gerais State, Brazil - Mineral Resource Estimate and Preliminary Economic Assessment” outlines all relevant data about the Bandeira Project (“The Project”). They are technical information and data related to the drilling program and the status of the current Lithium Mineral Resources contained in the spodumene-bearing pegmatites.

This Report and the estimates herein comply with the requirements of the Canadian Securities Administrators’ National Instrument 43-101 – Standard of Disclosure for Mineral Projects (“NI 43-101”) and Form 43-101F1 – Technical Report (“Form 43-101F1”).

The Project is located between Araçuaí and Itinga in Brazil’s “Lithium Valley” - a complex rock lithium district. The Preliminary Economic Assessment (PEA) includes only the Bandeira lithium deposits.

Lithium Ionic Corp. is headquartered in Toronto, Ontario (36 Lombard Street, Floor 4, Toronto, ON, Canada, M5C 2X3) with management offices in Nova Lima (Alameda Oscar Niemeyer, 1033 – sls 133/134 Vila da Serra – Nova Lima – Minas Gerais- CEP 34006-065 – Brazil) and Araçuaí (Recife Street 96, Araçuaí, Minas Gerais – CEP 39600-000, Brazil). It is a publicly traded Canadian exploration and development company listed on the TSX Venture Exchange (“TSXV”). The Company is acquiring, exploring, and developing mineral properties, primarily focusing on exploring in Brazil. Exploration is conducted through the Company’s wholly owned Brazilian subsidiary, MGLIT Empreendimentos Ltda. (“MGLIT”) and Neolit Minerals Participações Ltda. (“Neolit”).

The effective date of this report is August 30, 2023, and the information in this report, including the reported resource estimates, are all contained within a conceptual underground mineable MRE. The Report supports the disclosure by Lithium Ionic in the news release outlining the current MRE dated October 19, 2023.

2.1 Qualifications, Experience, and Independence

The Qualified Person responsible for the Mineral Resource Estimation, carried out at the Preliminary Economic Assessment level, is Geologist Carlos José Evangelista Silva, who has more than 15 years of relevant experience in Geology Exploration and Mineral Resource Estimation. Mr Silva is a full-time employee of GE21 Consultoria Mineral. He has considerable experience dealing with commodities, such as iron ore, lithium, and gold. Mr. Silva is a member of the Australian Institute of Geoscientists (MAIG).

The Qualified Person partially responsible for the mining studies carried out in the Preliminary Economic Assessment level is Mining Engineer Guilherme Gomides Ferreira. Mr. Gomides has 16 years of experience in the field of Mineral Reserve Estimate. Mr. Gomides is a full-time employee and Mining Manager in GE21 Consultoria Mineral. He possesses considerable experience dealing with various commodities. Mr. Gomides is a member of the Australian Institute of Geoscientists (MAIG).

The Qualified Person responsible for the environmental assessment carried out in the Preliminary Economic Assessment level is Ms. Branca Horta de Almeida Abrantes. Branca has 19 years of experience in the environmental sector. She works in the Environment area, from participating in the preparation of environmental studies to environmental management, as well as strategic studies. Throughout her professional career, she acquired experience in the industrial, mining, energy, and sanitation sectors. Ms. Branca Abrantes is a member of the Australian Institute of Geoscientists (MAIG).

The Qualified Person responsible for this report's content on issues related to Mineral Processing and Metallurgical Tests, and Recovery Methods is Paulo Bergman (FAusIMM, B.Sc.), a Mining Engineer of GE21 Consultoria Mineral, who has more than 40 years of experience in mining projects. Mr. Bergman is a Fellow of the Australasian Institute of Mining and Metallurgy (FAusIMM).

Porfirio Cabaleiro Rodriguez (FAIG, B.Sc.) is the reviewer of this technical report. Mr. Rodriguez has at least 45 years of experience in all aspects of mining project evaluation, from initial exploration to bankable feasibility studies. He is a senior mining engineer and managing director of GE21 Mineral Consulting.

Each of the authors of this report has the required qualifications, experience, competence, and independence to be considered a "Qualified Person," as defined by NI 43-101.

Neither GE21 nor the authors of this report have or have had, any material interest vested in Lithium Ionic Corp. or any of its related entities. GE21's relationship with Lithium Ionic is strictly professional, consistent with that held between a client and an independent consultant. This report was prepared in exchange for payment based on fees stipulated in a commercial agreement. Payment of these fees is not dependent on the results of this Report.

The Table 2.1 presents the QPs Matrix of responsibility.

Table 2.1: Presents the QPs Matrix of Responsibility.

| Company | Professional | Site Visit | Responsibility |
|--|----------------------------------|---------------------------|--|
| GE21 | Carlos José Evangelista Silva | September 13 and 14, 2023 | Items 2 to 12, 14 and partial responsibility on 1, 25, 26 and 27. |
| GE21 | Guilherme Gomides Ferreira | - | Items 15, 16, 19, 21 to 24 and partial responsibility on 1, 18, 25, 26 and 27. |
| GE21 | Paulo Bergman | - | Items 13, 17 and partial responsibility on 18, 25, 26 and 27. |
| GE21 | Branca Horta de Almeida Abrantes | - | Item 20 and partial responsibility on 1, 25, 26 and 27. |
| GE21 | Porfírio Cabaleiro Rodriguez | - | Report Peer Reviewer |
| All Qualified persons are responsible for the corresponding sections within Items related to the preceding Items of this Technical Report. | | | |

2.2 Effective Date

The current MRE and PEA effective date is August 30, 2023.

2.3 Units of Measure

Unless otherwise stated, the units of measurement in this Report are all metrics in the International System of Units (“SI”). Unless stated otherwise, all monetary units are expressed in United States Dollars (“US\$”). The UTM projection, Zone 24 South, SIRGAS 2000 datum, was adopted as a spatial reference.

3 RELIANCE ON OTHER EXPERTS

The Authors have not independently verified ownership or mineral title beyond the information that Lithium Ionic has provided. The Property description presented in this Report is not intended to represent a legal or any other opinion as to title.

Verification of information concerning Property status and ownership, which are presented in Item 4 below, has been provided to the Author by Carlos H C Costa, VP Exploration for Lithium Ionic by way of an Email on July 14, 2023. The Author only preliminary reviewed the land tenure and has not independently verified the legal status or ownership of the Property or any underlying agreements or obligations attached to ownership of the Property. However, the Author has no reason to doubt that the title situation is other than what is presented in this technical report (Item 4). The Author is not qualified to express any legal opinion concerning Property titles or current ownership.

4 PROPERTY DESCRIPTION AND LOCATION

4.1 Location

The Project is situated in the northeastern region of Minas Gerais State, Brazil, within the Jequitinhonha Valley area, approximately 600 km northeast of Belo Horizonte. It is positioned roughly 75 km south of the town of Salinas (population: approx. 42,000) and about 25 km east of Aracuaí (population: approx. 40,000), accessible via major paved roads (Figure 4.1)

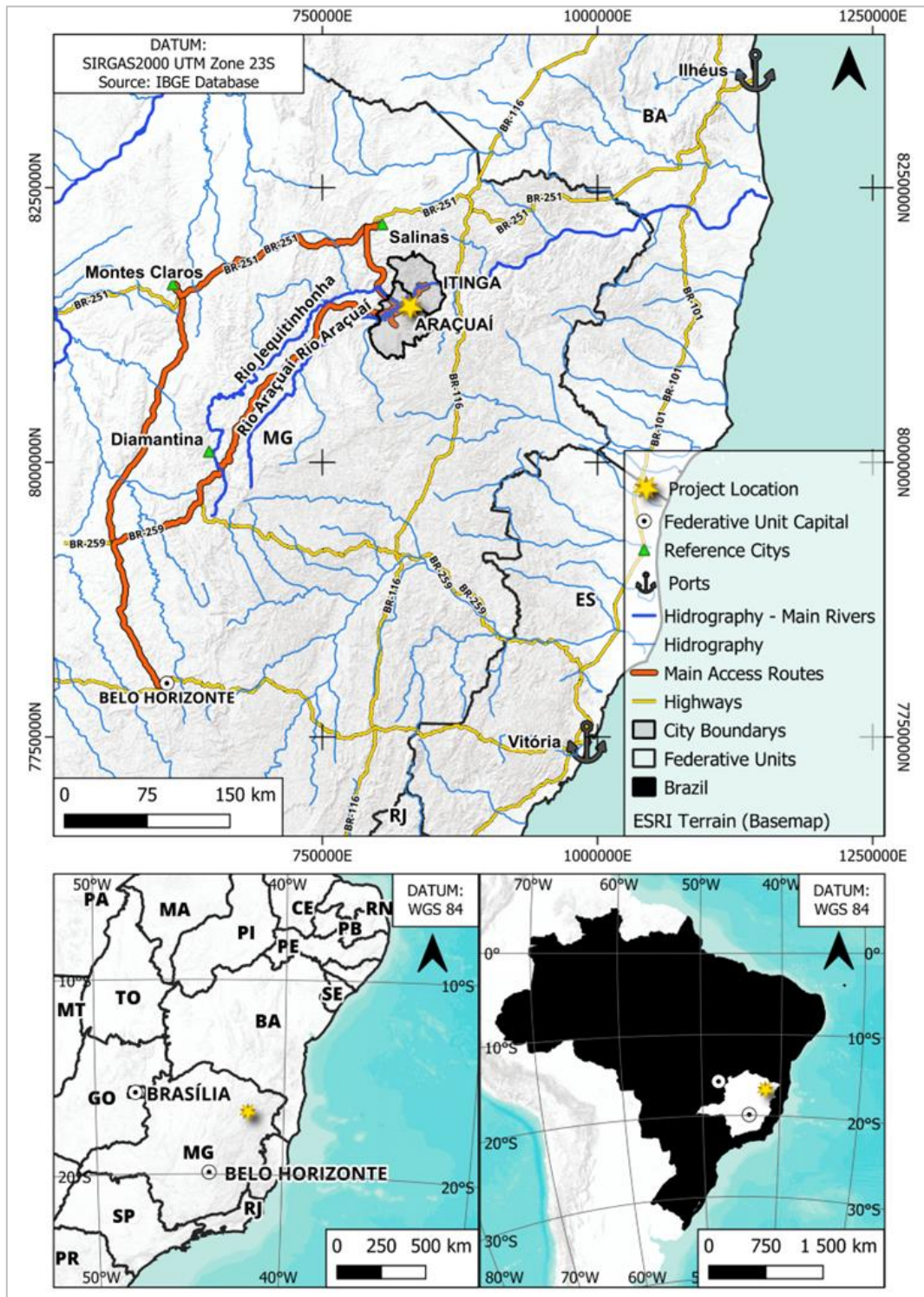


Figure 4.1: Project Localization.

This report will primarily focus on mineral resource estimates for one of the company's mineral exploration targets, namely, *Bandeira*. That target is located at Latitude 16° 47' S and Longitude 41° 53' W in the SIRGAS 2000 map projection. The SIRGAS 2000 UTM Zone 24S coordinates are 190,117 m E 8,141,940 m N.

4.2 Mineral Tenure

The legal framework for the development and use of mineral resources in Brazil was established by the Brazilian Federal Constitution, which was enacted on October 5, 1988 (the Brazilian Constitution) and the Brazilian Mining Code, which was enacted on January 29, 1940 (Decree-law 1985/40, later modified by Decree-law 227, of February 29, 1967). The National Mining Agency (Agência Nacional de Mineração, or ANM) oversees the Mining Code. There are two main legal regimes under the Mining Code regulating Exploration and Mining in Brazil: Exploration Authorization (“Autorização de Pesquisa”) and Mining Concession (“Concessão de Lavra”).

According to the Brazilian Constitution, all mineral resources in Brazil are the property of the Federal Government. The Brazilian Constitution also guarantees mining companies the entire property of the mineral products mined under their respective concessions. Mineral Rights come under the jurisdiction of the Federal Government, and mining legislation is enacted at the Federal level only. To apply for and acquire mineral rights, a company must be incorporated under Brazilian law, have its management domiciled within Brazil, and have its head office and administration in Brazil.

There are no restrictions on foreign investment in the Brazilian mining industry, except for mining companies that operate or hold mineral rights within a 150 km-wide strip of land parallel to the Brazilian terrestrial borders. In this instance, the equity interests of such companies must be majority Brazilian-owned. Exploration and mining activities in the border zone are regulated by the Brazilian Mining Code and supporting legislation.

Applications for an Exploration Authorization (“EA”) are made to the ANM and are available to any company incorporated under Brazilian law and maintaining a main office and administration in Brazil. EAs are granted following the submission of required documentation by a legally qualified Geologist or Mining Engineer, including an exploration plan and evidence of funds or financing for the investment forecast in the exploration plan. An annual fee per hectare, ranging from approximately US\$0.50/ha to US\$ 1.00/ha, is paid by the holder of the EA to the ANM, and a final report of the exploration work must be submitted by the end of the three years. No exploration work is permitted during the review period of a formal EA application.

EAs are valid for a maximum of three years, with a maximum extension equal to the initial period, issued at the discretion of the ANM. Annual fees per hectare increase by 50% during the extension period. After submitting a Final Exploration Report, the EA holder may request a mining concession. Mining concessions are granted by the Brazilian Ministry of Mines and Energy, have no set expiration date, and are valid until the total depletion of mineral resources. Mining concessions remain in good standing subject to submission of annual production reports and payments of royalties (CEFEM), which can be between 1% and 3%, to the federal government. CEFEM is 2% for Lithium in Brazil.

Areas where the maximum extension of an EA has expired, and a company has failed to submit a positive Final Exploration Report and mining concession request are designated with a status of “Public Offer.” Before Decree nº 9.406/2018, the public offer is auctioned. It is awarded to a company based on the best technical proposal regarding exploration activities and previous knowledge of the specific mineral right. The winning company bid is based on which company has offered the most cash in an auction procedure.

The project information and temporal evaluation connect current Brazilian regulations governing exploration and mining permits.

4.3 Mineral Tenure Status

Lithium Ionic's Project's encompass 30 claims, as detailed in Table 4.1 and Figure 4.2. These claims are split into two regions: the Itinga Project (18 claims) and the Salinas Project (12 Claims). This report will only approach the work accomplished in claim number 832439/2009 (Bandeira target), as shown in Figure 4.2.

The Exploration Permit area of Bandeira target is mostly in Itinga municipality, with a minor part in the Araçuaí municipality. The cities and their boundaries concerning the two project locations are shown in Figure 4.3.

The QPs have not reviewed the mineral tenure nor independently verified the legal status, ownership of the Project area, underlying property agreements or permits. The QPs have entirely relied upon and disclaimed responsibility for the information the Lithium Ionic management team via e-mails. This information is used in Item 4 of the report and supports the Mineral Resource estimate in Item 14.

The Bandeira target property area ("Bandeira Property") comprises one tenement covering approximately 6,928 ha (Table 4.1).

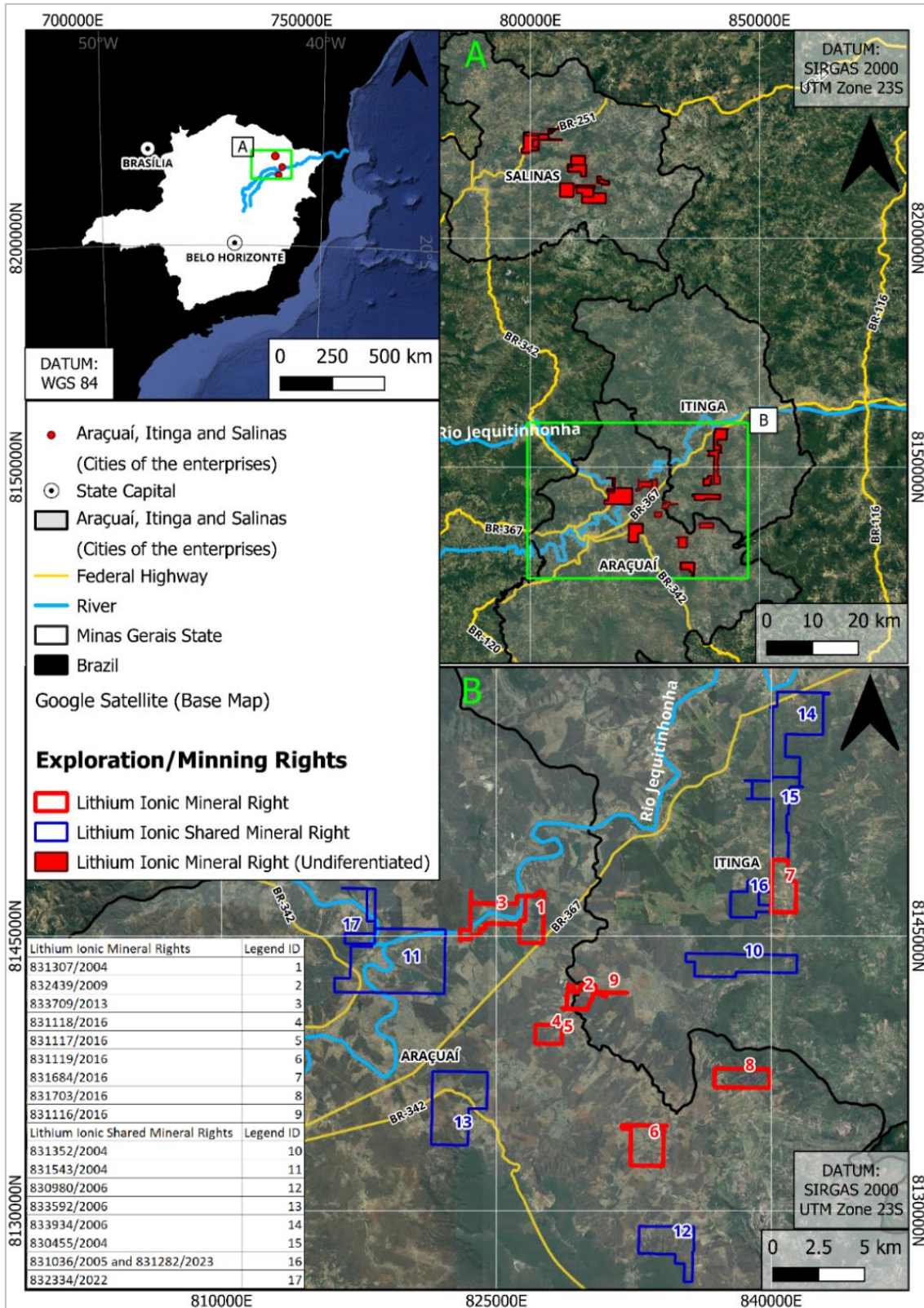


Figure 4.2: Lithium Ionic Tenements Map.

Source: Lithium Ionic, IBGE and ANM.

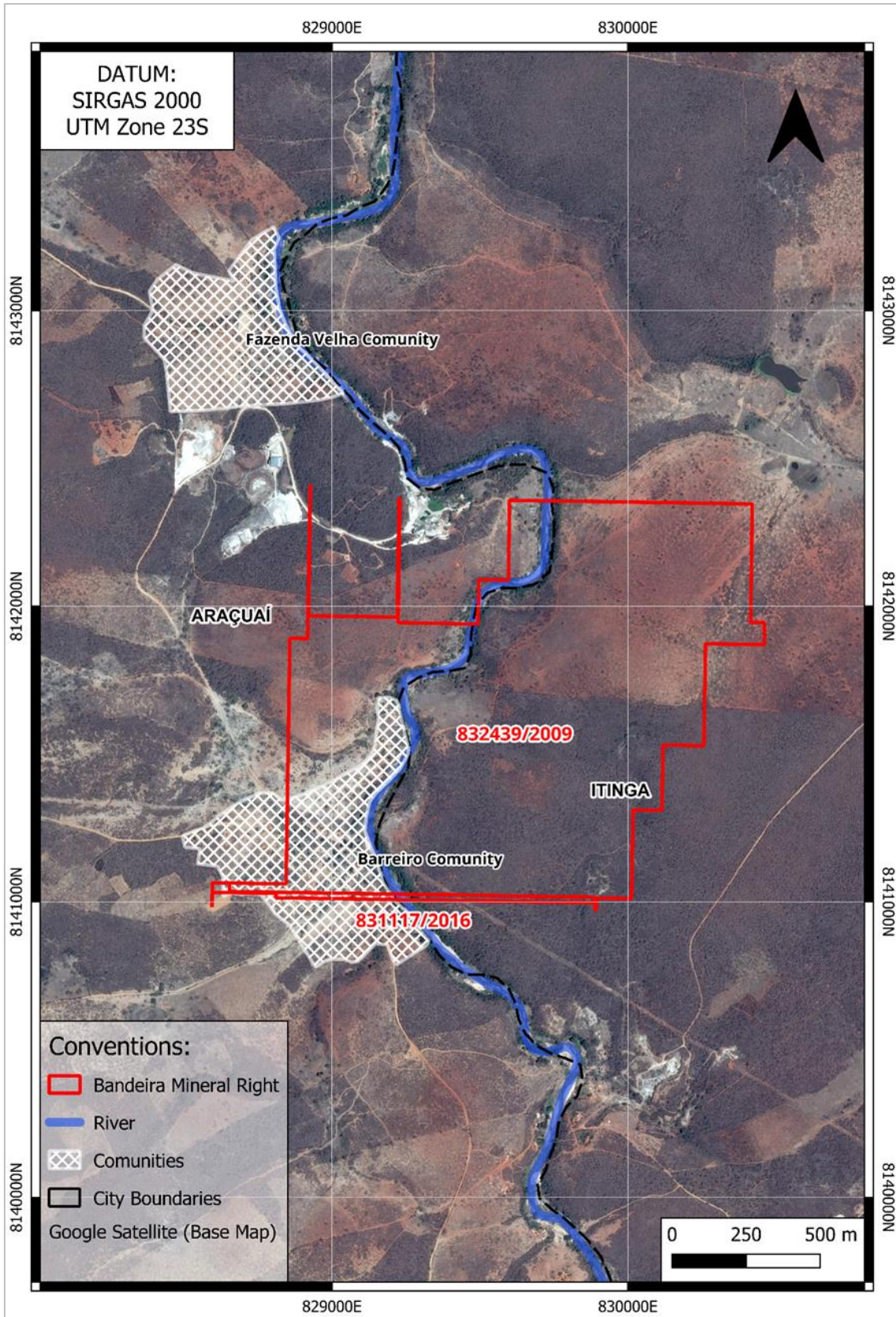


Figure 4.3: Bandeira Project Tenements Map.

Source: Lithium Ionic, IBGE and ANM.

Table 4.1: Lithium Ionic Land Tenure Information.

| Claim Number (ANM) | Area (ha) | Status | Name |
|--------------------|-----------------|----------------------------|----------------------------|
| 832.439/2009 | 156.77 | Permit Extension | MGLIT EMPREENDIMENTOS LTDA |
| 831.684/2016 | 325.66 | Permit Extension | MGLIT EMPREENDIMENTOS LTDA |
| 831.118/2016 | 146.88 | Permit Extension | MGLIT EMPREENDIMENTOS LTDA |
| 831.703/2016 | 305.87 | Permit Extension | MGLIT EMPREENDIMENTOS LTDA |
| 831.117/2016 | 2.27 | Permit Extension | MGLIT EMPREENDIMENTOS LTDA |
| 831.119/2016 | 401.65 | Permit Extension | MGLIT EMPREENDIMENTOS LTDA |
| 831.116/2016 | 15.79 | Permit Extension | MGLIT EMPREENDIMENTOS LTDA |
| 831.282/2023 | 315.68 | Application for Concession | MGLIT EMPREENDIMENTOS LTDA |
| 833.709/2013 | 414.96 | Approval Pending | MGLIT EMPREENDIMENTOS LTDA |
| 831.307/2004 | 300.19 | Approval Pending | MGLIT EMPREENDIMENTOS LTDA |
| TOTAL | 2 385.72 | | |
| 831.036/2005 | 48.70 | Application for Concession | MINERAÇÃO BORGES LTDA |
| 831.352/2004 | 622.64 | Approval Pending | MINERAÇÃO BORGES LTDA |
| 830.980/2006 | 540.57 | Application for Concession | MINERAÇÃO BORGES LTDA |
| TOTAL | 1 211.91 | | |
| 831.543/2004 | 1 738.87 | Approval Pending | EXOTIC MINERAÇÃO LTDA |
| 833.934/2006 | 879.54 | Approval Pending | EXOTIC MINERAÇÃO LTDA |
| 830.455/2004 | 523.18 | Approval Pending | EXOTIC MINERAÇÃO LTDA |
| TOTAL | 3 141.59 | | |
| 833.592/2006 | 1 000.00 | Approval Pending | CLESIO A G MINERAÇÃO |
| TOTAL | 1 000.00 | | |
| 830.986/2016 | 183.55 | Extension submitted | FERREIRA SANTOS |
| 830.929/2017 | 858.65 | Approval Pending | SALIT MINERAÇÃO LTDA |
| 830.926/2017 | 594.09 | Approval Pending | SALIT MINERAÇÃO LTDA |
| 830.925/2017 | 643.64 | Approval Pending | SALIT MINERAÇÃO LTDA |
| 830.970/2022 | 110.92 | Application | NEOLIT MINERALS LTDA |
| 830.972/2022 | 305.64 | Application | NEOLIT MINERALS LTDA |
| 831.200/2021 | 990.16 | Permit | FOLIUM EMPREENDIMENTOS |
| 830.833/2001 | 662.56 | Application for Concession | JOSÉ SILVA LAPA |
| 830.927/2017 | 912.05 | Approval Pending | SALIT MINERAÇÃO LTDA |
| 831.072/2022 | 727.87 | Permit | NEOLIT MINERALS LTDA |
| 832.361/2023 | 24.69 | Application | NEOLIT MINERALS LTDA |
| 832.362/2023 | 24.09 | Application | NEOLIT MINERALS LTDA |
| TOTAL | 6 037.91 | | |
| 832.347/2022 | 599.88 | Permit | FOLIUM EMPREENDIMENTOS |
| 832.334/2022 | 169.39 | Permit | FOLIUM EMPREENDIMENTOS |
| TOTAL | 769.27 | | |

Source: Lithium Ionic.

4.4 Property Surface Rights

The owner of an Exploration Authorization (“EA”) is guaranteed, by law, access to perform exploration fieldwork provided adequate compensation is paid to third-party landowners, and the owner of the EA accepts all environmental liabilities resulting from the exploration work.

According to Lithium Ionic Corp., agreements associated with the rights of the Bandeira Project are in place. Under the legislation of the Brazil Mining Code, mineral resources belong to the State and are granted under mineral licenses issued by the ANM. Surface rights belong to the landowner, who, under the Mining Code, are guaranteed remuneration that may arise from a mineral deposit being developed on their property. This participation is usually negotiated between the mineral rights owner and the landowner, with the remuneration being a small percentage of a production royalty or a monthly rental fee.

If an agreement is not reached, there is legislation whereby the Government will arbitrate a settlement agreement to ensure that exploration and development of the mineral rights can advance. Under the legislation, a surface right owner does not have the legal right to inhibit the exploration or development of mineral resources in Brazil.

Lithium Ionic has acquired some of the lands inside the Bandeira Mineral Rights area. Table 4.2 presents the current surface rights acquisition status. Table 4.3 and Figure 4.4 give the surface owners list and their respective land inside the Bandeira Mineral Right.

Table 4.2: Acquisition Status.

| Property Name | Former Owner | Negotiation Status |
|-------------------------------------|--|---|
| Fazenda Piauí - Barreiro – Part 01 | Ilton Lemes Pereira | Public Deed executed |
| Fazenda Piauí - Boa Vista – Part 01 | José Martins de Oliveira | Public Deed executed |
| Fazenda Piauí - Boa Vista – Part 02 | Demóstenes Soares Vieira | Public Deed executed |
| Fazenda Brejos | Agropecuária Internacional Ltda. | Sales Contract signed – Public Deed pending |
| - | Ilson Aparecido Pereira Moreira and others | Sales Contract in negotiation |

Table 4.3: Surface Owners.

| Surface Ownership | Situation | Area (ha) |
|--|------------------------|-----------|
| Acquired by Lithium Ionic | Acquired | 43.036 |
| Acquired by Lithium Ionic | Acquired | 2.624 |
| Acquired by Lithium Ionic | Acquired | 0.279 |
| Acquisition under negotiation | Under acquisition | 53.954 |
| Ilson Aparecido Pereira Moreira and others | Owned by Third Parties | 16.948 |
| Demóstenes Soares Vieira | Owned by Third Parties | 0.268 |
| Orlando Luiz Santos | Owned by Third Parties | 10.813 |
| Silvina Almeida Santos | Owned by Third Parties | 3.703 |
| Espólio de Laurita Costa Almeida | Owned by Third Parties | 6.144 |
| Espólio de Pedro Almeida Costa | Owned by Third Parties | 0.758 |
| Espólio de Elcino Almeida Santos | Owned by Third Parties | 0.265 |
| Gilda Almeida Santos | Owned by Third Parties | 0.398 |
| Espólio de Clemente Almeida Santos | Owned by Third Parties | 0.763 |
| Valdim Almeida Santos | Owned by Third Parties | 2.886 |
| Geraldo Gonçalves Jardim | Owned by Third Parties | 0.502 |
| Demóstenes Soares Vieira | Owned by Third Parties | 0.034 |
| Demóstenes Soares Vieira | Owned by Third Parties | 0.033 |

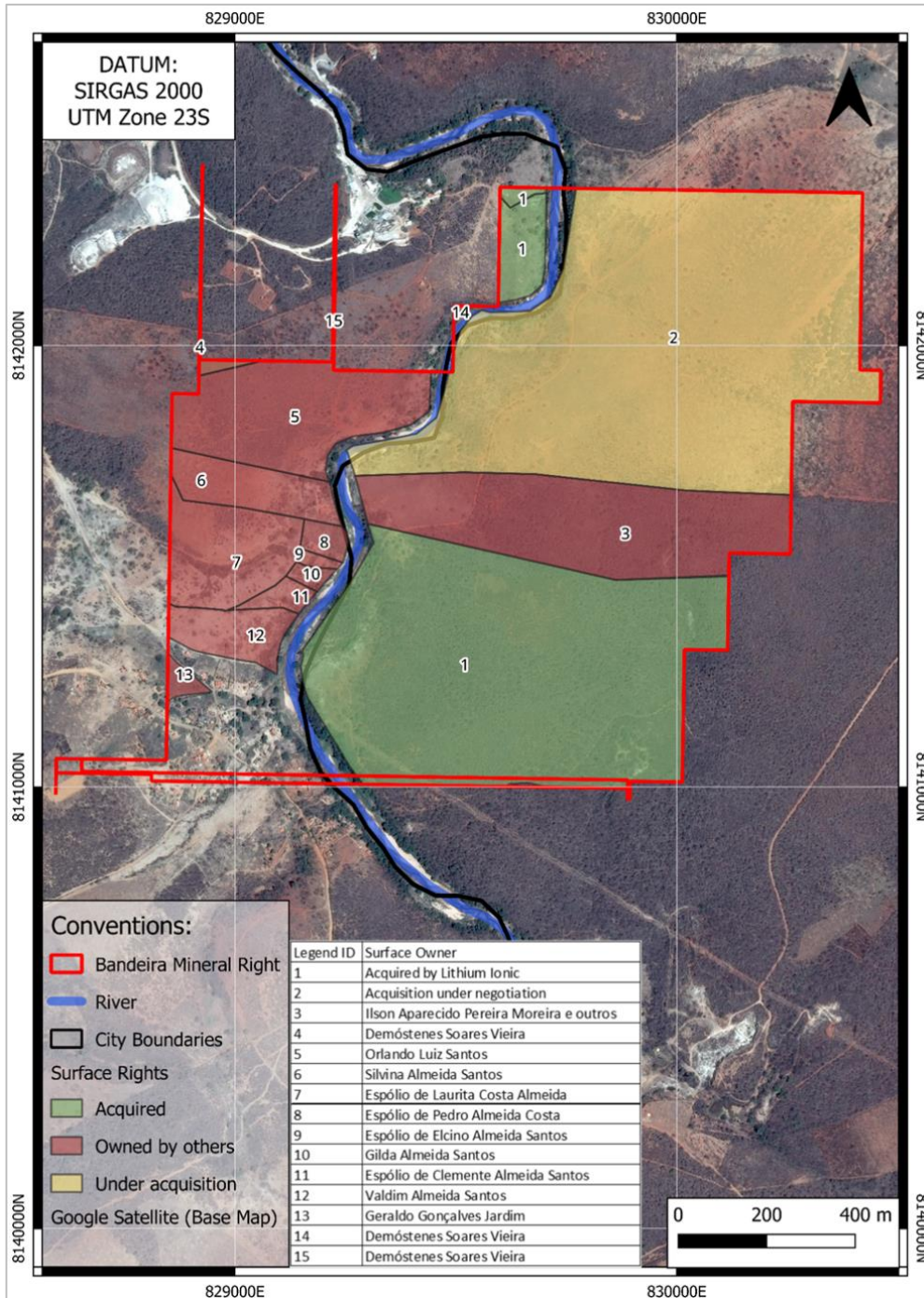


Figure 4.4: Bandeira Project Surface Rights Map.

Source: Lithium Ionic, IBGE and ANM.

4.5 Permits and Authorization

The Project currently entails only Exploration Permits; no other operational permits exist.

4.6 Environmental Considerations

The Project currently entails only Exploration Permits; no other operational permits exist.

4.7 Other Significant Factors and Risks

Neither the Authors of this Report nor Lithium Ionic Corp. are aware of any other significant factors or risks that may affect access, title, or the right or ability to perform work on the Property.

5 ACCESSIBILITY, CLIMATE, LOCAL RESOURCES, INFRASTRUCTURE AND PHYSIOGRAPHY

5.1 Accessibility

The Project is in northeastern Minas Gerais State, in the Municipalities of Itinga and Araçuaí, approximately 75 km south of Salinas and 600 km northeast of Belo Horizonte.

A public and private road network well serves the Project because of its proximity to National Highway BR-251 and BR-116. The Project is accessible year-round by a network of arterial and backcountry service roads.

National Highway BR-116 and BR-262 accesses the Port of Vitoria in the State of Espírito Santo, approximately 850 km from the Project site. This port could represent a potential export exit for spodumene production from the Project. The National Highways BR-116 and BR-415 access Ilhéus Port, which is 540 km from the project, and they are an option as a shipping port (Figure 4.1).

5.2 Climate

A semi-arid climate with high temperatures year-round characterizes the region. It has a temperature mean of 24.5 °C and a low annual average rainfall of 450 mm. Severe drought occurs from May to September, and torrential and sporadic rains occur from November to April. The average summer temperature high is 33 °C, and the average winter low is 18 °C. Exploration activities are currently conducted year-round. It is expected that any future mining activities will also be year-round.

5.3 Local Resources and Infrastructure

A network of arterial and backcountry service roads accesses the Project area. The Company has established an on-site core logging and processing facility at the Lithium Ionic Project in Araçuaí. Two significant communities are nearby, with a population of 40,000 or more.

Salinas is located approximately 75 km NNW of the town of Araçuaí (population: ~40,000), both connected by major sealed roads and serviced by the local municipal airports and by mobile phone network from the principal Brazilian service providers. Montes Claros is the closest major domestic airport, 230 km west of Salinas. The state of Minas Gerais is well-serviced by infrastructure, roads, hydroelectric power, and water. Also, the neighboring states of Espírito Santo and Bahia host the ports of Vitoria and Ilhéus, respectively. (Figure 4.1).

5.4 Physiography

The Project topography in the project region consists of gently rolling hills with less than 500 m difference in elevation. The hilltops are covered with a veneer of alluvium up to 5 m thick, which is not present on the hill slopes where bedrock is frequently exposed.

The Project area is characterized by thick thorn scrub and trees of medium height - except where it has been cleared for agriculture. The natural vegetation on the hilltops is typical of savannah grassland.

The average annual precipitation is moderate compared to other regions of Brazil. The indicated annual average measurements at the Araçuaí station are 707 mm, while the evapotranspiration averages about 2,000 mm, a deficit of 1,345 mm/year. This climatic condition is strongly semi-arid in characterization.

The low precipitation can result in better geotechnical stability conditions than in tropical regions, with rainy summers (due to the lower soil erosion of the rain). In this sense, this natural stability condition is a positive evaluation for the overall risk management of the Bandeira sites. However, water scarcity may require robust water management and planning for water use for the Bandeira.

6 HISTORY

The Bandeira site and all other Mineral Tenures have not had any drilling activity before 2022.

6.1 Historical Exploration

All works in the Bandeira target started in 2022 and do not have historical exploration data.

6.2 Historical Mineral Resource Estimates

Lithium Ionic Corp. and SGS Geological Services (SGS) released a MRE on August 10, 2023; the effective date of this MRE was June 24, 2023. From June until September of 2023, Lithium Ionic has substantially increased the drilling in Bandeira.

This MRE is presented in Table 6.1 and includes an in-pit and an underground (below pit) Mineral Resources (estimated from the bottom of the pit). Highlights of the Mineral Resource Estimate are as follows:

The Bandeira in-pit Mineral Resource includes, at a base case cut-off grade of 0.5 % Li₂O, 1.14 Mt grade 1.43 % Li₂O, in the Measured category, 3.1 Mt grade 1.33 % Li₂O, in the Indicated category and 5.9 Mt grade 1.40 % Li₂O, in the Inferred category.

The Bandeira below-pit Mineral Resource includes, at a base case cut-off grade of 0.8 % Li₂O, 3.0 Kt grade 1.1 % Li₂O, in the Measured category, 0.35 Mt grade 1.26 % Li₂O, in the Indicated category and 5.5 Mt grade 1.147 % Li₂O, in the Inferred category.

Table 6.1: Itinga Property; Bandeira and Outro Lado Deposits In-Pit and Underground (below-pit) Mineral Resource Estimate, June 24, 2023.

| <u>Deposit/Cut-Off Grade</u> | <u>Category</u> | <u>Resource (Mt)</u> | <u>Grade (% Li₂O)</u> | <u>Contained LCE (t)</u> |
|---|-----------------------------|----------------------|----------------------------------|--------------------------|
| Bandeira Open-Pit (0.5% Li ₂ O) | Measured | 1.14 | 1.43 | 40,000 |
| | Indicated | 3.11 | 1.33 | 102,000 |
| | Measured + Indicated | 4.24 | 1.36 | 142,000 |
| | Inferred | 5.92 | 1.40 | 205,000 |
| Bandeira Underground (0.8% Li ₂ O) | Measured | 0.003 | 1.10 | 0 |
| | Indicated | 0.35 | 1.26 | 11,000 |
| | Measured + Indicated | 0.36 | 1.26 | 11,000 |
| | Inferred | 5.53 | 1.47 | 201,000 |
| TOTAL | Measured | 1,14 | 1.43 | 40,000 |
| | Indicated | 3,46 | 1.32 | 113,000 |
| | Measured + Indicated | 4,60 | 1.35 | 153,000 |
| | Inferred | 11.45 | 1.43 | 406,000 |

Notes:

1. The effective date of the MRE is June 24, 2023.
2. The classification of the current Mineral Resource Estimate into Measured, Indicated and Inferred is consistent with the current 2014 CIM Definition Standards - For Mineral Resources and Mineral Reserves.
3. All figures are rounded to reflect the relative accuracy of the estimate, and numbers may not be added due to rounding.
4. All Resources are constrained by continuous 3D wireframe models (constraining volumes) and are considered to have reasonable prospects for eventual economic extraction.
5. Mineral resources which are not mineral reserves do not have demonstrated economic viability. An Inferred Mineral Resource has a lower level of confidence than that applying to an Indicated Mineral Resource and

- must not be converted to a Mineral Reserve. It is reasonably expected that the majority of Inferred Mineral Resources could be upgraded to Indicated Mineral Resources with continued exploration.
6. The pit optimization results are used solely to test the “reasonable prospects for economic extraction” by an open pit and do not represent an attempt to estimate mineral reserves. There are no mineral reserves on the Project. The results are used as a guide to assist in the preparation of a Mineral Resource statement and to select an appropriate resource reporting cut-off grade.
 7. It is envisioned that parts of the Bandeira deposit may be mined using open pit mining methods. In-pit mineral resources are reported at a cut-off grade of 0.5% Li_2O within a conceptual pit shell,
 8. The results from the pit optimization are used solely for the purpose of testing the “reasonable prospects for economic extraction” by an open pit and do not represent an attempt to estimate mineral reserves. There are no mineral reserves on the Property. The results are used as a guide to assist in the preparation of a Mineral Resource statement and to select an appropriate resource reporting cut-off grade.
 9. It is envisioned that parts of the Bandeira deposit may be mined using underground mining methods. Underground (below-pit) Mineral Resources are estimated from the bottom of the pit (base of transition mineralization) and are reported at a base case cut-off grade of 0.8% Li_2O . The underground Mineral Resource grade blocks were quantified above the base case cut-off grade, below the constraining pit shell and within the constraining mineralized wireframes.
 10. Based on the size, shape, location and orientation of the Bandeira and Outro Lado deposit, it is envisioned that the deposit may be mined using low-cost underground bulk mining methods.
 11. Bulk density values were determined based on physical test work from each deposit model and waste model.
 12. The pit optimization and in-pit base case cut-off grade of 0.5% Li_2O considers a mining cost of US\$2.50/t rock and processing, treatment and refining, transportation and G&A cost of US\$17.00/t mineralized material, an overall pit slope of 60°. The below-pit base case cut-off grade of 0.8% Li_2O considers a mining cost of US\$60.00/t rock and processing, treatment and refining, transportation and G&A cost of US\$17.00/t mineralized material.
 13. The estimate of Mineral Resources may be materially affected by environmental, permitting, legal, title, taxation, socio-political, marketing, or other relevant issues.

7 GEOLOGICAL SETTING AND MINERALIZATION

The Bandeira Project lies in the Middle Jequitinhonha River valley, northeastern Minas Gerais State, currently known as the Lithium Valley of Brazil. The region is part of the Eastern Brazilian Pegmatite Province (EBPP), one of the largest pegmatite provinces around the world with c. 150,000 km² (cf. synthesis and references in Pedrosa-Soares et al., 2011, 2023).

The EBPP resulted from the magmatic and tectono-metamorphic events that formed the Araçuaí Orogen from the Early Ediacaran (ca. 630 Ma) to the Late Cambrian (ca. 490 Ma). The major EBPP pegmatite populations found within the Araçuaí Orogen have been grouped into twelve pegmatite districts that include residual pegmatites (representing late silicate melts released by fractional crystallization of parent granites) and/or anatectic pegmatites (formed directly from partial melting of country rocks). Among them, the Araçuaí Pegmatite District includes hundreds of residual pegmatites of distinct subclasses, types, and sub-types (B, Be, Cs, Li, Sn, Ta) of the rare-element class.

They comprise two main groups of rare-element pegmatites:

- i* the generally thick (up to 100 m), zoned, complex LCT (Lithium-Cesium-Tantalum) pegmatites with several lithium minerals (e.g., elbaite, lepidolite, Li-phosphates, petalite and/or spodumene) and other rare-element minerals (e.g., beryl, Bi-minerals, cassiterite, pollucite, schorlite, Ta-minerals), displaying roughly concentric to irregularly-shaped primary zones (marginal, graphic or wall, and intermediate zones, and quartz cores) cut by albite-bearing replacement bodies and fracture fillings with gem-bearing pockets;
- ii* the relatively thinner, non-zoned to poorly zoned, spodumene-rich pegmatites (SRP) with rather simple mineralogical assemblages that include spodumene (up to 35 vol%), albite, perthite, quartz, and muscovite (together forming up to 90-95 vol%), and accessory minerals, such as cookeite, Li-phosphates, petalite, cassiterite, Nb-Ta oxides, graphite, Fe-Mn oxides, and zabuyelita.

Both LCT pegmatites and SRP bodies commonly show unidirectional solidification textures outlined by minerals (e.g., mica, spodumene, tourmaline) oriented roughly orthogonal to the contacts with the host rocks (or to any other lower temperature surface inside the pegmatite, such as host rock xenoliths).

The rare-element pegmatites of the Araçuaí District are related to granitic intrusions, mostly composed of peraluminous (S-type), sub-alkaline to alkaline, muscovite-bearing leucogranites with pegmatoid cupolas, of the Cambrian (535-500 Ma) post-collisional (post-tectonic) G4 supersuite of the Araçuaí Orogen.

Located in the central part of the Araçuaí Pegmatite District, the Itinga Pegmatite Field contains the most important lithium deposits of Brazil since the 1950's, both in terms of economic resources and geological potential. As with other lithium-rich pegmatite populations worldwide, the favorable geological conditions for the outstanding abundance of both SRP and LCT pegmatites in the Itinga Field are given by: i) the relatively low-pressure and high-temperature regimes of the regional and contact metamorphisms, recorded by the dominant country rocks (quartz-mica schists with andalusite and/or cordierite and/or sillimanite); and ii) the profusion of two-mica granite intrusions with pegmatoid cupolas emplaced in relatively shallow crustal levels. The Itinga Pegmatite Field includes the spodumene mines and deposits of CBL (Companhia Brasileira de Lítio) and Sigma Lithium, as well as Lithium Ionic's properties of its Itinga Project, such as the Bandeira spodumene deposit.

The lithium ore bodies exploited, since the early 1990's, in the CBL's underground mine display a closely spaced swarm of relatively narrow (6 m thick on average) but long (up to 700 m along strike) non-zoned spodumene-rich pegmatites. In the Sigma Lithium properties, where several large spodumene-rich pegmatites are found (e.g., Barreiro, Murial, and Xuxa), an open pit mine is currently being developed on the Xuxa SRP deposit (15 m thick x 1800 m long x 500 m). Regardless of their sizes, most pegmatites of the Itinga Field are (sub-)parallel to the prominent NE-SW structural trend outlined by the regional ductile foliation (the schistosity S1: NE strike /

NW dip) and late spaced cleavage (S2: NE strike / SE dip). However, flat-lying and high-angle dip joint systems can also host some lithium-mineralized pegmatites.

Also following the regional NE-SW structural trend, the Bandeira deposit comprises NE-striking swarms of spodumene-rich pegmatites (SRP), including concordant SRP bodies, hosted by the NW-dipping schistosity (S1), and discordant SRP bodies, emplaced along a SE-dipping fracture system (the S2 spaced cleavage), as well as a few mineralized pegmatites hosted by late flat-lying joints. They show sharp contacts with a cordierite-quartz-mica schist that may be enriched in decussate micas, tourmaline, and cordierite porphyroblasts, recrystallized along narrow (cm to dm) fringes of contact metamorphism which may also be anomalous in lithium content.

The Bandeira pegmatites are tabular bodies with convex lens-shaped terminations, arranged in tight and staggered (en-echelon) swarms, locally with branched connections linking ore bodies. Single SRP bodies normally reach hundreds of meters in length along the strike, ranging in thickness from a few decameters to decimeters, with the discordant SRP bodies tending to be thicker than the concordant ones. With known downdip-width up to 800 m, several Bandeira SRP bodies remain open in depth. The Bandeira orebodies show a rather simple mineralogical assemblage, consisting of medium (3–10 cm) to very coarse-grained (> 30 cm) spodumene crystals (up to 30 vol%) within a fine- to medium-grained matrix composed of albite, perthitic microcline, quartz, and muscovite, with generally scarce (< 5 vol% in total) accessory (montebrasite, Nb-Sn-Ta oxides) and secondary minerals (cookeite, sericite, zabuyelita, Fe-Mn oxides, clay minerals).

Petalite has been found in some drill cores and thin sections, mostly occurring in the SRP matrix as very fine- to fine-grained (sub-millimetric to 1 cm) crystals and, more rarely, in coarse-grained crystals locally found in a few core intervals. The thicker SRP bodies generally show a barren external zone rich in albite (which can be rather discontinuous), followed inwards by an internal zone rich in disseminated spodumene (although spodumene may also be more ROM in some domains than others along the internal zone).

The thinner SRP bodies generally lack the external lithium-barren zone, showing disseminated spodumene along the whole orebody. Unidirectional solidification textures outlined by tabular to telescope-shaped spodumene crystals are common in the Bandeira SRP orebodies. Thin albite-rich pegmatites, barren to poor in lithium, are also found in the Bandeira SRP swarms. The exploration drilling work revealed two main SRP swarms in the Bandeira deposit: i) the northern swarm, with thicker and longer SRP bodies, and ii) the southern swarm, with smaller SRP bodies.

The synthesis presented in 7.1, 7.1.1, and 7.2 were compiled from Pedrosa-Soares et al. (2009, 2011, 2020, 2023), Paes et al. (2016), and references quoted on those publications, whose repeatedly citations are removed for easier readability of the following text.

7.1 Regional Lithium History and Geology

The Project lies in the Eastern Brazilian Pegmatite Province (EBPP), located in terranes of the Araçuaí Orogen (Figure 7.1 and Figure 7.3). The EBPP, one of the largest pegmatitic populations in the world with c. 150,000 km², contains pegmatite districts located in eastern Minas Gerais (c. 90% of the whole province), southeastern Bahia, and Espírito Santo States of Brazil.

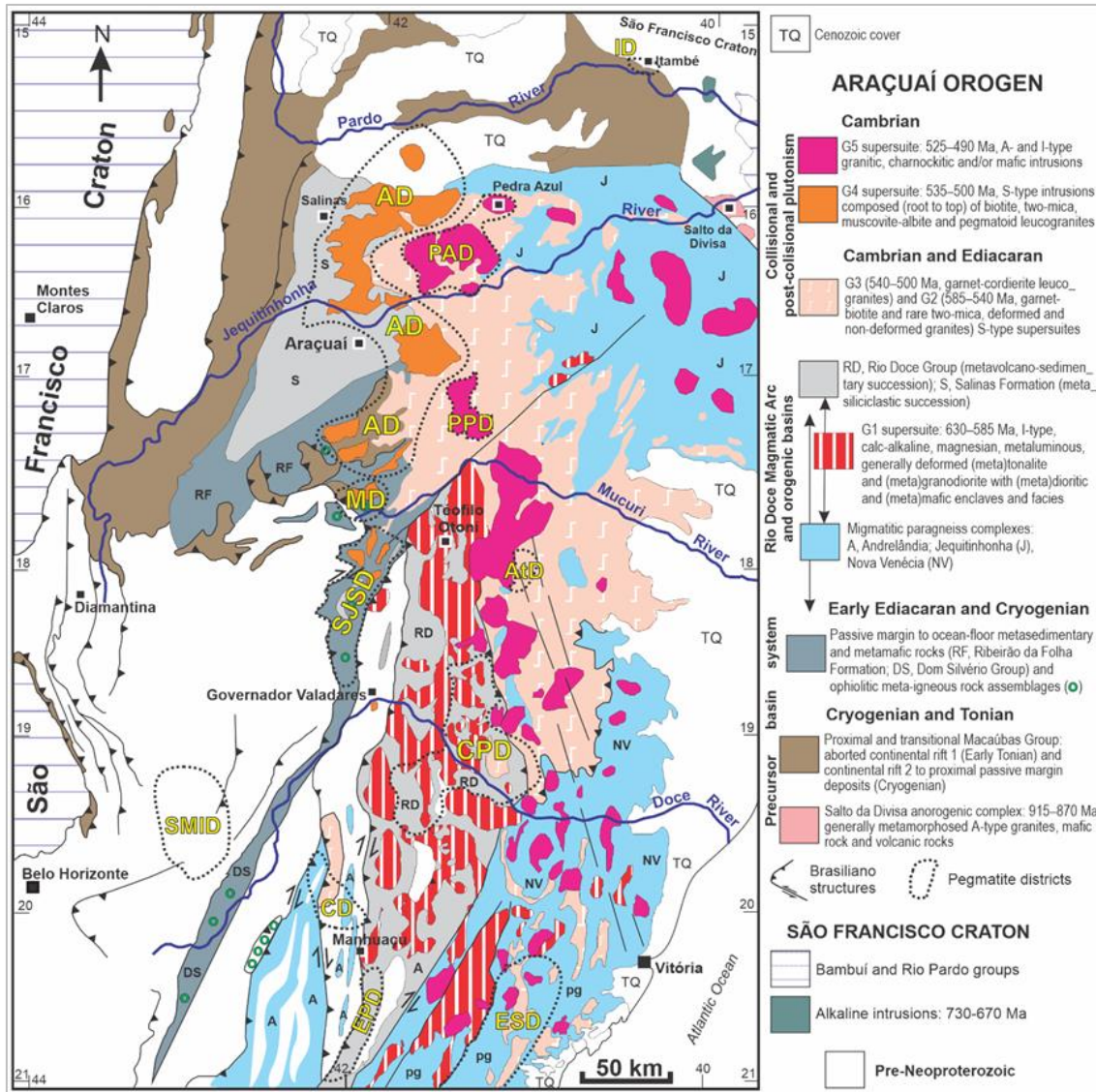


Figure 7.1: Simplified geologic map of the Araçuaí Orogen (modified from Pedrosa-Soares et al., 2020),

Highlighting the granite supersuites and pegmatite districts of the Eastern Brazilian Pegmatite Province (cf. Pedrosa-Soares et al., 2011, 2023): AD, Araçuaí; AtD, Ataléia; CD, Caratinga; CPD, Conselheiro Pena; ESD, Espírito Santo; ID, Itambé; MD, Malacacheta; PAD, Pedra Azul; PPD, Padre Paraíso; SJSD, São José da Safira; SMID, Santa Maria de Itabira. (Figure from Pedrosa-Soares et al., 2023).

The Eastern Brazilian Pegmatite Province is the most important region in the history of pegmatite studies and development of lithium deposits in Brazil. Pegmatite gemstones are officially known in Brazil since the last decades of the 17th century, when green tourmalines, initially mistaken for emeralds, were found by the explorer Fernão Dias Paes Leme in the region of São José da Safira, a pegmatite district very rich in gem-quality elbaite (Li-bearing tourmaline). Long after, in the first decades of the 19th century, pioneer naturalists and geologists, such as Eschwege, Spix, Martius, and Saint-Hilaire, described pegmatite gem deposits located in the Jequitinhonha and Doce river valleys. In 1818, Spix and Martius reached the headwaters of the Calhauzinho and Piauí rivers in the Araçuaí region (Figure 7.4), searching for the gemstones' primary sources, particularly chrysoberyl (then called "chrysolite" locally) that was already mined there. They found a "white granite with little mica, but rich in black tourmaline" (i.e., pegmatite). At that time, spodumene (discovered and named by the Brazilian mineralogist José Bonifácio de Andrada in a volume of the Journal der Chemie, 1800) was already called "rotten chrysolite" by pioneer prospectors and

gemstone diggers (“garimpeiros” in Brazilian Portuguese) of the Jequitinhonha Valley. In 1866, Charles Hartt described the N45E-trending structure of the mica schists hosting very coarse-grained “granite” veins between Araçuaí and Itinga. In 1882, Costa Sena published the first paper directly referring to spodumene (also called “triphane” at that time) in the Middle Jequitinhonha region, after identifying “andalusite, cymophane (chrysoberyl) and triphane with sharp edges, in sands and gravels from streams of the Piauí river valley” and suggested that the primary deposits would also be located there. Several spodumene occurrences, among other pegmatite minerals, of the Middle Jequitinhonha Valley are described by Luiz Caetano Ferraz in his “Compendio dos Minerães do Brasil”, published in 1928.

The importance of pegmatites as economic mineral deposits greatly increased in Brazil from the Second World War, due to the large production of mica, beryl, and quartz to supply the military industry of allied countries, to the end of the Cold War in early 1990’s. Just after the Second World War, in 1946, the largest pegmatitic populations of Brazil were grouped into provinces by Glaycon de Paiva. Among them the Eastern Brazilian Pegmatite Province was first defined. Since then, more than one thousand pegmatites have been mined there for gemstones, cassiterite, Li and Be ores, Nb-Ta oxides, industrial minerals (K-feldspar, muscovite, albite, quartz), collection and rare minerals, dimension stone, and minerals for esoteric purposes.

Historical milestones in the discoveries and mining of lithium deposits in the Araçuaí-Itinga region were reported by Haroldo de Sá in his PhD thesis (1977). According to him:

- “The discoveries and production of cassiterite, lepidolite, and amblygonite in pegmatites of the Piauí river valley (e.g., Fumal, Generosa, Jenipapo, and Urubu) by the Estanífera do Brasil and Produco companies dated back to the early 1950s. Although spodumene has been known for a long-time by gem diggers (“garimpeiros”), who called it “cambalacho” or “crisólita podre” (i.e., rotten chrysolite in reference to its similarity to chrysoberyl), its commercial production only started at the end of the 1960s at the Cachoeira mine (then owned by Companhia Estanífera do Brasil) to supply the increasing demand of the national market.

Petalite, formerly called “escória branca” (white scoria) and very often mistaken for feldspar, was correctly identified at the end of the 1960’s and immediately mined for exportation by the Companhia Estanífera do Brasil until 1972, followed by Companhia Arqueana de Minérios e Metais Ltda. Around 1977, this mining company has more than twenty distinct pegmatite bodies producing petalite, spodumene, amblygonite, lepidolite, beryl, cassiterite and columbite-tantalite.”

For his PhD thesis (1977), Haroldo de Sá compiled map, sections and other data from the archives of the Companhia Arqueana de Minérios e Metais Ltda. and produced the first geochronological data for the local granites and pegmatites (whose similar ages, around 500 Ma, is evidence of a genetic link between them). He also produced the first geochemical data (K, Rb, Cs) for minerals of non-economic and pegmatites with mineralization of petalite, spodumene, lepidolite and/or pollucite. His spatial interpretation of the distribution and zoning of different Li-rich pegmatites, even with present-day knowledge, remains realistic.

Khalil Afgouni, an outstanding pioneer of the lithium mining in Brazil and the owner of Companhia Arqueana de Minérios e Metais Ltda, together with Haroldo de Sá published a farseeing article entitled “Lithium Ore in Brazil” in the prestigious magazine Energy in 1978 (vol. 3, pp. 247-253). In the article, they predict that “another new use (for that metal) is in lithium batteries for electric cars and, if this application becomes reality, Brazil will be a big consumer, ranking at same level as the most developed countries in the world, with the advantage of being one of few countries producing its own raw material.” Although this is not yet a full reality, the remarkable increase in lithium ore production in the Jequitinhonha Lithium Valley is a result of the invaluable heritage of Arqueana’s discoveries of world-class lithium deposits.

The assets were later bought by CBL (Cachoeira mine) in the early 1990’s and, more recently, by Sigma Lithium (Xuxa mine, and other spodumene and petalite deposits such as Barreiro, Maxixe, Murial, and others). That heritage continues to drive new companies to the region, whose exploration efforts have led to the discovery of subsurface spodumene deposits in areas lacking outcrops, such as the Bandeira deposit of Lithium Ionic.

Since the early 1980s, the region encompassing the Eastern Brazilian Pegmatite Province (EBPP) has been completely covered by systematic geological mapping (in 1:100,000 scale) and experienced an outstanding increasing in scientific studies supported by robust analytical data. That allowed genetic and metallogenetic links between pegmatite populations and the tectono-magmatic events of the regional geological evolution to be established. In fact, the EBPP is the result of the magmatic and tectono-metamorphic events that formed the Araçuaí Orogen from the Early Ediacaran (ca. 630 Ma) to the Late Cambrian (ca. 490 Ma).

These events comprise the regional deformation, metamorphism and partial melting of sedimentary and volcanic successions deposited in the Tonian-Cryogenian precursor (rift to passive margin) basin system and the Ediacaran orogenic (arc-related) basins (Figure 7.2), as well as of the continental basement. The melting events resulted in the production of huge volumes of orogenic granitic rocks and thousands of pegmatites grouped into five supersuites (G1 to G5; Figure 7.1, Table 7.1).

The sedimentary and volcano-sedimentary successions involved in the tectono-metamorphic-anatectic processes that generated granites and pegmatites show two contrasting distributions of U-Pb ages for detrital grains of zircon (Figure 7.2). One is a classic multimodal age spectrum of a basin system evolved from continental rift to passive margin, represented by the Macaúbas Group and Jequitinhonha Complex.

The other age distribution shows an unimodal spectrum typical of orogenic basins largely filled by material from a rather dominant zircon source (e.g., an active magmatic arc), representing the Salinas Formation and Rio Doce Group that host most Li-bearing pegmatites in the EBPP (Figure 7.1). The Salinas Formation, comprising quartz-mica schist (metapelite) with lenses of calc-silicate rock (metamarl), metawacke (metasandstone) and metaconglomerate, is the main host unit of Li-rich pegmatites in the whole EBPP, including the spodumene-rich pegmatites of the Bandeira deposit of Lithium Ionic.

Tectono-metamorphic events and the G1 to G5 granitic supersuites of the Araçuaí Orogen play distinct roles in relation to pegmatite abundance, distribution, genesis, and metallogenetic specialization, imposing important prospecting constraints with regards to metallic potential of distinct pegmatite populations along the EBPP (see 7.2).

The G4 is the most important granitic supersuite related to Li-rich pegmatites, followed by the G2 supersuite, while the G5 and G1 supersuites are related to Be-rich pegmatites generally free of or poor in Li-minerals. Tourmaline-bearing pegmatites are widespread in the EBPP, except in some clusters of Be-rich and Li-rich pegmatites.

The G4 intrusions and batholiths show the classical distribution of granitic facies, from pluton root to top, found in other Li-rich pegmatite districts around the world, comprising biotite leucogranite, two-mica leucogranite, muscovite leucogranite, albite leucogranite and pegmatoid granite. Apatite, beryl, tourmaline, and garnet occur in the pegmatoid granites, and muscovite-albite leucogranites. The Salinas Formation is also the main host unit of G4 intrusions associated with Li-rich pegmatites (Figure 7.1).

7.1.1 Pegmatites

Granitic pegmatites represent silica-saturated magmas variably rich in H₂O and bearing fluids, as well as in other hyperfusible (fluxing) components (e.g., Li, Na), crystallized in rather closed chemical systems (cf. Cerný, 1991; London, 2008). The EBPP comprises the two known genetic types of pegmatites, both formed during the evolution of the Araçuaí Orogen: i) the anatectic pegmatites generated directly from the partial melting of country rocks; and ii) the residual pegmatites, representing late silicate melts released by fractional crystallization of parental granites. Genetic affiliation and other criteria allow pegmatite districts to be distinguished in the EBPP (Figure 7.3; Table 7.2).

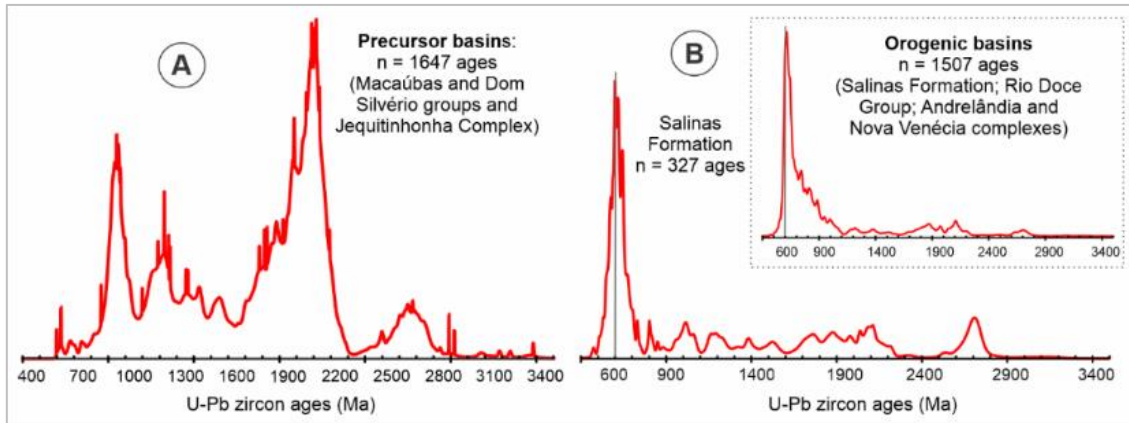


Figure 7.2: Distributions of U-Pb ages for detrital zircon grains from metamorphosed sedimentary and volcanic rocks (Figure from Pedrosa-Soares et al., 2023).

(A) precursor basins (e.g., Macaúbas Group and Jequitinhonha Complex), and (B) orogenic basins (e.g., Salinas Formation, Rio Doce Group) of the Araçuaí Orogen within the Eastern Brazilian Pegmatite Province.

Table 7.1: Main features of the orogenic igneous supersuites of the Araçuaí Orogen (simplified from Pedrosa-Soares et al. 2023).

| Supersuites | G ₁ | G ₂ | G ₃ | G ₄ | G ₅ |
|-------------------------------|---|--|--|---|--|
| Ages (Ma) | 630 – 585 | 585 – 540 | 540 – 500 | 535 – 500 | 525 – 490 |
| Lithotypes | mostly tonalite and granodiorite, minor diorite to gabbro-norite, with biotite, amphibole and/or pyroxenes; poor in pegmatites | mostly biotite-garnet syenogranite to alkali feldspar granite, garnet-rich monzogranite to tonalite, and garnet-two-mica granite, locally with sillimanite; associated with external rare element pegmatites | alkali feldspar granite to syenogranite with cordierite and/or garnet and/or sillimanite, free of or poor in biotite; poor in pegmatites | from pluton root to top: biotite granite, two-mica leucogranite, muscovite and/or albite and/or schorlomite granite, pegmatoid granite; associated with external rare element pegmatites | alkali feldspar granite to granodiorite, orthopyroxene-bearing charnockitic rocks, basic (norite) to ultrabasic rocks, and beryl-topaz pegmatites |
| Field Relations | batholiths and stocks, generally rich in dioritic to mafic enclaves and facies, showing solid-state deformation and migmatization, local well-preserved igneous fabrics, associated with the arc-related metavolcano-sedimentary Rio Doce Group | batholiths, stocks and stratoid bodies, showing solid-state deformation, metamorphism and migmatization, with common restites and xenoliths of metasedimentary rocks, and localized well-preserved igneous fabrics | mostly autochthonous, non-deformed patches, veins, and lodes of G ₃ leucosome, and minor stocks, free of the regional foliation, hosted by migmatites with G ₂ paleosome | balloon- to stratoid-shaped intrusions, post-kinematic in relation to the regional ductile foliation, locally imposing late deformation on the regional structural trend (circumscribed intrusions) | balloon-shaped plutons and multiple intrusions, locally rich in mafic and/or microgranular enclaves with magma mixing features, and norite-rich bodies, post-kinematic in relation to the regional ductile foliation |
| Geochemical Signatures | metaluminous to slightly peraluminous, magnesian, calcic to alkali-calcic, medium- to high-K, expanded calc-alkaline series | strongly to weakly peraluminous, calc-alkalic to sub-alkalic (K > Na) | peraluminous, sub-alkalic (K > Na) | peraluminous, sub-alkalic (K > Na) to alkalic (Na > K) | metaluminous to slightly peraluminous, ferroan, high-K calc-alkalic, minor tholeiite |
| Petrogenetic Type | metaluminous I-type, locally peraluminous I-type | peraluminous S-type, locally peraluminous I-type | S-type | S-type | A-type and I-type |
| Tectonic Stage | pre-collisional to early collisional magmatic arc | late pre-collisional to late collisional | late collisional to post-collisional | post-collisional | post-collisional |

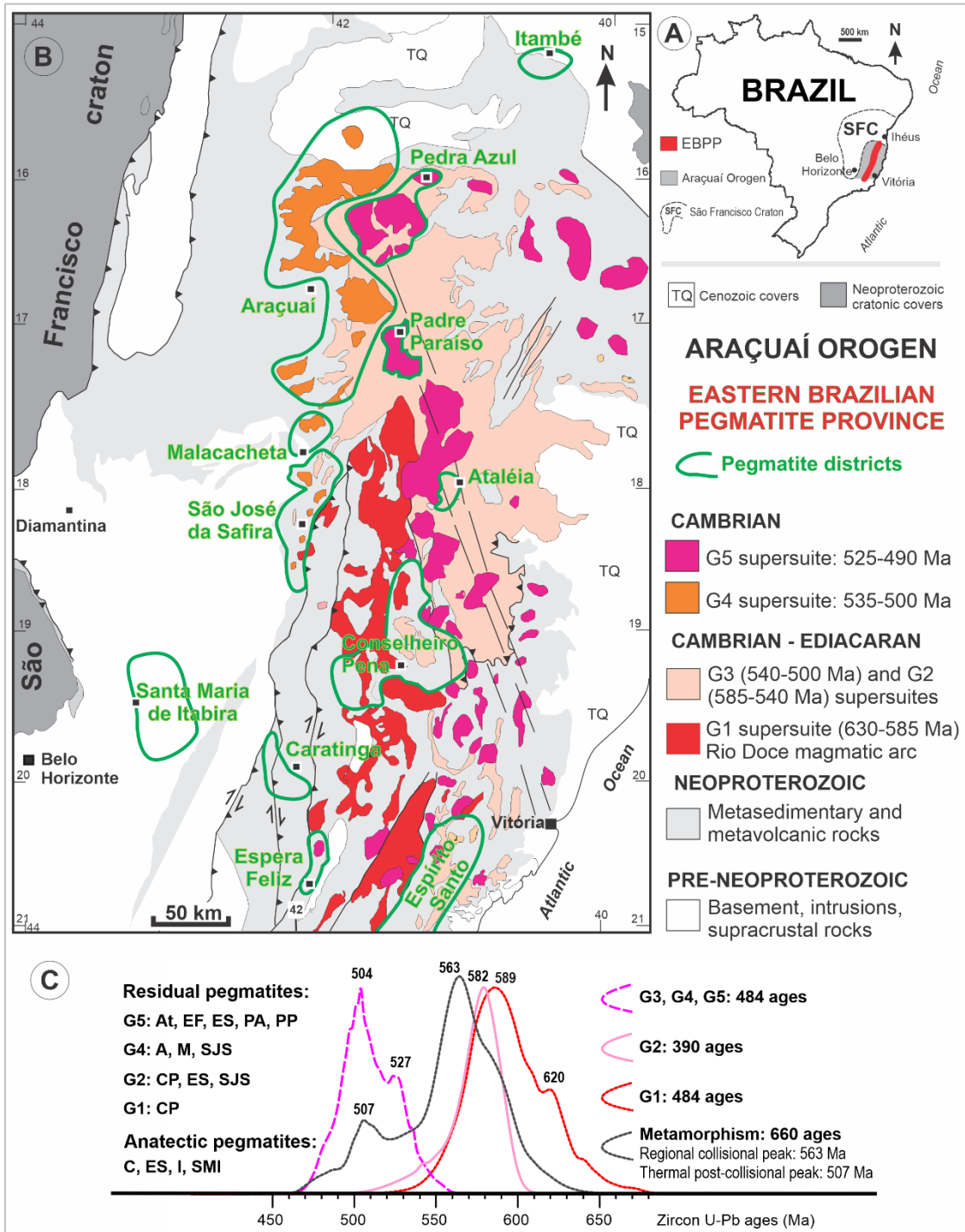


Figure 7.3: Araçuaí Orogen – Eastern Brazilian Pegmatite Province

A) Location of Eastern Brazilian Pegmatite Province (EBPP). B) Simplified geological map highlighting the granite supersuites (G1 to G5) and EBPP pegmatite districts: A, Araçuaí; At, Ataléia; C, Caratinga; CP, Conselheiro Pena; EF, Espera Feliz; ES, Espírito Santo; I, Itambé; M, Malacacheta; PA, Pedra Azul; PP, Padre Paraíso; SMI, Santa Maria de Itabira; SJS, São José da Safira. C) Distribution of zircon U-Pb ages from orogenic granite supersuites (G1 to G5), regional metamorphism and post-collisional thermal events, correlated to pegmatite districts. (Figure from Pedrosa-Soares et al., 2023).

The anatectic pegmatites are coarse-grained quartz-feldspathic bodies (i.e., granitic leucosomes) hosted by migmatitic gneisses and micaschists, mostly formed in the collisional tectono-metamorphic event (585 – 540 Ma) and in the post-collisional thermal event (540 – 490 Ma). Therefore, their spatial distribution, and genetic and metallogenetic features are directly related to the melted country rocks. Conversely, the residual pegmatites, especially those enriched in rare elements, have restricted spatial distributions and genetic links directly related to the distinct granite types from which they ultimately inherited their geochemical characteristics and metallogenetic specializations (Figure 7.3; Figure 7.2).

Therefore, residual pegmatites released from peraluminous, subalkalic to alkalic, hydrous, S-type, two-mica leucogranites formed from the partial melting of metasedimentary rocks might have a rather distinct metallogenetic specialization (e.g., richer in Li, Cs, Ta, Sn, and P) in relation to residual pegmatites (e.g., richer in Be, F, and Fe) from metaluminous, high-K calc-alkalic, ferroan, relatively anhydrous, A-type, amphibole-biotite granites formed from the partial melting of mainly igneous rocks. The first case (S-type granites) refers to Li-bearing pegmatites associated with the G4 and G2 supersuites, while the second (A-type granites) stands for the Be-bearing (but Li-free) pegmatites comprised by the G5 supersuite (Figure 7.3; Table 7.2).

(Pedrosa-Soares et al., 2023, updated after Pedrosa-Soares et al., 2011. (*) Cerný et al. (1991, 2012). LCT, Lithium-Cesium-Tantalum; and NYF, Niobium- Fluorine pegmatites).

Table 7.2: Features of the Main Pegmatite Districts of the Eastern Brazilian Pegmatite Province

| District names and ages (Ma) | Historical and present-day mineral production, and rare minerals | Genetic affiliation; class, subclass, type, subtype, and family (*) | Parent and host rocks |
|------------------------------|--|---|--|
| Itambé 508 Ma | K-feldspar, quartz crystals, mica, beryl, columbite, monazite | anatectic; muscovite-rare element, REE, allanite-monazite, NYF | biotite-hornblende gneisses, sillimanite-feldspar-mica schists |
| Pedra Azul 501 Ma | quartz, beryl (aquamarine), topaz | residual; REE, beryl-topaz, NYF | A-type G ₅ granites |
| Padre Paraíso 519 Ma | quartz, beryl (aquamarine), topaz, quartz crystals, goshenite, chrysoberyl | residual; REE, beryl-topaz, NYF | A- and I-types G ₅ granites and charnockites |
| Araçuaí 535-500 Ma | Greenish to pinkish spodumene, petalite, lepidolite, Li-phosphates, cookeite, cassiterite, columbite-tantalite, industrial minerals (perthitic K-feldspar, albite, muscovite), tourmalines (elbaite, schorlite), beryl ore and gems (aquamarine, morganite), pollucite, quartz crystals, cleavelandite, herderite and other rare phosphates, topaz, bismuthinite | residual; mostly rare element and minor muscovite-rare element, Li, beryl, complex (spodumene, petalite, lepidolite, elbaite, amblygonite), albite-spodumene (SRP), albite, LCT | S-type G ₄ leucogranites; low-P/high-T (andalusite, cordierite, sillimanite) to medium-PT (garnet, staurolite, kyanite, sillimanite) mica schists to paragneisses, metasandstones, calc-silicate rocks, meta-ultramafic rocks |
| Ataléia 502 Ma | quartz crystals, beryl (aquamarine), topaz, chrysoberyl | residual; REE, beryl-topaz, NYF | A- and I-types G ₅ granites and charnockites |
| São José da | tourmalines (elbaite, schorlite), industrial minerals (perthitic K- | residual; muscovite-rare element and rare element, | S-type G ₄ and G ₂ leucogranites; medium- |

| | | | |
|------------------------------------|---|--|--|
| Safira 545-490 Ma | feldspar, albite, muscovite), beryl ore and gems (aquamarine, heliodor, morganite), lepidolite, Li-phosphates, spodumene, garnet, cleavelandite, columbite-tantalite, cassiterite, bertrandite, microlite, zircon, rare phosphates | Li, beryl, complex (elbaite, lepidolite, Li-phosphates, spodumene), LCT | PT (garnet, staurolite, kyanite, sillimanite) mica schists to paragneisses, metasandstones, calc-silicate rocks, meta-ultramafic rocks |
| Conselheiro Pena 570-545 Ma | industrial minerals (perthitic K-feldspar, albite, muscovite), tourmalines (elbaite, schorl), beryl ore and gem, spodumene (kunzite), lepidolite, Li-phosphates, quartz crystals, cleavelandite, columbite-tantalite, cassiterite, rare phosphates (arrojadite, barbosalite, brasilianite, childrenite, correianevesite, eosphorite, roscherite, vivianite, etc.) | residual; muscovite-rare element and rare element; Li, beryl, complex (elbaite, Li-phosphates, lepidolite, spodumene), LCT | S-type G ₂ (and I-type G ₁ ?) granites; medium-PT to intermediate low-P (garnet, staurolite, cordierite, kyanite, sillimanite), mica schists to paragneisses, metasandstones, calc-silicate rocks, meta-ultramafic rocks |
| Malacacheta 535-500 Ma | muscovite, beryl, chrysoberyl; alexandrite, sapphire | residual; muscovite-rare element, beryl, LCT; and anatectic to hydrothermal processes | S-type G ₄ leucogranites; mica schists, meta-ultramafic rocks, migmatites |
| Santa Maria de Itabira, 545-500 Ma | emerald, alexandrite, aquamarine, amazonite | quartz-feldspathic hydrothermal deposits, and pegmatites | ultramafic schists, banded iron formations, migmatites |
| Caratinga, 570 Ma | kaolin, corundum (sapphire, ruby), beryl | anatectic; abyssal, ceramic | migmatitic paragneisses |
| Espera Feliz, 500 | quartz crystals, beryl (aquamarine), topaz | residual; REE, beryl-topaz; NYF | G ₅ granites |
| Espírito Santo 570-500 Ma | kaolin, quartz, beryl (aquamarine), topaz, tourmalines (and spodumene?) | anatectic; ceramic; and residual; REE, beryl-topaz, NYF (and LCT?) | migmatitic paragneisses, G ₅ (and G ₂ ?) granites |

The EBPP was subdivided into twelve pegmatite districts based on the mineral production, genetic and metallogenetic affiliation and classification, parental granite type, host rocks and metamorphic regime, and crystallization ages of a relatively large and clustered pegmatite population (Figure 7.3; Table 7.2). Most of them are districts of residual pegmatites of the rare element class, distinguished by their affinities with the LCT (Lithium-Cesium-Tantalum) or NYF (Niobium-Yttrium-Fluorine) geochemical-metallogenetic families that, in turn, are related to distinct types of parental granites. Beryl-topaz (NYF) pegmatites cluster in districts almost completely circumscribed or very close to A-type and I-type G₅ intrusions, encompassing granitic and igneous charnockitic (orthopyroxene-bearing) rocks with features of magma mingling-mixing involving mafic melts.

Contrastingly, complex LCT pegmatites and albite-spodumene-rich pegmatites (SRP) are found in the external aureoles of S-type intrusions mostly composed of two-mica leucogranites with pegmatoid cupolas, generally hosted by metasedimentary rocks of the greenschist to amphibolite facies. Among the EBPP Li-bearing districts, the Araçuaí Pegmatite District stands out by having the largest historical and current production of lithium ore and the only world-class spodumene

deposits of Brazil. Those deposits include the CBL, Sigma, and the newly discovered deposits by other companies, such as the Bandeira and other spodumene-rich deposits of Lithium Ionic Corporation.

The Araçuaí Pegmatite District includes several LCT pegmatite fields distinguished by their mineral production, pegmatite types and subtypes, and pressure-temperature (P-T) conditions of both the regional and contact metamorphisms (Figure 7.4). Besides complex LCT pegmatites, spodumene-rich pegmatites (SRP) are known in the Curralinho, Itinga, Neves-Tesouras and Salinas pegmatite fields. However, the Itinga Pegmatite Field remains the most important for spodumene production and prospecting, owing to the outstanding abundance of non-zoned to poorly zoned SRP ranging from a few to dozens of meters thick, hundreds to a few thousand meters in length along strike, and dozens of meters in down-dip width. Many spodumene orebodies mined by Arqueana, CBL and Sigma, as well as those discovered by Lithium Ionic at Bandeira and other targets, belong to the SRP (or albite-spodumene) type.

7.2 Structural Geology

In the Araçuaí Pegmatite District (Figure 7.4), the present-day structural framework was established after four deformation events (D1, D2, DG, and DNt). Two of them (D1, D2) are directly related to the regional tectono-metamorphic evolution of the Araçuaí Orogen in the Ediacaran-Cambrian. The third deformation event (DG) was caused by the widespread and voluminous intrusions of Cambrian G4 granites that caused thermal metamorphism and significant structural disturbance on the regional fabrics along areas relatively close to granitic stocks and batholiths (Pedrosa-Soares et al. 1987, 1993, 2011; Alkmim et al., 2006; Santos et al., 2009; Peixoto et al., 2017). Much later, the last deformation event (DNt) resulted from neotectonics reactivation in the Late Tertiary (Saadi and Pedrosa-Soares, 1989). The Ediacaran-Cambrian deformation events (D1, D2, and DG) formed the structural framework that passively hosts the rare element pegmatites in the Araçuaí District (Figure 7.4). The much younger neotectonic deformation (DNt) reworked prior structures in upper crustal levels in the Late Tertiary (Miocene), forming normal faults and graben basins (e.g., the Virgem da Lapa Graben, Figure 7.4) filled by the fluvial to lacustrine sandstone-mudstone piles of the São Domingos Formation that reach more than 100 m in thickness (Saadi and Pedrosa-Soares, 1989; Pedrosa-Soares, 1997). Locally, neotectonic faults may cut and displace blocks with pegmatite deposits.

The D1 deformation results from regional tectono-metamorphic processes imposed by compressive stresses during the collisional stage (580-540 Ma) of the Araçuaí Orogen. Megascopic to macroscopic D1 structures are asymmetric tight folds with long limbs and short hinges, parasitic folds, and ductile shear zones related to thrust ramps and oblique to transcurrent strike-slip domains.

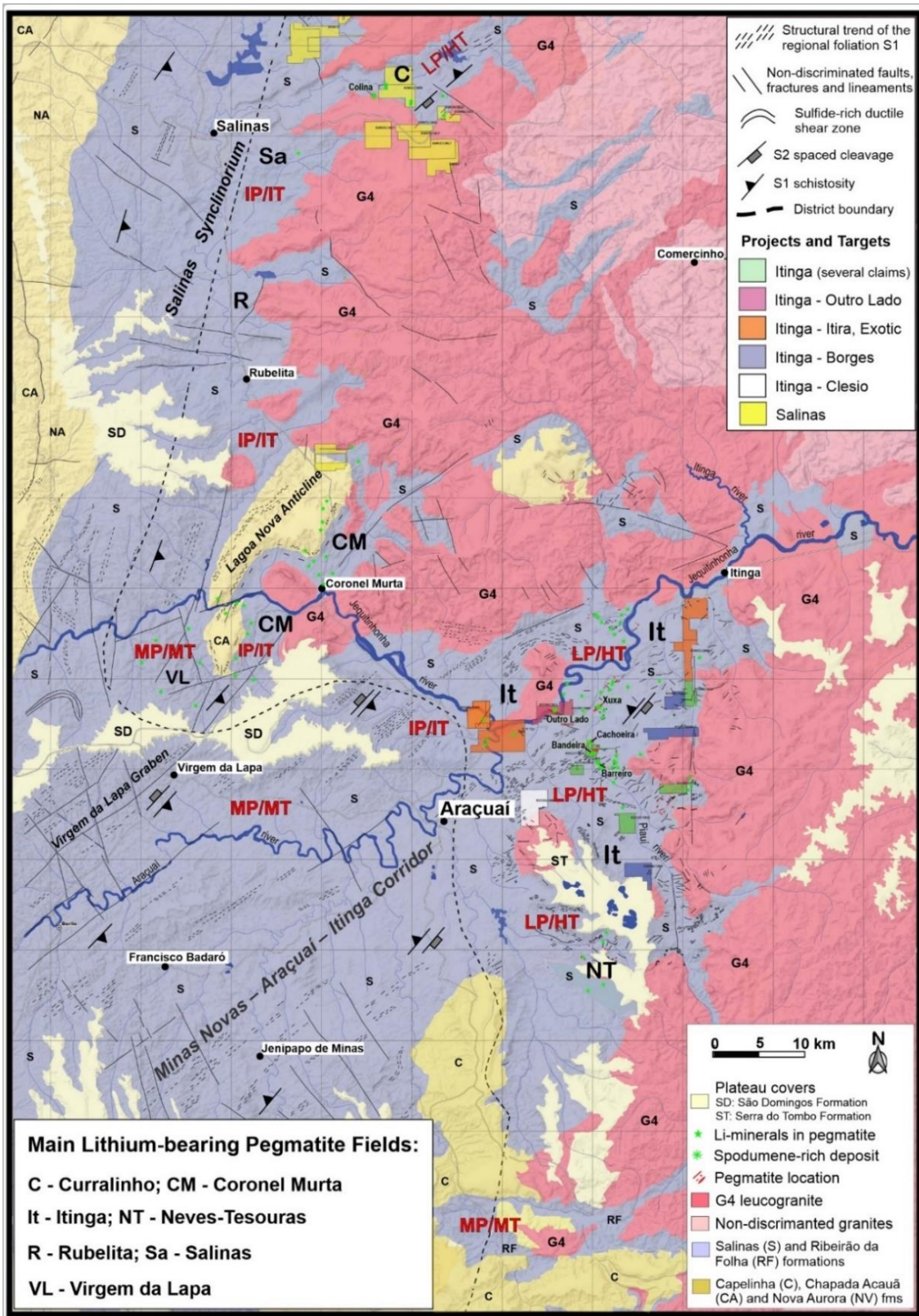


Figure 7.4: Geological map of the Araçuaí Pegmatite District.

Highlighting lithium-bearing pegmatite fields (see inbox), major tectonic domains (names in italics on map), metamorphic regimes according to relative pressure (P) and temperature (T) conditions (LP/HT, low-P/high-T; IP/IT, intermediate-low P and T; and MP/MT, medium P and T), spodumene active mines (Cachoeira, Xuxa) and main spodumene deposits: Bandeira and Outro Lado

(Lithium Ionic), Barreiro (Sigma), and Colina (Latin Resources). Map modified and updated by Pedrosa-Soares et al. (2023) based on the district map by Paes et al. (2016).

The macroscopic to microscopic D1 structures include the main regional planar structure that evolved from a cleavage to the schistosity S1 (Figure 7.5) that contains the L1 mineral/stretching lineation. S1 is generally (sub)parallel to the layering (S0) along D1 fold limbs, becoming an axial-plane surface in fold hinges (Figure 7.5). Anastomosed and S-C foliations characterizes higher strain shear zones syn-kinematic to S1. Although it generally is a very penetrative structure, the S1 foliation also provides host surfaces for pegmatites.

Distinct metamorphic regimes related to the D1 deformation of schists and gneisses rich in micas have been recognized in the region encompassing the Araçuaí Pegmatite District (Pedrosa-Soares et al., 1984, 1993, 1996; Costa et al., 1984; Costa, 1989; Santos et al., 2009; Peixoto et al., 2017). In the western and southwestern sectors of the region (Figure 7.4), the S1 schistosity shows syn-kinematic (syn-S1) assemblages with Fe-rich garnet (almandine), staurolite, kyanite and/or sillimanite. Such index-minerals series is typical of a medium pressure and medium temperature (MP/MT) metamorphic regime (Figure 7.4). This, together with quantitative geothermobarometric data, characterize the M1 metamorphic event as a syn-collisional (syn-D1) Barrovian-type (MP/MT) metamorphism dating between 575 – 550 Ma. P and T increase from c. 3.5 kbar at 450 °C in the garnet zone at the southwest of Francisco Badaró, passing northeastwards through the staurolite, kyanite and sillimanite zones, and reaching up to 8.5 kbar at 650 °C at the southeast of Coronel Murta (Figure 7.4).

In the northeastern and northern sectors of the region, the S1 schistosity shows syn-kinematic (syn-S1) assemblages with biotite, Mn-rich garnet (spessartine), andalusite, cordierite and/or sillimanite. Such index-minerals series is typical of a low pressure and high temperature (LP/HT) metamorphic regime (Figure 7.4). From the most northeastern andalusite zone to the southwest of Itinga, quartz-feldspathic leucosomes with aplitic to pegmatitic textures formed from the breakdown of muscovite along the S1 foliation of cordierite-quartz-mica schists. Northeastwards, through the andalusite-cordierite, cordierite-sillimanite, sillimanite, and K-feldspar zones, increasing metamorphism and partial melting of quartz-mica schists formed migmatitic paragneisses in the eastern tip of the Itinga Pegmatite Field (Figure 7.4). Regionally, the metamorphic event (M2) records a low-P/high-T metamorphism with pressures from 2 kbar to 5.5 kbar under temperatures from 400 °C to 700 °C, at around 540-530 Ma. The M2 metamorphism reached partial melting conditions on quartz-mica schists of the Salinas Formation with increasing anatexis rates that formed leucosome-rich migmatites (diatexites) in the easternmost sector of the Araçuaí Pegmatite District. This implies that, in deeper crustal levels, the widespread anatexis on the Salinas Formation could have produced large volumes of S-type granitic magmas in the late collisional to post-collisional stages of the Araçuaí Orogen. Indeed, the time interval of the M2 metamorphism (540-530 Ma) fits well with the oldest ages of G4 granites (535-525 Ma). This, together with the fact that the M2 metamorphism culminated in partial melting of quartz-mica schists and paragneisses in the easternmost Araçuaí Pegmatite District, indicate that the S-type G4 magmas were formed from the anatexis of thick metasedimentary packages in deep levels of the Salinas Formation.

Along the boundary between the M1 and M2 metamorphic domains (Figure 7.4), the syn-S1 mineral assemblages include almandine and/or staurolite and andalusite and/or cordierite, characterizing an intermediate-low pressure (Buchan-type) metamorphic regime (IP/IT, Figure 7.4) transitional between the M1 Barrovian-type (MP/HT) and the M2 low-P/high-T (LP/HT) metamorphic regimes found in the Araçuaí Pegmatite Districts. Bearing in mind the relations between distinct pegmatite populations, their metallogenetic specializations and metamorphic regimes (Cerný, 1991; Cerný et al., 2012), such metamorphic characterization is of great importance for prospecting different rare element pegmatites, as Li-rich pegmatites are typically found in terranes with relatively low-P/high-T metamorphism.

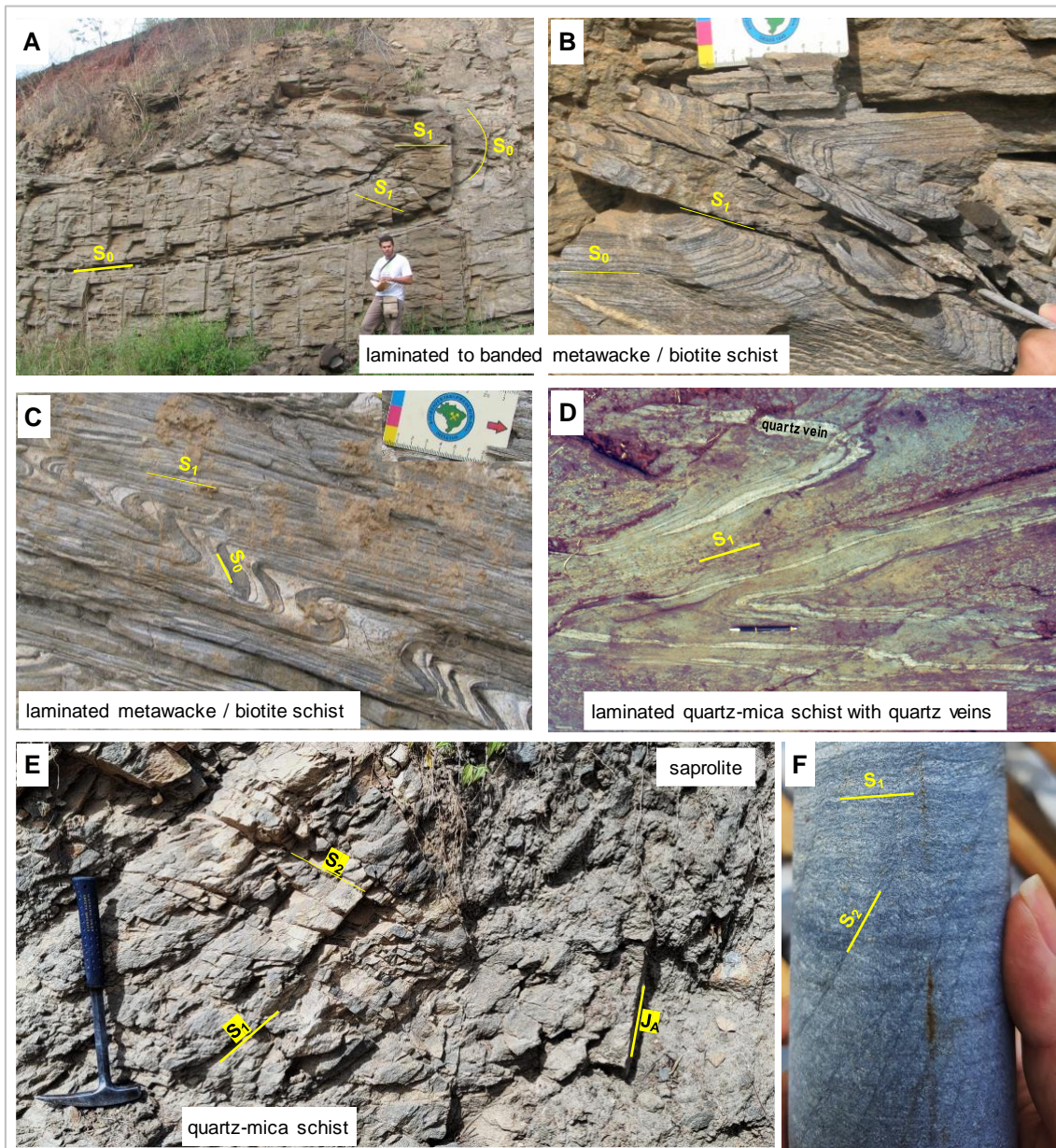


Figure 7.5: Photos from outcrops and a drill core showing structures of the deformation events D_1 and D_2 on the Salinas Formation in the Araçuaí Pegmatite District.

(A and B) Large tight fold (A) with a hinge (B) showing the sedimentary layering (S_0) cut by the low-angle dip to flat axial-plane S_1 cleavage. C) Tight folds with limbs transposed by S_1 foliation. D) Hinges of tight folds with metamorphic quartz veins in quartz-mica schist. E) Spaced cleavage S_2 cutting the schistosity S_1 , and sub-vertical joints (J_A) cutting across both S_1 and S_2 in the Bandeira area. F) S_2 spaced foliation marked by recrystallized mica, cutting the S_1 schistosity in a drill core sample from the Bandeira deposit.

The D_2 deformation developed from the late collisional to the post-collisional stages of the Araçuaí Orogen, when increasing decompression conditions, imposed by the orogen gravitational collapse, gradually replaced the tangential D_1 compressive stresses. In the Araçuaí Pegmatite District, the D_2 deformation comprises mostly brittle structures, such as the S_2 spaced cleavage, joint families, and normal faults, as well as large open folds (flexures). The spacing between surfaces of the S_2 cleavage ranges from less than one centimeter to decimeters (Figure 7.5). Locally, S_2 may be very well developed in micaschists, becoming a tight crenulation cleavage to schistosity. The S_2 spaced cleavage and other brittle structures, as being more open surfaces

than the S1 schistosity, provided host surfaces for Li-rich pegmatites, generally the thicker ones, in the Itinga Pegmatite Field.

The latest Cambrian deformation event (DG) was caused by the intrusion of large volumes of S-type magmas that formed the G4 granites and cut across and disturbed the regional framework imprinted by the D1 and D2 deformations. The DG event deformed the regional structural trend of the host rocks around granitic plutons, forming radial fractures irradiating from the granitic plutons, and imprinting ring-shaped fracture systems that reworked regional structures around the intrusions. All these DG structures can host late orogenic rare element pegmatites.

During emplacement and cooling, the G4 plutons caused contact metamorphism on their country rocks and released residual silicate melts that formed pegmatites that either crystallized within the parental granite or migrated outwards and were hosted by D1, D2 and DG structures of the Salinas Formation and other metasedimentary units. While barren and beryl-bearing pegmatites are found both within parental G4 granites and country rocks, the Li-bearing pegmatites have been only found in places rather far from (> 1 km) granite massifs, emplaced in the Salinas Formation and other metasedimentary units. The G4 batholith emplaced along the whole eastern boundary of the Araçuaí Pegmatite District is formed by multiple coalescent plutons and places an eastern limit for the occurrence of Li-bearing pegmatites.

Regionally, the deformational events formed large structures with distinct implications for the occurrence and structural control of pegmatites in the Araçuaí District, such as the Salinas Synclinorium, the Lagoa Nova Anticline, and the Minas Novas - Araçuaí - Itinga Corridor (Figure 7.4).

The axial zone of the Salinas Synclinorium shows the best-preserved section of the Salinas Formation, comprising non-deformed to weakly deformed metawacke, metapelite and metaconglomerate, metamorphosed in the biotite and garnet zones of the low greenschist facies. This low-grade metasedimentary section reaches up to 2 km in thickness, with no evidence of pegmatite along the synclinorium keel. However, a Li-rich pegmatite cluster, including SRP bodies, was recently found to the east of the Salinas Synclinorium, along the andalusite-cordierite-bearing, low-pressure/high-temperature metamorphic zone of the Curralinho Pegmatite Field (Figure 7.4).

In the case of the Lagoa Nova Anticline, although there are LCT pegmatites emplaced along its structural surfaces, no SRP was yet found there, much probably due to the rather unfavorable pressure-temperature conditions of the regional and contact metamorphisms (between the medium PT (MP/MT) and intermediate PT (IP/IT) regimes).

The Minas Novas - Araçuaí - Itinga Corridor, in turn, plays a special role in the understanding of the structural control and the most favorable pressure-temperature conditions for the SRP occurrence in the Araçuaí Pegmatite District. That corridor has been characterized as a flower-shaped transpressive (during D1) to transtensive (during D2) structure (Pedrosa-Soares et al., 1993, 1996; Alkmim et al., 2006) with the S1 foliation dipping to SE in the NW flank, and to NW in the SE flank (Figure 7.4).

In the Itinga Pegmatite Field, the S1 schistosity and S2 spaced cleavage show NE-trending strikes, with the S1 schistosity dipping to NW and the S2 cleavage dipping to SE (if they have not been disturbed by later deformations, i.e., DG and Dnt). The S1 foliation, as well as the S2 spaced cleavage and other brittle surfaces (i.e., the flat-lying and subvertical joints) host many Li-rich pegmatites, with the thicker SRP bodies generally emplaced in more open surfaces of brittle structures.

The regional metamorphism associated with the S1 schistosity gradually increases from southwest to northeast along the corridor, reaching c. 3.5 kbar at c. 550 °C at the andalusite-cordierite zone in the Piauí river valley, where the contact metamorphism was imposed by G4 granitic intrusions also under relatively low-pressure conditions. All those tectono-metamorphic and magmatic features favorable to SRP occurrence characterize the Itinga Pegmatite Field

where several of the most important spodumene deposits already found in Brazil are located, such as those of the CBL and Sigma, and the SRP deposits of Lithium Ionic.

7.3 Local Geology

Field mapping in the Bandeira area revealed the existence of two geological units: (i) Salinas Formation, characterized by banded quartz-mica schists with lenses of calcsilicate rocks; and (ii) G4 Supersuite, represented by an extensive pegmatite dike-swarm (pegmatite veins) composed of spodumene-rich orebodies and some non-mineralized pegmatites (Figure 7.6).

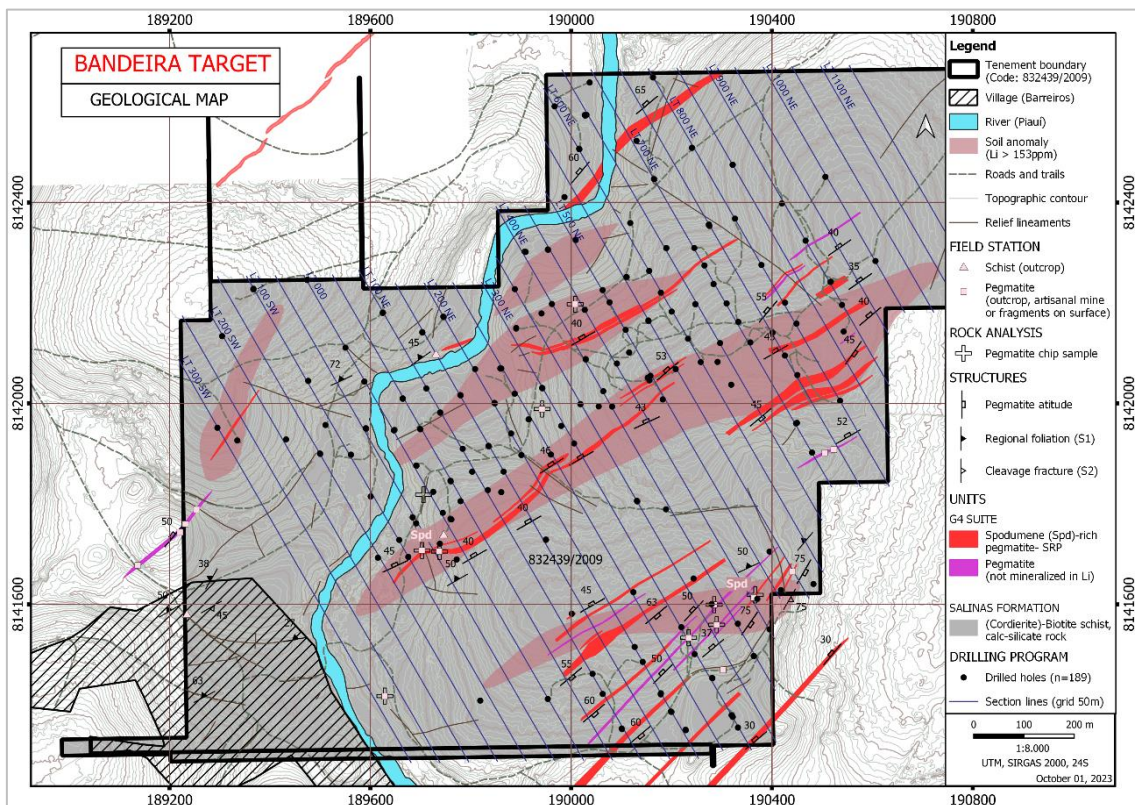


Figure 7.6: Geological Map of the Bandeira Deposit.

Owing to the significant weathering typical of tropical regions, the surface of the Bandeira area predominantly comprises recent residual soils resulting from the decomposition of the underlying rocks. The residual soil from the schists is a red to brown fine-grained (silt to clay) eluvium. In contrast, the pegmatite soil is typically a whitish, fine to coarse-grained, powdered eluvium, with a composition dominated by quartz, kaolinized feldspar and altered muscovite. In cases of lithium mineralization, this soil can also contain fine-grained, partially to almost wholly weathered spodumene fragments.

Based on the few exposed outcrops, the Salinas Formation in the Bandeira area is composed of biotite schist and cordierite-biotite schists of gray color and medium-grained size. When these rocks contain a higher concentration of mica, the schistosity is more penetrative, and they also tend to be more fractured (Figure 7.7a). When the amount of quartz is greater, a preserved original bedding can be observed marked by the alternance of dark biotitic and light quartz-feldspathic layers (Figure 7.7b). Cordierite-biotite schist was also identified in the Bandeira target, and they are characterized by the enrichment of millimetric to centimetric cordierite porphyroblasts (Figure 7.7c), which can be stretched along the schistosity (syn-tectonic) or undeformed and late-stage (post-tectonic). Based on observations in the drill cores it is also possible to verify the presence of calc-silicate rocks interlayered in the schists, which can be classified in three types (based on the mineralogy): (i) biotite-quartz schist; (ii) quartz-biotite schist; and (iii) cordierite-quartz-biotite schist.

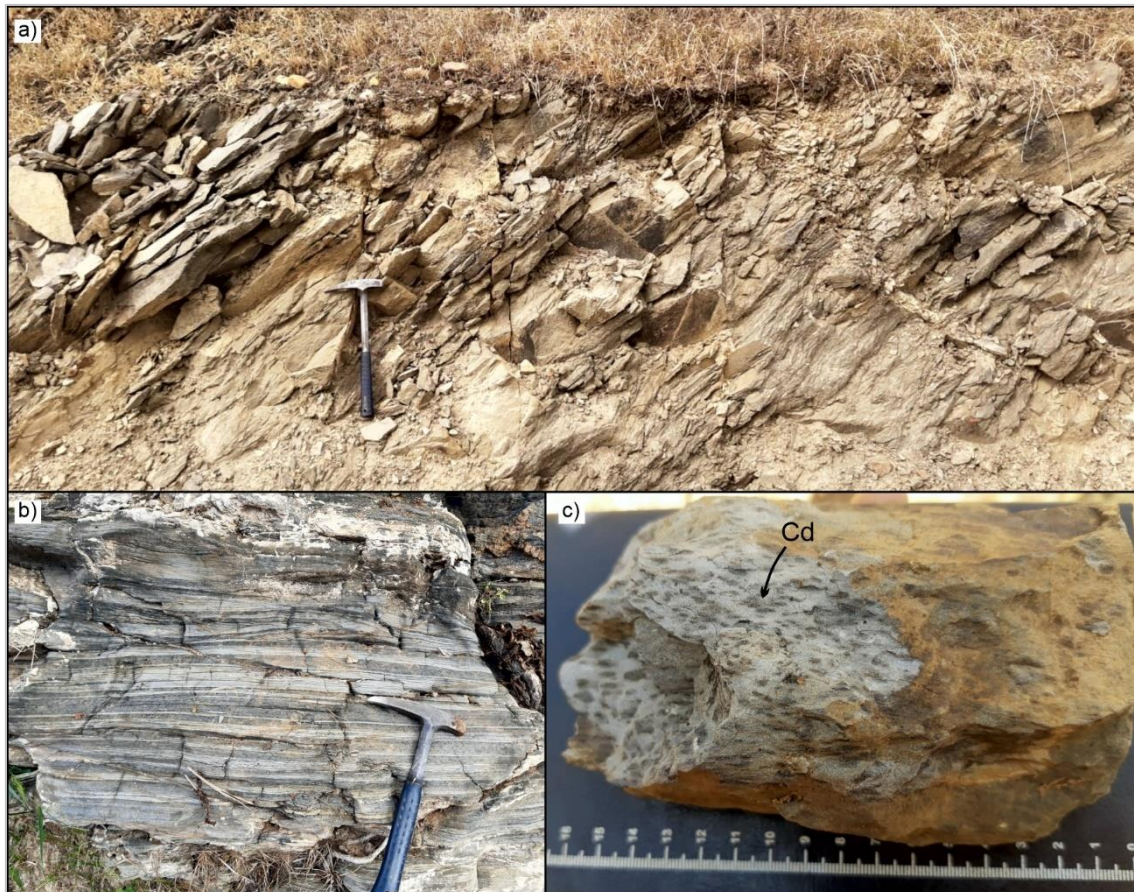


Figure 7.7: Schists of the Salinas Formation observed in the Bandeira Deposit.

a) fractured biotite schist (UTM: 189,232 / 8,141,577); b) banded biotite-schist with preserved original bedding (UTM: 189,733 / 8,142,094); c) detail of the cordierite-biotite schist (UTM: 190,441 / 8,141,664). Coordinates in SIRGAS 2000, zone 24S. Abbreviation: Cd-cordierite).

The pegmatites in the Bandeira target constitute a swarm of several dikes with variable thickness (metric to decametric). They are normally concordant to the Salinas Formation schistosity (50-55°NE/40-50°NW). The nature of the contact between the pegmatite and the host rock is abrupt and sharp (Figure 7.3a). Records of the pegmatites mineralized in lithium in the Bandeira area (i.e.: Spodumene-Rich Pegmatites – SRP) can be observed in some exposed outcrops that show centimetric coreless to greenish spodumene crystals, with whitish color when weathered. In such veins, it is common the occurrence of euhedral prismatic centimetric crystals with a preferred orientation indicative of mineral growth orthogonal to the borders of the dike (Figure 7.3b).

Based on the observations from these outcrops, and the intercepts from the drill cores, it is possible to define the Bandeira mineralized bodies as non-zoned pegmatitic dikes with a simple and consistent mineralogy composed essentially of albite (33%), perthitic K-feldspar (25%), spodumene (19%), quartz (15%), and muscovite (5%). Accessory phases (3%) vary from petalite, columbite, tantalite, cassiterite, apatite, tourmaline, and sphalerite. The log analysis unveiled well-preserved spodumene crystals of variable sizes, typically centimeter-scale and disseminated throughout the rock. Notably decimeter-sized crystals also occur (Figure 7.3b).

The concordant SRP pegmatites in the Bandeira area are dominantly concordant with the regional schistosity (S1) but discordant bodies, with similar strike and dipping to southeast, also occur. The best example are the pegmatites observed in the southeastern region (Figure 7.3), where a more flattened large discordant body fed smaller intrusions that dips towards southeast. These discordant bodies share identical mineralogical composition with the concordant bodies, leading to the interpretation as both products of the same coeval magmatism.



Figure 7.8: Spodumene-Rich Pegmatites observed in the Bandeira Deposit.

a) pegmatite of ca. 2 m thick concordant to the regional foliation (S1) of the host schists; b) outcropping and weathered prismatic spodumene crystals that grew perpendicular to the contact; c) detail of the cordierite-biotite schist (UTM: 190,441 / 8,141,664). Coordinates in SIRGAS 2000, zone 24S. Abbreviation: Cd-cordierite.

7.4 Mineralization Model

The following text and illustrations were compiled from Pedrosa-Soares et al. (2023) and complemented with data from Lithium Ionic public and internal reports, if not otherwise specified.

The Bandeira spodumene deposit is located immediately to the southeast of the CBL's Cachoeira mine (Figure 7.9). This mine has played a major role in the understanding of the mineralogical, petrographic, geochemical, and structural features of spodumene-rich pegmatites (SRP) through the scientific and technical studies carried out on the Cachoeira Pegmatite Group, a specific pegmatitic population of the Itinga Pegmatite Field (e.g., Sá, 1977; Afgouni and Sá, 1978; Correia-Neves et al., 1986; Afgouni and Marques, 1997; Pedrosa-Soares et al., 2009, 2011, 2023; Romeiro, 1998; Quéméneur and Lagache, 1999; Romeiro and Pedrosa-Soares, 2005; Dias, 2015; Chaves et al., 2018; Luiz, 2023). The Cachoeira Pegmatite Group comprises a SRP swarm that has been mined at least since the 1970's by the Arqueana Company (Figure 7.10), followed by the production of spodumene ore in industrial scale by CBL since 1993 (Figure 7.11). It is yet the best characterized spodumene deposit in Brazil, providing solid information to support the mineralization model that was applied to the exploration work on the Bandeira deposit (Figure 7.4).

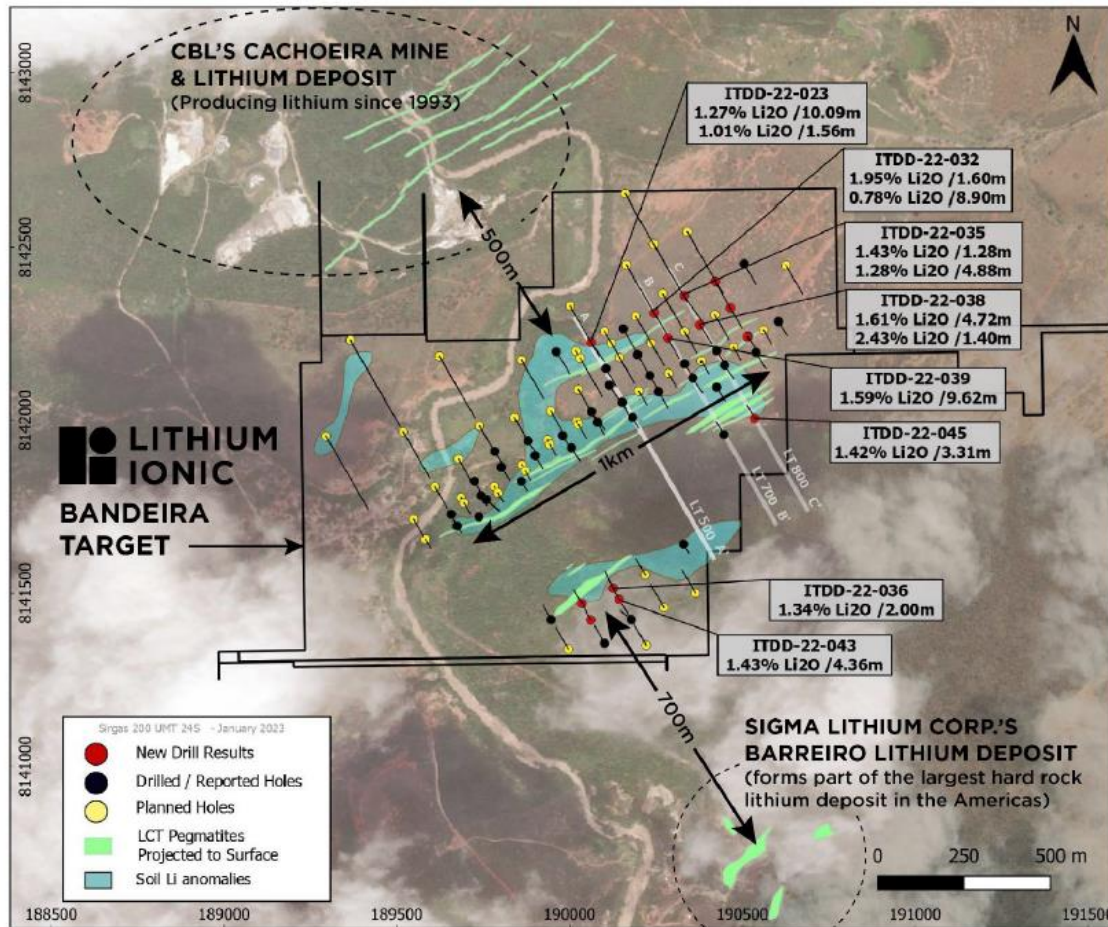


Figure 7.9: Location of the Bandeira deposit in relation to the CBL's Cachoeira mine and the Sigma's Barreiro deposit (cf. Corporate Presentation, Lithium Ionic Corporation, March 2023).
<https://www.lithiumionic.com/projects/itinga-project/>.

The typical SRP orebodies of the Cachoeira Pegmatite Group are non-zoned but rather inequigranular pegmatites composed of spodumene (on average 23 vol%), perthitic microcline, albite, quartz, and muscovite, generally totalizing more than 95% of the whole orebody volume. Montebasite, beryl, cassiterite, columbite-tantalite, cookeite, zabuyelite and petalite are scarce accessory minerals.

The Cachoeira SRP cluster forms a pegmatite swarm characterized by a staggered (en-échelon) spatial distribution of parallel to subparallel, locally branched orebodies showing lateral and vertical offsets among them (Figure 7.11 and Figure 7.12). They are roughly tabular bodies with lens-shaped terminations, ranging from decimeters up to 30 m in thickness orthogonal to dip, from a few meters to many hundreds of meters in length along strike, and up to many hundreds of meters downdip. The Cachoeira pegmatites were emplaced in the Salinas Formation that consists of banded cordierite-quartz-mica schist with intercalations of calcsilicate rock, recording P-T conditions suitable for SRP occurrence. In the Salinas Formation, the main host surfaces for pegmatites are the regional foliation (schistosity) S1 and the S2 spaced cleavage, although late joint surfaces can also host SRP bodies (Figure 7.10, Figure 7.11, and Figure 7.12).

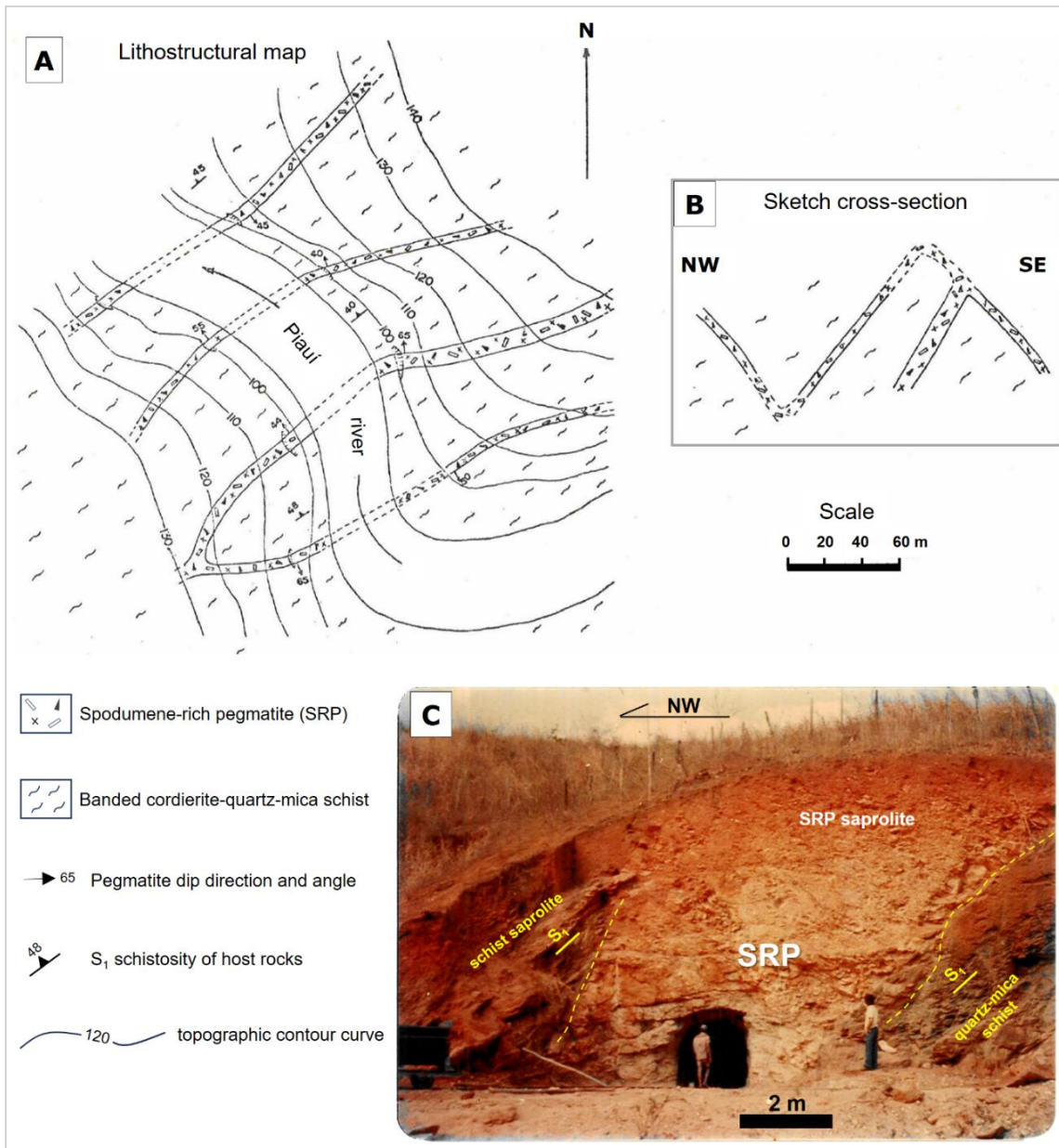


Figure 7.10: The Cachoeira mine in the mid 1970's.

A (map) and B (section) showing four NE-trending, parallel to sub-parallel, branched, tabular-shaped, spodumene-rich pegmatites (SRP) both concordant with the NW-dipping S1 schistosity of host rocks and discordant with S1, (i.e., emplaced in the SE-dipping S2 spaced cleavage). B (photo) shows a concordant, c. 7 m thick SRP hosted by cordierite-quartz-mica schist, with both rocks increasingly weathered (saprolites to soils) towards the topographic surface. (Map, cross-section, and photo adapted from Sá, 1977).

The tectonic structure of the Salinas Formation behaved passively during the intrusion of Li-rich magmas that crystallized as spodumene-rich pegmatites, which in turn do not record any evidence of ductile or brittle deformations (Figure 7.11 and Figure 7.12), except for small faults that locally cut pegmatite contacts and may be related to the latest D2 or DG deformations (Figure 7.12; see also section 7.2).

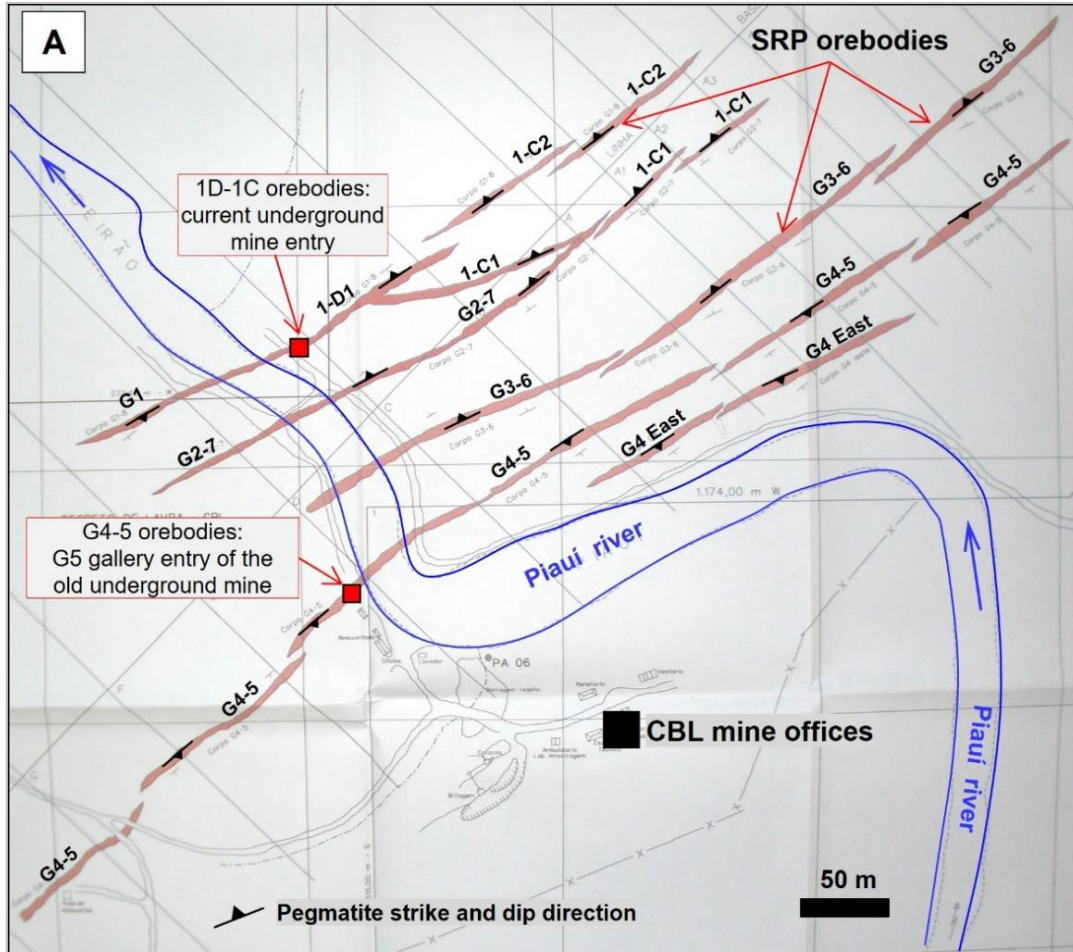


Figure 7.11: Map of the Cachoeira Pegmatite Group in CBL's mine area (adapted and updated from Romeiro, 1998).

Showing the staggered (en-échelon) spatial pattern of parallel to subparallel, locally branched, NE-trending orebodies of spodumene-rich pegmatites (SRP, in light brown) with indications of mapped strike and dip directions of the pegmatite bodies. SRP concordant bodies, emplaced along the S1 schistosity, dip to NW. SRP discordant bodies, hosted by the S2 spaced cleavage, dip to SE. B) A fractal example of the en-échelon distribution pattern of SRP bodies shown by three smaller veins (above the main SRP orebody) in CBL's Cachoeira mine (photo by A.C. Pedrosa Soares, August 2022).

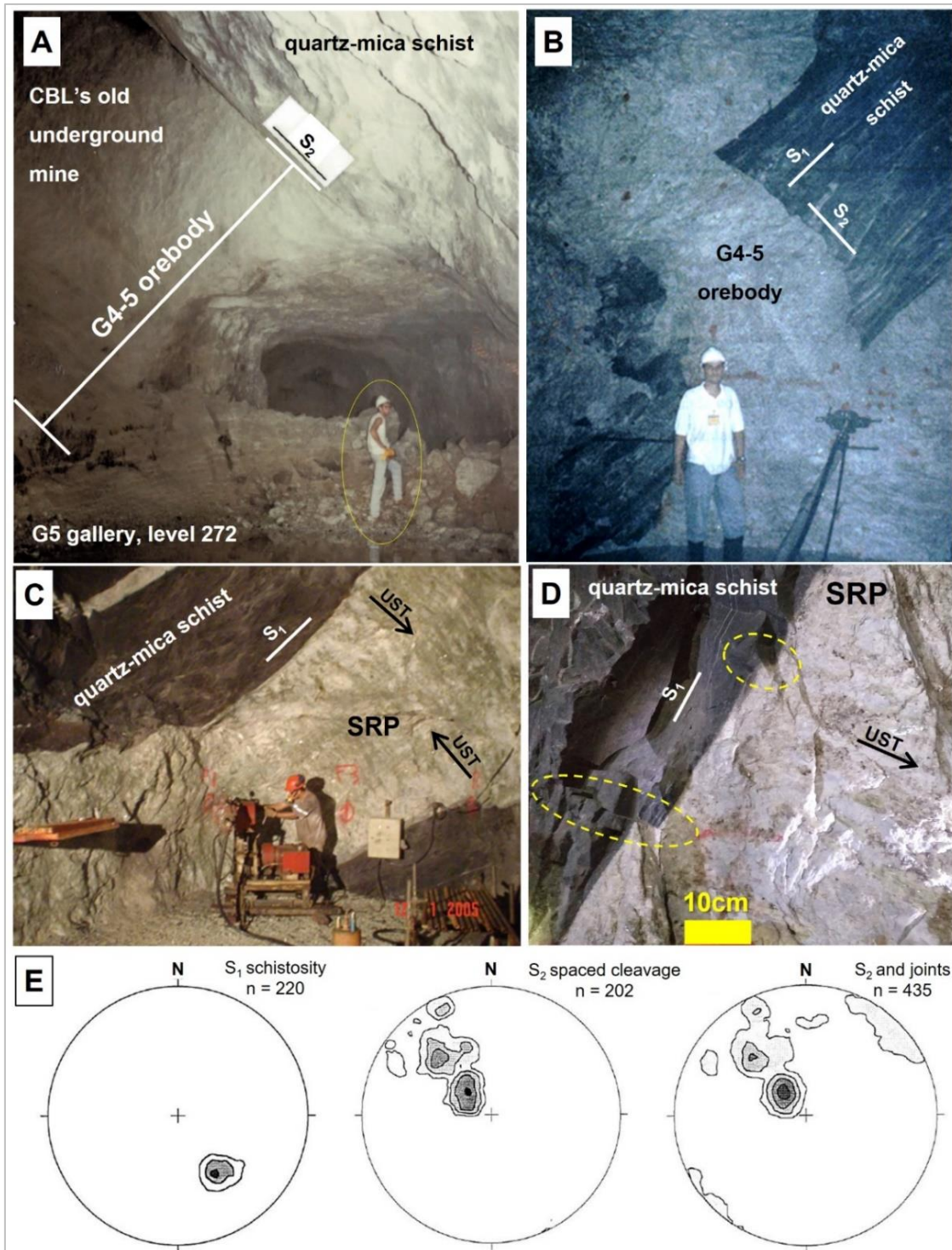


Figure 7.12: 13 Photos from spodumene-rich pegmatites (SRP) in the Cachoeira underground mine (CBL).

A) The G4-5 SRP in the G5 gallery, level 272, showing a discordant orebody (c. 7 m thick) hosted by the S2 spaced cleavage (photo from Romeiro, 1998). B) A closing edge of the main G4-5 orebody, showing SRP branches cutting across the host quartz-mica schist (photo from Romeiro, 1998). C) Mining front showing a concordant SRP orebody (1D/1C gallery) ranging from c. 3 m to more than 4 m thick, hosted by the S1 foliation dipping to NW, with unidirectional solidification texture (UST, black arrows) outlined by orientated greenish spodumene crystals orthogonal to the SRP contacts (photo from Romeiro and Pedrosa-Soares, 2005). D) Sharp lithological contact, concordant with S1, between a SRP and the host schist, showing small offsets along short brittle

surfaces (yellow ellipses) and unidirectional solidification texture (UST, black arrow) outlined by oriented spodumene and feldspar (photo by Pedrosa-Soares, August 2022). E) Stereograms (Schmidt projection, lower hemisphere) for the SRP host structures in the Cachoeira underground mine and surface outcrops showing that both S1 and S2 are Ne-trending but dip to opposite directions: S1 to NW and S2 to SE (stereograms adapted from Romeiro, 1998).

Based on available information from the Cachoeira Pegmatite Group and CBL's underground mine (Figure 7.10 to Figure 7.12), a mineralization model for spodumene-rich pegmatites (SRP) was conceived to assist in the exploration work on the Bandeira target. After a soil geochemistry campaign, Li anomalies roughly parallel to the Cachoeira SRP swarm were revealed and, together with lithological and structural data from few outcrops, old diggings, and new exploration trenches (Figure 7.13) provided the basis for a very successful drilling campaign that discovered dozens of new SRP bodies rather close to each other from the near surface to more than 800 m in depth. The newly discovered Bandeira deposit comprises spodumene-rich orebodies, arranged along the same structural trend of Cachoeira's SRP swarm (Figure 7.14).

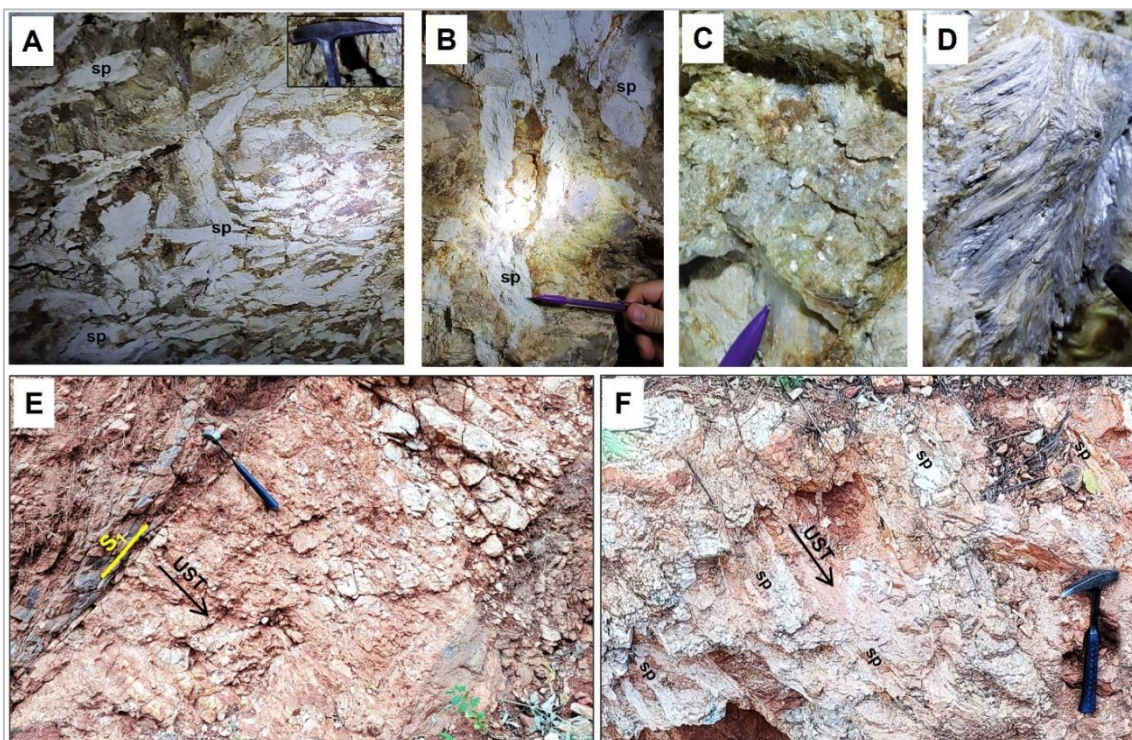


Figure 7.13: Photos from underground galleries of an old digging for gem prospecting (Garimpo in Brazilian Portuguese),

Showing a rather weathered pegmatite very rich in pseudomorphs of spodumene (sp) replaced by white clay (A and B), with local mica-rich rich metasomatic bodies, small miarolitic cavities and rare lepidolite books (D) at the pegmatite top. A new trench (E) revealed another rather weathered pegmatitic body concordant with the S1 foliation of the host quartz-mica schist, showing pseudomorphs of tabular-shaped spodumene (sp) replaced by white clay (F), depicting unidirectional solidification texture (UST) orthogonal to the pegmatite/schist contact.

Following the regional NE-SW structural trend, the Bandeira deposit comprises SRP swarms of NE-striking orebodies mostly hosted by and concordant with the NW-dipping schistosity (S1), but also some discordant SRP emplaced along the SE-dipping fracture system (S2 spaced cleavage), as well as a few SRP bodies hosted by late flat-lying joints (Figure 7.14). The Bandeira pegmatites are tabular bodies with convex lens-shaped terminations, arranged in tight and staggered (en-echelon) swarms, locally with branched connections linking ore bodies. Single SRP bodies normally reach hundreds of meters in length along the strike, ranging in thickness from a few decameters to decimeters, with the discordant SRP bodies tending to be thicker than the concordant ones. With known downdip-width up to 800 m, several Bandeira SRP bodies remain

open in depth. The exploration drilling work revealed two main SRP swarms in the Bandeira deposit: i) the northern swarm, with thicker, longer, and wider SRP bodies concordant to the S1 foliation of host rocks; and ii) the southern swarm, with somewhat smaller SRP bodies (Figure 7.14).

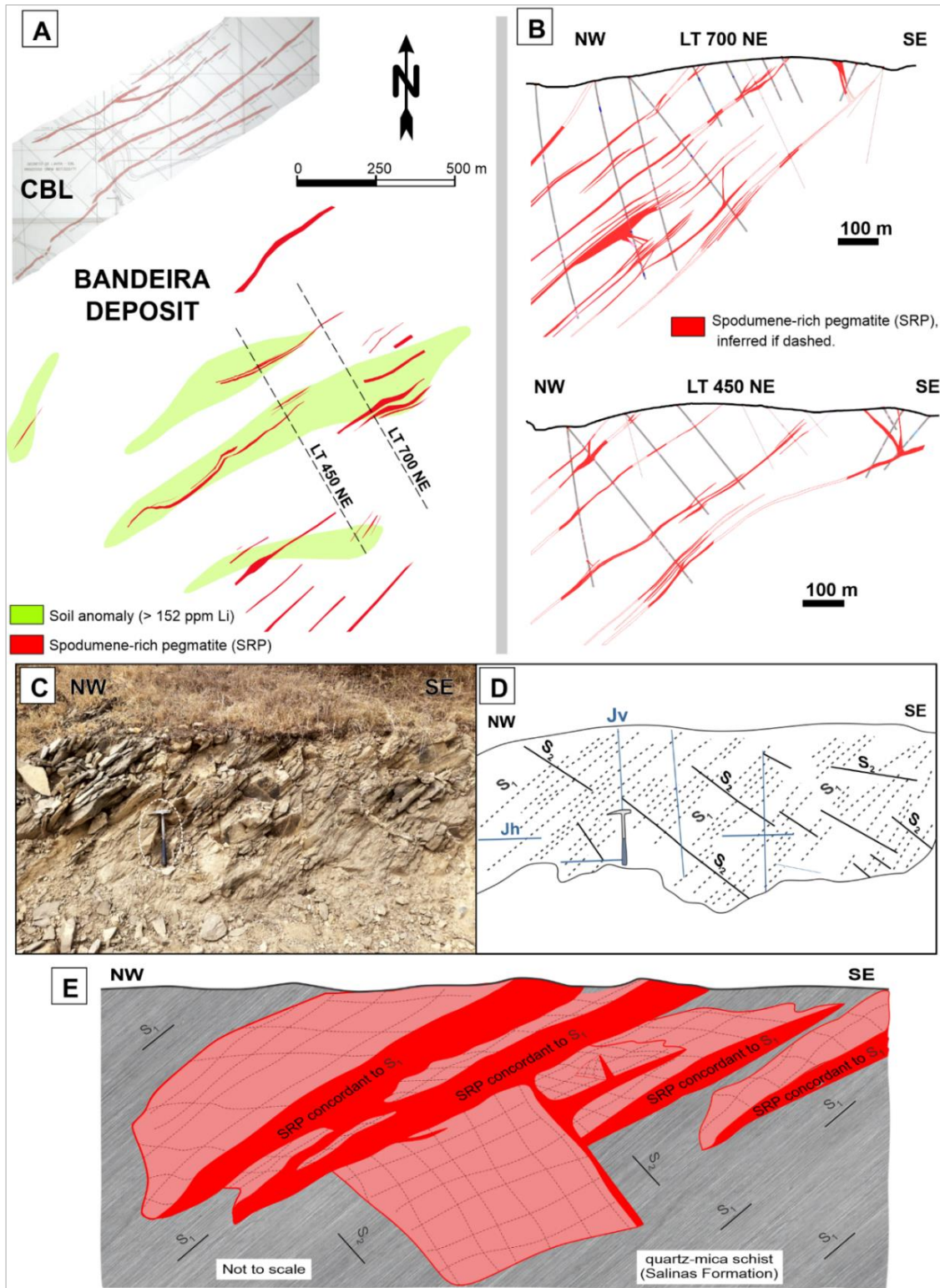


Figure 7.14: Spodumene Pegmatites interpretations.

A) Simplified map showing the distributions of Li anomalies in soil and drilled SRP bodies projected to surface in the Bandeira deposit, and CBL's SRP swarm (see Figure 7.11). B) Simplified cross-sections showing the SRP swarm discovered in depth by Lithium Ionic after exploration work. C and D) Outcrop and structural sketch illustrating the tectonic surfaces of the country rocks (Salinas Formation) that host pegmatites in the Bandeira deposit: S1, regional ductile foliation (schistosity); S2, post-S1 spaced cleavage; Jh, late horizontal joints; and Jv, late vertical joints. E) Cartoon illustrating a model for the spatial distribution and lateral relations of SRP orebodies in the Bandeira deposit. (Map and sections for A and B from Lithium Ionic reports, and CBL map from Romeiro, 1998. C, D, and E by Geologist Anderson Victoria).

The host rocks of SRP orebodies in the Bandeira deposit are banded to laminated cordierite-quartz-mica schists, locally containing disseminated sulfide and/or graphite-rich bands, with intercalations of massive calcsilicate rocks (Figure 7.15 and Figure 7.16). Most cordierite forms ellipsoidal (egg-shaped) stretched poikiloblasts syn-kinematic to the regional S1 schistosity (Figure 7.15).

The banded to laminated quartz-mica schists represent metamorphosed sand-mud sediments, and the calcsilicate rocks are metamorphosed Ca-rich carbonate-mud sediments (marls). They show sharp contacts with the SRP orebodies that generally are concordant to the regional S1 foliation (often parallel to the compositional layering S0) but are also hosted by the S2 cleavage or foliation (Figure 7.16). The host schists may be enriched in decussate muscovite and/or biotite, black to green tourmaline, and recrystallized cordierite along narrow (cm to dm) fringes of contact metamorphism imposed by pegmatites (Figure 7.17). Although the host schists may be anomalous in lithium content close to pegmatites, they show no Li-ore mineral.

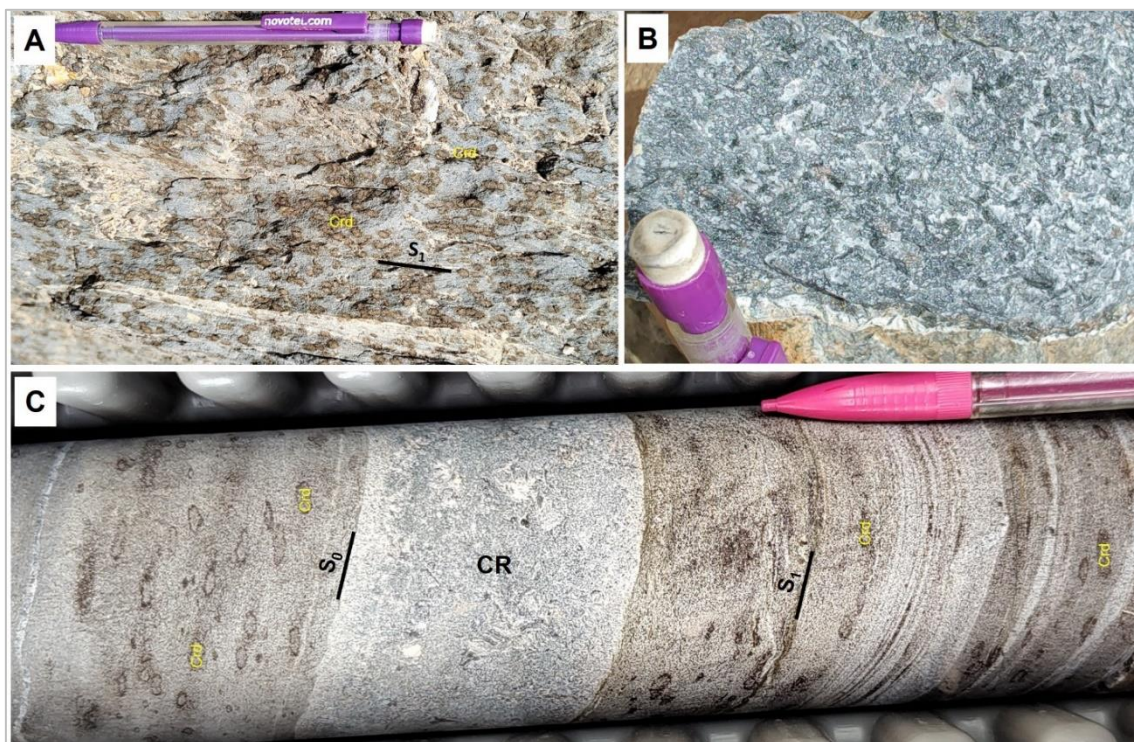


Figure 7.15: Photos from host rocks of spodumene-rich orebodies in the Bandeira deposit.

A) Partially weathered cordierite-quartz-mica schist rich in poikiloblasts (dark spots) of egg-shaped (ellipsoidal) cordierite (Crd) crowded of biotite and/or quartz inclusions and coronated by biotite. B) Calcsilicate rock with porphyroblasts of amphibole (dark green) and grossular garnet (light pink) within a massive matrix (greenish gray) mostly composed of quartz and plagioclase. C) Drill core segment showing the banded to laminated cordierite-quartz-mica schist with ellipsoidal cordierite (Crd; light spots coronated by biotite), light-colored quartz-rich laminae, and an intercalation of calcsilicate rock (CR).

The Bandeira spodumene orebodies show a rather simple mineralogical assemblage (Figure 7.16 and Figure 7.17), consisting of medium - to very coarse-grained spodumene phenocrysts, reaching up to 35 vol% on average, within a fine - to medium-grained matrix mostly composed of albite, perthitic K-feldspar (microcline), quartz, muscovite, and petalite, summing up to 95 vol% of the total matrix. The scarce accessory (mainly montebrasite, and Nb-Sn-Ta oxides) and secondary minerals (cookeite, sericite, zabuyelita, Fe-Mn oxides, clay minerals) generally comprise less than 5 vol% in total. In drill cores, the spodumene crystals are mostly free of hydrothermal and weathering alterations and very poor in mineral inclusions (Figure 7.16 and Figure 7.17). Conversely, surface outcrops, shallow diggings and exploration trenches cutting SRP bodies generally show weathered spodumene (Figure 7.13), forming pseudomorphs composed of white clay (kaolinite and montmorillonite). Rare spodumene-quartz intergrowth (SQUI) may be found associated with spodumene crystals (Figure 7.17). Petalite has been found in SRP's drill cores and thin sections, mostly occurring in the matrix as very fine- to fine-grained (sub-millimetric to 1 cm) crystals (Figure 7.17) and, more rarely, as coarser crystals locally found in rather restricted intervals.

The thicker SRP bodies may show a lithium-barren and thin marginal zone rich in albite, generally rather discontinuous, followed inwards by a thick internal zone rich in disseminated spodumene (although spodumene may also be more ROM in some domains than others along the internal zone). Owing to the upward migration of H₂O-rich fluids, flat-lying SRP sections close to the hanging-wall contact, as well as the top termination ("head") of high-angle dip bodies, may show metasomatic units with miarolitic cavities that partially replaced the primary mineral assemblage. Many SRP bodies lack the external lithium-barren zone, showing disseminated spodumene along virtually the whole orebody (Figure 7.16 and Figure 7.17). Unidirectional solidification textures outlined by tabular to telescope-shaped spodumene crystals are common in the Bandeira's SRP orebodies. Thin albite-rich pegmatites, barren to poor in lithium, are also found in the Bandeira pegmatite swarms.

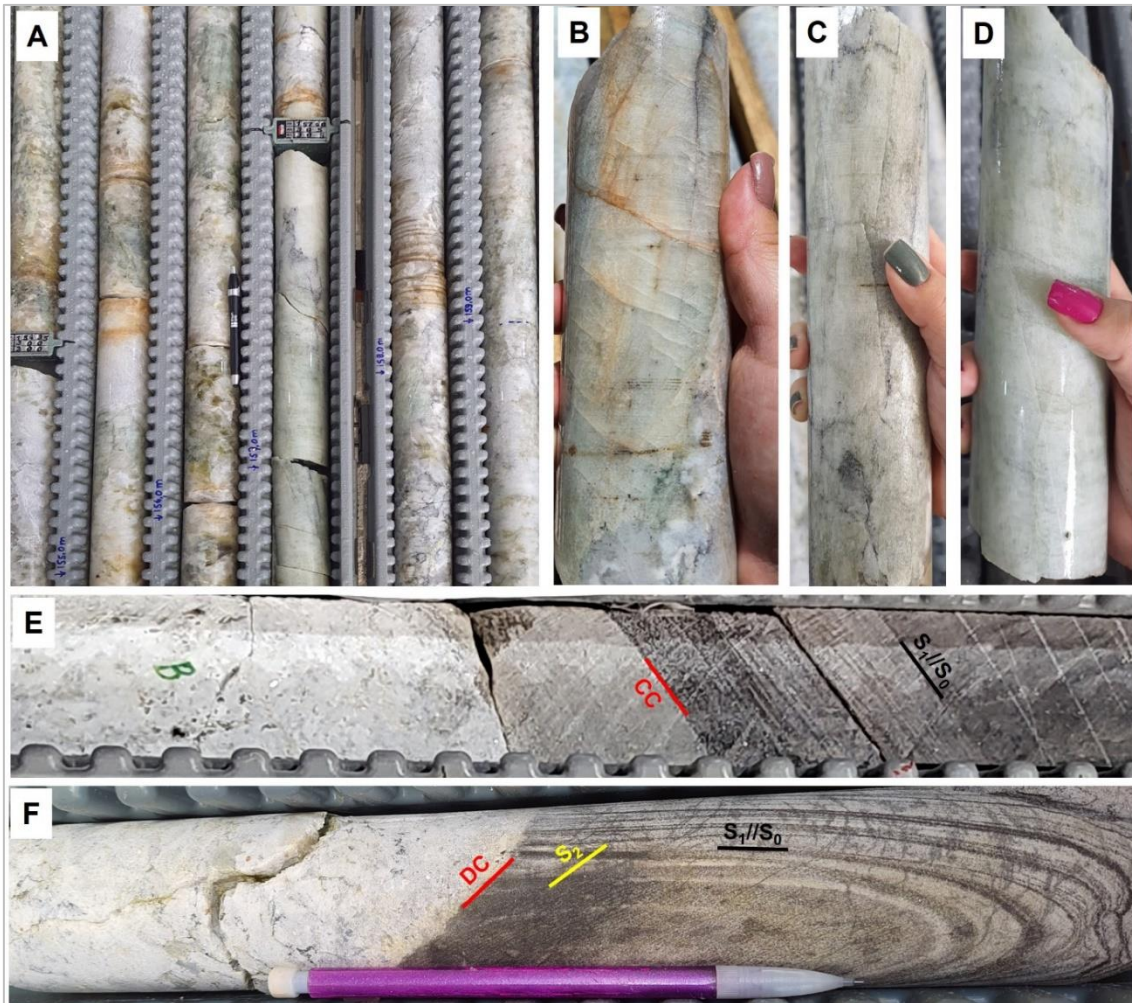


Figure 7.16: Drill core samples from spodumene-rich orebodies and their host rocks in the Bandeira deposit (photos by Geologist Fabiana Guimarães).

A) Segment of a non-zoned SRP body with medium - to coarse-grained greenish spodumene disseminated in the quartz-albite-microcline-muscovite matrix; black minerals in spots and fracture fillings are Nb-Sn-Ta oxides and graphite. B to D) Features of roughly tabular, greenish to white spodumene crystals free of or poor in inclusions. E) Concordant contact (CC) between albite-rich pegmatite border and laminated quartz-mica schist; the host surface is the regional schistosity S1 parallel to the compositional (sedimentary) layering S0. F) Discordant contact (DC) between albite-rich pegmatite border and laminated cordierite-quartz-mica schist; the host surface is the S2 cleavage/foliation.

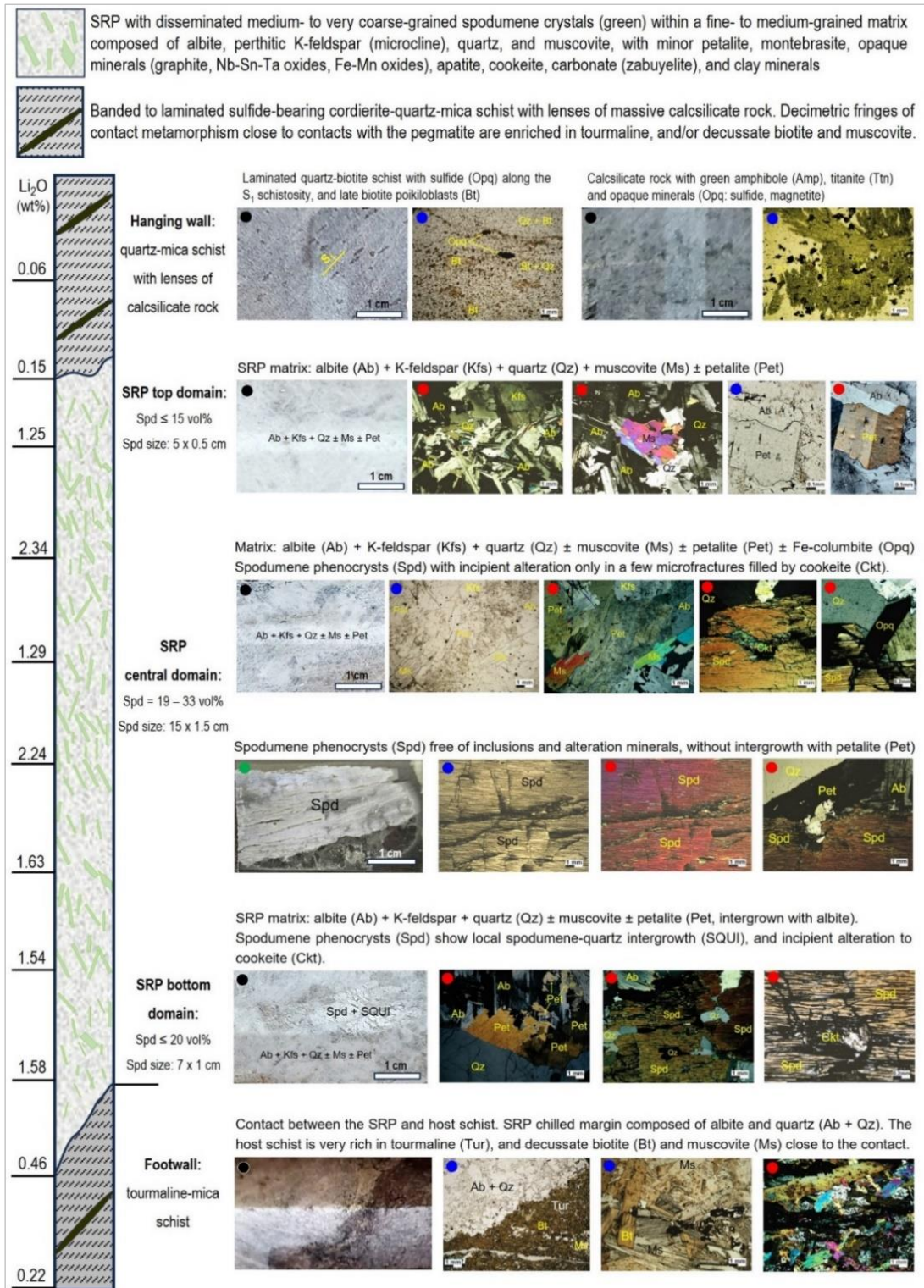


Figure 7.17: Characterization illustrated summary for a typical spodumene-rich pegmatite (SRP) of the Bandeira deposit, based on intercept with 6,75 m thick and 1.99 wt% Li₂O.

Pegmatitic textures based on average grain size (cm): fine < 2.5; medium = 2.5–10; coarse = 10–30; and very coarse > 30. Spd size (e.g., 15 x 1.5 cm) based on average length and thickness of spodumene crystals. Photo types indicated by dots: black, photo from unpolished sample; blue, photomicrography under parallel polarizers light; green, photo from polished thin section; red: photomicrography under crossed polarizers light. Drill core and thin sections described by Geologists Fabiana Guimarães and Laura Wisniowski, respectively. Figure from Pedrosa-Soares et al. (2023).

8 DEPOSIT TYPES

The following text and illustrations were compiled from Pedrosa-Soares et al. (2023) and complemented with data from Lithium Ionic public and internal reports, if not otherwise specified.

According to the most accepted petrologic-metallogenetic classification of pegmatites, published by Cerný (1991) and updated by Cerný and Ercit (2005) and Cerný et al. (2012), all the spodumene-rich pegmatites found within the Bandeira deposit, as well as in the whole Cachoeira Pegmatite Group, belong to the rare element class, Li subclass, and albite-spodumene type.

Although generally included in the LCT (Lithium-Cesium-Tantalum) family, the non- to poorly zoned spodumene-rich pegmatites (SRP) found in the Bandeira deposit, as well as all the orebodies mined in CBL's Cachoeira Mine since the 1990's (Romeiro and Pedrosa-Soares, 2005), the Xuxa and other spodumene-rich deposits of Sigma Lithium (Sá, 1977; Delboni et al., 2023), and the Outro Lado deposit of Lithium Ionic, are rather poor both in Ta and Cs when compared with the complex zoned LCT pegmatites (e.g., Generosa, Jenipapo, Murundu, Urubu and others) found in the Itinga Pegmatite Field (cf. Sá, 1977; Romeiro, 1998; Quéméneur and Lagache, 1999; Dias, 2015) and elsewhere (e.g., Cerný 1991; London, 2008; Cerný et al., 2012).

The SRP deposits consist of non-zoned to poorly zoned spodumene-rich pegmatites with spodumene reaching up to 35 vol% on average, and the total modal content of spodumene, albite, K-feldspar, quartz, and white mica (muscovite and/or Li-rich mica) summing up more than 90 vol% of the whole body. Therefore, SRP bodies are very poor in accessory minerals, which are generally represented by Li-micas, Li-phosphates, Nb-Sn-Ta oxides, cookeite, carbonate and graphite. They are also poor in secondary (metasomatic) units due to their rather fluid-poor (anhydrous) nature (Figure 7.12, Figure 7.16, and Figure 7.17).

As a corollary, the scarcity of rare elements, except for lithium, imposes constraints on the geochemical prospecting methods to be applied on searching for spodumene-rich deposits. Conversely, the high Li content (1.4 wt% Li₂O on average) in SRP-type magmas promotes a significant decrease in the crystallization temperature and viscosity of the silicate melt, leading to the high mobility that allows such a Li-rich magmas to crystallize as very large but relatively narrow SRP bodies, with hundreds to thousands of meters in length and width, but only decimeters to a few decameters in thickness.

Therefore, for prospection and exploration work related to spodumene-rich deposits, it is very important to distinguish between the non- to poorly zoned spodumene-rich pegmatites (SRP, i.e., pegmatites of the albite-spodumene type) and the complex zoned LCT pegmatites.

9 EXPLORATION

Fieldwork was conducted in the Bandeira deposit together with an approach that encompassed chip rock sampling, soil sampling, a trench program, structural analysis and a drilling program (see chapter 10-DRILLING). These activities objected to achieve a more profound comprehension of the local geology and the identification of potential spodumene-rich pegmatites.

9.1 Chip Rock Sampling

Despite the extensive residual soil cover, the field mapping led to the recognition of pegmatites in artisanal mines (garimpos), in situ outcrops or as fragments dispersed on the surface. Spodumene crystals were only identified in pegmatites founded in artisanal mines, and surrounding areas. The chip rock map (Figure 9.1) shows the location of each collected sample, with their respective lithium content (Li ppm), and the location of the outcropping pegmatites, mineralized in spodumene or not.

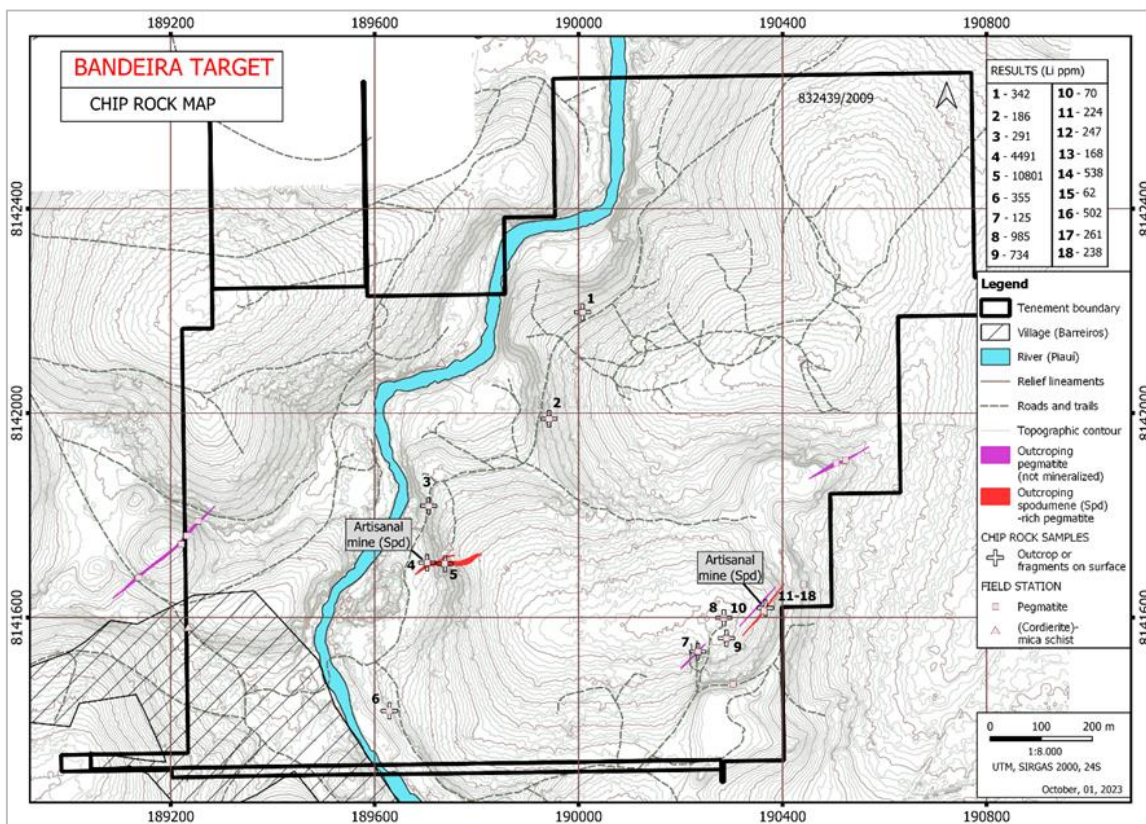


Figure 9.1: Chip Rock Map in the Bandeira Deposit emphasizing the Distribution of Each Collected Sample [Li (ppm)] and the Regions where the Pegmatites are Exposed on the Surface.

9.2 Soil Sampling Program

The soil program in the Bandeira area was conducted in two distinct campaigns. In the first survey, the lines were oriented along the azimuth N120° and were spaced at regular intervals of 250 meters. Within each of these lines, samples were collected every 50 meters. In the second campaign, the lines were oriented at N150°, were spaced at regular intervals of 150 meters and the samples were collected every 25 meters.

A total of 537 samples were collected in the Bandeira area and the content of lithium in the soil varied from 10 ppm to 573 ppm. Calculations based on the distribution of the results indicated a subdivision of the content as low grade (< 69 Li ppm); low to moderate grade (70-107 Li ppm); moderate to high grade (108-152 ppm); and high grade (> 153ppm). Based on the distribution of the results, it was possible to interpreted at least five high grade anomalous zones that represent more favorable spots to prospect spodumene-rich pegmatites (Figure 9.2). These anomalous

regions are strongly oriented along the NE-SW direction, which is the same strike of the regional foliation and the mapped pegmatites in the Bandeira area and adjacent region.

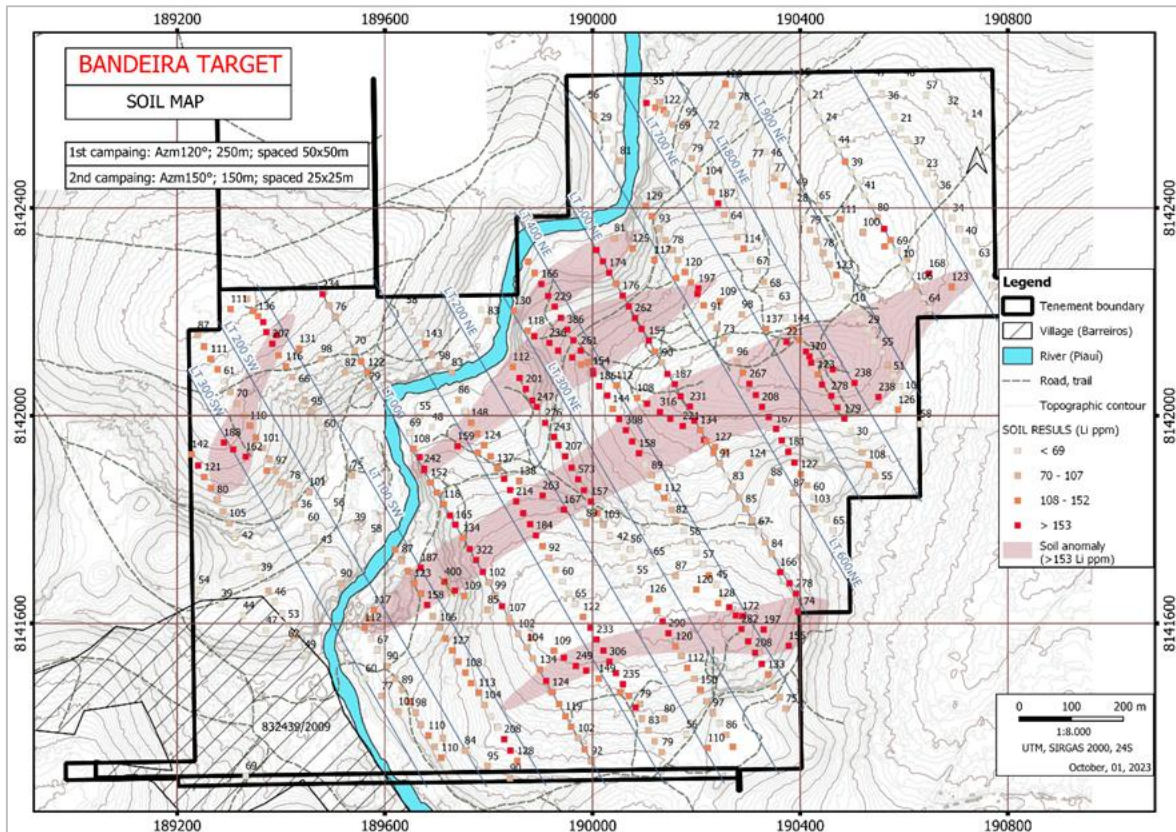


Figure 9.2: Soil Geochemical Map of the Bandeira Deposit. The Remarkable NE-SW Anomalous Trend is coincident with the Direction of the Spodumene-Rich Pegmatites.

9.3 Trench Program

After the soil geochemistry survey, a trench program was devised to investigate the anomalous areas. A total of 22 trenches were executed, totaling 1401m of excavated lines (see Table 9.1). The trenches were preferably positioned on top of the soil anomalies and the majority were positive, with pegmatite intercepts (Figure 9.3). Due to the high weathering, the exposed pegmatites are very decomposed in some trenches, exhibiting a characteristic whitish color that show a significant contrast with the host schist (see example of trench ITTRE-22-006 in Figure 9.4 a and b). These pegmatites are friable, and it was possible to diagnose only quartz, kaolin and flake muscovite. In other trenches, however, it was possible to observe more preserved pegmatites, with visible spodumene centimetric crystals (see example of trench ITTRE-22-001 in Figure 9.4 c and d). Independent of the conservation state, as part of the procedure, every pegmatite higher than 30cm mapped in the trench was sampled to verify the lithium content (see channel sampling line on the pegmatite excavated in trench ITTRE-22-001 shown in the scheme of Figure 9.4 e).

In addition to confirming the presence of pegmatites and studying their mineral composition, the trenches played an important role in determining the strike and dip of the dikes. This valuable information contributed significantly to the mapping of the area and provided a higher level of confidence in planning the boreholes for the drilling campaign.

Table 9.1: Summary of the Trenches Executed in the Bandeira Deposit.

| TRENCH | X | Y | Z | AZIMUTH (°) | DIP (°) | LENGHT (m) |
|---------------|--------|---------|-----|-------------|---------|------------|
| ITTRE-22-001 | 189772 | 8141689 | 296 | 308 | 0 | 43 |
| ITTRE-22-002 | 190395 | 8141705 | 304 | 155 | 0 | 67 |
| ITTRE-22-003 | 190156 | 8142046 | 336 | 150 | 0 | 41 |
| ITTRE-22-003B | 190158 | 8142055 | 336 | 146 | 0 | 11 |
| ITTRE-22-004 | 189960 | 8141898 | 298 | 155 | 0 | 45 |
| ITTRE-22-005 | 190401 | 8142141 | 343 | 151 | 0 | 47 |
| ITTRE-22-006 | 190451 | 8142056 | 343 | 150 | 0 | 52 |
| ITTRE-22-007 | 190292 | 8142082 | 340 | 149 | 0 | 50 |
| ITTRE-22-008 | 190055 | 8141994 | 324 | 150 | 0 | 79 |
| ITTRE-22-009 | 189941 | 8142179 | 325 | 150 | 0 | 74 |
| ITTRE-22-010 | 189888 | 8142019 | 279 | 150 | 0 | 91 |
| ITTRE-22-011 | 190001 | 8141581 | 324 | 150 | 0 | 140 |
| ITTRE-22-012 | 190077 | 8142201 | 311 | 149 | 0 | 51 |
| ITTRE-22-014 | 190280 | 8141600 | 325 | 150 | 0 | 53 |
| ITTRE-22-015 | 190480 | 8141902 | 317 | 150 | 0 | 8 |
| ITTRE-22-016 | 190124 | 8141624 | 353 | 150 | 0 | 66 |
| ITTRE-22-017 | 190319 | 8142037 | 335 | 150 | 0 | 109 |
| ITTRE-22-018 | 190189 | 8141789 | 339 | 150 | 0 | 102 |
| ITTRE-22-020 | 190543 | 8142143 | 340 | 150 | 0 | 51 |
| ITTRE-23-014A | 190244 | 8141651 | 324 | 150 | 0 | 53 |
| ITTRE-23-021 | 189819 | 8141408 | 350 | 150 | 0 | 98 |
| ITTRE-23-023 | 189335 | 8141926 | 350 | 330 | 0 | 70 |
| Total | | | | | | 1401 |

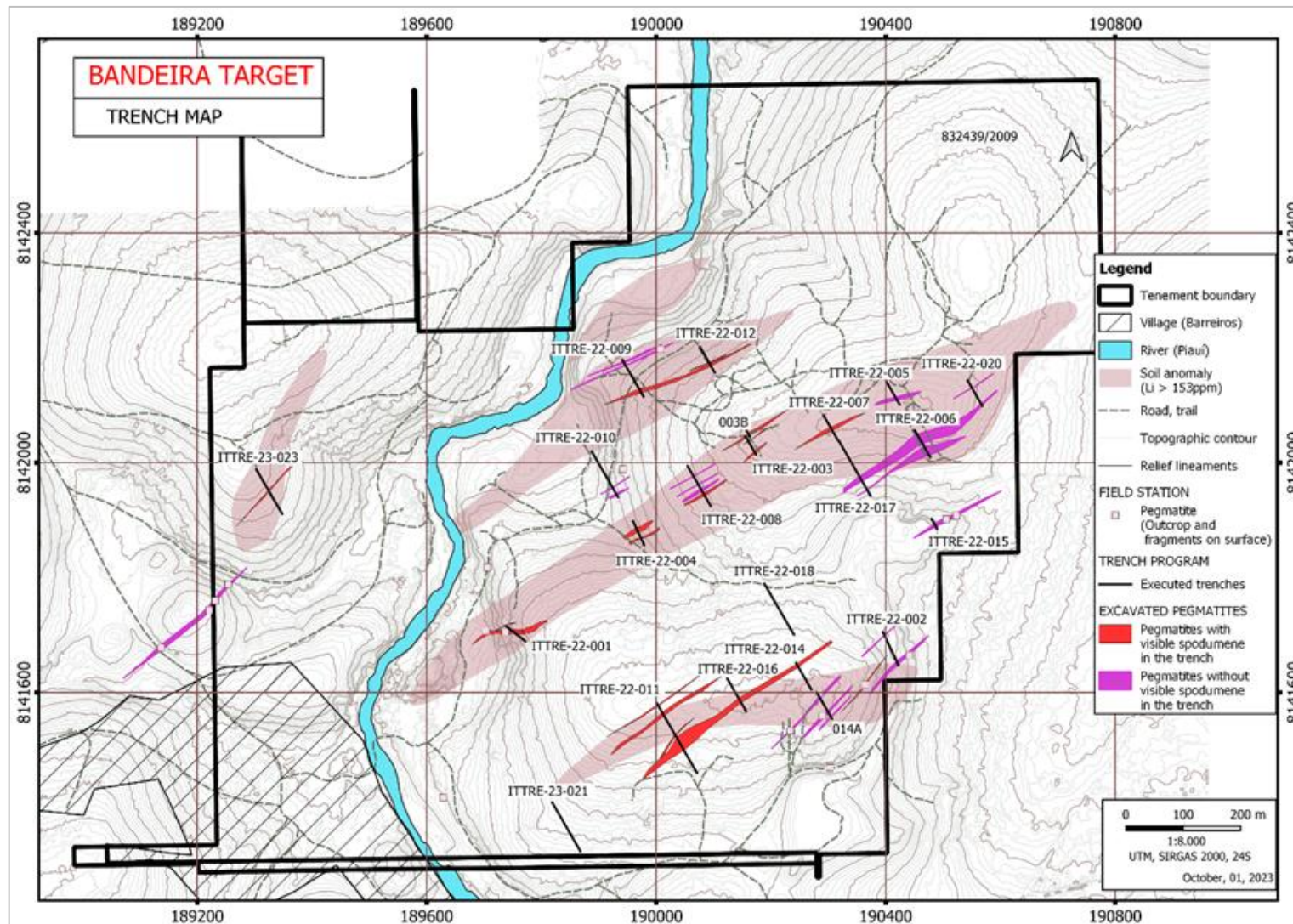
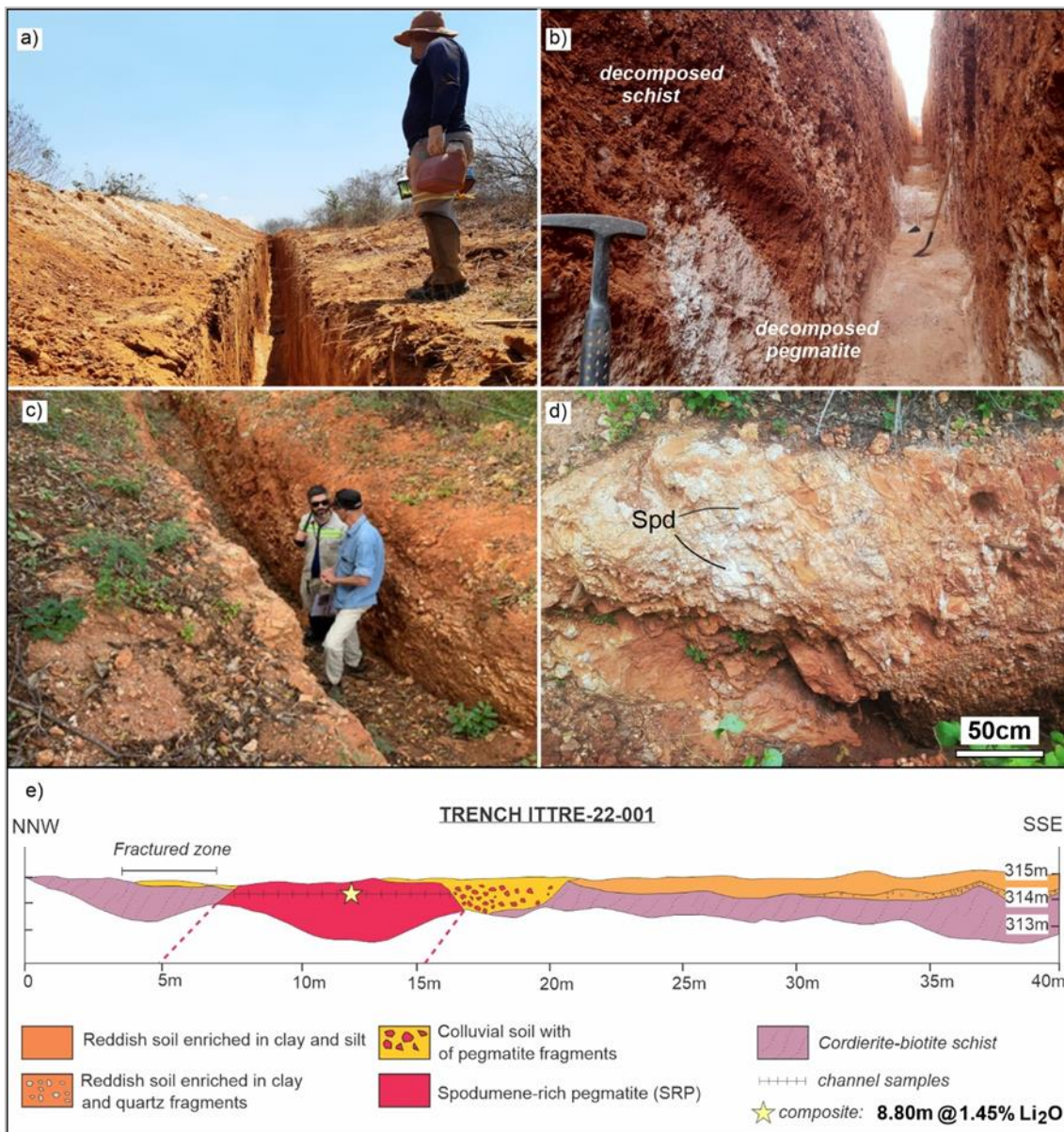


Figure 9.3: Trench Map of the Bandeira Deposit. Twenty-two trenches were executed, preferably in the soil anomalous region. Most of them intercepted pegmatites.



9.4 Structural Analysis

Although lacking outcrops, the few exposures of mica schists from the Salinas Formation are very relevant and helpful to understanding the structures in the Bandeira deposit. Ductile and brittle structures are recognized. The ductile structures were produced during the progressive metamorphism related to the syn-collisional phase of the Araçuaí orogen. In contrast, the brittle structures are younger and have been interpreted as related to the gravitational collapse of the orogen during the post-collisional phase. The structural map of the Bandeira target (Figure 9.5) shows the distribution of the structures and the projection of the non-exposed pegmatites. In that case, the attitude of each body was measured considering the interpreted geological model.

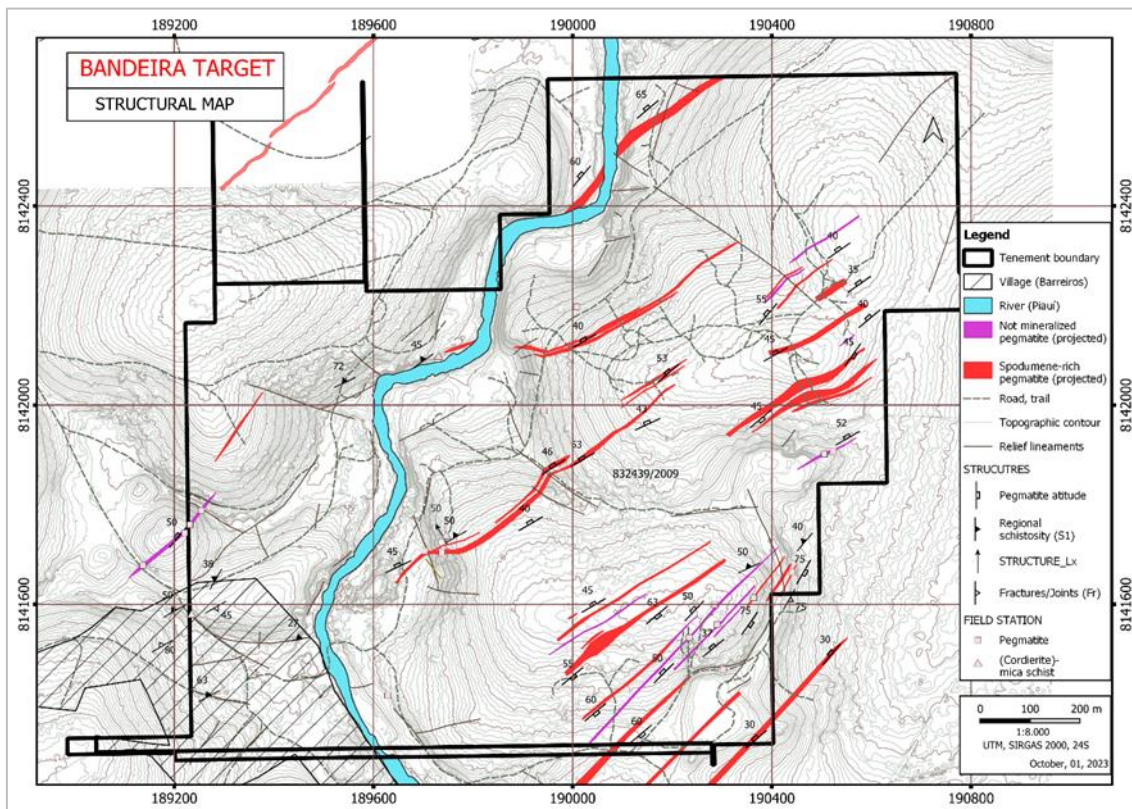


Figure 9.5: Structural Map of the Bandeira Target emphasizing the Distribution of the Mapped Structures.

Not that the pegmatites veins are projections of the known intrusions based on the intercepts in drillholes. The attitude of each of vein is based on the modeled veins.

The dominant ductile structural feature is the pervasive regional schistosity (S1), which exhibits a consistent orientation in both strike and dip across the entire area (modal: N50E/45NW). The stretched lineation (Lx) complements the ductile structural framework, often manifested as elongated micas or ellipsoidal cordierite porphyroblasts crystallized along S1. This lineation is downdip and indicates tectonic transport along the NW-SE direction.

The brittle structures are represented by a series of fractures, occasionally joints, that intersect the S1 schistosity and seem part of a conjugate system (Figure 9.6). Each structure was denoted as either F1 (fractures with a moderate dip to the southeast) or F2 (sub-vertical fractures), and their presence and prevalence may vary depending on the outcrop. The F1 structure seems more pervasive in the entire region, which also allows the interpretation of these structures as related to the development of a cleavage fracture system (secondary foliation S2). All these planar structures in the Bandeira area (S1, F1 and F2) consistently display a standard orientation along the NE-SW strike, with variations only in their dip angles.

Understanding the structural patterns in the host rocks is crucial for prospecting pegmatites since these structures serve as the surfaces that guide the migration of the silicate magmatic residues. Consequently, they profoundly influence the shape and continuity of the pegmatite bodies enriched in spodumene in the Bandeira area.

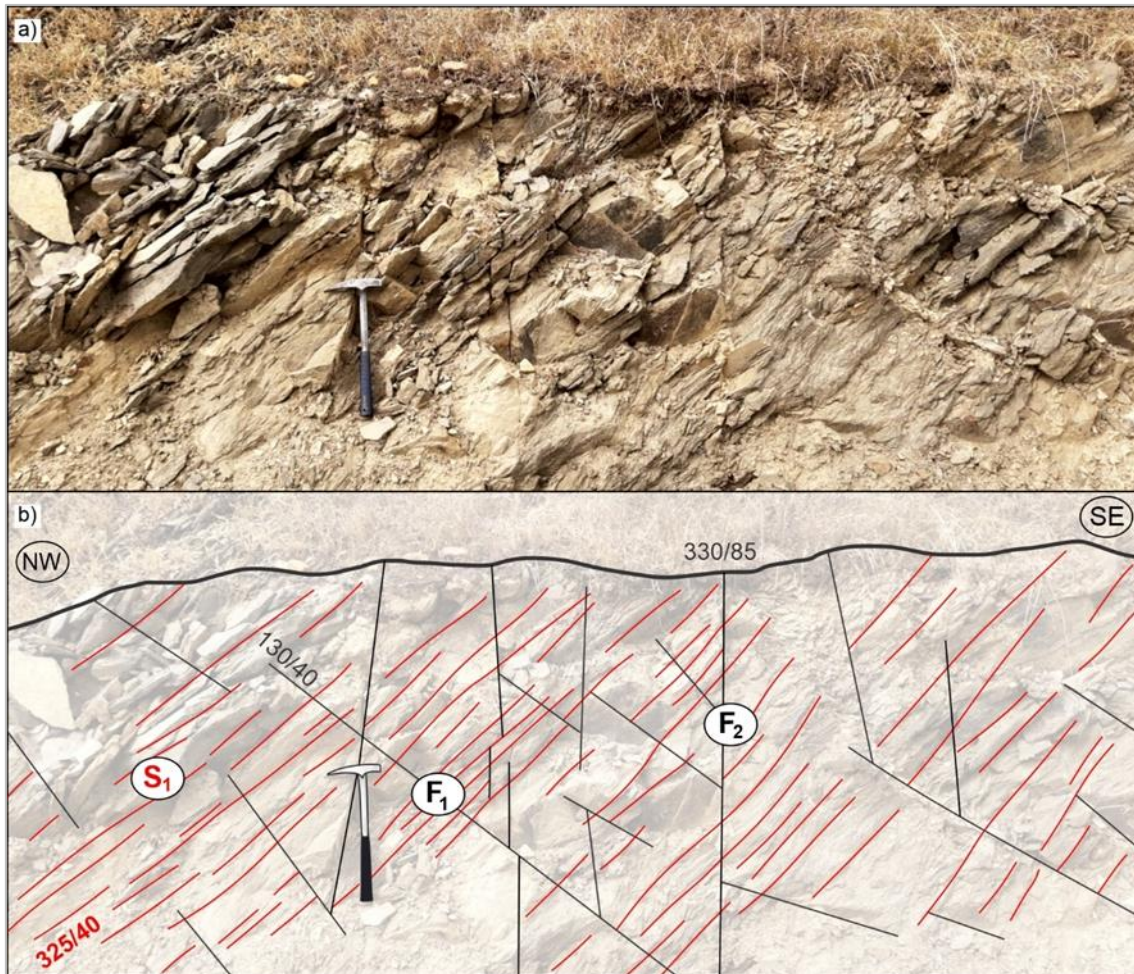


Figure 9.6: a) fractured biotite-schist in the Bandeira area (UTM: 189,232 / 8,141,577); b) scheme emphasizing the interpreted structures in the same outcrop (a): regional ductile foliation (schistosity S_1) and spaced brittle structures possibly related to conjugated system (F_1 , with moderate dip to southeast; and F_2 , subvertical).

9.5 Geophysical Surveys

A small-scale geophysical survey consisting of Induced Polarization was conducted on both Bandeira and Outro Lado prospects in 2022.

Induced polarization (IP) and resistivity (RES) are commonly used to delineate the resistive or conductive portions of the pegmatites subsurface. Although common in use by some operators, the inverted data is not always helpful or productive in the very early stages of exploration; however, in the case of Lithium Ionic, there were sufficient outcrops to measure some attitude data, so the general trend of the pegmatites could be extrapolated using the subsurface IP anomalies. Energy-induced data were acquired through the dipole-dipole arrangement in two distinct areas: Area 1 involved six lines and totaled 5,150 m linear. Area 2 had five lines totaling 2,850 m linear profiling executed in March and April 2022.

The principle for this prospecting method is based on the injection of current through several electrodes into the ground. Data acquired depended on the resistivity values at each point, terrain geometry and the electrodes' geometric arrangement (arrays). For an uninterrupted flow of current, the induced polarization depends on the terrain's impedance and the current's frequency. The induced polarization can be measured in the time and frequency domains. Despite being complex, IP resembles the discharge of a capacitor (time domain), or the impedance variation of an alternating current (frequency domain) can be measured. Once processed, the raw data can be viewed in 2D or, if available, in a 3D environment. Resistivity and induced polarization data were acquired in Areas 1 and 2 with the dipole-dipole arrangement (AB=MN=25 m). The map in

Figure 9.7 shows the location of the lines and measuring stations of the Chargeability and Resistivity data. Some pseudo-sections of apparent chargeability and apparent resistivity 2D models of the processed data are shown below.



Source: Stevanato, 2022

Figure 9.7: Location of the Lines and Measuring Stations of the Chargeability and Resistivity data of Area 1 and Area 2 of the Lithium Project.

The top panels of Figure 9.8 to Figure 9.11 show some examples of the actual chargeability sections and the lower panels the real resistivity sections of some of the lines, are shown below.

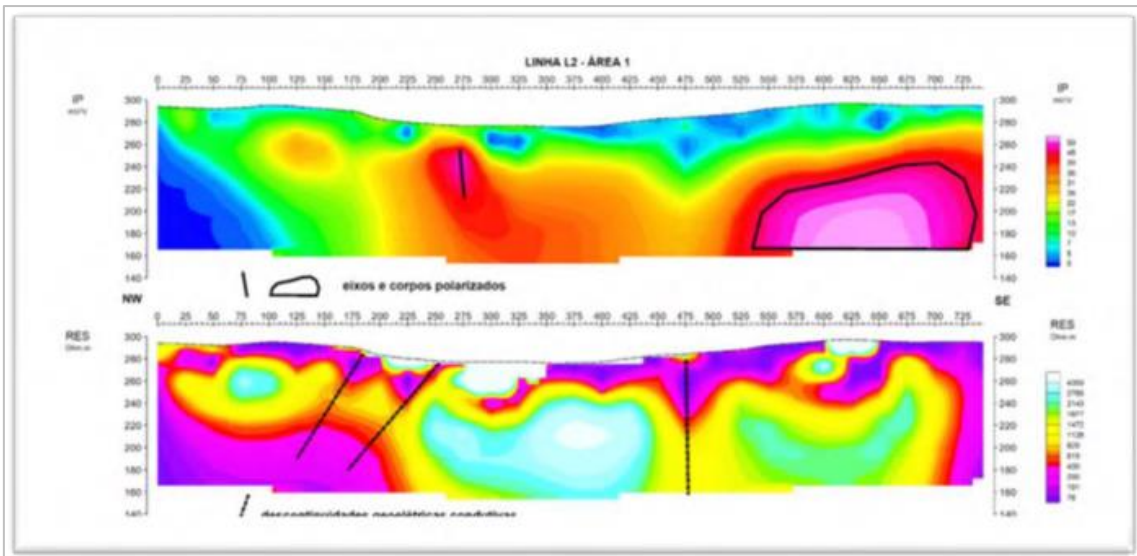


Figure 9.8: Depth Model of the Chargeability (Top Panel) and the Actual Resistivity (Bottom Panel) of Line 2 of Area 1.

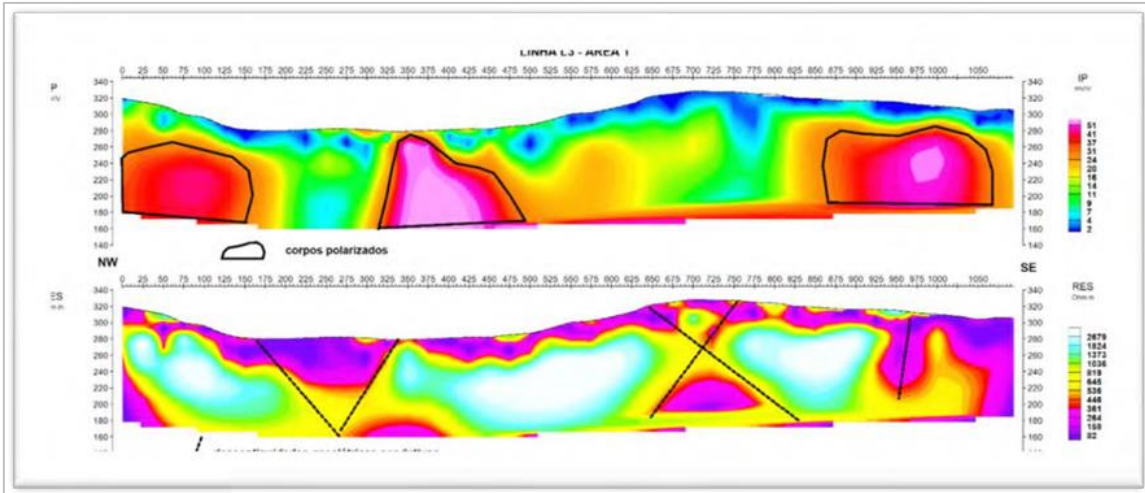


Figure 9.9: Depth Model of the Actual Chargeability (Top Panel) and the Actual Resistivity (Bottom Panel) of Line 3 of Area 1.

Source: Stevanato, 2022.

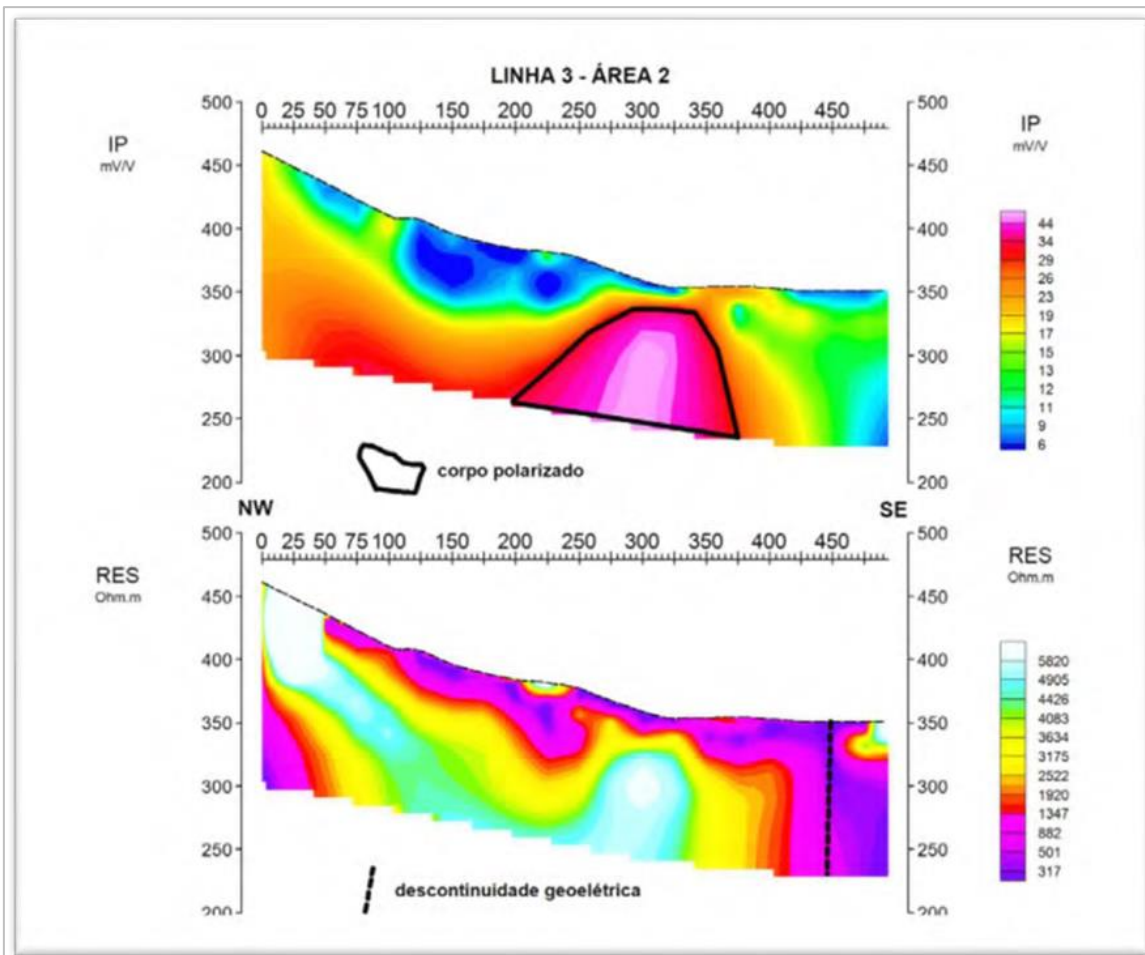


Figure 9.10: Depth Model Chargeability (Top Panel) and Resistivity (Bottom Panel) of Line 3 Area 2.

Source: Stevanato, 2022.

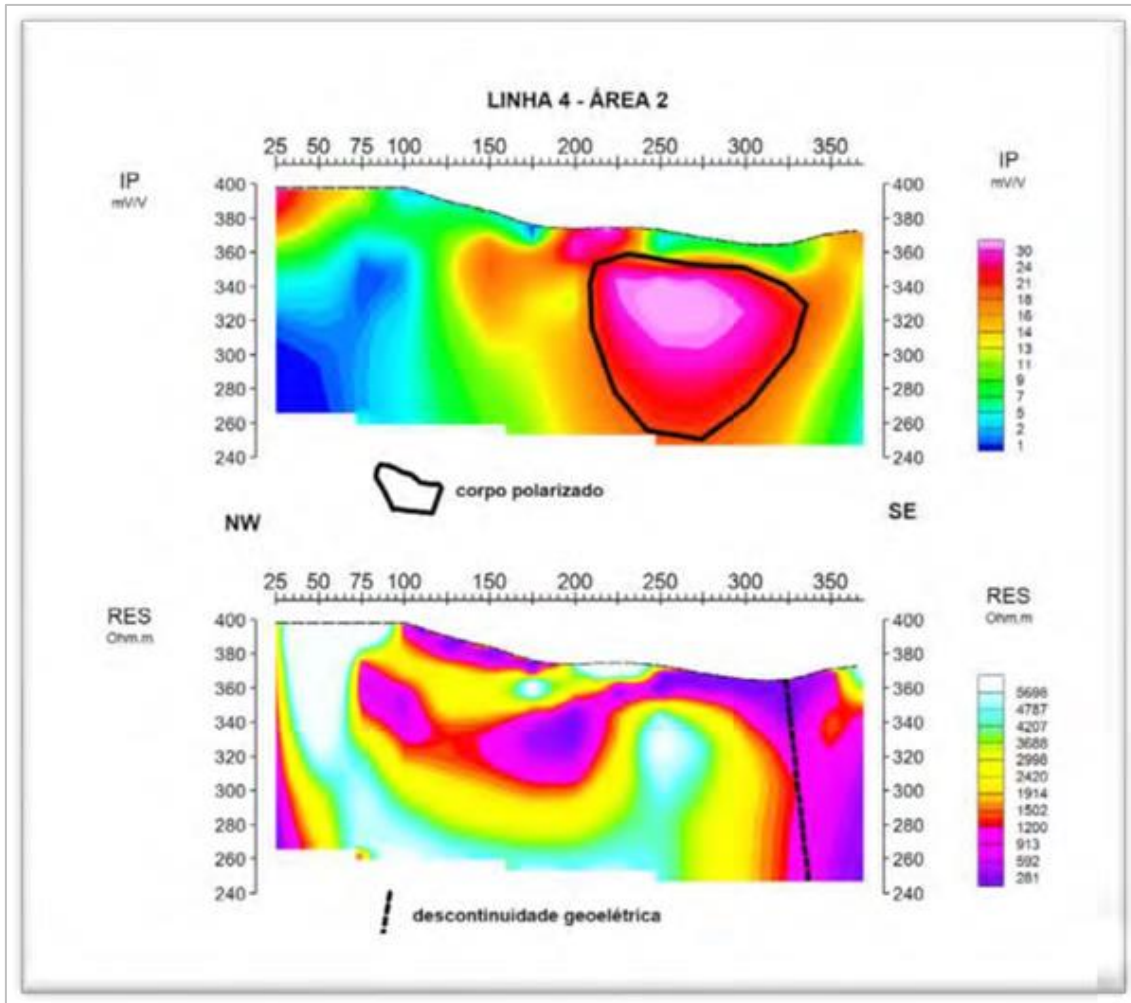


Figure 9.11: Depth Model Chargeability (Top Panel) and Resistivity (Bottom Panel) of Line 4 Area 2.
 Source: Stevanato, 2022.

The Geophysical-Geological model was designed from the accurate resistivity data of Line 3 of Area 1. This model was parameterized from the log data of the ITDD-22-001 rotary drilling and is composed of a unit of shales throughout the length measured by geophysics. Superimposed on this homogeneous unit is another consisting of soil and conductive shale that in the probing carried out intercepted the pegmatite lenses to a depth of 13.7 meters. Other interpretations suggest the presence of conductive geoelectric discontinuities that probably correspond to fault and/or fracture systems.

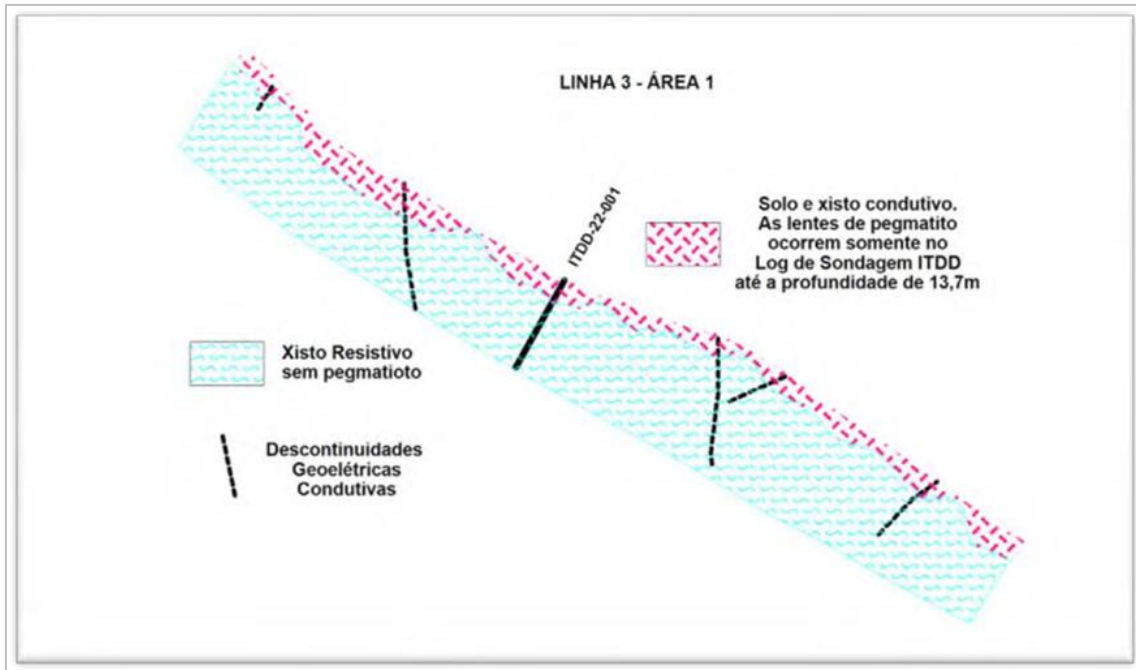


Figure 9.12: Conceptual Geological Model from Geophysics Data.

Source: Stevanato, 2022.

The inverted data was reviewed by Lithium Ionic geoscientists to determine some baseline information to choose a general attitude of the pegmatitic dykes and, if possible, to assist in designing some drill hole targets.

10 DRILLING

10.1 Lithium Ionic Drilling Campaigns

As of August 30, 2023, Lithium Ionic has successfully executed 182 diamond drill holes within the Bandeira Property, as detailed in Table 10.1 to Table 10.3 and Figure 10.1.

All diamond drilling activities conducted within the Bandeira Property until August 2023 have been incorporated into the Mineral Resource estimation process. It is important to note that any drill holes completed in 2023 after this date, as well as pending sample assay results, have not been considered in the present resource statement.

Table 10.1: Bandeira Drill Holes Summary.

| Drill Type | Year | Number Drill | Length (m) |
|------------|--------------|--------------|---------------|
| DDH | 2022 | 52 | 5,930 |
| | 2023 | 130 | 33,749 |
| | Total | 182 | 39,679 |

10.2 Drill Type

All drilling operations were conducted using core techniques with NQ core size specifications, featuring a 47.6 mm core diameter. This approach was chosen to ensure the retrieval of pristine and representative core samples, which are essential for accurate geological logging, adequate sample support, and to secure a material supply for future metallurgical testing purposes.

10.3 Lithium Ionic Drilling Campaigns

Three Brazilian-based companies undertook the 2022-2023 Drill Program in Bandeira:

- Servdrill Perfuração e Sondagens Ltda (<http://servdrill.com.br/>);
- Servitec Foraco Sondagem AS (<https://www.foraco.com.br/>);
- GEOSOL Ltda (<https://www.geosol.com.br/>).

10.4 Drill Collar Monuments

All Drill Core Monuments were surveyed by a Differential GPS and the monuments were placed by the driller once the hole had been completed.

10.5 Drillhole Surveying

The drill holes were drilled with a plunge between 50° to 90°. Core holes are generally oriented at azimuth 340° and 152°, perpendicular to both general orientations of the pegmatite intrusions.

Lithium Ionic used the REFLEX GYRO IQ downhole survey tool to obtain all downhole survey data.

According to The REFLEX GYRO-IQ™ website, the tool can maintain high accuracy of surveys. The device is connected to a cloud-based data hub, with a secure chain of custody and QA/QC application with real-time access to drilling survey data. Data transfer from field to office ensures minimum clerical errors related to processing and interpretation.

Lithium Ionic rented the downhole Reflex tool and completed all hole surveys at various locations and attitudes, where all necessary survey were done in real-time. Lithium Ionic staff had quick access to results through the cloud-based data hub. The design of the high-speed survey allowed Lithium Ionic field staff (including geologists and drillers) to obtain the following:

- Survey speeds of more than 150 meters surveyed per minute,

- There were no significant issues with the accuracy of results, which was confirmed once holes were plotted on a 3D modelling software.
- Continuous survey data comes from the tool's north-seeking sensors assisted with GPS.

The report's authors have no way to verify the accuracy of the survey method; hence, the authors will rely on the statements and information provided by Lithium Ionic.

10.6 Core Orientation

Lithium Ionic began implementing REFLEX ACT III to establish core orientation for drill holes within the Bandeira project after July 2023. As of the effective date, core orientation has been determined for four drill holes. Lithium Ionic has consistently integrated core orientation into its drilling program and will now prioritize its application in strategically significant sections of the geological model moving forward.”

The Reflex core orientation system is based on recovering the core barrel orientation after a run. The Reflex orientation tool begins the orientation process by inserting the device in the core barrel using a specially made shoe. The tool records core barrel orientation each minute during a core run. The Reflex sleeve that attaches to the upper drill rod measures the direction of the top-of-hole using built-in accelerometers. Upon completion of a run, the drill string is left undisturbed while the communication tool, which is on the surface, counts down the time to the next reading; after this, the barrel can be withdrawn. On the surface, the tool is inserted into the end of the barrel, and the barrel is rotated until it indicates that the barrel is in the same up-down position as it was in the hole. The core, barrel, and shoe are then marked using a level to confirm verticality upward position. After the line is split, the top of the core marks is transferred along the length of the recovered core.

The report's authors have no way to verify the accuracy of the orientation method; the authors will rely on the statements and information provided by Lithium Ionic.

10.7 Drill Core Chain custody

The drill cores are primarily stored in plastic or wooden boxes.

It is always transported by the drilling companies from the drilling site directly to the Lithium Ionic core sheds in Araçuaí. Lithium Ionics's staff receives all core boxes delivered.

10.8 Core Logging Procedures

Lithium Ionic adheres to a core logging methodology, carried out by geologists and technicians.

In summary, the following procedures are conducted:

- Preparation of drilling site.
- Collar Drilling location.
- Verify and validate meterage and quality of drill cores in the field.
- Core survey drilling.
- Photographs of the core box.
- Detailed petrographic and geological structural core logging.
- Geotechnical logging (RQD, weathering types).
- Sample geochemistry logging programming and QAQC procedures.

- Drill core density determinations for each programmed sample.
- Core sample preparation for geochemistry analysis.
- Logistics protocols for sending samples to the laboratory.

Each procedure has its respective sheet and is stored in digital form within Lithium Ionic customized database system.

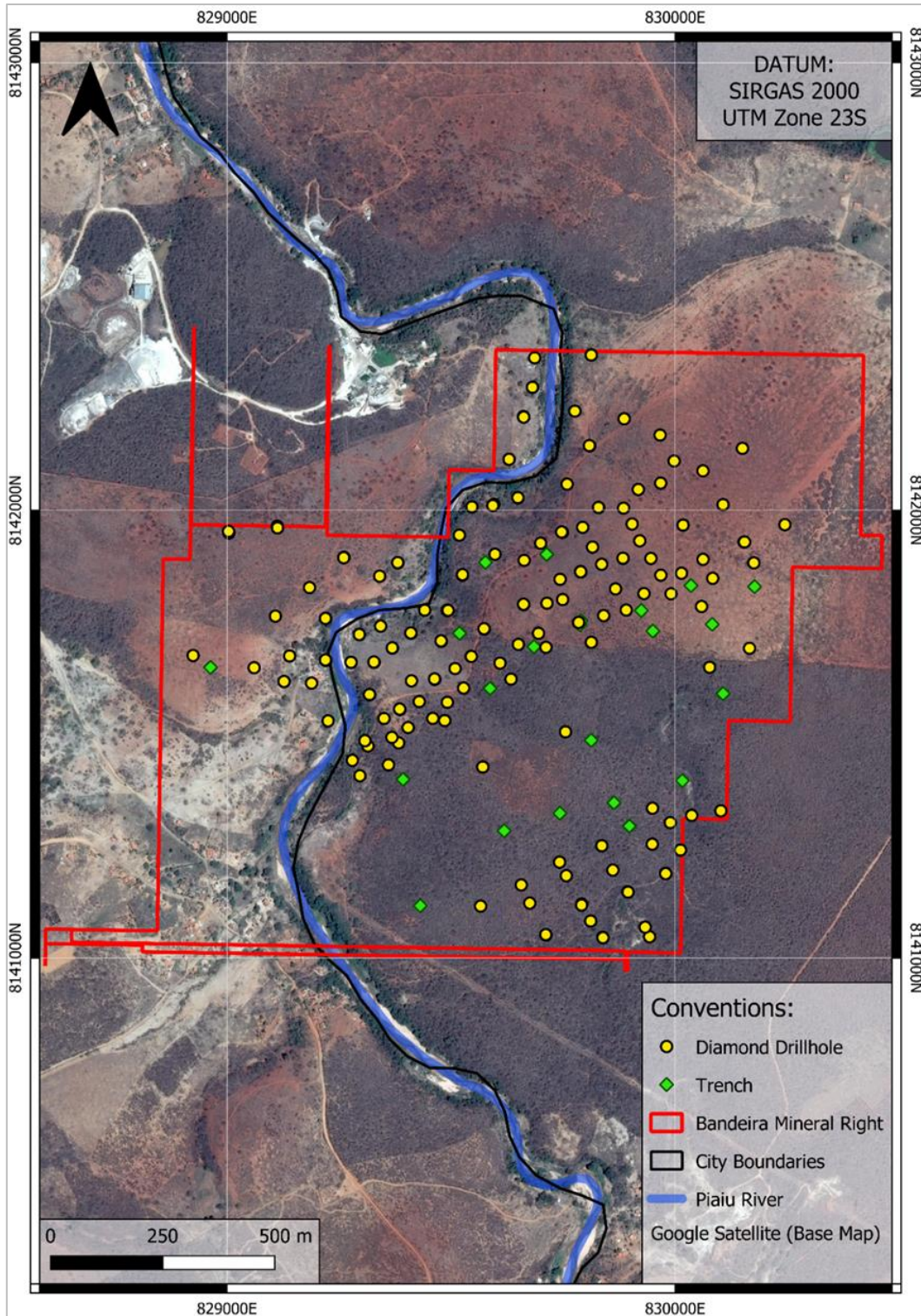


Figure 10.1: Lithium Ionic Drill Holes and Trenches

Table 10.2: Bandeira Drill Holes.

| HOLE-ID | LOCATION-X | LOCATION-Y | LOCATION-Z | maxdepth | METHOD | Year | HOLE-ID | LOCATION-X | LOCATION-Y | LOCATION-Z | maxdepth | METHOD | Year | HOLE-ID | LOCATION-X | LOCATION-Y | LOCATION-Z | maxdepth | METHOD | Year |
|--------------|------------|------------|------------|----------|--------|------|-------------|------------|------------|------------|----------|--------|------|-------------|------------|------------|------------|----------|--------|------|
| ITDD-22-001 | 189738 | 8141720 | 296 | 101 | DDH | 2022 | ITDD-22-038 | 190379 | 8142276 | 327 | 150 | DDH | 2022 | ITDD-23-079 | 190483 | 8141640 | 320 | 171 | DDH | 2023 |
| ITDD-22-002 | 189760 | 8141770 | 302 | 96 | DDH | 2022 | ITDD-22-039 | 190284 | 8142238 | 331 | 150 | DDH | 2022 | ITDD-23-080 | 190241 | 8142509 | 305 | 310 | DDH | 2023 |
| ITDD-22-003 | 190330 | 8141641 | 323 | 60 | DDH | 2022 | ITDD-22-040 | 190063 | 8141421 | 306 | 151 | DDH | 2022 | ITDD-23-081 | 190418 | 8141628 | 304 | 172 | DDH | 2023 |
| ITDD-22-004 | 190153 | 8142051 | 336 | 76 | DDH | 2022 | ITDD-22-041 | 190467 | 8142324 | 338 | 151 | DDH | 2022 | ITDD-23-082 | 190009 | 8142326 | 275 | 298 | DDH | 2023 |
| ITDD-22-004B | 190153 | 8142051 | 336 | 40 | DDH | 2022 | ITDD-22-042 | 190606 | 8142283 | 341 | 110 | DDH | 2022 | ITDD-23-083 | 190017 | 8142506 | 275 | 420 | DDH | 2023 |
| ITDD-22-005 | 190183 | 8142008 | 336 | 68 | DDH | 2022 | ITDD-22-043 | 190143 | 8141485 | 314 | 151 | DDH | 2022 | ITDD-23-084 | 189625 | 8142181 | 306 | 305 | DDH | 2023 |
| ITDD-22-006 | 190116 | 8142101 | 331 | 125 | DDH | 2022 | ITDD-22-044 | 190420 | 8142398 | 334 | 202 | DDH | 2022 | ITDD-23-085 | 190246 | 8141501 | 315 | 115 | DDH | 2023 |
| ITDD-22-007 | 189861 | 8141823 | 302 | 71 | DDH | 2022 | ITDD-22-045 | 190536 | 8142005 | 333 | 101 | DDH | 2022 | ITDD-23-086 | 190241 | 8142509 | 305 | 341 | DDH | 2023 |
| ITDD-22-008 | 189744 | 8141782 | 299 | 75 | DDH | 2022 | ITDD-22-046 | 190179 | 8141423 | 305 | 120 | DDH | 2022 | ITDD-23-087 | 190322 | 8141375 | 296 | 90 | DDH | 2023 |
| ITDD-22-009 | 190426 | 8142095 | 345 | 110 | DDH | 2022 | ITDD-22-047 | 190507 | 8142451 | 340 | 157 | DDH | 2022 | ITDD-23-088 | 190118 | 8142359 | 300 | 304 | DDH | 2023 |
| ITDD-22-010 | 190379 | 8142168 | 341 | 4 | DDH | 2022 | ITDD-22-048 | 190448 | 8141960 | 326 | 100 | DDH | 2022 | ITDD-23-089 | 190371 | 8141611 | 317 | 184 | DDH | 2023 |
| ITDD-22-011 | 189803 | 8141864 | 292 | 100 | DDH | 2022 | ITDD-22-050 | 190200 | 8142183 | 327 | 151 | DDH | 2022 | ITDD-23-090 | 190037 | 8142639 | 276 | 589 | DDH | 2023 |
| ITDD-22-012 | 189901 | 8141897 | 288 | 100 | DDH | 2022 | ITDD-22-049 | 190179 | 8141421 | 305 | 109 | DDH | 2022 | ITDD-23-091 | 189367 | 8142228 | 335 | 544 | DDH | 2023 |
| ITDD-22-013 | 189881 | 8141940 | 284 | 100 | DDH | 2022 | ITDD-23-051 | 190101 | 8141351 | 298 | 91 | DDH | 2023 | ITDD-23-092 | 189847 | 8142001 | 277 | 130 | DDH | 2023 |
| ITDD-22-014 | 189784 | 8141910 | 285 | 103 | DDH | 2022 | ITDD-23-052 | 190166 | 8142446 | 294 | 481 | DDH | 2023 | ITDD-23-093 | 190200 | 8141385 | 302 | 75 | DDH | 2023 |
| ITDD-22-015 | 189675 | 8141694 | 275 | 51 | DDH | 2022 | ITDD-23-053 | 190109 | 8142146 | 325 | 141 | DDH | 2023 | ITDD-23-094 | 189943 | 8142030 | 300 | 109 | DDH | 2023 |
| ITDD-22-016 | 189980 | 8141955 | 308 | 103 | DDH | 2022 | ITDD-23-054 | 189739 | 8141981 | 275 | 145 | DDH | 2023 | ITDD-23-095 | 189746 | 8142172 | 277 | 250 | DDH | 2023 |
| ITDD-22-017 | 189725 | 8141824 | 293 | 100 | DDH | 2022 | ITDD-23-055 | 190101 | 8141352 | 298 | 130 | DDH | 2023 | ITDD-23-096 | 189942 | 8142031 | 300 | 118 | DDH | 2023 |
| ITDD-22-018 | 190064 | 8142024 | 326 | 154 | DDH | 2022 | ITDD-23-056 | 190228 | 8141350 | 299 | 76 | DDH | 2023 | ITDD-23-097 | 189780 | 8141805 | 299 | 49 | DDH | 2023 |
| ITDD-22-019 | 189658 | 8141728 | 276 | 102 | DDH | 2022 | ITDD-23-058 | 189739 | 8141982 | 275 | 156 | DDH | 2023 | ITDD-23-098 | 189760 | 8141845 | 294 | 350 | DDH | 2023 |
| ITDD-22-020 | 190082 | 8141993 | 327 | 91 | DDH | 2022 | ITDD-23-059 | 190229 | 8141349 | 299 | 57 | DDH | 2023 | ITDD-23-099 | 189836 | 8141914 | 284 | 79 | DDH | 2023 |
| ITDD-22-021 | 190258 | 8142082 | 339 | 131 | DDH | 2022 | ITDD-23-060 | 190165 | 8142447 | 292 | 490 | DDH | 2023 | ITDD-23-100 | 189691 | 8141761 | 278 | 50 | DDH | 2023 |
| ITDD-22-022 | 190006 | 8141920 | 311 | 100 | DDH | 2022 | ITDD-23-061 | 190281 | 8141453 | 297 | 105 | DDH | 2023 | ITDD-23-101 | 189835 | 8141915 | 284 | 100 | DDH | 2023 |
| ITDD-22-023 | 190063 | 8142225 | 304 | 149 | DDH | 2022 | ITDD-23-062 | 190163 | 8142649 | 278 | 433 | DDH | 2023 | ITDD-23-102 | 189745 | 8142173 | 277 | 262 | DDH | 2023 |
| ITDD-22-024 | 190156 | 8142264 | 313 | 180 | DDH | 2022 | ITDD-23-063 | 190281 | 8141452 | 297 | 121 | DDH | 2023 | ITDD-23-103 | 189511 | 8141957 | 273 | 221 | DDH | 2023 |
| ITDD-22-025 | 190233 | 8142129 | 335 | 130 | DDH | 2022 | ITDD-23-065 | 190130 | 8142523 | 283 | 505 | DDH | 2023 | ITDD-23-104 | 189684 | 8141773 | 278 | 67 | DDH | 2023 |
| ITDD-22-026 | 190357 | 8142121 | 342 | 121 | DDH | 2022 | ITDD-23-066 | 190332 | 8141354 | 297 | 151 | DDH | 2023 | ITDD-23-105 | 189907 | 8142302 | 277 | 421 | DDH | 2023 |
| ITDD-22-027 | 190449 | 8142159 | 342 | 109 | DDH | 2022 | ITDD-23-067 | 190364 | 8141497 | 301 | 130 | DDH | 2023 | ITDD-23-106 | 189700 | 8141948 | 279 | 142 | DDH | 2023 |
| ITDD-22-028 | 190333 | 8142162 | 339 | 112 | DDH | 2022 | ITDD-23-068 | 189692 | 8141876 | 287 | 136 | DDH | 2023 | ITDD-23-107 | 189588 | 8142044 | 273 | 241 | DDH | 2023 |
| ITDD-22-029 | 189962 | 8142198 | 299 | 171 | DDH | 2022 | ITDD-23-069 | 190364 | 8141496 | 302 | 220 | DDH | 2023 | ITDD-23-108 | 189760 | 8141846 | 294 | 95 | DDH | 2023 |
| ITDD-22-030 | 190426 | 8142200 | 337 | 110 | DDH | 2022 | ITDD-23-070 | 190163 | 8142649 | 280 | 423 | DDH | 2023 | ITDD-23-109 | 189780 | 8142016 | 275 | 316 | DDH | 2023 |
| ITDD-22-031 | 190540 | 8142196 | 339 | 130 | DDH | 2022 | ITDD-23-071 | 190332 | 8141561 | 320 | 153 | DDH | 2023 | ITDD-23-110 | 189915 | 8141968 | 288 | 72 | DDH | 2023 |
| ITDD-22-032 | 190245 | 8142309 | 320 | 163 | DDH | 2022 | ITDD-23-072 | 189691 | 8141876 | 287 | 140 | DDH | 2023 | ITDD-23-111 | 189834 | 8141827 | 299 | 41 | DDH | 2023 |
| ITDD-22-033 | 190516 | 8142242 | 339 | 100 | DDH | 2022 | ITDD-23-073 | 190016 | 8142507 | 275 | 480 | DDH | 2023 | ITDD-23-113 | 189601 | 8141814 | 273 | 109 | DDH | 2023 |
| ITDD-22-033A | 190517 | 8142242 | 339 | 22 | DDH | 2022 | ITDD-23-074 | 189848 | 8142000 | 276 | 121 | DDH | 2023 | ITDD-23-114 | 189916 | 8141968 | 288 | 92 | DDH | 2023 |
| ITDD-22-034 | 190043 | 8141461 | 311 | 121 | DDH | 2022 | ITDD-23-075 | 190395 | 8141550 | 303 | 169 | DDH | 2023 | ITDD-23-115 | 189866 | 8141864 | 294 | 48 | DDH | 2023 |
| ITDD-22-035 | 190326 | 8142368 | 320 | 205 | DDH | 2022 | ITDD-23-076 | 190009 | 8142325 | 276 | 260 | DDH | 2023 | ITDD-23-116 | 189859 | 8142069 | 276 | 139 | DDH | 2023 |
| ITDD-22-036 | 190127 | 8141515 | 317 | 121 | DDH | 2022 | ITDD-23-077 | 190220 | 8141554 | 322 | 100 | DDH | 2023 | ITDD-23-117 | 189891 | 8142149 | 297 | 220 | DDH | 2023 |
| ITDD-22-037 | 189954 | 8141411 | 305 | 122 | DDH | 2022 | ITDD-23-078 | 189625 | 8142181 | 306 | 362 | DDH | 2023 | ITDD-23-118 | 189592 | 8141949 | 273 | 184 | DDH | 2023 |

Table 10.3: Bandeira Drill Collars.

| HOLE-ID | LOCATION-X | LOCATION-Y | LOCATION-Z | maxdepth | METHOD | Year |
|-------------|------------|------------|------------|----------|--------|------|
| ITDD-23-120 | 189859 | 8142070 | 277 | 280 | DDH | 2023 |
| ITDD-23-112 | 189699 | 8141949 | 279 | 320 | DDH | 2023 |
| ITDD-23-119 | 189779 | 8142016 | 275 | 139 | DDH | 2023 |
| ITDD-23-121 | 189891 | 8142150 | 297 | 362 | DDH | 2023 |
| ITDD-23-122 | 189591 | 8141950 | 273 | 340 | DDH | 2023 |
| ITDD-23-123 | 189712 | 8142030 | 275 | 351 | DDH | 2023 |
| ITDD-23-124 | 190154 | 8142164 | 327 | 130 | DDH | 2023 |
| ITDD-23-125 | 189648 | 8141947 | 273 | 330 | DDH | 2023 |
| ITDD-23-126 | 190154 | 8142165 | 327 | 170 | DDH | 2023 |
| ITDD-23-127 | 190029 | 8142087 | 320 | 151 | DDH | 2023 |
| ITDD-23-128 | 189591 | 8141950 | 273 | 206 | DDH | 2023 |
| ITDD-23-129 | 189665 | 8142009 | 274 | 199 | DDH | 2023 |
| ITDD-23-130 | 190154 | 8142164 | 327 | 300 | DDH | 2023 |
| ITDD-23-131 | 190029 | 8142088 | 320 | 301 | DDH | 2023 |
| ITDD-23-132 | 189664 | 8142010 | 274 | 210 | DDH | 2023 |
| ITDD-23-133 | 189561 | 8141898 | 277 | 184 | DDH | 2023 |
| ITDD-23-134 | 189648 | 8141947 | 273 | 165 | DDH | 2023 |
| ITDD-23-135 | 190179 | 8142220 | 321 | 250 | DDH | 2023 |
| ITDD-23-136 | 190248 | 8142197 | 331 | 334 | DDH | 2023 |
| ITDD-23-137 | 189664 | 8142010 | 274 | 401 | DDH | 2023 |
| ITDD-23-138 | 189476 | 8142045 | 298 | 330 | DDH | 2023 |
| ITDD-23-140 | 190208 | 8142068 | 338 | 80 | DDH | 2023 |
| ITDD-23-141 | 190297 | 8142120 | 339 | 61 | DDH | 2023 |
| ITDD-23-142 | 190111 | 8142251 | 306 | 200 | DDH | 2023 |
| ITDD-23-144 | 190247 | 8142198 | 331 | 120 | DDH | 2023 |
| ITDD-23-139 | 189550 | 8142111 | 304 | 367 | DDH | 2023 |
| ITDD-23-143 | 190190 | 8142309 | 316 | 439 | DDH | 2023 |
| ITDD-23-145 | 189625 | 8142180 | 306 | 330 | DDH | 2023 |
| ITDD-23-146 | 189809 | 8142068 | 274 | 295 | DDH | 2023 |
| ITDD-23-147 | 190110 | 8142251 | 306 | 510 | DDH | 2023 |
| ITDD-23-148 | 190310 | 8142199 | 335 | 350 | DDH | 2023 |
| ITDD-23-149 | 189367 | 8142227 | 335 | 469 | DDH | 2023 |
| ITDD-23-150 | 189861 | 8142069 | 276 | 349 | DDH | 2023 |
| ITDD-23-151 | 189474 | 8142246 | 327 | 442 | DDH | 2023 |
| ITDD-23-152 | 190190 | 8142309 | 316 | 315 | DDH | 2023 |
| ITDD-23-153 | 189295 | 8141951 | 322 | 450 | DDH | 2023 |
| ITDD-23-154 | 190266 | 8142274 | 325 | 550 | DDH | 2023 |
| ITDD-23-155 | 190109 | 8142252 | 307 | 241 | DDH | 2023 |
| ITDD-23-156 | 190189 | 8142309 | 316 | 341 | DDH | 2023 |
| ITDD-23-157 | 189881 | 8142238 | 284 | 380 | DDH | 2023 |
| ITDD-23-158 | 189475 | 8142242 | 326 | 481 | DDH | 2023 |
| ITDD-23-159 | 190027 | 8142186 | 309 | 314 | DDH | 2023 |
| ITDD-23-160 | 190081 | 8142092 | 328 | 259 | DDH | 2023 |
| ITDD-23-161 | 190277 | 8142352 | 314 | 420 | DDH | 2023 |
| ITDD-23-162 | 189366 | 8142231 | 334 | 487 | DDH | 2023 |
| ITDD-23-163 | 190034 | 8142573 | 277 | 534 | DDH | 2023 |
| ITDD-23-164 | 189956 | 8142309 | 278 | 480 | DDH | 2023 |
| ITDD-23-165 | 189907 | 8142302 | 277 | 358 | DDH | 2023 |
| ITDD-23-166 | 190131 | 8141806 | 314 | 121 | DDH | 2023 |
| ITDD-23-167 | 189706 | 8142141 | 284 | 412 | DDH | 2023 |
| ITDD-23-168 | 190131 | 8141806 | 314 | 146 | DDH | 2023 |
| ITDD-23-169 | 190322 | 8142475 | 323 | 435 | DDH | 2023 |
| ITDD-23-170 | 189949 | 8141722 | 316 | 141 | DDH | 2023 |
| ITDD-23-171 | 190020 | 8141998 | 319 | 249 | DDH | 2023 |
| ITDD-23-172 | 190277 | 8142352 | 314 | 375 | DDH | 2023 |
| ITDD-23-173 | 189949 | 8141722 | 316 | 150 | DDH | 2023 |
| ITDD-23-174 | 189706 | 8142141 | 284 | 363 | DDH | 2023 |
| ITDD-23-175 | 190034 | 8142573 | 277 | 530 | DDH | 2023 |
| ITDD-23-177 | 189954 | 8142306 | 276 | 391 | DDH | 2023 |
| ITDD-23-178 | 189500 | 8141899 | 273 | 190 | DDH | 2023 |
| ITDD-23-179 | 189432 | 8141928 | 294 | 250 | DDH | 2023 |
| ITDD-23-180 | 189987 | 8142411 | 276 | 500 | DDH | 2023 |
| ITDD-23-181 | 189588 | 8142043 | 273 | 250 | DDH | 2023 |
| ITDD-23-182 | 190355 | 8142418 | 327 | 381 | DDH | 2023 |
| ITDD-23-183 | 189500 | 8141899 | 273 | 186 | DDH | 2023 |

10.9 Ore Drilling Intercepts

Drill spacing typically ranges from 50m to 150m, with narrower spacing observed in the central portion of the drill pattern and wider spacing towards the pattern's edges. The ore intercepts vary in thickness, ranging from approximately 85% of the true width to nearly the true width of the mineralization.

The average pegmatite intersection spans from 0.3m to 25m, with an average true thickness of about 5m. In total, 257 mineralized intercepts from diamond drill holes (DDH) were utilized for modelling the 23 mineralized solids within the Bandeira Project. Each solid was assigned a numerical code in the tag column.

Table 10.4 and Table 10.5 list the mineralized intervals from Bandeira drill holes that were incorporated into the 3D modeling of the mineralized solids (Figure 10.2 and Figure 10.3).

Table 10.4: Mineralized Intercepts by Bandeira Drill Holes.

| holeid | from | to | Length | Li2O% | Model | holeid | from | to | Length | Li2O% | Model | holeid | from | to | Length | Li2O% | Model | holeid | from | to | Length | Li2O% | Model |
|--------------|--------|--------|--------|-------|--------|--------------|--------|--------|--------|-------|--------|-------------|--------|--------|--------|-------|--------|-------------|--------|--------|--------|-------|--------|
| ITDD-22-001 | 8.5 | 13.7 | 5.2 | 1.53 | 1 | ITDD-22-038 | 55.73 | 56.81 | 1.08 | 0.39 | 04B-NE | ITDD-23-061 | 61.5 | 78.58 | 17.08 | 1.43 | SE-A | ITDD-23-074 | 85.77 | 89.55 | 3.78 | 1.58 | 01A-SW |
| ITDD-22-002 | 33.08 | 38.74 | 5.66 | 2.02 | 1 | ITDD-22-038 | 67.32 | 71.32 | 4 | 1.04 | 1 | ITDD-23-062 | 104.43 | 117.43 | 13 | 1.68 | 03-NE | ITDD-23-074 | 96.84 | 100.25 | 3.41 | 1.98 | 1 |
| ITDD-22-006 | 54.9 | 57.6 | 2.7 | 2.23 | 1 | ITDD-22-038 | 98.13 | 104.85 | 6.72 | 1.24 | 04-NE | ITDD-23-062 | 119.43 | 124.43 | 5 | 2.03 | 03-NE | ITDD-23-075 | 130.1 | 141.9 | 11.8 | 1.00 | SE-B |
| ITDD-22-007 | 21.62 | 27.58 | 5.96 | 1.33 | 1 | ITDD-22-039 | 86.24 | 91.95 | 5.71 | 2.13 | 1 | ITDD-23-062 | 349.55 | 353.47 | 3.92 | 1.05 | 04-NE | ITDD-23-076 | 82.64 | 84.05 | 1.41 | 2.03 | 02-NE |
| ITDD-22-011 | 53.14 | 59.89 | 6.75 | 1.99 | 1 | ITDD-22-039 | 94.19 | 95.86 | 1.67 | 1.71 | 04-NE | ITDD-23-062 | 384.5 | 385.6 | 1.1 | 0.67 | 04C-NE | ITDD-23-076 | 85.55 | 86.84 | 1.29 | 2.24 | 02A-NE |
| ITDD-22-012 | 37.03 | 42.03 | 5 | 1.70 | 1 | ITDD-22-043 | 38.05 | 42.41 | 4.36 | 1.43 | SE-A | ITDD-23-062 | 386.68 | 388.67 | 1.99 | 1.67 | 04C-NE | ITDD-23-076 | 167.12 | 168.98 | 1.86 | 1.43 | 1 |
| ITDD-22-013 | 53.18 | 57.08 | 3.9 | 1.56 | 01A-SW | ITDD-22-045 | 41.57 | 44.88 | 3.31 | 1.42 | 08-NE | ITDD-23-063 | 41.67 | 55.24 | 13.57 | 1.73 | SE-A | ITDD-23-078 | 321.95 | 323.43 | 1.48 | 0.86 | 1 |
| ITDD-22-013 | 62.9 | 65.66 | 2.76 | 1.66 | 1 | ITDD-22-046 | 63 | 68 | 5 | 1.17 | SE-A | ITDD-23-065 | 159.62 | 164.6 | 4.98 | 1.12 | 02-NE | ITDD-23-078 | 324.44 | 337.78 | 13.34 | 1.56 | 1 |
| ITDD-22-014 | 77.1 | 82.8 | 5.7 | 1.14 | 1 | ITDD-22-048 | 57.5 | 60.11 | 2.61 | 0.70 | 09-NE | ITDD-23-065 | 203.93 | 208.16 | 4.23 | 1.53 | 02B-NE | ITDD-23-080 | 255.45 | 256.94 | 1.49 | 2.87 | 04-NE |
| ITDD-22-015 | 6.16 | 8.74 | 2.58 | 1.04 | 1 | ITDD-22-048 | 69.39 | 74.2 | 4.81 | 1.08 | 08-NE | ITDD-23-065 | 271.2 | 277.29 | 6.09 | 2.53 | 1 | ITDD-23-080 | 260.45 | 261.66 | 1.21 | 1.99 | 04-NE |
| ITDD-22-016 | 39.5 | 45.35 | 5.85 | 1.27 | 1 | ITTRE-22-001 | 25 | 32.123 | 7.123 | 1.46 | 1 | ITDD-23-065 | 321.2 | 324.22 | 3.02 | 1.24 | 04-NE | ITDD-23-081 | 120.07 | 129.07 | 9 | 1.49 | SE-B |
| ITDD-22-017 | 62.21 | 67.15 | 4.94 | 1.06 | 1 | ITTRE-22-001 | 32.459 | 34 | 1.541 | 1.46 | 1 | ITDD-23-065 | 336.67 | 339.41 | 2.74 | 1.32 | 04C-NE | ITDD-23-082 | 50.63 | 56.4 | 5.77 | 2.17 | 02C-NE |
| ITDD-22-019 | 29.83 | 33.57 | 3.74 | 1.97 | 1 | ITTRE-22-004 | 12.8 | 15.8 | 3 | 0.70 | 01A-SW | ITDD-23-065 | 354.23 | 378.23 | 24 | 1.32 | 05A-NE | ITDD-23-082 | 99.92 | 102.23 | 2.31 | 1.04 | 02-NE |
| ITDD-22-021 | 31.9 | 34.73 | 2.83 | 1.29 | 04-NE | ITTRE-22-012 | 42 | 46 | 4 | 0.50 | 02A-NE | ITDD-23-065 | 390.1 | 397.82 | 7.72 | 1.88 | 05-NE | ITDD-23-082 | 196.2 | 201 | 4.8 | 1.48 | 1 |
| ITDD-22-022 | 14.31 | 18.31 | 4 | 0.55 | 1 | ITDD-22-050 | 96.6 | 99.31 | 2.71 | 0.81 | 04-NE | ITDD-23-065 | 431.25 | 434.45 | 3.2 | 0.67 | 06-NE | ITDD-23-083 | 59.09 | 66.12 | 7.03 | 1.37 | 03-NE |
| ITDD-22-023 | 38.53 | 43.59 | 5.06 | 2.13 | 02A-NE | ITDD-22-049 | 64.87 | 67.87 | 3 | 0.86 | SE-A | ITDD-23-065 | 441.88 | 445.37 | 3.49 | 2.04 | 06A-NE | ITDD-23-083 | 171.31 | 177.15 | 5.84 | 1.90 | 02-NE |
| ITDD-22-023 | 114.34 | 115.9 | 1.56 | 1.01 | 1 | ITDD-23-052 | 108.25 | 109.28 | 1.03 | 1.32 | 02A-NE | ITDD-23-065 | 456.28 | 457.62 | 1.34 | 0.86 | 07-NE | ITDD-23-083 | 310.73 | 314.78 | 4.05 | 1.11 | 04-NE |
| ITDD-22-024 | 28.14 | 31 | 2.86 | 2.04 | 02-NE | ITDD-23-052 | 205.44 | 209.44 | 4 | 1.79 | 1 | ITDD-23-065 | 458.05 | 459.74 | 1.69 | 1.01 | 07-NE | ITDD-23-083 | 372.67 | 379.76 | 7.09 | 2.29 | 05-NE |
| ITDD-22-024 | 32.22 | 33.86 | 1.64 | 2.34 | 02-NE | ITDD-23-052 | 223.63 | 225.63 | 2 | 2.33 | 04-NE | ITDD-23-065 | 460.29 | 461.88 | 1.59 | 1.17 | 07-NE | ITDD-23-084 | 275.42 | 278.93 | 3.51 | 1.60 | 1 |
| ITDD-22-024 | 159.72 | 161.72 | 2 | 2.46 | 04-NE | ITDD-23-052 | 256.39 | 257.46 | 1.07 | 0.56 | 04C-NE | ITDD-23-066 | 28.16 | 37.16 | 9 | 0.73 | SE-A | ITDD-23-084 | 279.2 | 284.87 | 5.67 | 1.16 | 1 |
| ITDD-22-025 | 67.62 | 71.31 | 3.69 | 2.22 | 04-NE | ITDD-23-052 | 308.2 | 310.33 | 2.13 | 1.32 | 05-NE | ITDD-23-067 | 86.96 | 103.96 | 17 | 1.21 | SE-A | ITDD-23-086 | 272.46 | 274.84 | 2.38 | 1.52 | 04-NE |
| ITDD-22-027 | 22.78 | 26.78 | 4 | 0.47 | 04-NE | ITDD-23-052 | 311.08 | 312.46 | 1.38 | 0.80 | 05-NE | ITDD-23-068 | 92.23 | 93.97 | 1.74 | 1.03 | 1 | ITDD-23-086 | 276 | 282.45 | 6.45 | 1.07 | 04-NE |
| ITDD-22-027 | 27.78 | 29.09 | 1.31 | 0.45 | 04-NE | ITDD-23-052 | 381.3 | 386 | 4.7 | 1.11 | 06-NE | ITDD-23-068 | 112.79 | 114.45 | 1.66 | 0.38 | 01B-SW | ITDD-23-086 | 293.7 | 299.86 | 6.16 | 1.33 | 04C-NE |
| ITDD-22-028 | 34.3 | 35.35 | 1.05 | 2.17 | 04B-NE | ITDD-23-052 | 395.2 | 398.52 | 3.32 | 1.79 | 06A-NE | ITDD-23-069 | 60.55 | 75.48 | 14.93 | 1.44 | SE-A | ITDD-23-088 | 83.32 | 86.32 | 3 | 0.96 | 02-NE |
| ITDD-22-028 | 38.64 | 40.25 | 1.61 | 1.95 | 1 | ITDD-23-052 | 433.13 | 435.39 | 2.26 | 2.16 | 07-NE | ITDD-23-070 | 78.3 | 84.3 | 6 | 1.06 | 03-NE | ITDD-23-088 | 199.94 | 202.63 | 2.69 | 1.59 | 04-NE |
| ITDD-22-028 | 51.39 | 53.39 | 2 | 0.67 | 04-NE | ITDD-23-052 | 436.36 | 438.74 | 2.38 | 2.14 | 07-NE | ITDD-23-070 | 89.3 | 97.3 | 8 | 1.32 | 03-NE | ITDD-23-088 | 206 | 210.19 | 4.19 | 1.87 | 04-NE |
| ITDD-22-029 | 44.28 | 46.93 | 2.65 | 1.29 | 02A-NE | ITDD-23-053 | 74.65 | 77.19 | 2.54 | 1.95 | 1 | ITDD-23-070 | 332.74 | 336.36 | 3.62 | 2.15 | 04-NE | ITDD-23-088 | 272.46 | 274.62 | 2.16 | 2.21 | 05-NE |
| ITDD-22-029 | 145.91 | 149.08 | 3.17 | 1.21 | 1 | ITDD-23-054 | 118 | 123 | 5 | 1.66 | 1 | ITDD-23-070 | 339.94 | 341.09 | 1.15 | 0.72 | 04C-NE | ITDD-23-089 | 63.26 | 72.02 | 8.76 | 1.37 | SE-A |
| ITDD-22-030 | 46.6 | 53.3 | 6.7 | 1.49 | 04-NE | ITDD-23-055 | 36.97 | 38.95 | 1.98 | 0.42 | SE-A | ITDD-23-070 | 341.39 | 343.42 | 2.03 | 1.41 | 04C-NE | ITDD-23-089 | 155.53 | 161.53 | 6 | 1.22 | SE-B |
| ITDD-22-032 | 18.35 | 19.95 | 1.6 | 1.95 | 02A-NE | ITDD-23-056 | 37.75 | 49.02 | 11.27 | 0.88 | SE-A | ITDD-23-072 | 99.14 | 100.94 | 1.8 | 1.37 | 1 | ITDD-23-090 | 161.74 | 169.95 | 8.21 | 1.03 | 03-NE |
| ITDD-22-032 | 130.3 | 133.92 | 3.62 | 0.71 | 1 | ITDD-23-058 | 122.55 | 128.55 | 6 | 1.96 | 1 | ITDD-23-072 | 113.69 | 117.69 | 4 | 1.38 | 01B-SW | ITDD-23-090 | 259.5 | 263.5 | 4 | 1.80 | 02-NE |
| ITDD-22-032 | 137.4 | 139.2 | 1.8 | 1.58 | 04-NE | ITDD-23-059 | 28.72 | 32.96 | 4.24 | 1.32 | SE-A | ITDD-23-073 | 77.82 | 83.66 | 5.84 | 1.99 | 03-NE | ITDD-23-090 | 386.98 | 389.98 | 3 | 1.62 | 1 |
| ITDD-22-033A | 6.05 | 10.05 | 4 | 0.41 | 04B-NE | ITDD-23-060 | 225.23 | 229.5 | 4.27 | 2.03 | 1 | ITDD-23-073 | 206.62 | 213.3 | 6.68 | 1.99 | 02-NE | ITDD-23-090 | 442.9 | 445.66 | 2.76 | 1.79 | 04-NE |
| ITDD-22-035 | 103.27 | 105.17 | 1.9 | 1.04 | 04A-NE | ITDD-23-060 | 283.3 | 284.48 | 1.18 | 2.16 | 04C-NE | ITDD-23-073 | 243.54 | 245.1 | 1.56 | 1.43 | 02B-NE | ITDD-23-090 | 466.85 | 471.85 | 5 | 1.72 | 04C-NE |
| ITDD-22-035 | 111.93 | 113.21 | 1.28 | 1.43 | 04B-NE | ITDD-23-060 | 319.4 | 321.2 | 1.8 | 0.99 | 05A-NE | ITDD-23-073 | 352.92 | 360.92 | 8 | 1.66 | 04-NE | ITDD-23-090 | 564.45 | 567.45 | 3 | 1.56 | 06-NE |
| ITDD-22-035 | 171.62 | 176.5 | 4.88 | 1.28 | 04-NE | ITDD-23-060 | 332.62 | 334 | 1.38 | 2.04 | 05-NE | ITDD-23-073 | 408.21 | 411.86 | 3.65 | 1.83 | 05A-NE | ITDD-23-091 | 479.83 | 482 | 2.17 | 2.04 | 1 |
| ITDD-22-035 | 179.3 | 181.02 | 1.72 | 0.56 | 04C-NE | ITDD-23-060 | 399.67 | 402.45 | 2.78 | 1.79 | 06-NE | ITDD-23-073 | 413.9 | 423.97 | 10.07 | 1.30 | 05A-NE | ITDD-23-091 | 486.04 | 489.24 | 3.2 | 0.82 | 1 |
| ITDD-22-036 | 39.1 | 45.1 | 6 | 0.90 | SE-A | ITDD-23-060 | 405.94 | 408.44 | 2.5 | 0.81 | 06A-NE | ITDD-23-073 | 425.1 | 426.35 | 1.25 | 1.25 | 05A-NE | ITDD-23-092 | 92.81 | 95.83 | 3.02 | 1.57 | 01A-SW |
| ITDD-22-038 | 43.26 | 44.66 | 1.4 | 2.43 | 04A-NE | ITDD-23-060 | 444.29 | 449.43 | 5.14 | 1.44 | 07-NE | ITDD-23-073 | 443.07 | 447.07 | 4 | 2.10 | 05-NE | ITDD-23-092 | 103.81 | 109.42 | 5.61 | 1.23 | 1 |

Table 10.5: Mineralized Intercepts by Bandeira Drill Holes.

| holeid | from | to | Length | Li2O% | Model | holeid | from | to | Length | Li2O% | Model | holeid | from | to | Length | Li2O% | Model |
|-------------|--------|--------|--------|-------|--------|-------------|--------|--------|--------|-------|--------|-------------|--------|--------|--------|-------|--------|
| ITDD-23-093 | 43.65 | 51.65 | 8 | 1.47 | SE-A | ITDD-23-117 | 151.89 | 153.46 | 1.57 | 0.79 | 01A-SW | ITDD-23-137 | 81.68 | 85.18 | 3.5 | 1.48 | 01C-SW |
| ITDD-23-094 | 80.58 | 81.72 | 1.14 | 1.25 | 1 | ITDD-23-117 | 166.63 | 169.18 | 2.55 | 0.74 | 1 | ITDD-23-137 | 182.18 | 183.7 | 1.52 | 0.92 | 01A-SW |
| ITDD-23-094 | 83.88 | 88.26 | 4.38 | 2.17 | 1 | ITDD-23-118 | 155.35 | 156.56 | 1.21 | 1.76 | 01A-SW | ITDD-23-137 | 186.06 | 187.39 | 1.33 | 1.38 | 01A-SW |
| ITDD-23-095 | 46.35 | 48.48 | 2.13 | 0.70 | 02C-NE | ITDD-23-118 | 161.16 | 164.07 | 2.91 | 1.12 | 1 | ITDD-23-137 | 189.8 | 196.65 | 6.85 | 1.44 | 1 |
| ITDD-23-095 | 205.4 | 206.91 | 1.51 | 1.13 | 01A-SW | ITDD-23-120 | 109.66 | 114.98 | 5.32 | 1.33 | 01A-SW | ITDD-23-138 | 289.52 | 291.29 | 1.77 | 1.56 | 1 |
| ITDD-23-095 | 216.19 | 217.88 | 1.69 | 1.98 | 1 | ITDD-23-120 | 126.06 | 127.18 | 1.12 | 0.52 | 1 | ITDD-23-138 | 292.62 | 296.62 | 4 | 0.97 | 1 |
| ITDD-23-095 | 218.84 | 223.07 | 4.23 | 1.38 | 1 | ITDD-23-120 | 253.93 | 259.63 | 5.7 | 1.86 | 05-NE | ITDD-23-140 | 28.83 | 30.62 | 1.79 | 1.22 | 1 |
| ITDD-23-096 | 88.95 | 90.4 | 1.45 | 1.03 | 1 | ITDD-23-112 | 124.79 | 131.18 | 6.39 | 1.74 | 1 | ITDD-23-141 | 39.98 | 44.45 | 4.47 | 1.32 | 1 |
| ITDD-23-096 | 91.2 | 97.18 | 5.98 | 1.91 | 1 | ITDD-23-112 | 142.43 | 144.36 | 1.93 | 1.20 | 01B-SW | ITDD-23-141 | 47.25 | 49.25 | 2 | 0.52 | 04-NE |
| ITDD-23-097 | 38.7 | 44.12 | 5.42 | 1.48 | 1 | ITDD-23-119 | 124.13 | 130.85 | 6.72 | 1.57 | 1 | ITDD-23-141 | 49.58 | 51.61 | 2.03 | 0.69 | 04-NE |
| ITDD-23-098 | 62.59 | 67.59 | 5 | 1.64 | 1 | ITDD-23-121 | 38.85 | 40.85 | 2 | 0.80 | 02-NE | ITDD-23-142 | 36.36 | 41.36 | 5 | 1.39 | 02-NE |
| ITDD-23-098 | 194.04 | 196.69 | 2.65 | 1.02 | 05-NE | ITDD-23-121 | 165.12 | 169.82 | 4.7 | 2.15 | 01A-SW | ITDD-23-142 | 126.7 | 128.7 | 2 | 2.05 | 1 |
| ITDD-23-099 | 63.04 | 65.04 | 2 | 1.91 | 01A-SW | ITDD-23-121 | 182.04 | 183.59 | 1.55 | 2.59 | 1 | ITDD-23-144 | 94.46 | 99.42 | 4.96 | 1.85 | 04-NE |
| ITDD-23-099 | 67.96 | 72.49 | 4.53 | 1.10 | 1 | ITDD-23-121 | 331.55 | 337.47 | 5.92 | 1.83 | 05-NE | ITDD-23-139 | 304 | 315.16 | 11.16 | 1.63 | 1 |
| ITDD-23-101 | 76.74 | 81.74 | 5 | 1.55 | 1 | ITDD-23-122 | 164.11 | 168.11 | 4 | 1.49 | 1 | ITDD-23-147 | 41.3 | 44.43 | 3.13 | 1.96 | 02-NE |
| ITDD-23-102 | 52.6 | 56.09 | 3.49 | 1.16 | 02C-NE | ITDD-23-123 | 151.75 | 159.4 | 7.65 | 2.39 | 1 | ITDD-23-147 | 45.04 | 47.62 | 2.58 | 1.35 | 02A-NE |
| ITDD-23-102 | 202.45 | 204.35 | 1.9 | 0.99 | 01A-SW | ITDD-23-125 | 133.72 | 134.77 | 1.05 | 0.60 | 1 | ITDD-23-147 | 138.02 | 140.27 | 2.25 | 1.11 | 1 |
| ITDD-23-102 | 228.55 | 233.36 | 4.81 | 1.63 | 1 | ITDD-23-125 | 144.94 | 147.92 | 2.98 | 1.44 | 01B-SW | ITDD-23-147 | 268.3 | 271.03 | 2.73 | 1.63 | 05-NE |
| ITDD-23-103 | 197 | 200 | 3 | 1.33 | 1 | ITDD-23-126 | 105.8 | 108.37 | 2.57 | 1.02 | 1 | ITDD-23-147 | 285.15 | 287.81 | 2.66 | 1.57 | 05B-NE |
| ITDD-23-104 | 55.89 | 57.89 | 2 | 0.84 | 1 | ITDD-23-128 | 179.31 | 183.31 | 4 | 2.43 | 1 | ITDD-23-147 | 393.84 | 395.03 | 1.19 | 0.75 | 07-NE |
| ITDD-23-104 | 58.89 | 59.89 | 1 | 0.84 | 01B-SW | ITDD-23-129 | 153.61 | 155 | 1.39 | 0.83 | 01A-SW | ITDD-23-147 | 396.66 | 398.68 | 2.02 | 1.30 | 07-NE |
| ITDD-23-105 | 97.01 | 99.52 | 2.51 | 1.47 | 02C-NE | ITDD-23-129 | 157.1 | 160.35 | 3.25 | 1.97 | 1 | ITDD-23-155 | 44.5 | 50.49 | 5.99 | 1.71 | 02-NE |
| ITDD-23-105 | 110.73 | 116.4 | 5.67 | 1.49 | 02-NE | ITDD-23-130 | 88.49 | 91.08 | 2.59 | 1.15 | 1 | ITDD-23-155 | 149.36 | 151.36 | 2 | 1.67 | 1 |
| ITDD-23-105 | 220.44 | 229.59 | 9.15 | 1.32 | 1 | ITDD-23-130 | 201.33 | 203.33 | 2 | 0.60 | 05-NE | | | | | | |
| ITDD-23-105 | 370.38 | 372.7 | 2.32 | 1.46 | 05-NE | ITDD-23-130 | 240.32 | 242.41 | 2.09 | 1.46 | 05B-NE | | | | | | |
| ITDD-23-105 | 373.42 | 375.38 | 1.96 | 1.19 | 05-NE | ITDD-23-131 | 99.48 | 101.48 | 2 | 1.98 | 1 | | | | | | |
| ITDD-23-106 | 133.08 | 135.23 | 2.15 | 0.95 | 01B-SW | ITDD-23-131 | 272.94 | 278 | 5.06 | 0.96 | 05-NE | | | | | | |
| ITDD-23-107 | 197.74 | 199.94 | 2.2 | 1.37 | 1 | ITDD-23-132 | 69.558 | 72.73 | 3.172 | 1.66 | 01C-SW | | | | | | |
| ITDD-23-107 | 209.54 | 213.54 | 4 | 1.81 | 01B-SW | ITDD-23-132 | 166.14 | 167.86 | 1.72 | 1.75 | 01A-SW | | | | | | |
| ITDD-23-108 | 75.26 | 81.26 | 6 | 1.59 | 1 | ITDD-23-132 | 172.68 | 178.59 | 5.91 | 1.59 | 1 | | | | | | |
| ITDD-23-108 | 86.52 | 88.52 | 2 | 1.73 | 01B-SW | ITDD-23-133 | 150.2 | 154.79 | 4.59 | 1.20 | 1 | | | | | | |
| ITDD-23-109 | 120.09 | 126.07 | 5.98 | 1.34 | 1 | ITDD-23-134 | 32.45 | 34.95 | 2.5 | 2.43 | 01C-SW | | | | | | |
| ITDD-23-109 | 247.87 | 255.66 | 7.79 | 1.69 | 05-NE | ITDD-23-134 | 135.63 | 137.16 | 1.53 | 0.50 | 01A-SW | | | | | | |
| ITDD-23-110 | 58.58 | 62.84 | 4.26 | 2.15 | 1 | ITDD-23-134 | 138.85 | 141.96 | 3.11 | 2.24 | 1 | | | | | | |
| ITDD-23-111 | 27.8 | 34.4 | 6.6 | 1.51 | 1 | ITDD-23-135 | 121.85 | 123.46 | 1.61 | 1.74 | 1 | | | | | | |
| ITDD-23-113 | 97.33 | 99.89 | 2.56 | 1.75 | 1 | ITDD-23-135 | 136.02 | 137.59 | 1.57 | 2.96 | 04-NE | | | | | | |
| ITDD-23-114 | 71.78 | 78.15 | 6.37 | 0.96 | 1 | ITDD-23-135 | 247.22 | 248.46 | 1.24 | 0.31 | 05B-NE | | | | | | |
| ITDD-23-115 | 34.08 | 41 | 6.92 | 1.26 | 1 | ITDD-23-136 | 85.97 | 89.97 | 4 | 1.73 | 04-NE | | | | | | |
| ITDD-23-116 | 112.82 | 117.36 | 4.54 | 2.18 | 01A-SW | ITDD-23-136 | 318.38 | 319.63 | 1.25 | 0.32 | 07-NE | | | | | | |

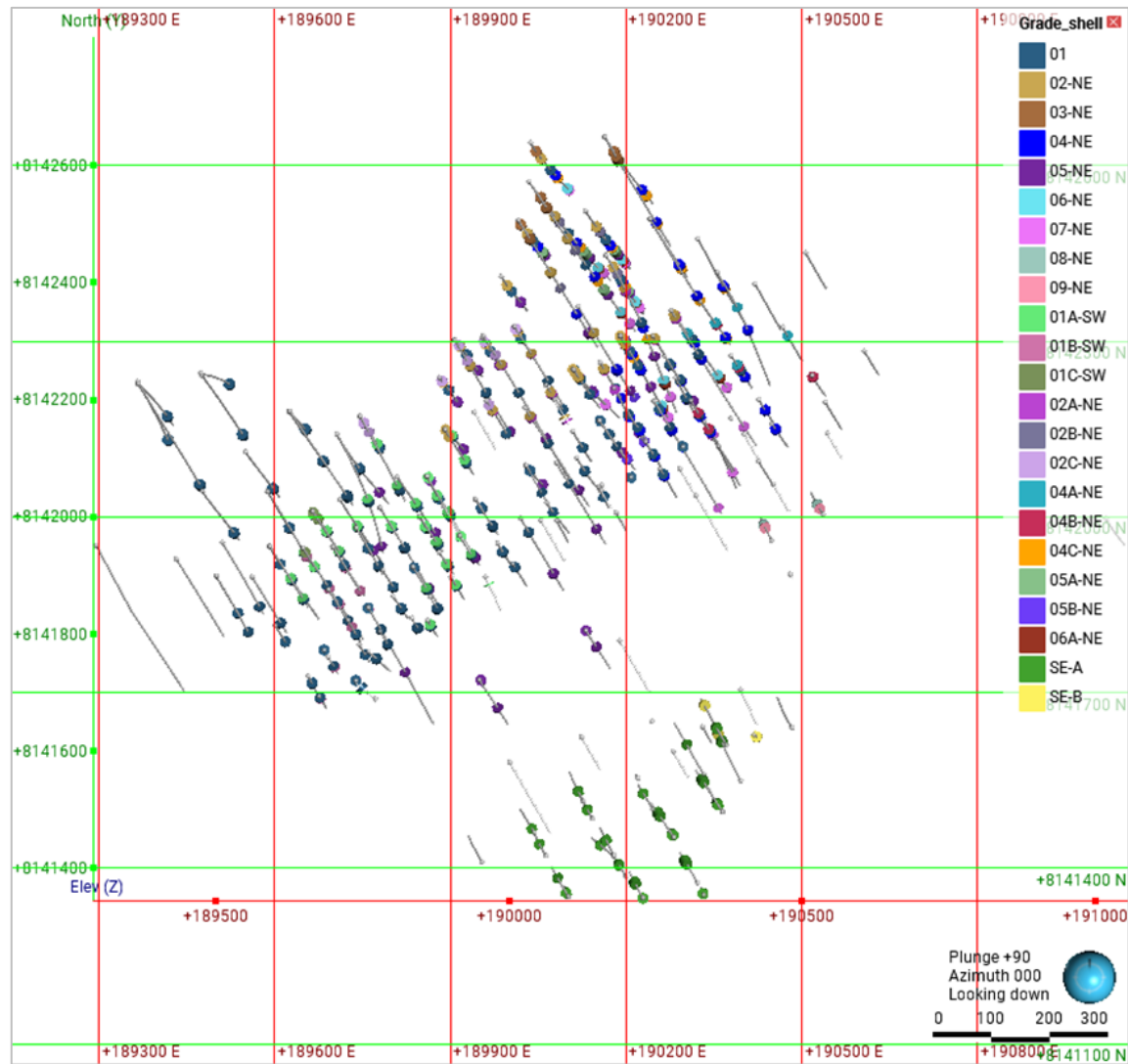


Figure 10.2: Horizontal Projection of Bandaiera Drilling Holes with Mineralized Intercepts.

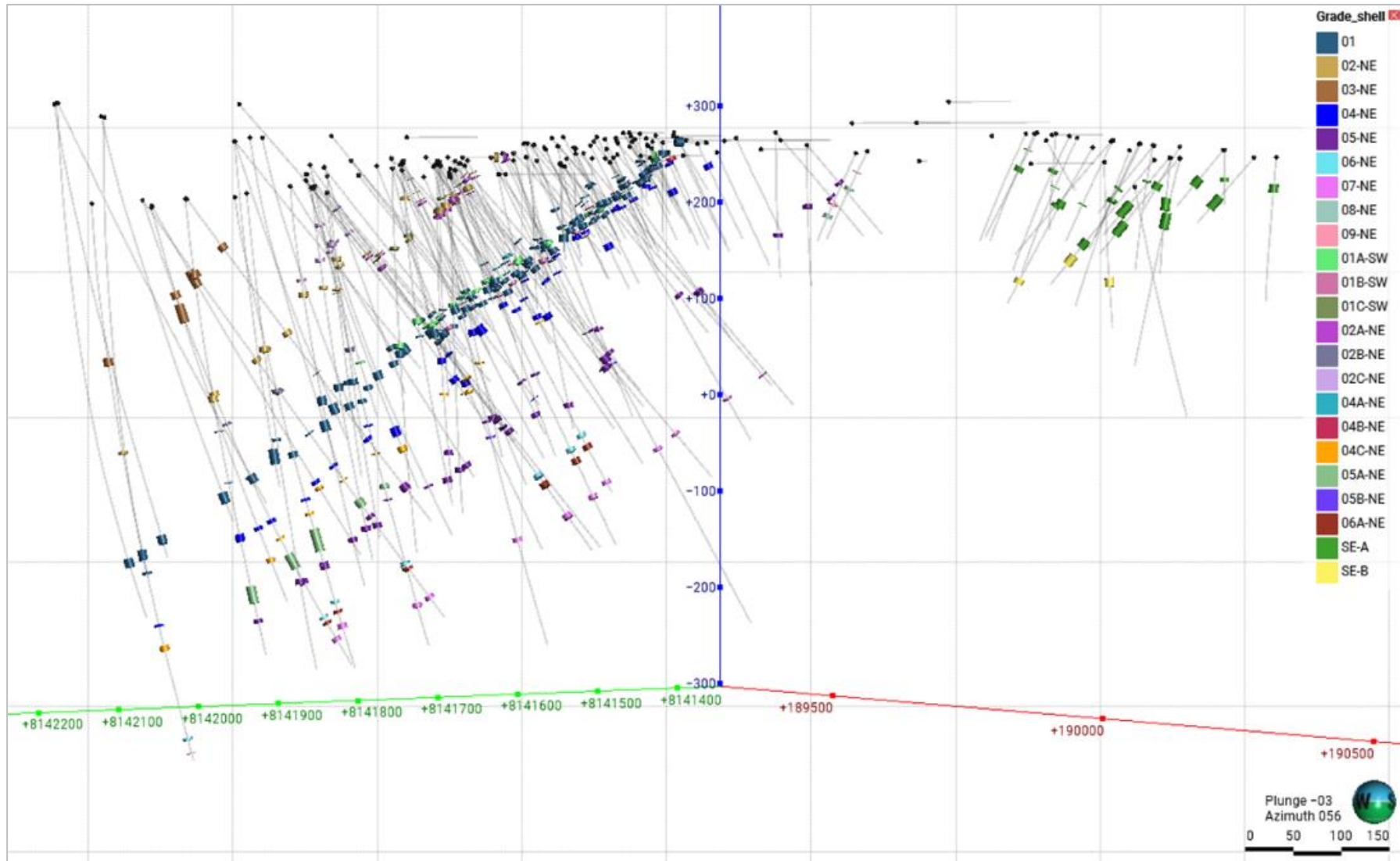


Figure 10.3: Oblique View of Drill Holes with Mineralized Intercepts.

10.1 QP's Comments

No significant drilling, sampling or recovery factors would impact the outcome of the drilling results and the estimated MRE (covered in Item 14).

In the Author's opinion, based on a review of all possible information, the drilling procedures put in place by Lithium Ionic meet acceptable industry standards, and the data can be and has been used for Geological and Resource Modelling.

11 SAMPLE PREPARATION, ANALYSIS AND SECURITY

11.1 Sampling

Samples are prepared from NQ diameter drill cores (47.6mm core diameter). The sampling procedures described in this section reflect the current Standard Operational Procedures (SOP) in use by Lithium Ionic.

Sample intervals in the mineralized zones are defined based on a 1.00m support. Mineralized samples must have a minimum length of 1.00m and a maximum length of 1.50m. In some specific situations, samples shorter than 1.00m can be generated. These situations are described in detail in the SOP.

Outside the mineralized domains, the sampling support is 1.50m, and samples can range from 1.00m to 3.00m.

The visual indicators for sample interval definition include lithological contacts, structures, and mineralization.

The sample collection and sample definition procedures adopted by Lithium Ionic are described below:

- Drill core is brought in by the drilling contractor team, one or more times per shift, from the drill rig to a drill logging and sampling area.
- The disposition and orientation of boxes are checked, and the depth lengths are marked.
- Core boxes are photographed (three boxes per picture) and logged.
- Sample intervals are marked with a pencil in the core box.
- Before sampling, the drill core is marked by a line drawn along the core at high angles to the foliation to orient the saw cut. The right side of the core is selected as a sample. The other half of the core is retained for future reference.
- Sample tags are attached to the core box at the end of each sample.
- Sample bags are numbered before sampling.
- Sample tags are inserted in the bags only after samples are bagged.
- After the samples are tagged and bagged, they are weighted.
- The core is cut lengthwise along the core axis. A Geologist defines the position of the cut, and a Geology Technician performs the cutting.
- For weathered material, a spatula or a machete is used to split the sample into two subsamples along the drilling direction.
- Fresh rock cores are cut in half using a diamond saw and flushed with water between cuts.
- After bagging, the samples are weighted, and the weight is registered.
- Batches are assembled and sent to the laboratory.

The standard batch size is 35 samples, consisting of 29 core samples and 6 quality control samples.

11.2 Sample Preparation, Security and Custody Chain of Custody

Samples are defined and marked on-site after logging and entering the data into the database. Cores are split in half using a diamond saw. Half of the core is left in the core box, while the other half is stored in plastic bags, accompanied by a printed sample tag, and sent to the lab.

Drill core samples are prepared and analyzed by an independent commercial laboratory (SGS Geosol). The SGS Geosol facility is ISO 9001, ISO 14001, and ISO 17025 certified. The sample shipment is delivered to the SGS Geosol facility in Vespasiano, Minas Gerais, Brazil, via a parcel transport company. At all times, samples are in the custody and control of the Company's representatives until delivery to the laboratory, where samples are held in a secure enclosure until processing. SGS Geosol sends a confirmation e-mail with details of samples received upon delivery. The chain of custody of the batches was carefully maintained from collection at the drill rig to delivery at the laboratory to prevent accidental contamination or mixing of samples and render active tampering as tricky as possible.

All samples received at SGS Geosol are inventoried and weighted before processing. Samples are dried at 105°C, crushed to 75% passing a 3 mm sieve, homogenized, split (Jones riffle splitter), and pulverized (250 to 300 g of sample) in a steel mill to 95% passing 150 mesh.

11.3 Density Measurements

The density SOP currently in use by Lithium Ionic states that density measurements should be taken for every geochemical sample generated. In the cases where the drill core quality does not allow for the density assay, this should be registered in the density sampling plan with a specified tag. The high frequency of the density sampling aims for the acquisition of a statistically robust database.

For the geochemical samples with more heterogeneity 3 samples should be taken, one on the top of the sample, other in the middle and other in the base. Homogenous geochemical samples should generate only one density sample. Density samples must have a minimum length of 10 cm and a maximum of 25 cm. Density is commonly measured in the unsampled half-cores, reflecting on a faster and more dynamic drillhole data collection process. All density data is stored in a database. A summary of the procedures described in the density SOP is presented next:

- Sample selection and registration in the density plan.
- Weighing of the sample.
- Weighing of the sample while submerged.
- Density values are acquired from the following formula:

$$D = P_A / (P_A - P_B)$$

D = Density.

P_A = Sample weight (in the air).

P_B = Sample weight (submerged in water).

The density assay procedures do not include drying or sample sealing with paraffin. Considering the climate and the lithological characteristics of the deposit, not implementing the mentioned procedures might be acceptable.

For a more conclusive evaluation of the effect of those procedures on the density results, GE21 recommends duplicate density assays, using the SOP procedure in one sample and a procedure that includes drying and sealing in the other sample. For the sealed samples, the density formula to be used is:

$$D_s = P_s / [(P_p - P_j) - (P_p - P_s) * d_p]$$

D_s = Dry Density.

P_s = Dry sample weight (in the air).

P_p = Sealed sample weight (in the air).

P_j = Sealed sample weight (submerged in water).

D_p = Paraffin density.

11.4 Sample Analysis

After the preparation, the core samples are analyzed by SGS Geosol. The chemical assays are performed using SGS's analytical method ICP90A, a multi-element analysis using fusion by sodium peroxide (Na_2O_2) and finish with ICP-OES analysis. If lithium results are above 15000 ppm, SGS Geosol re-analyzes for lithium through the ICP90Q_Li method, which is similar to the ICP90A but with higher Detection Limits.

All the chemical analyses conducted by SGS Geosol are reported to Lithium Ionic on PDF format certificates, which are also accompanied by an MS Excel digital file.

11.5 Quality Assurance and Quality Control (QAQC)

The Quality Assurance and Quality Control program implemented was proposed by the independent company GE21. The sample batch composition includes 5 Quality Control Samples for every 30 regular samples. The Quality Control composition of the batches is described next:

- Coarse (Preparation) and Fine (Analytical) Blanks: 6% of the batch, or two blanks per batch, one of each type.
- Standards: 6% of the batch, or two standards per batch.
- Crushed Duplicates: 3% of the batch, or 1 sample per batch.
- Pulverized Duplicates: 3% of the batch, or 1 sample per batch.

Additionally, for every sample batch one sample is selected for the Check Assay procedure, representing 3% of the batch. Check samples are selected from the pulverized material of a regular sample, reserved by the primary laboratory. These samples are sent to a secondary laboratory, ALS Vancouver, monthly. ALS Vancouver is ISO 17025 accredited. The same control sample proportion criteria should be respected on Check Assay batches: 2 standards, 2 blanks, 2 duplicates. Particle Size Analysis (PSA) are also performed on the Check Assay samples. Figure 11.1 present the batch composition scheme for batches with mineralized samples or zones and for unmineralized batches. Table 11.1 presents the proportion of Quality Control samples in the Lithium Ionic geochemical database.

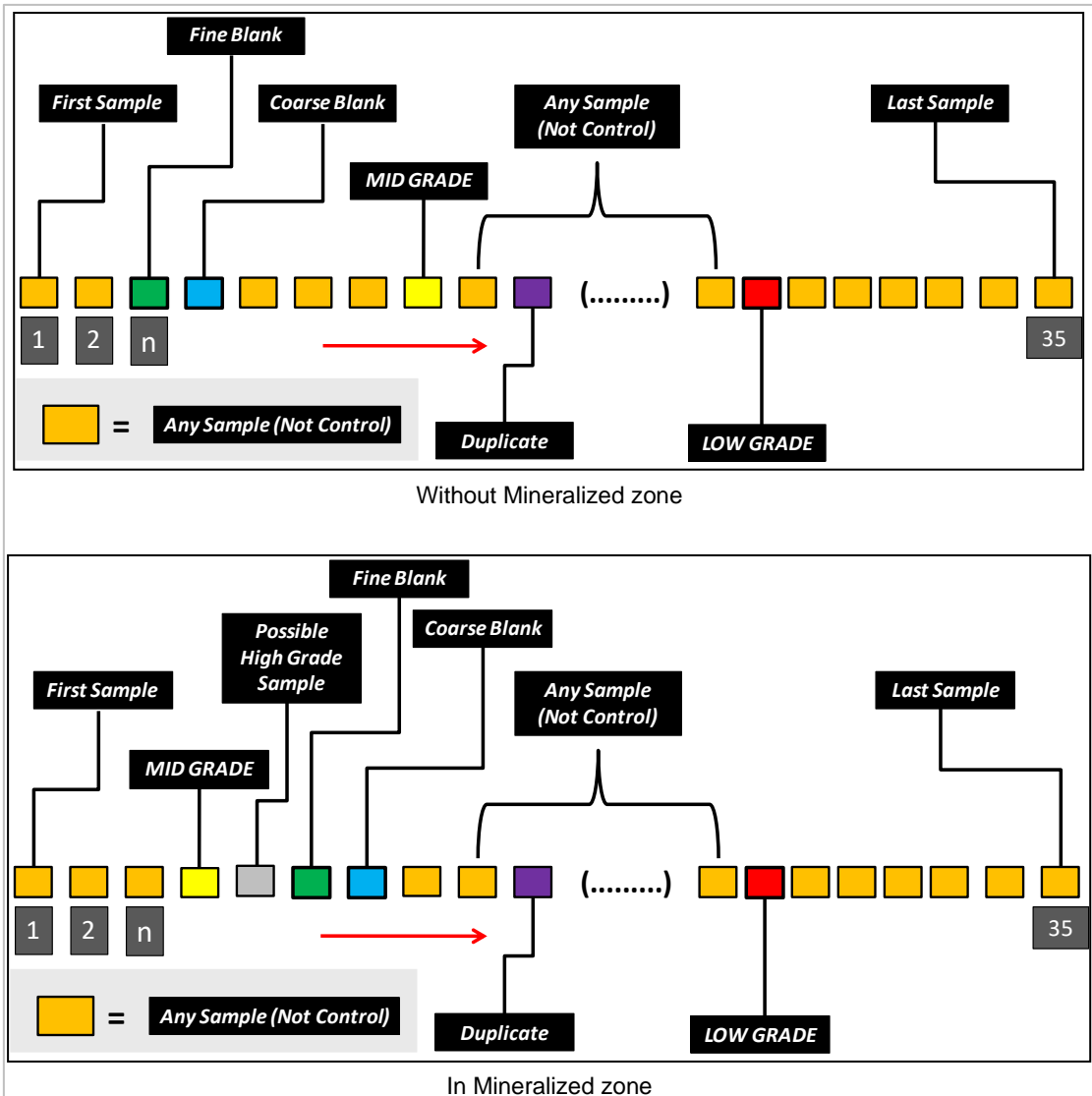


Figure 11.1: QAQC Program.

Table 11.1: QAQC Program Summary.

| CRM/SRM | Crushed Duplicates | Pulverized Duplicates | Preparation Blanks | Analytical Blanks | Total QAQC Samples | Total Database |
|---------|--------------------|-----------------------|--------------------|-------------------|--------------------|----------------|
| 353 | 161 | 161 | 176 | 178 | 1,029 | 7,562 |
| 4.7% | 2.1% | 2.1% | 2.3% | 2.4% | 13.6% | 100.0% |

11.5.1 Preparation Blank – Coarse Blank

Preparation blank samples are inserted in the sample batch before the physical preparation of the samples. This measure helps to track any contamination problems that might occur in the granulometric reduction processes or the sample-splitting processes. Blank samples are inserted in the beginning of the possibly mineralized intervals, following the sequence:

- Mineralized sample.
- Analytical/Fine Blank.
- Preparation/Coarse Blank.

- If an unmineralized batch is assembled, blank samples must be inserted at the beginning of the batch.
- Lithium Ionic uses a commercial blank, ITAK-QG-01, as its Coarse Blank material. More than 95% of the Coarse Blank samples are below the 5x Detection Limit threshold, indicating no major contamination problems. Figure 11.2 presents the Preparation Blank control chart for Lithium.

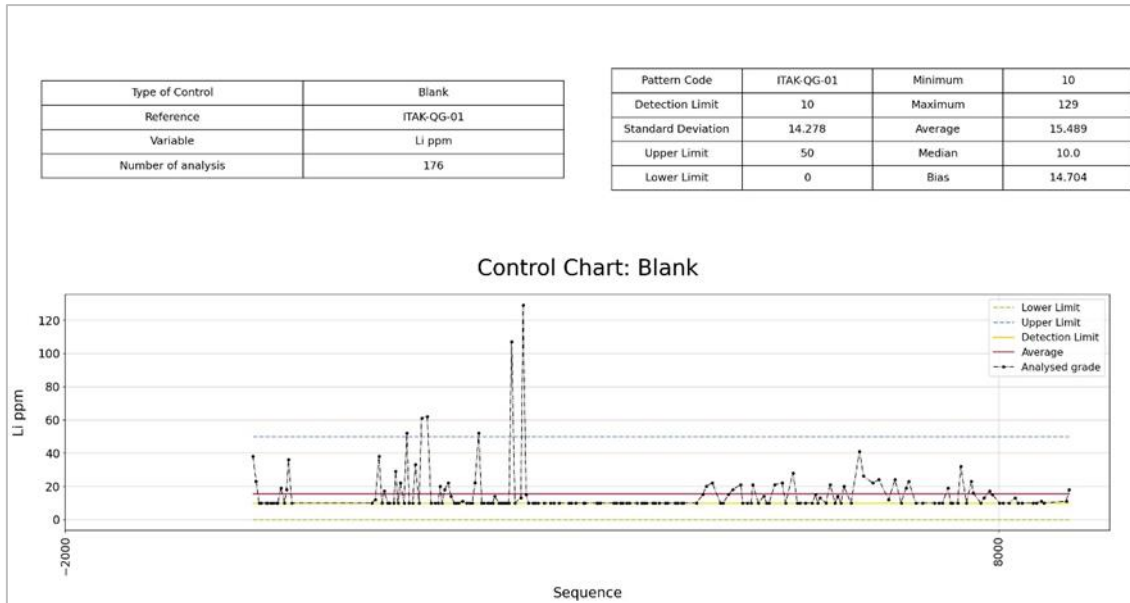


Figure 11.2: Blank Control Chart – ITAK QG-01.

11.5.2 Analytical Blank – Fine Blank

Analytical or Fine Blank samples are inserted in the analytical batches after the samples' physical preparation. This type of blank sample is used to assess contamination problems that might occur in the sample digestion or sample fusion processes and/or to evaluate analytical equipment (in this case, ICP-OES) miscalibrations. Blank Samples are inserted at the beginning of the possibly mineralized intervals, following the sequence:

- Mineralized sample.
- Analytical/Fine Blank.
- Preparation/Coarse Blank.

If an unmineralized batch is assembled, blank samples must be inserted at the beginning of the batch.

For its QAQC Program, Lithium Ionic uses two commercial Fine Blank samples: ITAK-QF-15 and ITAK-QF-16. Only two of the 178 samples of this control have returned grades higher than the 5x Detection Limit threshold, indicating no contamination or calibration problems in the final stages of the geochemical analysis. Figure 11.3 and Figure 11.4 present the Analytical Blanks control charts for Lithium:

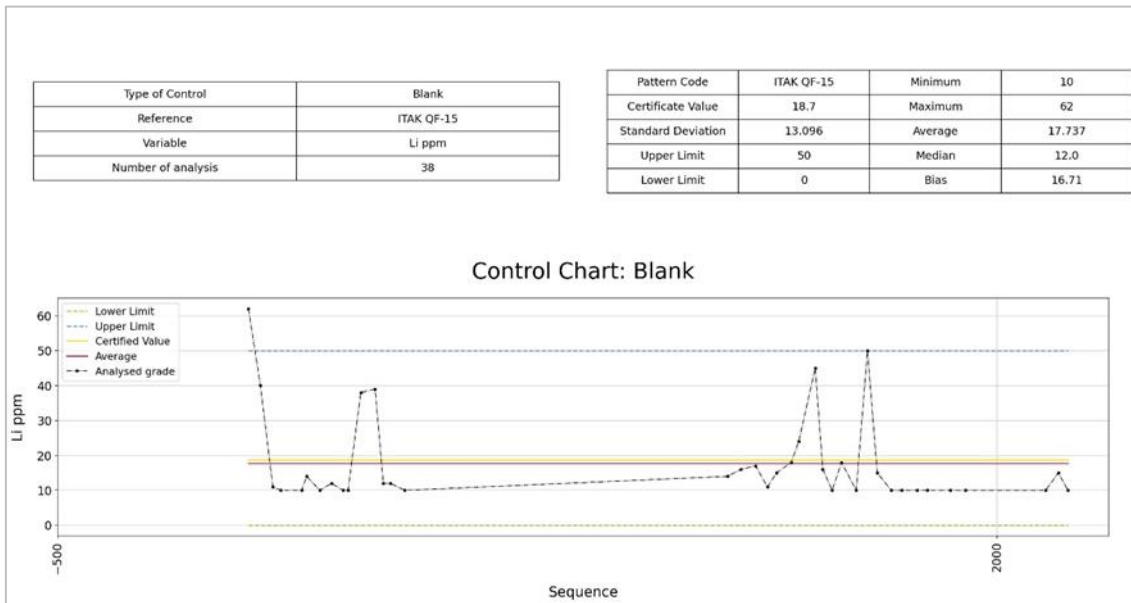


Figure 11.3: Blank Control Chart – ITAK QF-15.

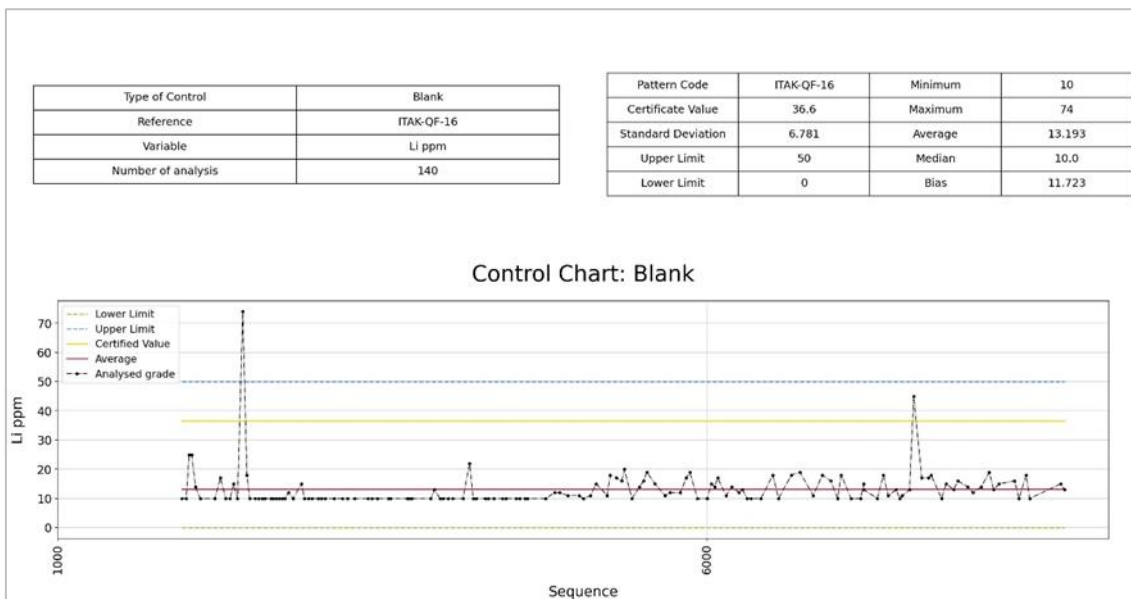


Figure 11.4: Blank Control Chart – ITAK QF-16.

11.5.3 Certified/Standard Reference Material – CRM/SRM

Certified or Standard Reference Materials are reference materials for which one or more parameters have been certified by a technically valid and recognized procedure. A certifying body has issued a Certificate or other accurate documentation. These materials are used as Quality Control Samples to evaluate the accuracy of the analytical methods and procedures used.

Lithium Ionic uses 4 CRMs/SRMs: ITAK – 1100, ITAK – 1101, OREAS 750 and OREAS 752. These Reference Materials evaluate high, medium, and low-grade assay results.

Medium-grade or high-grade Reference Materials are inserted at the beginning of the possible mineralized zones. The insertion can occur immediately or a few samples before the mineralized zone. The low-grade Materials are inserted at the end of the zone where the Geologist interprets mineralization. The insertion can be immediately after or a few samples after the mineralized

zone. The order of the Reference Materials can be changed based on geological features or mineralization characteristics.

Figure 11.5 to Figure 11.8 present Lithium's CRM/SRM control charts. More than 90% of the samples are constrained within the 2x Standard Deviation limits, with only four samples outside the 3x Standard Deviation limits. Samples outside the 3x Standard Deviation boundaries are most likely related to sample swaps.

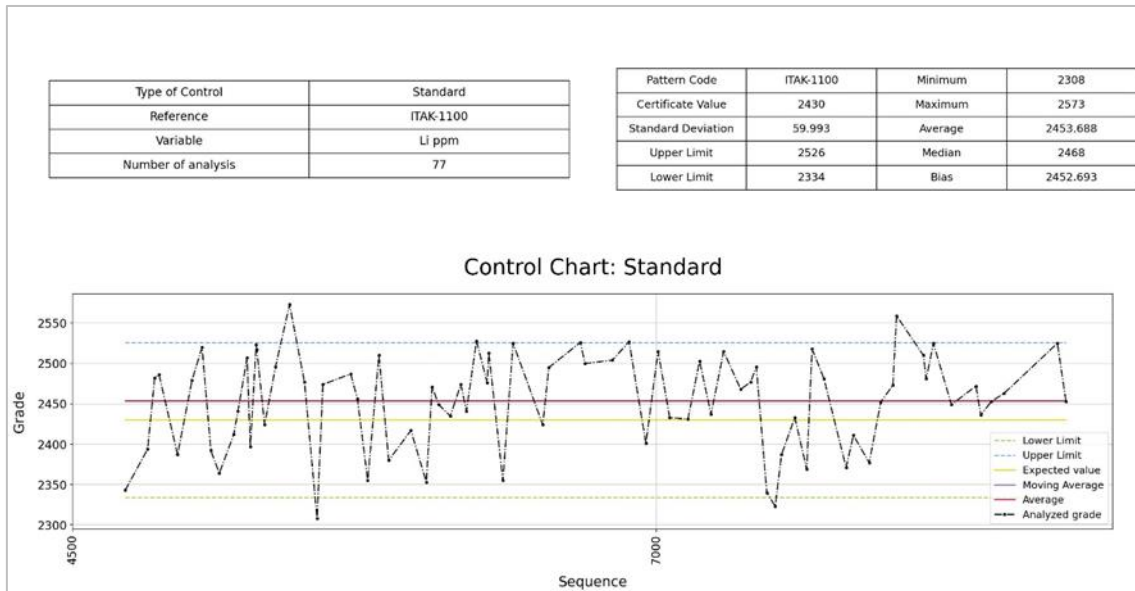


Figure 11.5: Standard Reference Material Chart – ITAK 1100.

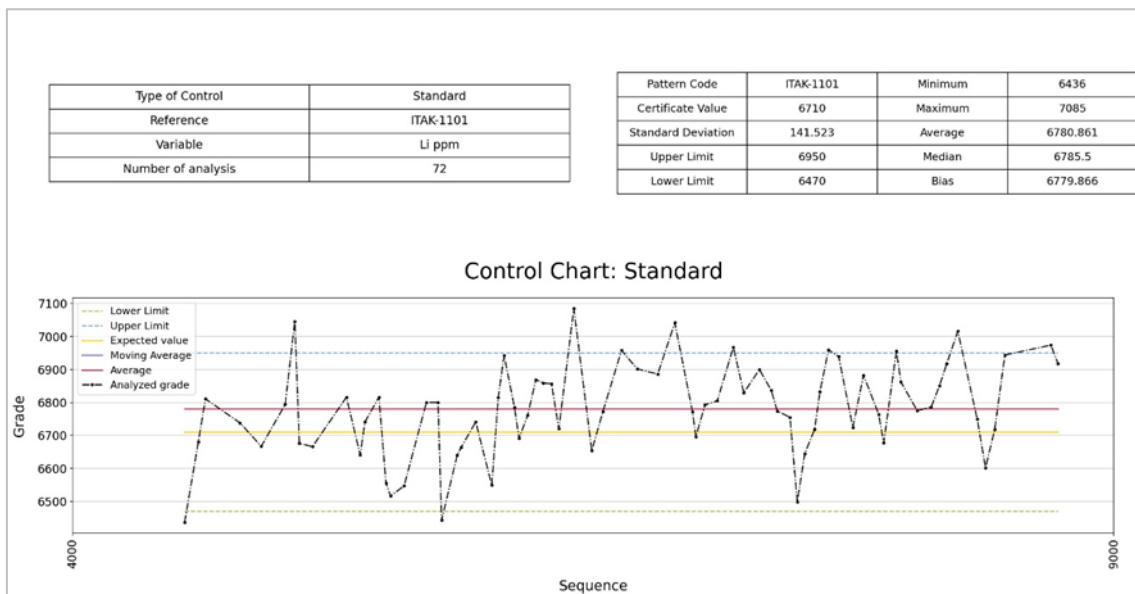


Figure 11.6: Standard Reference Material Chart – ITAK 1101.

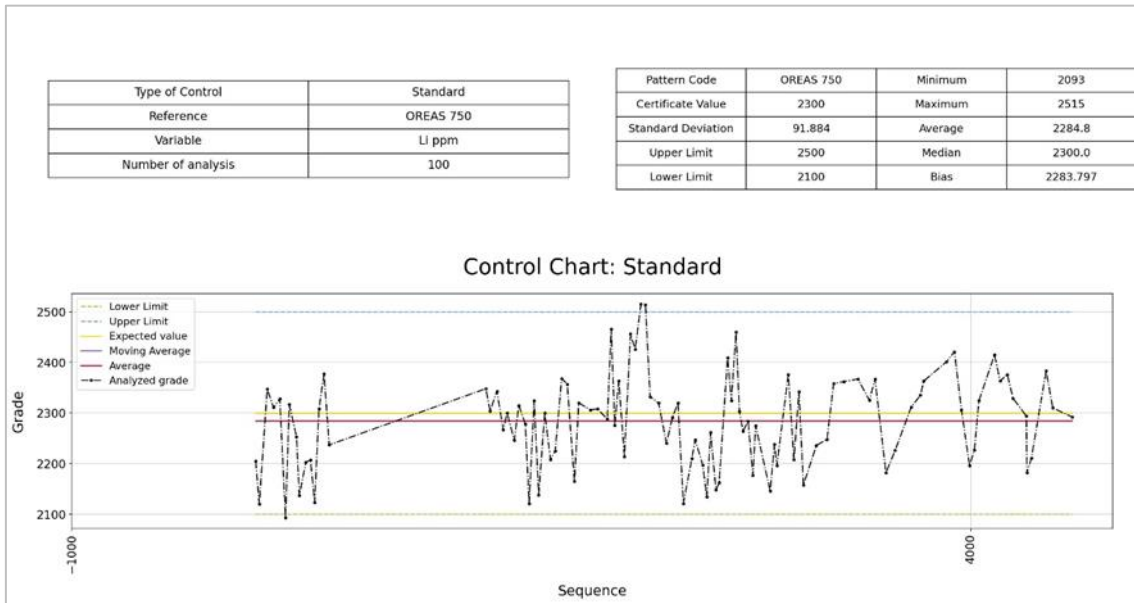


Figure 11.7: Standard Reference Material Chart – OREAS 750.

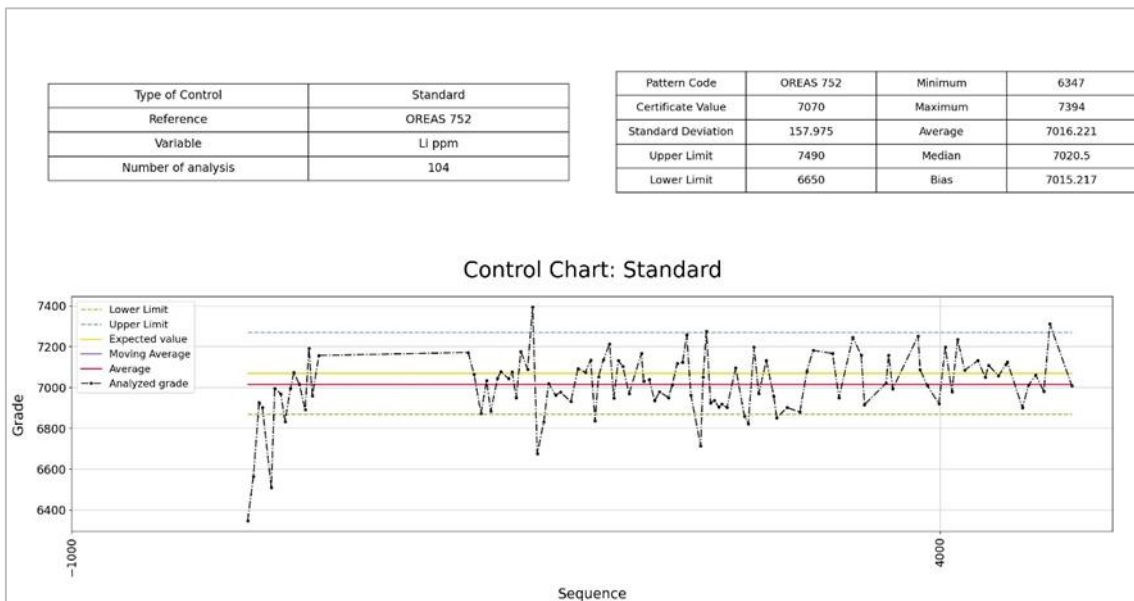


Figure 11.8: Standard Reference Material Chart – OREAS 752.

11.5.4 Crushed Duplicates

Duplicates are used in the Quality Control program as a means of evaluating the precision of the geochemical analysis. Insertion of blind duplicates of crushed material are used to test the laboratory's reproducibility and if the crushing process is generating bias or imprecision in the results.

A total of 161 crushed duplicates were evaluated. Control charts for this control type show high correlations and a good reproducibility, with over 90% of the samples falling below the 20% HARD limit. Figure 11.9 presents the control chart.

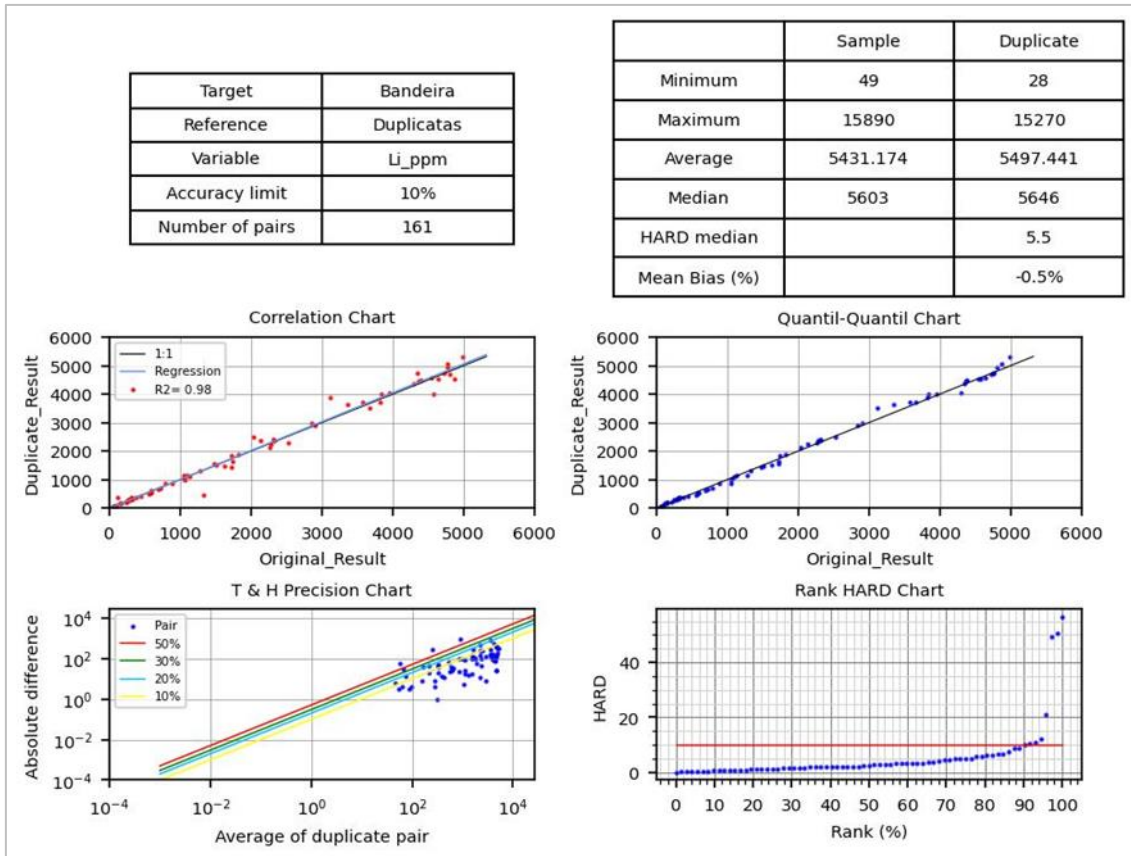


Figure 11.9: Crushed Duplicates Control Chart.

11.5.5 Pulverized duplicates

Duplicates are used in the Quality Control program to evaluate the geochemical analysis' precision. Insertion of blind duplicates of pulverized material is used to test the laboratory's reproducibility and if the milling process is not generating bias or imprecision in the results.

A total of 161 pulverized duplicates were evaluated. Control charts for this control type show high correlations and good reproducibility, with approximately 80% of the samples falling below the 10% HARD limit. Figure 11.10 presents the control chart.

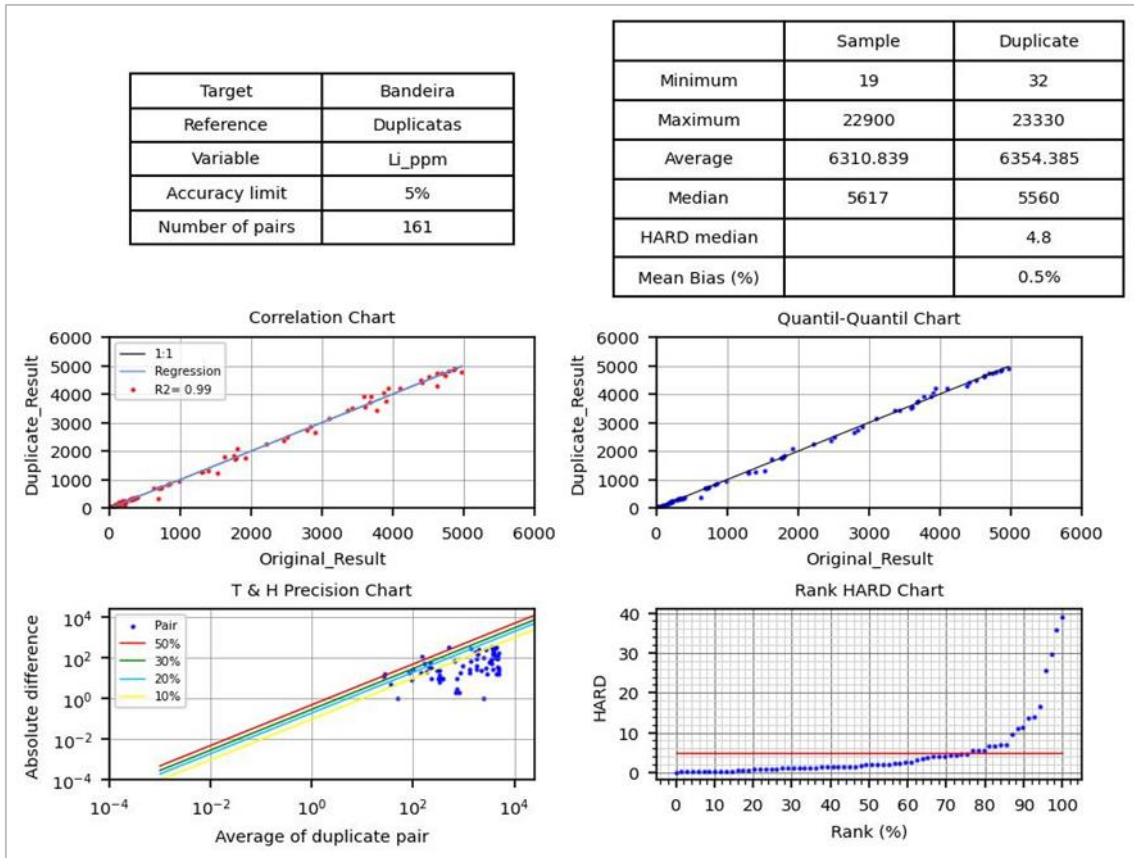


Figure 11.10: Pulverized Duplicates Control Chart.

11.5.6 Check Assay

Lithium Ionic has submitted Check Assay batches for analysis at the ALS Laboratory in Vancouver, British Columbia, Canada. This procedure is used to verify the reliability of the primary laboratory results by crosschecking it with a secondary reference laboratory. Check Assay results are presented in the following control chart (Figure 11.11). Only 1 sample of 72 has returned a pair above the 30% HARD limit, representing 1.4% of the total Check Assays presents the control chart of the Check Assay results.

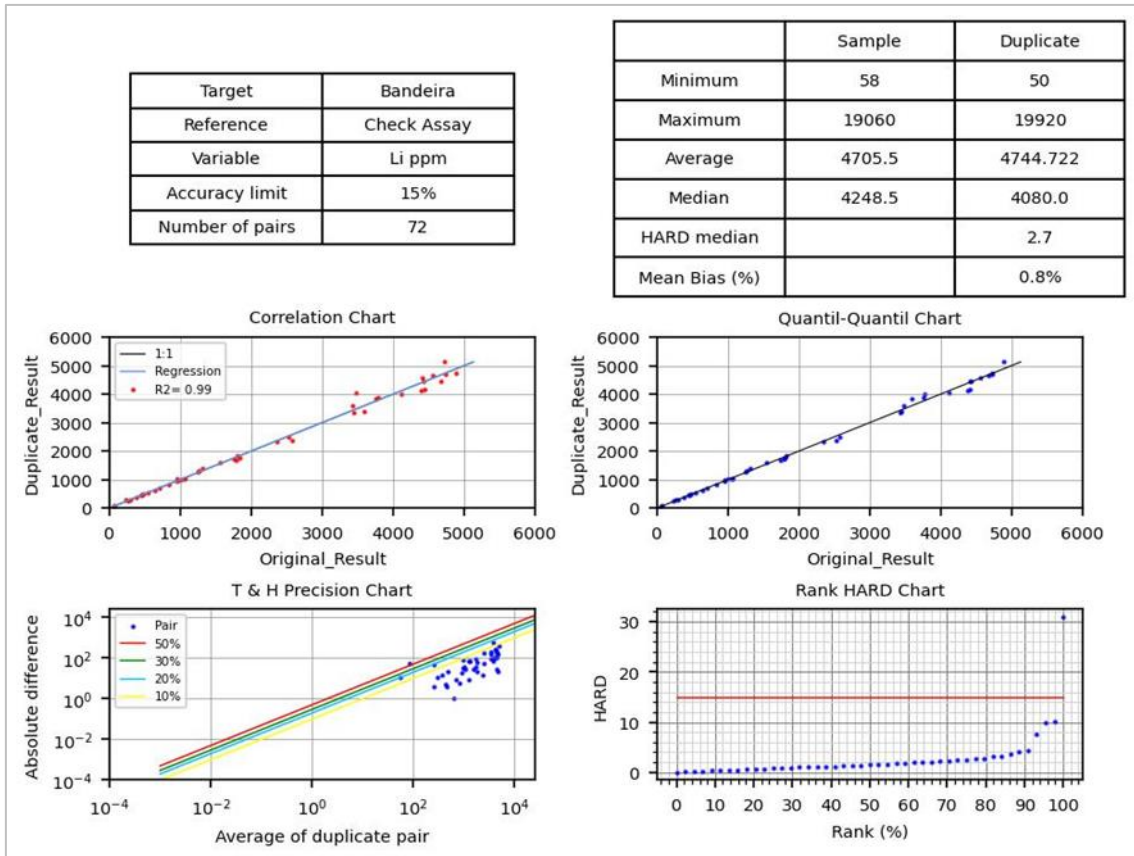


Figure 11.11: Check Assay Control Chart.

11.6 QP Opinion

The Qualified Person thinks that the sampling, sample preparation, security and analysis performed by Lithium Ionic and hired companies are suited for a Mineral Resource Estimation study. Quality Assurance procedures follow the industry’s best practices, and Quality Control results are within industry standards, attesting to the quality of the Database information.

12 DATA VERIFICATION

12.1 QP Verification

Mr. Carlos José E. Silva, an independent QP for Geology Exploration and Mineral Resource Estimate, carried out a site visit on the Bandeira Project between 13 and 14 of September 2023. Lithium Ionic allowed unlimited access to the Company's facilities during this time.

The Author of this Report inspected mainly the following points:

- u) Drilling Sites and Trenches (Figure 12.1 to Figure 12.2):
 - Collar landmarks.
 - Trenches.
 - Drilling Rings.
- v) Drill Core Shed (Figure 12.3 to Figure 12.9):
 - Installations and Overall core shed procedures flowchart.
 - Core box archive and Drillhole landmark checking.
 - Drill core saw and Drill core sample bags.
 - Batches of sample bags.
 - Pulverized samples and Crushed samples returned from labs.
 - Density test procedures by water displacement methodology.
 - Physical files storage for drillhole loggings and bulletins.
 - Checking of mineralization style and sampling procedures.
- w) The cross-checked the assay data within the drill sample database. Digital assay records were randomly selected and scrutinized against the available laboratory assay certificate reports.
- x) Additionally, a comprehensive review of the assay database was conducted to identify errors, including overlaps, gaps in intervals, and typographical errors in assay values. The database generally exhibited high accuracy, requiring no adjustments to the assay values contained within.

All verified procedures related to sampling management, storage, logging, sample preparation and assay were checked, and it is considered inside acceptance limits and in compliance with mineral industry practices. Rock-type descriptions fit with the checked mineralization style.

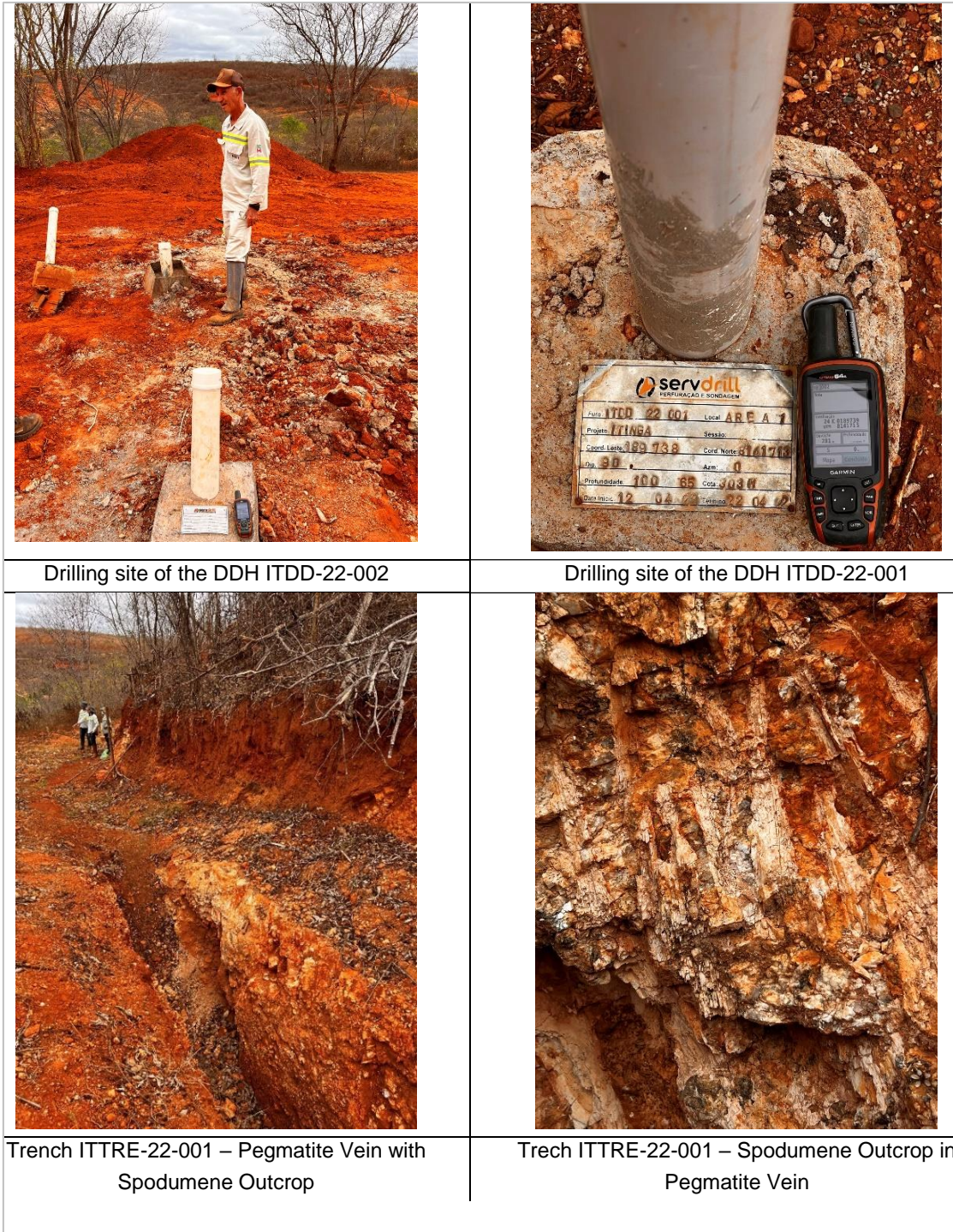


Figure 12.1: Collar Moments and Trench on Lithium Ionic Bandeira Property.



Drill Ring on site of the Bandeira, drilling in 13/09/2023 the DDH ITDD-23-192 o azimuth 140 – dip ~70



Drill Ring on site of the Bandeira, drilling in 13/09/2023 – DDH ITDD-23-192 - Technicians recovering the cores and using the REFLEX ACT III for core orientation



Drill Ring on site of the Bandeira, drilling in 13/09/2023 - DDH ITDD-23-192 – Spodumene in pegmatite veins cores recovered from drilling – depth 355m



Drill Ring on site of the Bandeira, drilling in 13/09/2023 the DDH ITDD-23-192 - REFLEX GYRO IQ used by Lithium Ionic Staff to do the survey measurement

Figure 12.2: Drilling Ring and Survey Equipment on Lithium Ionic Bandeira Property.

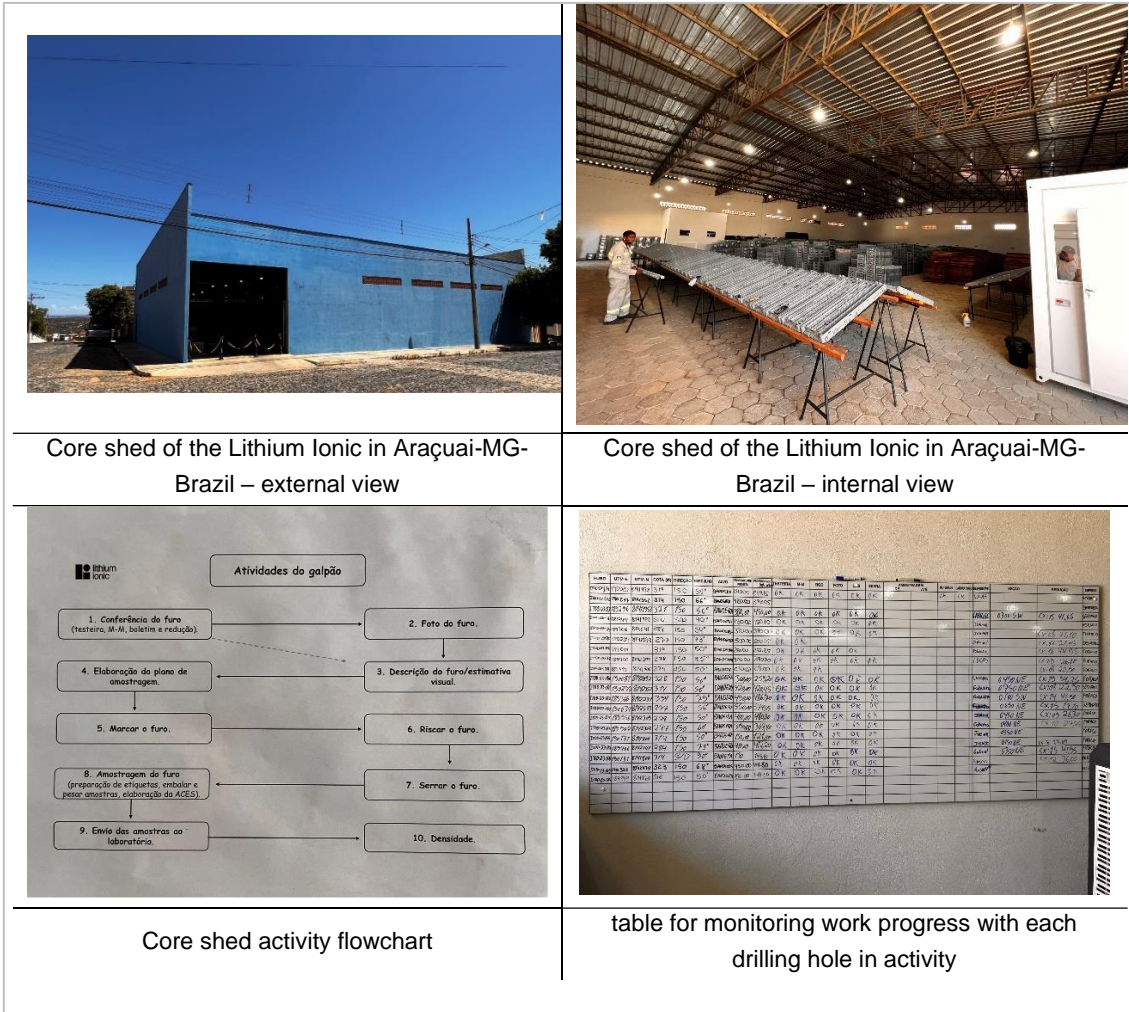


Figure 12.3: Lithium Ionic Core Shed Storage House in Araçuaí.

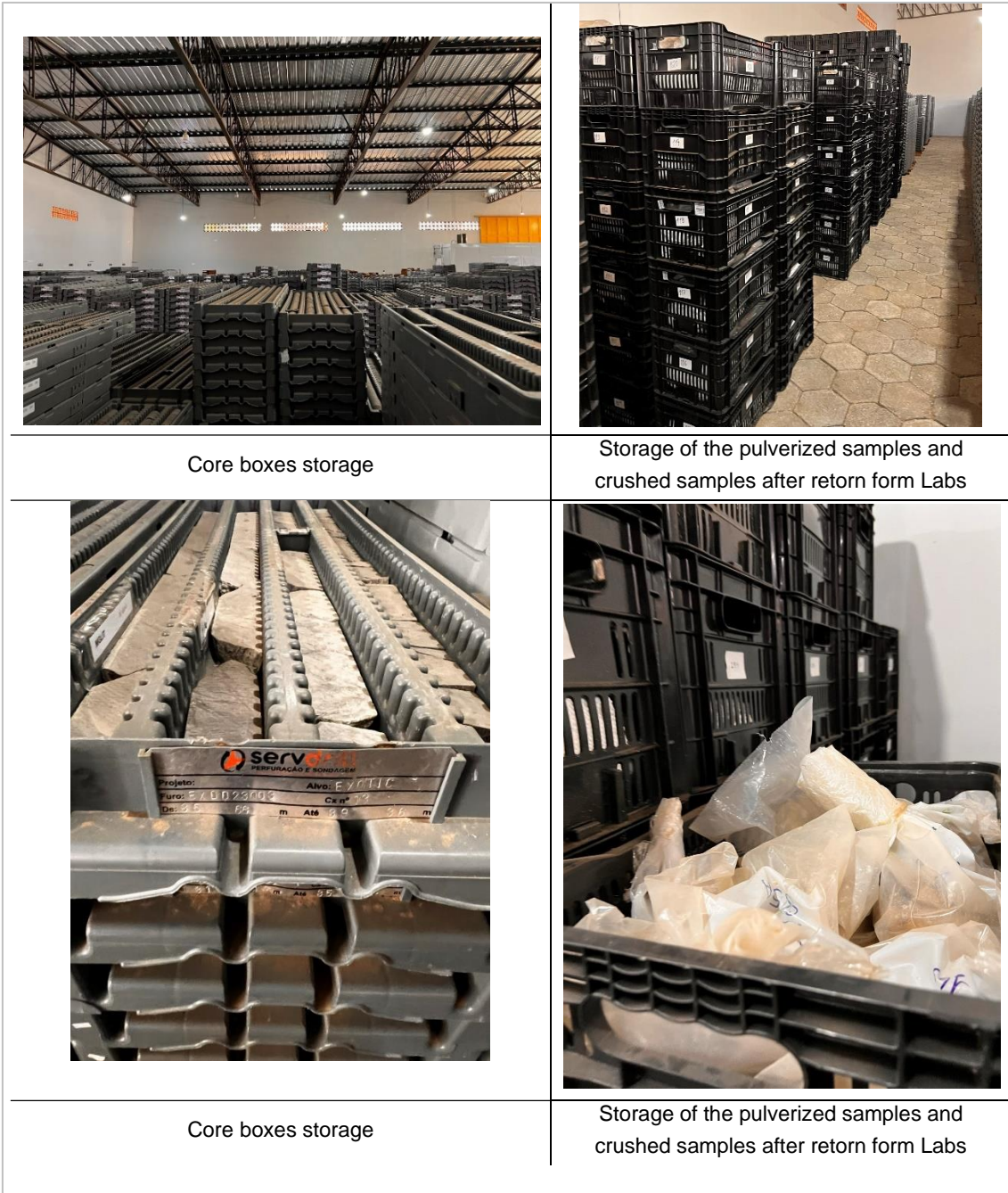


Figure 12.4: Cores Boxes Storage in Lithium Ionic Core Shed.



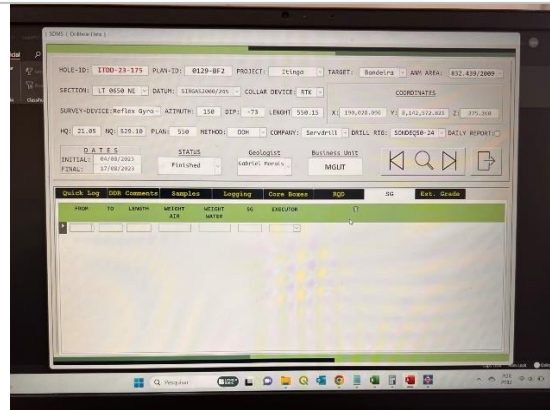
Figure 12.5: Lithium Ionic Staff Working in Logs and Sampling Procedures.



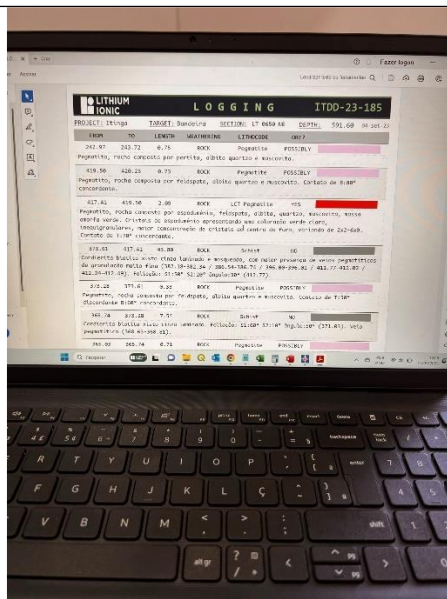
Figure 12.6: Lithium Ionic Density Procedures and QAQC Standards Stock.



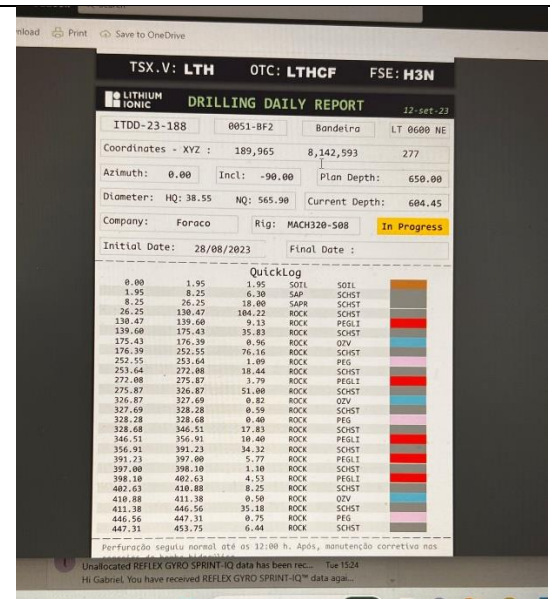
customized database management system for mineral research from Lithium Ionic



customized database management system for mineral research from Lithium Ionic – Registration of Collar Drilling



customized database management system for mineral research from Lithium Ionic -Registration of the Geological log



customized database management system for mineral research from Lithium Ionic -Registration of the Drilling daily report

Figure 12.7: Lithium Ionic Data Base System Interface.



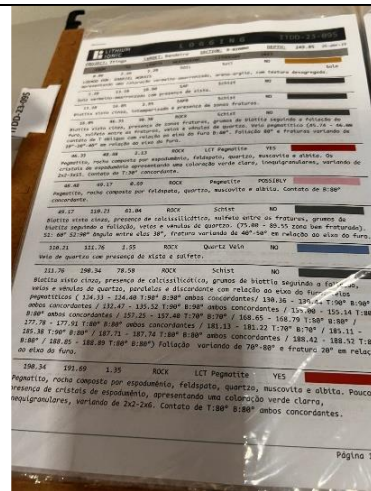
Physical Drillhole Files Storage



binder with drill hole documents



binder with drill hole documents



binder with drill hole documents – geological log



binder with drill hole documents - Daily Drilling Bulletin



binder with drill hole documents – assays results certificates

Figure 12.8: Lithium Ionic Drilling Files Storage.



Figure 12.9: Lithium Ionic Bandeira Property Spodumene Pegmatites Intercepts.

13 MINERAL PROCESSING AND METALLURGICAL TESTING

The ROM from the Bandeira Project's underground mine will be consisted of pegmatite mineralized with minerals such as spodumene, albite, quartz, muscovite, K-feldspar, cookeite, and minor amounts of petalite. The technological characterization of this material to define the process flowchart for size reduction, classification, and concentration by dense media was carried out using 2" (50.8 mm) diameter drill samples.

This technological characterization is always carried out through chemical and mineralogical analyses, physical tests to determine hardness, particle size distribution in crushing tests, level of abrasiveness and metallurgical tests to understand the response of the ore material when subjected to the simulation of the industrial process of concentrating the mineral, spodumene.

13.1 Mineralogical Characterization

The lithium minerals present in a pegmatite of economic interest can be various, as shown in Table 13.1 below. This table shows lithium oxide's reduced chemical formula, density, hardness, and stoichiometric content, expressed as Li₂O %.

Table 13.1: Lithium Minerals Found in Pegmatite Rocks.

| Mineral | Chemical formula | Density | Hardness | % Li ₂ O |
|--------------|--|-----------|-----------|---------------------|
| Ambligonite | LiAl (PO ₄) F | 3,0 - 3,1 | 5,5 - 6,0 | 11,90 |
| Eucryptite | LiAlSiO ₄ | 2,66 | 6,5 | 11,90 |
| Lepidolite | K (Li,Al ₃)(Si,Al) O ₄₁₀ (F,OH) ₂ | 2,8 - 2,9 | 2,5 - 3,5 | 3,3 - 7,8 |
| Montebrasite | LiAl (PO ₄)(OH) | 3,0 | 5,5 - 6,0 | 7,00 |
| Petalite | LiAlSi O ₄₁₀ | 2,4 | 6,5 | 4,90 |
| Spodumenio | LiAlSi O ₂₆ | 3,1 - 3,2 | 6,5 - 7,0 | 8,00 |
| Zinnwaldita | KLiFe ²⁺ Al (AlSi O ₃₁₀)(F,OH) ₂ | 2,9 - 3,0 | 2,5 - 4,0 | 5,60 |
| Hectorite | Na _{0,3} (Mg,Li) ₃ (Si O ₄₁₀)(F,OH) ₂ | 2,3 | 1,0 - 2,0 | 1,22 |
| Triphyllite | LiFe ²⁺ PO ₄ | 3,4 -3,6 | 4 | 9,47 |
| Zabuyelite | Li ₂ CO ₃ | 2,09 | 3 | 40,44 |

Spodumene, petalite and zabuelite was shown in the Bandeira drilling cores.

The mineralogical characterization of the Bandeira ore was carried out using visual modal analysis by the project's geologists in Araçuaí. This visual analysis is quick and very useful for developing geological exploration work. In this phase of the work, around 12 (twelve) drill cores were observed to compose an average mineralogical analysis of the deposit. The average chemical analysis is shown in Table 13.2 below.

Table 13.2: Mineralogical Analysis of the Bandeira Project (Visual Modal).

| Mineral | Chemical formula | Composition (%) |
|--------------|---|-----------------|
| Albite | NaAlSi ₃ O ₈ | 28,40 |
| Quartz | SiO ₂ | 27,85 |
| K-feldspar | KAlSi ₃ O ₈ | 19,50 |
| Spodumene | LiAlSi ₂ O ₆ | 17,25 |
| Muscovite | KAl ₂ (Si ₃ Al)O ₁₀ (OH, F) ₂ | 3,70 |
| Cookeite | LiAl ₄ (Si ₃ Al)O ₁₀ (OH) ₈ | 1,80 |
| Petalite | LiAlSi ₄ O ₁₀ | 0,50 |
| Accessories* | | 1,00 |

*Accessories: Opaques, sphalerite, blue tourmaline, beryl, cassiterite, columbite/tantalite, lithiophyllite/triphyllite, apatite and zabuelite. Variation of +/- 5.00% is acceptable by this methodology.

13.2 Chemical Analysis of the Mineralized Material

The average analysis of the Bandeira deposit, considering core samples and metallurgical test results, is shown below in Table 10.3. This average chemical analysis is comparable to the pegmatites mineralized with spodumene in the Itinga and Araçuaí region, as characterized by the companies that extract and beneficiate lithium ores in the region.

Table 13.3: Average Chemical Analysis of Mineralized Intervals from Bandeira Cores (Typology = PegLi).

| Metal Oxides | Composition |
|--------------------------------------|-------------|
| Li ₂ O, % | 1,41 |
| Fe ₂ O ₃ , % | 0,86 |
| SiO ₂ , % | 74,15 |
| Al ₂ O ₃ , % | 14,40 |
| K ₂ O, % | 3,60 |
| P ₂ O ₅ , % | 0,45 |
| CaO, % | 0,45 |
| On ₂ O, % | 3,20 |
| SnO ₂ , ppm | 210 |
| Ta ₂ O ₅ , ppm | 80 |
| WO ₃ , ppm | 35 |
| Nb ₂ O ₅ , ppm | 100 |

13.3 Metallurgical Tests

For the sake of more understanding, the word “ore” in this item is used to describe the plant feed.

Preliminary metallurgical tests using dense media were carried out by SGS Geosol in Vespasiano, Brazil, and Sepro Minerals in Vancouver, Canada. In addition, ore sorter tests were conducted by TOMRA in Germany.

13.3.1 Dense Media Separation

- The dense media separation process is based on the principle of density to concentrate minerals and eliminate gangue, using a fluid with a density intermediate

to separate materials. The types of dense medium used are (i) aqueous solutions of inorganic salts, (ii) organic liquids, and (iii) suspensions of solids in water (AQUINO et al., 2007; CAMPOS et al., 2018).

- The first application of dense medium separation was carried out using aqueous solutions of inorganic salts for the industrial separation of coal. This type of dense medium is less expensive than organic liquids, but the maximum density achieved is 1.95 g/cm³ (BURT, 1984).
- Organic liquids are not used industrially as they are toxic, corrosive and have a low vapour pressure. They are used in the laboratory for preliminary concentration studies and to determine the degree of release.
- Suspending solids in water is an alternative for separating metallic minerals industrially. The solid must have a high density, friability, resistance to abrasion and easy recovery of the ore fines retained in the dense slurry. Initially, galena was developed, which allowed separation, but it became unfeasible due to the low efficiency of mineral recovery. The use of magnetite and ferrosilicon has become widespread since it is possible to recover ore fines by magnetic separation with high efficiency. The maximum application density for magnetite is 2.5 g/cm³, used for low-density minerals, and for ferrosilicon, it is 3.4 g/cm³, the primary dense medium used industrially. It is worth noting that the silicon content in the alloy must be between 15 and 22% to minimize iron oxidation and maximize magnetic recovery.
- Separation in dense media can be applied for pre-concentration or to obtain the final concentrate. According to Wills (1988), dense media separation is generally used for particles larger than 0.6 mm.
- The equipment used in the dense media separation process can be static (drum or cone) or dynamic (cyclone or dynawhirpool). Static dense media separation is suitable for coarse-grained material since the sedimentation speed is proportional to the diameter of the particles, and in this case, only gravitational force acts. In the case of the dynamic process, separation is proportional to centrifugal acceleration, which allows for greater capacity and separation of finer particles compared to the static dense medium.
- The drum used in static dense media separation consists of a rotating cylindrical tube into which the ore material and viscous media are fed separately at the top of the equipment (Figure 13.1). The heavy particles sediment in the lower part of the tube and are transported to the upper part through perforated plates attached to the inside of the cylinder, where they are directed to a collection chute, as indicated in point 2 of Figure 13.1. The light particles are dragged through the center of the cylinder and exit by overflow at the end opposite to the feed (point 3 in Figure 13.1). The dimensions of the cylinder vary according to the particle size range of the application, which can include particles from 5 to 300 mm, so cylinders up to 4.3 m in diameter and 6 m in length can be used (CAMPOS et al., 2018).

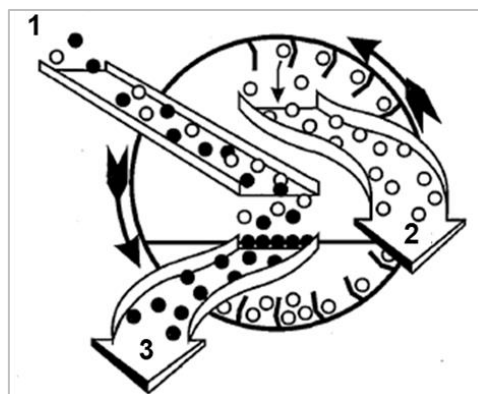


Figure 13.1: Schematic Representation of Dense Medium Drum.

(1) Ore feed and Dense Medium. (2) Heavy Particle Outlet. (3) Light Particle Outlet. Source: Dorr-Oliver Eimco USA Inc. 2003.

The dense medium cone is a conical tank with sufficient agitation to keep the dense medium in suspension and aid separation, as shown in Figure 13.2. The light particles float and overflow at the top of the cone. The heavy particles sink and are removed from the cone using pumps or an upward flow of air (internal or external). The conical separator can be used to process particles up to 10cm in size and can be found in sizes up to 6 m in diameter (CAMPOS et al., 2018).

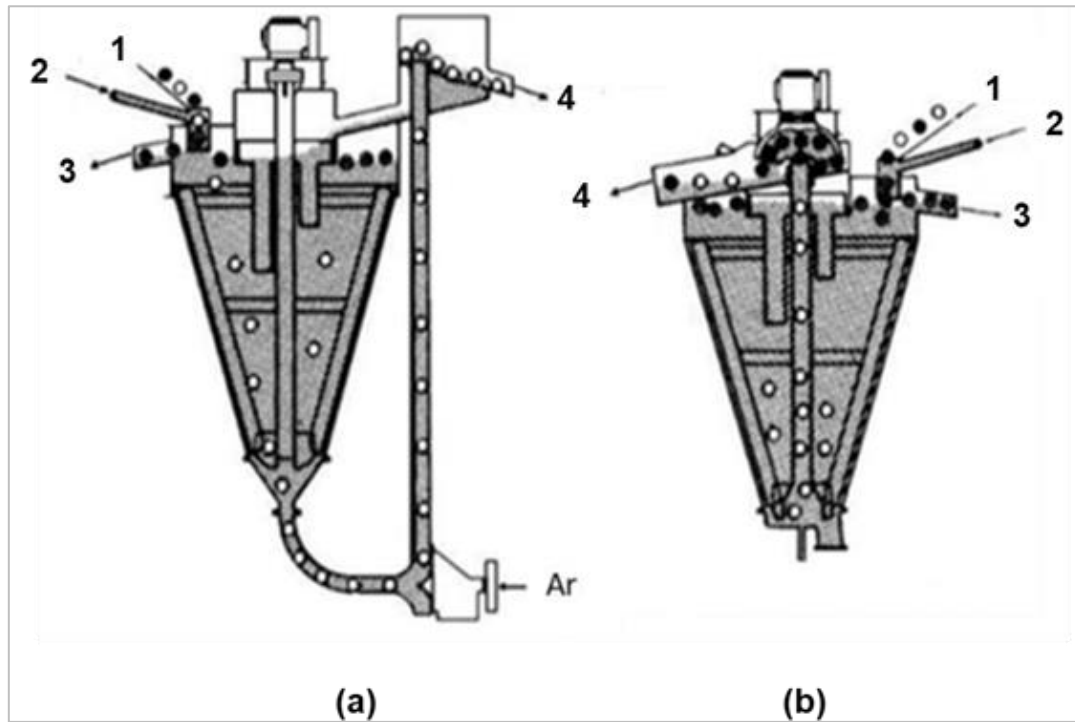


Figure 13.2: Schematic Representation of Cone.

(a) Cone with External Upward Flow. (b) Cone with Internal Upward Flow. (1) Ore Feed. (2) Dense Medium Feed. (3) Light Particle Outlet. (4) Heavy particle outlet.

The dense media cyclone comprises a cylindrical and conical part, with the ore and dense media mixture fed tangentially to the cylindrical portion, as indicated in point 1 of Figure 13.3. The heavy particles move along the wall in the vortex formed inside the cyclone and are discharged at the bottom (apex). The vortex drags the light particles to exit at the top of the cyclone. The performance of the cyclone is a function of (i) the feed pressure, (ii) the density of the dense medium pulp, (iii) the grain size of the dense medium, (iv) the ore material (particle shape, particle size distribution, partitioning of light and heavy particles), and (v) the angle of the conical section of the cyclone. The recommended ore size for this application is between 0.5 and 20 mm (AQUINO et al., 2007).

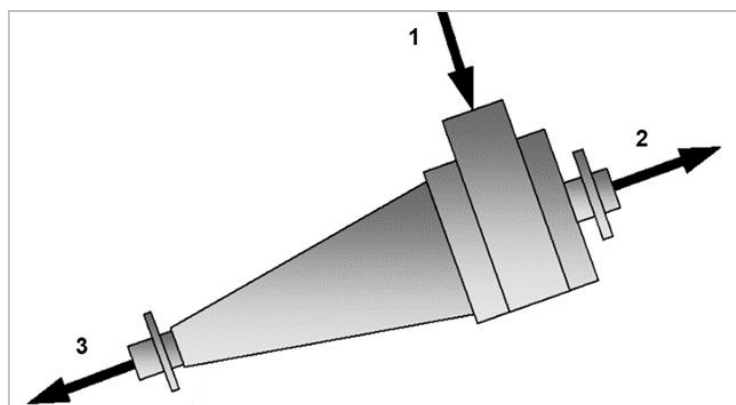


Figure 13.3: Schematic Representation of a Dense Medium Cyclone.

(1) Ore feed and dense medium. (2) Light particles exit. (3) Heavy particles exit.

The dynawhirlpool consists of a cylinder installed at an inclination of 25° to the horizontal for ore treatment. The ore is fed into the upper part of the cylinder diluted with 10% of the dense medium, as shown in point 1 of Figure 13.4.

The rest of the dense medium is fed under pressure tangentially to the cylinder, forming an upward-moving vortex, which directs the heavier particles towards the wall of the cylinder and transports them to the top, where they are discharged into the side opening of the cylinder, point 4 of Figure 13.4.

The light particles float along the longitudinal axis inside the cylinder and are discharged at the bottom, point 3 in Figure 13.4. The control of the vortrateex is a function of the geometric parameters of the dynawhirlpool, such as (i) the dimensions of the cylinder, (ii) the diameter and internal length of the feed pipe and the outlet pipe of the float, (iii) the diameter of the dense medium feed and the outlet of the sink. In addition to operational variables such as the dense medium feed pressure and the float outlet pressure, the latter is adjusted by the height of the hose connected to the outlet pipe.

The upper limit of the feed particle size ranges from ½" (13mm) to 1 ½" (38mm), for which 6" (15cm) to 18 ½" (47cm) cylinders are used, respectively. The potential lower grain size limit is up to 0.2 mm, regardless of the equipment size. However, the high viscosity of the medium limits feeding to particles between 0.6 and 0.8mm due to the difficulty of sieving through very close meshes (AQUINO et al., 2007; CAMPOS et al., 2018).

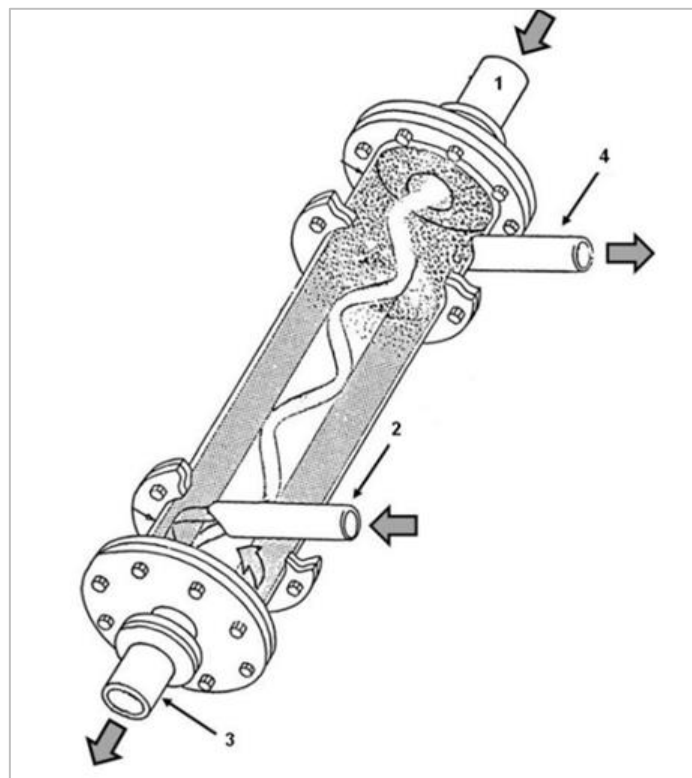


Figure 13.4: Schematic Representation of the Dynawhirlpool.

(1) Ore feed. (2) Dense medium feed under pressure. (3) Light particles outlet. (4) Heavy Particles Outlet.

13.3.1.1 SGS

Samples from boreholes ITDD-22-001, 002 and 007 were sent to SGS and prepared according to the procedure shown in Figure 13.5 for the HLS test. The objective of the test is to evaluate the performance of dense media separation in obtaining lithium concentrate for the Bandeira Project, according to market specifications, by varying the particle size and density of the viscous media.

The approximately 20kg sample was dried and crushed in a jaw crusher with openings of 31.5, 25.4 and 12.5 mm to obtain 100% material in 12.5mm. Once this was done, particle size analysis was carried out using a sequence of 12.5, 6.3, 1.7 and 0.5mm sieves, and a representative sample was taken from each range to send for chemical analysis. In addition, for the -12.5+6.3mm, -6.3+1.7mm and -1.7+0.5 bands, HLS tests were carried out for densities of 3.0, 2.9, 2.8 and 2.7g/cm³.

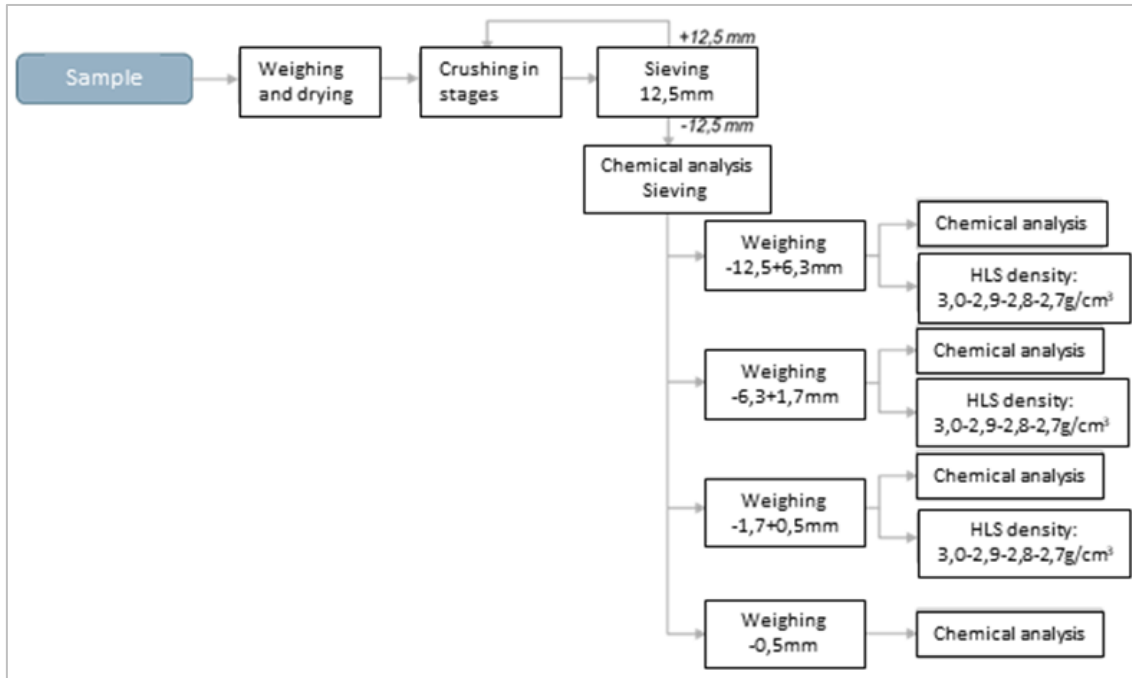


Figure 13.5: Flowchart of the Sample Preparation Procedure and HLS Test.

The particle size distribution of the 100% material passing 12.5mm is shown in Figure 13.6. It is worth noting that approximately 12% of the mass does not have a particle size suitable for the dense separation stage, i.e., it is smaller than 0.5mm. The Bandeira Project's process route considers concentrating this material by flotation.

The chemical analysis identified a major composition of aluminum (9.04%), potassium (1.83%) and lithium (0.76%), as shown in Figure 13.7. The presence of aluminum can be explained mainly by the presence of albite, K-feldspar and spodumene. Potassium is mostly present in K-feldspar and lithium in spodumene. Regarding iron, the main contaminant for market specifications, the concentration in the ore is 0.16%. The mineral origin of iron is mainly shale (biotite). In addition to the presence of iron, another point of attention regarding shale is its density, which can vary between 2.40 and 3.05g/cm³, similar to the cut-off density of the dense medium separation generally used to concentrate spodumene, since the density of the mineral of interest varies between 3.15 and 3.20g/cm³ (PEIXOTO, et al., 2016).

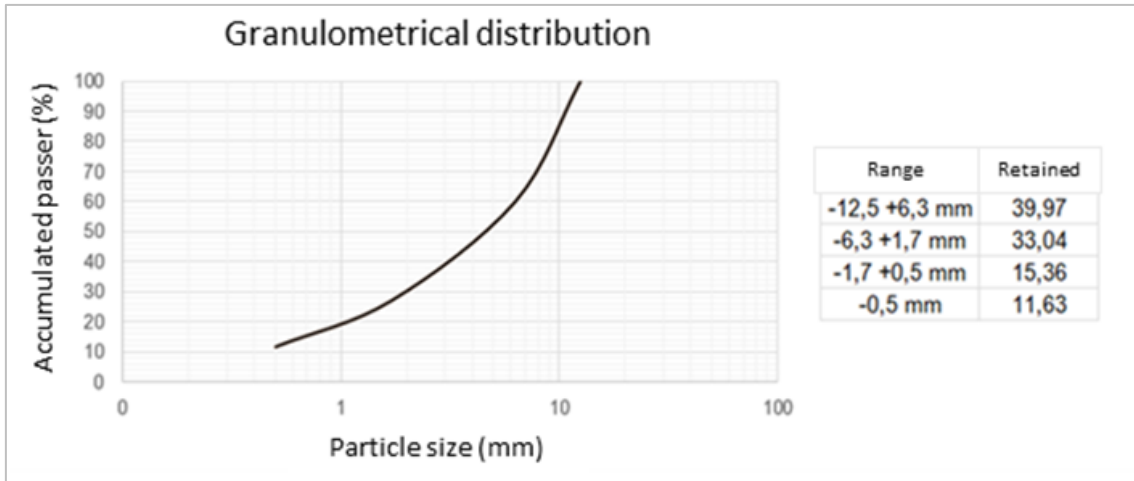


Figure 13.6: Particle Size Distribution of the 12.5mm Crushing Product.

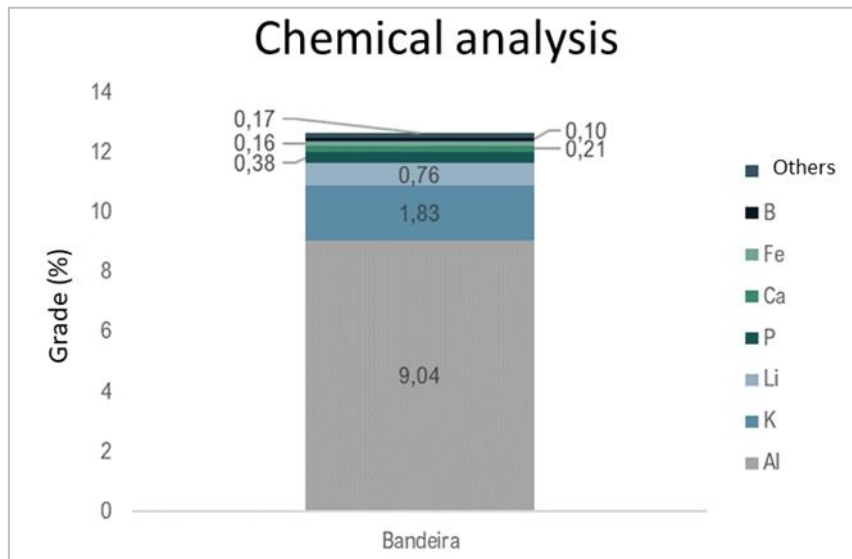


Figure 13.7: Chemical Composition of the Bandeira Sample.

The separation tests in dense media were carried out by particle size range, namely (i) -12.5 +6.3mm, (ii) -6.3 +1.7mm and (iii) -1.7 +0.5mm, using organic liquids to assess the optimum density to achieve the market specification for lithium concentrate, i.e., a minimum of 5.5% Li₂O and a maximum of 1% Fe₂O₃.

The densities evaluated were (i) 2.7g/cm³, (ii) 2.8g/cm³, (iii) 2.9g/cm³ and (iv) 3.0g/cm³, for which solutions were prepared with different proportions of methylene iodide (3.29g/cm³) and acetone (0.79g/cm³). The tests for the particle size ranges of -12.5 +6.3mm and -6.3 +1.7mm were carried out in beakers, while the test for the finest particle size (-1.7 +0.5mm) was carried out in a separator funnel.

The test involves mixing the ore and the dense medium solution in the reactor (beaker or separating funnel) and waiting for separation. Once this is done, the sinking material, the dense medium and the floating material are collected separately. The densities were evaluated in sequence, as presented in Figure 13.8. For each stage, chemical composition and mass partitioning were also assessed.

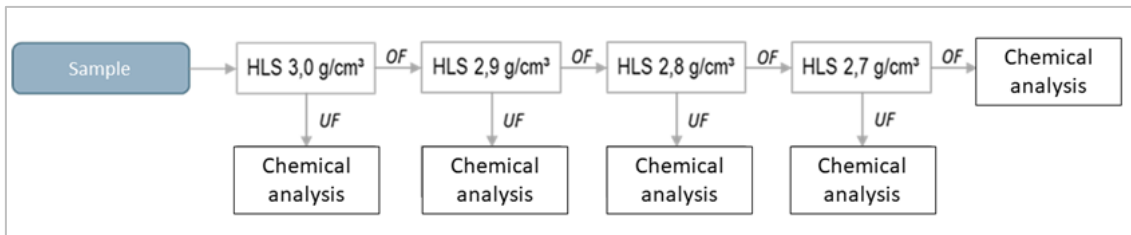


Figure 13.8: HLS Test Flowchart.

Figure 13.9 shows the cumulative result of the Li₂O and Fe content by density for the three particle size ranges evaluated; the value was calculated for the individual content of each sample and the mass split.

Results show that the cutting density increases with particle size, i.e., for finer particles, it is possible to obtain a concentrate, as specified, using a cutting density of 2.7g/cm³; however, for the intermediate particle size range, the cut should be made at 2.8g/cm³ and for coarser material at 2.9g/cm³. In addition, the Li₂O content in the float of the coarser material is three times higher than the float of the finer fabric, which indicates less release of spodumene in the coarser particle size range. About iron, the maximum content limit was met for all densities.

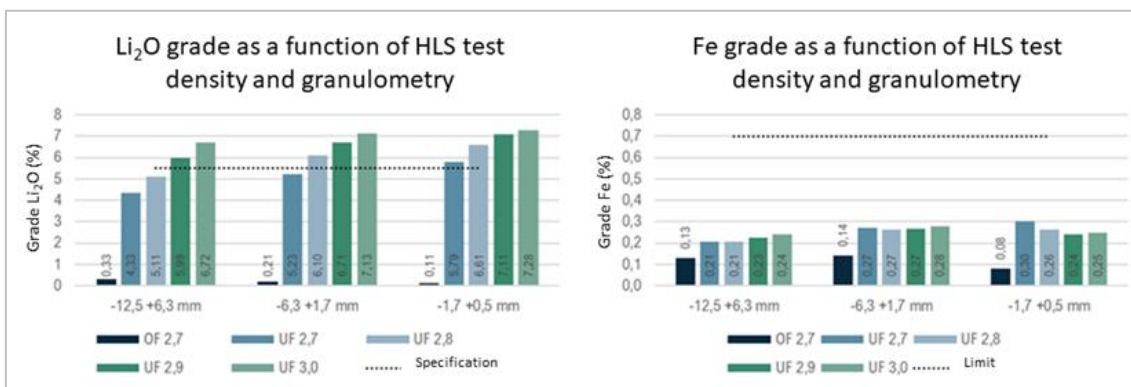


Figure 13.9: Result of chemical analysis of Li₂O and Fe by HLS test step.

The recovery results per particle size range and the overall HLS recovery are shown in Figure 13.10 as the Li₂O content in the concentrate. For the -12.5 +6.3mm particle size range, the cut-off density was 2.84g/cm³, representing a recovery of 70.5%; the values were obtained by interpolation.

The density of the -6.3 +0.5mm range was 2.71g/cm³, and the recovery was 90.1%. However, when considering the loss of fines, i.e., the fraction smaller than 0.5mm, which represents 12% of the mass and 11% of the lithium, the HLS recovery was 74.8%.

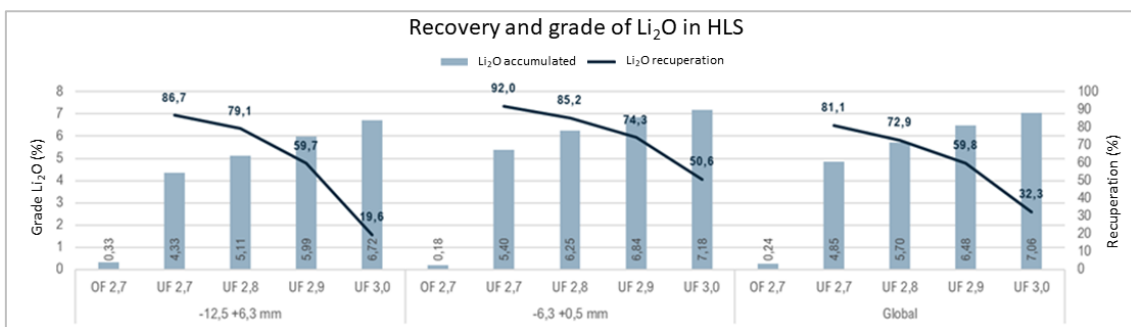


Figure 13.10: Recovery and Li₂O Content in the HLS.

13.3.1.2 SEPRO

The HLS and DMS tests were conducted on underground samples from a mine near the Bandeira project. Two samples were selected, "C1" and "S1", with sample C1 having a higher concentration of shale, to assess the impact of shale on the specification of the DMS concentrate. Tests were carried out for two particle size ranges: -19 +0.85mm and -6.3 +0.85mm.

The HLS tests were carried out in two stages for 2.90 and 2.70g/cm³ densities. Similarly, pilot tests with Condor DMS were carried out for densities of 2.77/2.76 and 2.91g/cm³. The test flowchart is shown in Figure 13.11.

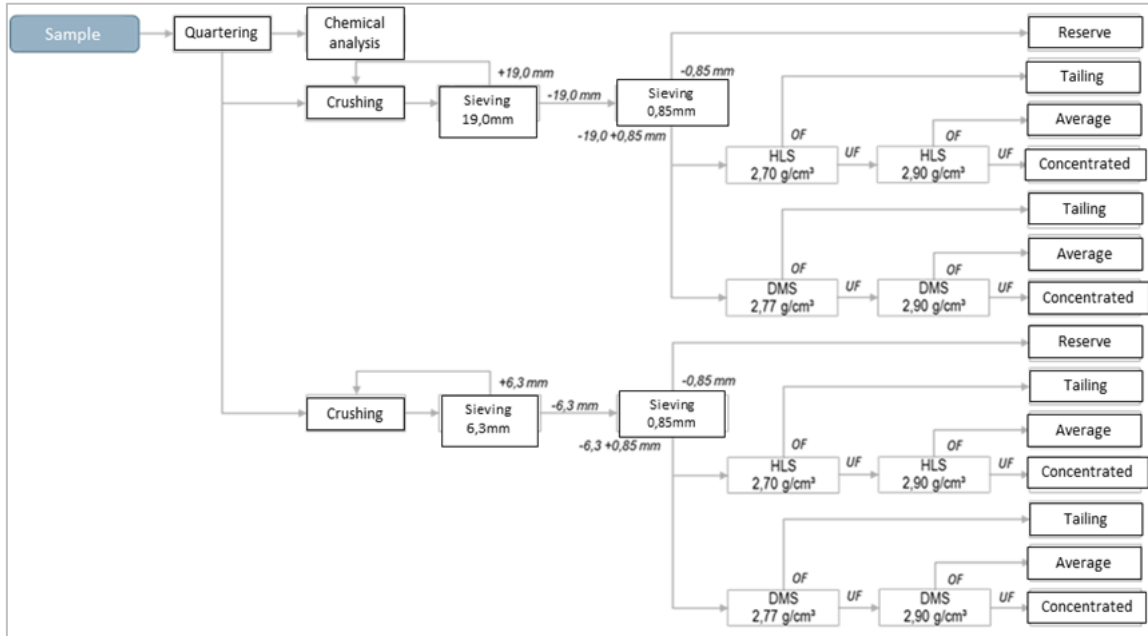


Figure 13.11: Sevro's Sample Preparation and Testing Flowchart.

The result of the chemical analysis of the feed sample is shown in Figure 13.12. The sample is mainly composed of silicon, aluminum, potassium, and iron. Iron in the material above the specification limit of the concentrate is a point of attention.

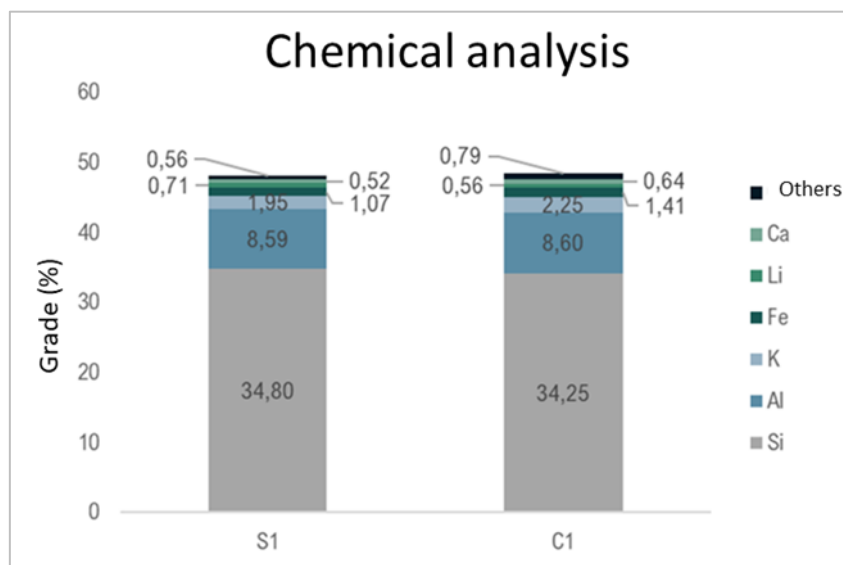


Figure 13.12: Result of Chemical Analysis Feed Sevro Tests.

The results of the HLS and DMS tests are shown in Figure 13.13. In general, dilution did not significantly impact the recovery of lithium by separation in dense media. Regarding particle size, finer particle size increased the partial recovery of the unit operation (HLS or DMS) since it promoted greater material of economic interest liberation. However, it decreased overall recovery, as it increased the proportion of loss in the fines.

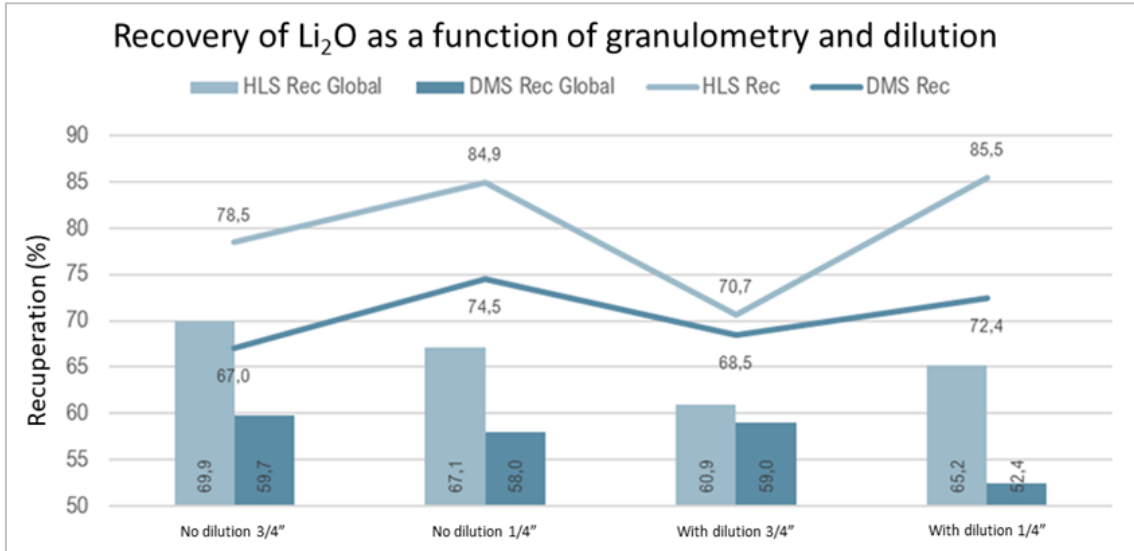


Figure 13.13: Sepro Test Results.

Figure 13.14 shows the results of the chemical analysis for the HLS and DMS concentrate. About the Li₂O content, it can be seen that for all conditions and types of tests, the value obtained was higher than specified. Therefore, a lower density in the dense separation stages is recommended. The iron content in the concentrate was also higher than specified.

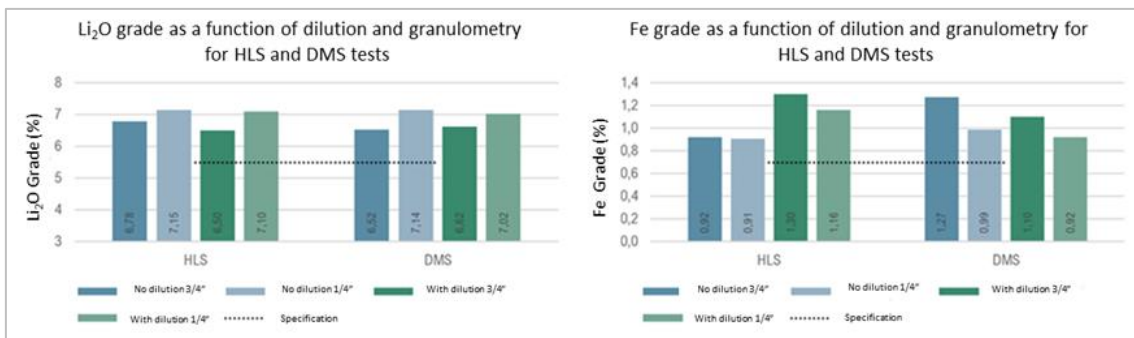


Figure 13.14: Result of chemical analysis of Li₂O and Fe by condition of the HLS and DMS tests.

13.3.2 Ore Sorter

The principle of manual sorting dates to the Bronze and Iron Ages, and technological advances have been developed to improve the efficiency of this process. Initially, sorting was carried out on a table; later, conveyors were used to increase productivity. However, manual sorting by visual inspection is limited to grain sizes larger than 50 or 60mm and represents a high labour cost (REVUELTA, 2018).

In the 1940s, using sensors in mining, the first sensor-based sorting technology using a radiometric source was developed to classify rocks according to natural radioactive concentrations in Canada (YOUNG, 2017; VERAS, 2018). In 1950, the photometric colour sensor was used to preconcentrate uranium ore in Australia. Subsequently, sensor-based sorting spread to gold, zinc, and copper mining (VERAS, 2018). In the 1960s, optical sorting was applied to diamond recovery (WILLS and NAPIER-MUNN, 2006).

In 1970, an automatic classifier for coal was developed using X-ray attenuation, a method already studied by Marie Curie in separating potatoes (VERAS, 2018). The automatic classifier can be applied either for pre-concentration, for example, in the processing of gold and uranium, eliminating particles with lower than desired content, or to obtain the final concentrate, as is the case with limestone and diamonds (WILLS and NAPIER-MUNN, 2006).

The system consists of a controlled feed of ore onto the belt, on which a detector is installed that captures the properties of each particle and analyzes them to subsequently eject them at the end of the belt, as shown in Figure 13.5.

The feed must be between 5 and 300mm, the size ratio between the smallest and largest particles must be 2 or 3 times, and the material must be sufficiently liberated at the feed particle size. In addition, all the particles must be exposed to the sensor, so overlapping should be avoided, and a monolayer of material should be aimed for.

Current sorters have a capacity of 150t/h for grain sizes between -25 +5mm and 500t/h for grain sizes between -300 +80mm. The performance of the sensor-based sorter depends on the computer processing capacity, the feed condition, and the performance of the blowers (WILLS and NAPIER-MUNN, 2006; VERAS, 2018).

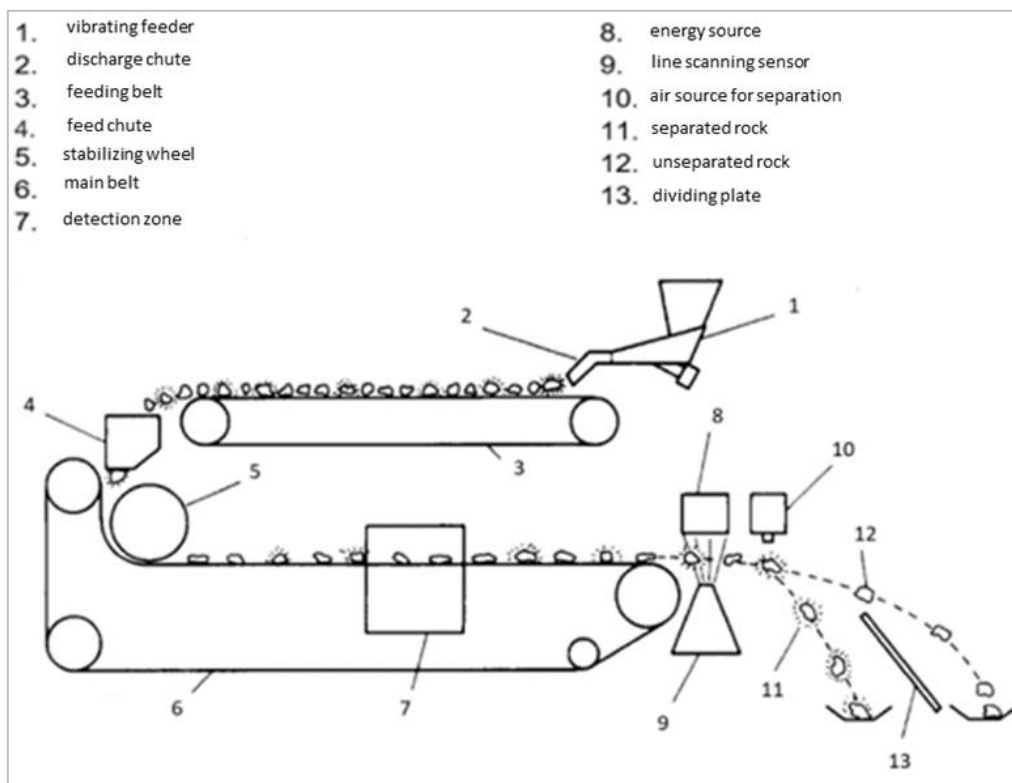


Figure 13.15: Schematic Representation of the Sensor-based Sorter (VERAS, 2018).

Table 13.4 shows the main properties analyzed and the respective applications of the different sensors used in classification. Electromagnetic interactions in different energy ranges with the ore generate characteristic responses that make it possible to identify the particles (WOTRUBA and HARBECK, 2012).

The reactions from the interaction between electromagnetic radiation and the sample can be (i) fluorescence, (ii) diffusion, (iii) reflection, (iv) remission, (v) absorption, (vi) refraction and (vii) transmission.

The sensors analyze the variation in irradiation and convert the photon energy into an electrical signal, which is then converted into a colour scale. Sensors can also be combined to distinguish the particles of interest.

Currently, the most used sensors in the mineral industry are X-ray, colour and infrared transmission (VERAS et al., 2016).

Table 13.4: Properties and Applications of Sensor-based Classification (Revuelta, 2018; Wotruba and Harbeck, 2012).

| Sensor technology | Property | Application |
|--------------------------------|--|---|
| Radiometric (RM) | Natural Gamma Radiation | Radoactive Ores |
| X-ray Transmission (XRT) | Atomic Density | Base Metals Heavy Metals Precious Metals Industrial Minerals Coal Diamond Scrap |
| X-ray Fluorescence (XRF) | X-ray Visible Fluorescence | Metal Sulphides Limestone Iron Ore Diamonds |
| Color | Reflection Absorption Transmission | Base Metals Precious Metals Industrial Minerals Diamonds Glass |
| Photometric (PM) | Monochrome Reflection Absorption | Coal Sulphides Phosphates Oxides Precious Stones Diamonds |
| Near Infrared (NIR) | Reflection Absorption | Base Metals Industrial Minerals |
| Infrared (IR) | Heat Conductivity Heat Dissipation | Metal Sulphides Precious Metals Industrial Metals Graphite Coal |
| Electromagnetic (EM) | Conductivity | Metal Sulphides Native Metals |
| Electrostatic (Revuelta, 2018) | | Salts Halita Silvita |
| Magnetic (Revuelta, 2018) | | Iron ore Andalusian Quartz Kimberlites |

13.3.2.1 TOMRA

A sample made up of 6 boreholes (ITDD-22-013, 015, 029, 032, 035 and 036) with a Li₂O content of between 1.31 and 1.52% was sent to TOMRA, in Germany, to assess the applicability of the Ore Sorter in the pre-concentration stage. The material was crushed to obtain 100% throughput at 31.5mm and separated into 3 particle size ranges (-31.5 +19mm; -19 +9.5mm and -9.5mm).

The tests were carried out on two particle size ranges, -31.5 +19mm and -19 +9.5mm, and the -9.5mm material was weighed, and the content determined to make up the metallurgical balance of the test. A preliminary analysis was carried out on the sample and the use of the X-ray transmission sensor (XRT) was recommended for the test.

The X-ray transmission sensor is related to the atomic density of the material, so the higher the intensity of the X-ray transmitted, the lower the absorption and the lower the atomic density. Electromagnetic radiation between 90 and 200keV is incident on the sample and the transmitted radiation is detected pixel by pixel and converted into an electrical signal to generate a grayscale image. Thus, a light color indicates low absorption and therefore low atomic density. To distinguish thickness and atomic density, two sensors are used, acquiring different energy bands (VERAS, 2018; WOTRUBA and HARBECK, 2012).

The tests were carried out using the cascade classification principle, as shown in Figure 13.16. The sample was fed via a vibrating feeder onto a belt and analyzed by the Duoline X-ray sensor.

The initial configuration of the equipment was programmed to eliminate all particles with at least 30% high atomic density pixels. Next, the material previously classified as low density was classified again, eliminating all particles with at least 80% high and medium atomic density pixels. Finally, the particles that were not ejected in the intermediate stage underwent a new classification, where particles with at least 50% of high and medium density pixels were eliminated and particles with low atomic density were kept, i.e., the material sorter concentrate.

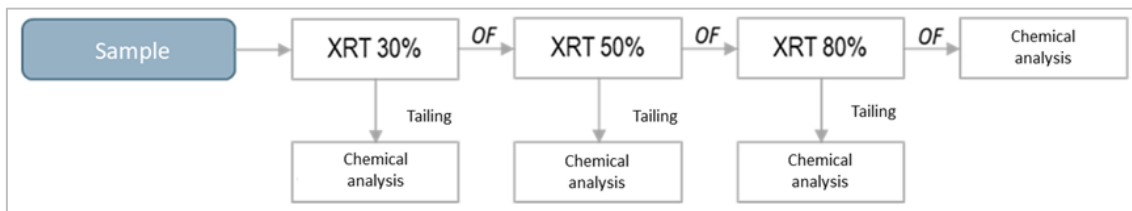


Figure 13.16: XRT Sorter Cascade Sorting Flowchart.

The results are shown in Table 13.5 and Table 13.6 for the particle size ranges of -31.5 +19mm and -19 +9.5mm, respectively. The fine fraction (-9.5mm) accounted for 16.9% of the mass, which will be sent to the dense media concentration stage.

The results show that as the average atomic density of the ROM sorter cut decreases, the concentrate content increases and the metallurgical recovery decreases for both particle size ranges.

Configuration 2 was therefore selected as the most interesting since it was possible to enrich the content of the dense medium feed by between 25 and 26%, recovering 91 to 94% of the lithium.

Table 13.5: Pre-Concentration Ore Sorter Results for -31.5 +19mm.

| Configuration | Mass Reduction (%) | Content Li ₂ O Ore (%) | Li ₂ O content Tailings (%) | Li ₂ O Recovery (%) | Enrichment (%) |
|---------------|--------------------|-----------------------------------|--|--------------------------------|----------------|
| 1 | 17.15 | 1.46 | 0.23 | 96.85 | 17 |
| 2 | 24.81 | 1.56 | 0.30 | 93.97 | 25 |
| 3 | 48.43 | 1.74 | 0.73 | 71.69 | 39 |

Table 13.6: Pre-Concentration Ore Sorter Results for -19 +9.5mm.

| Configuration | Mass Reduction (%) | Li ₂ O Ore (%) | Li ₂ O content Tailings (%) | Li ₂ O Recovery (%) | Enrichment (%) |
|---------------|--------------------|---------------------------|--|--------------------------------|----------------|
| 1 | 16.49 | 1.52 | 0.29 | 96.37 | 16 |
| 2 | 26.86 | 1.65 | 0.43 | 91.26 | 26 |
| 3 | 55.01 | 1.95 | 0.80 | 66.51 | 50 |

14 MINERAL RESOURCE ESTIMATES

GE21 conducted comprehensive 3D geological modelling, statistical and geostatistical studies, and grade estimation for the Lithium Ionic Bandeira Property. This estimation considered various factors, such as the quantity and distribution of available data, interpreted controls on mineralization, mineralization style, and the quality of the sampling data.

The geological modelling and estimation processes were executed utilizing Leapfrog 2023.1 software. The UTM Projection – Zone 22 South in SIRGAS 2000 Datum was adopted as the reference coordinate system for the database in this project.

14.1 Drilling Database

The database underwent a comprehensive visual validation, considering the interrelation of tables, identifying gaps and overlaps, and ensuring the inclusion of crucial information. Additionally, using Leapfrog Geo software, GE21 conducted validation checks on the Collar, Survey, Assay, and Lithology tables. This stage of the work did not reveal any significant inconsistencies, as these had already been verified during the Data Verification stage.

Mineral Resource estimates were based on data derived from drill hole and trench databases, incorporating lithology logs and assay results from HQ drill core samples. The topographic surface bounds the extent of these estimates. Figure 14.1 illustrates the spatial distribution of the utilized drill holes.

The original dataset provided by Lithium Ionic encompassed data from 182 surface diamond drill holes (totaling 39,679 meters) and 22 trench channels (1417 meters) executed by Lithium Ionic from 2022 until August 30, 2023.

The Bandeira database contains 4,876 assay intervals covering 4,592 meters, comprising 164 assays from trenches totaling 157 meters and 4,712 assay intervals from drill holes totaling 4,434 meters.

The assay table includes data for various elements, including Li (ppm), Li₂O (%), Al (%), As (ppm), B (%), Ba (ppm), Be (ppm), Ca (%), Cd (ppm), Co (ppm), Cr (ppm), Cu (ppm), Fe (%), K (%), La (ppm), Mg (%), Mn (ppm), Mo (ppm), Nb (ppm), Ni (ppm), P (%), Pb (ppm), Sb (ppm), Sc (ppm), Sn (ppm), Sr (ppm), Ta (ppm), Ti (%), V (ppm), W (ppm), Y (ppm), and Zn (ppm). Following a thorough review of the database, the Li₂O (%) data was extracted explicitly for subsequent statistical analysis, block modelling, and resource estimation.

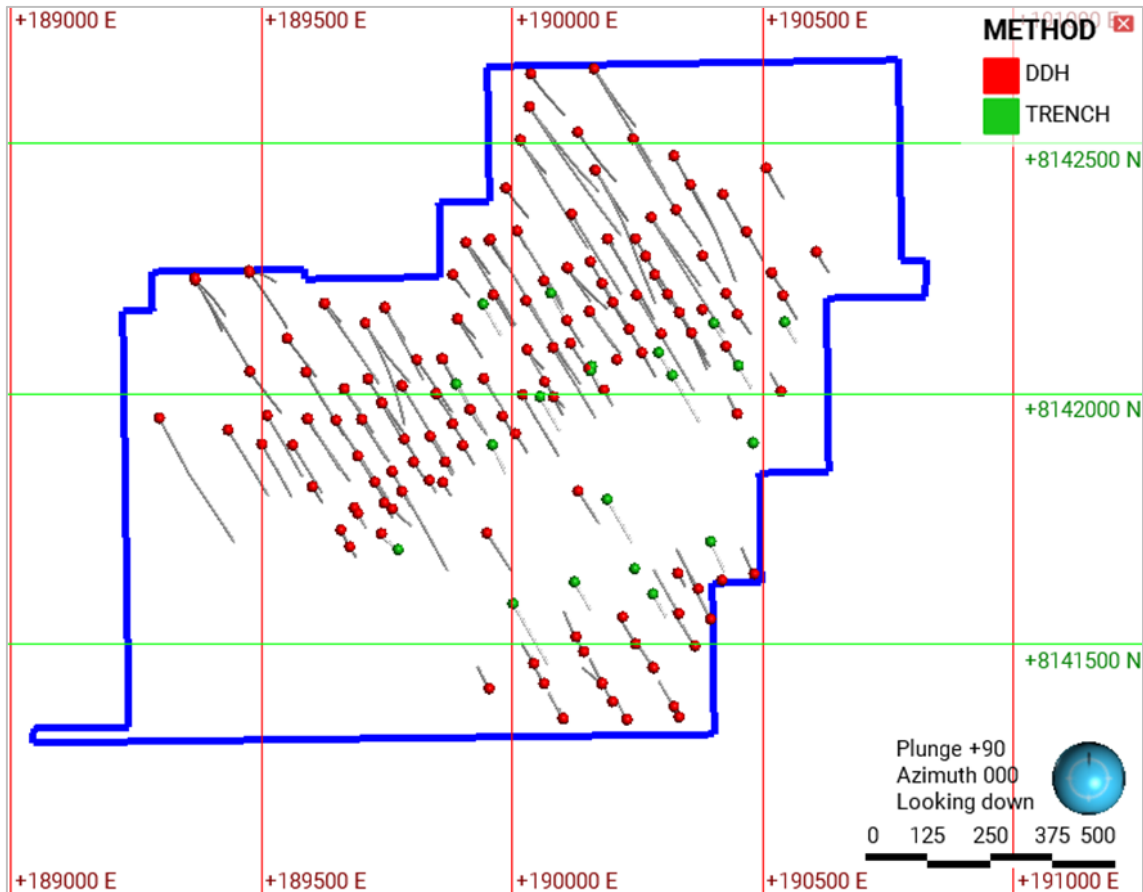


Figure 14.1: Drillhole Location Map.

14.2 Geological Modeling

Lithium Ionic undertook a geological interpretation, encompassing all documented pegmatite intervals within the Bandeira deposits. Initially, cross-sectional interpretations were crafted, utilizing traditional manual techniques and advanced cartographic software platforms such as QGIS, ArcGIS, and Leapfrog. These initial steps laid the groundwork for a robust modelling process.

A set of grade shell sections, with an envelope delimiting zones with a cut-off grade of 0.3% Li₂O (%), was interpreted by the Lithium Ionic team (Figure 14.2 and Figure 14.3). The resulting interpretations were developed into a series of implicit 3D models, aligned with a prevailing strike direction of 235° and 140° (Figure 14.4 and Figure 14.5).

Lithium Ionic also conducted weathering modelling, basing the analysis on the descriptions provided in the logs (Figure 14.6).

The Qualified Person thinks the geological interpretations and modelling suit a Mineral Resource Estimation study. Quality Assurance procedures follow the industry's best practices, and the model is honouring the mineralized pegmatite intervals and has adequate continuity of the modelled bodies.

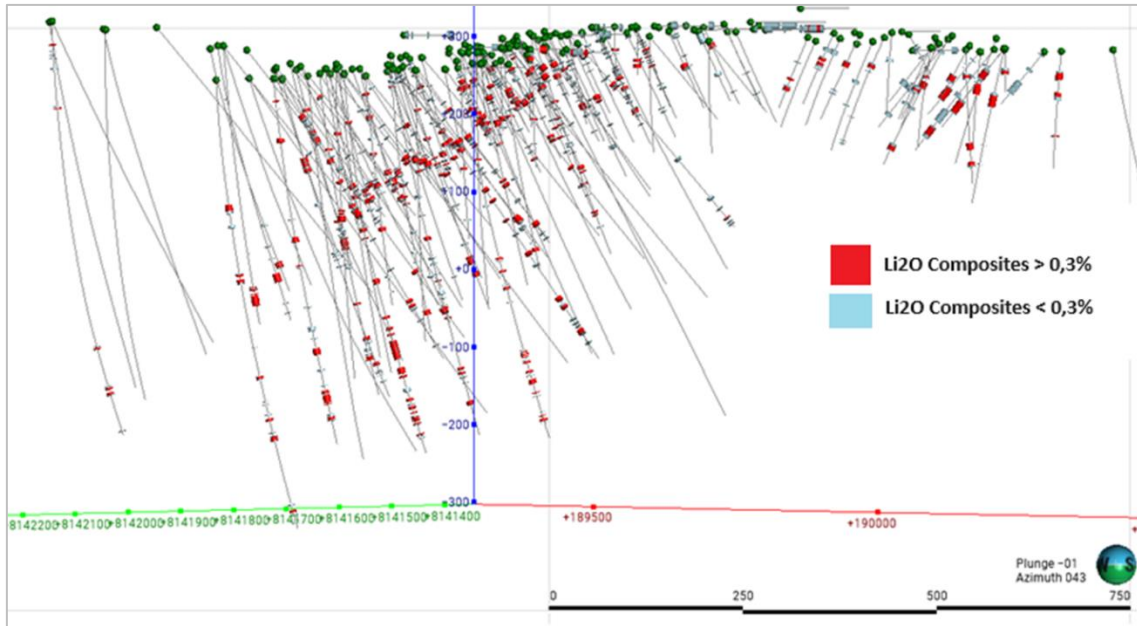


Figure 14.2: Assay Composites Classified by Li₂O > 0.3% Grade Limit in Pegmatites Veins.

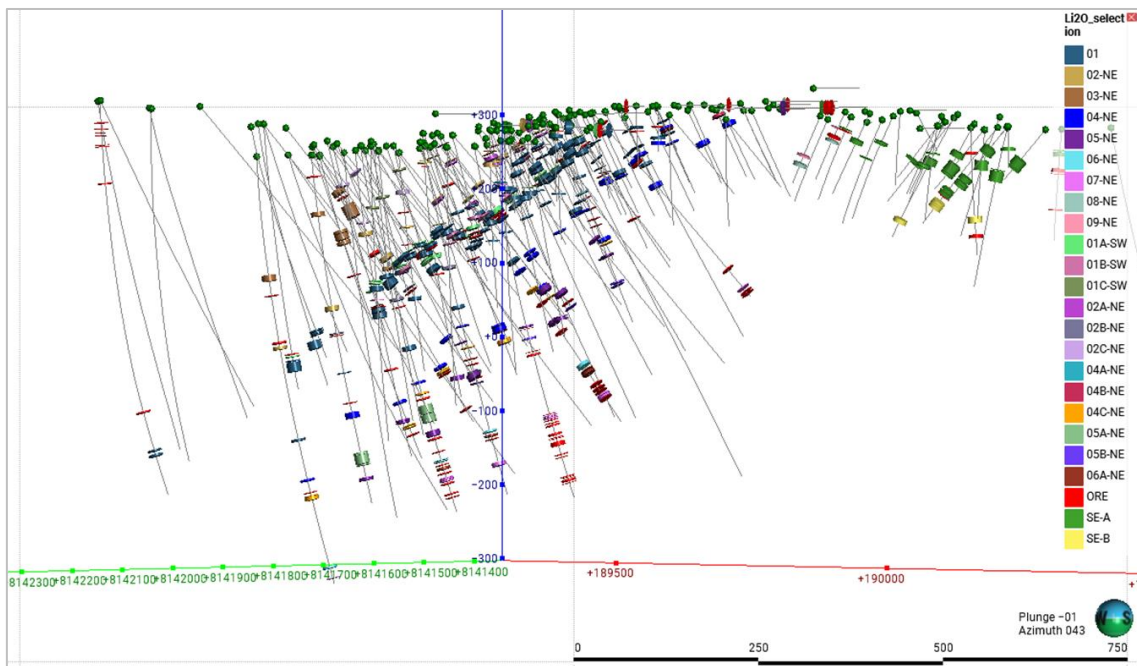


Figure 14.3: Assays Composites within the Li₂O > 0.3% limit in pegmatites veins grouped by separated lenses and dykes.

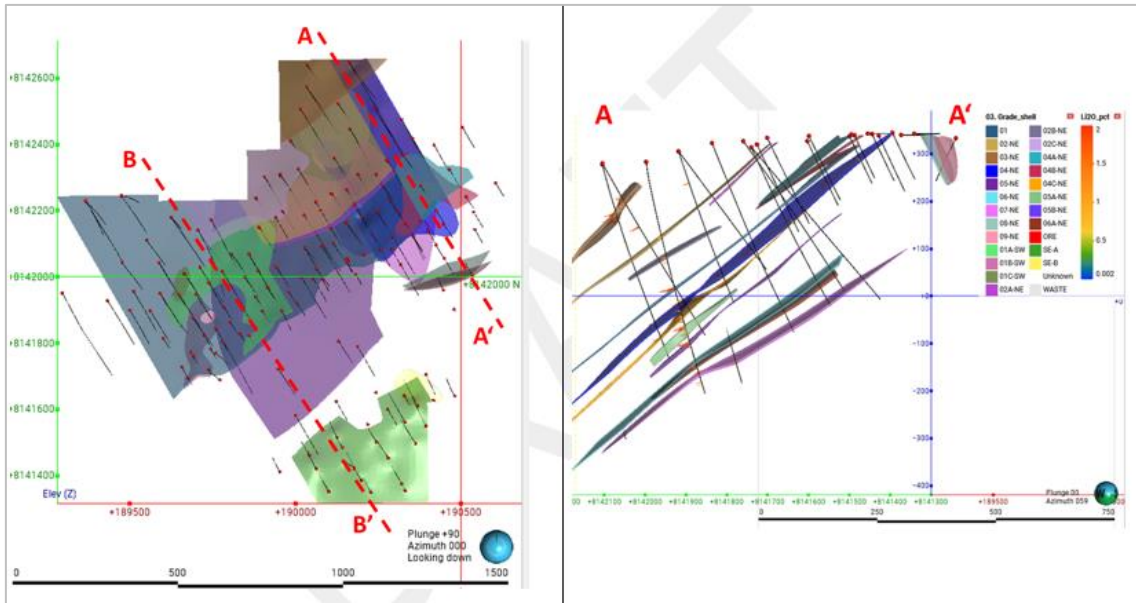


Figure 14.4: Spodumene grade shells modeled with assays composites Li₂O > 0.3 % - horizontal view plan (left side) and section view (right view plan).

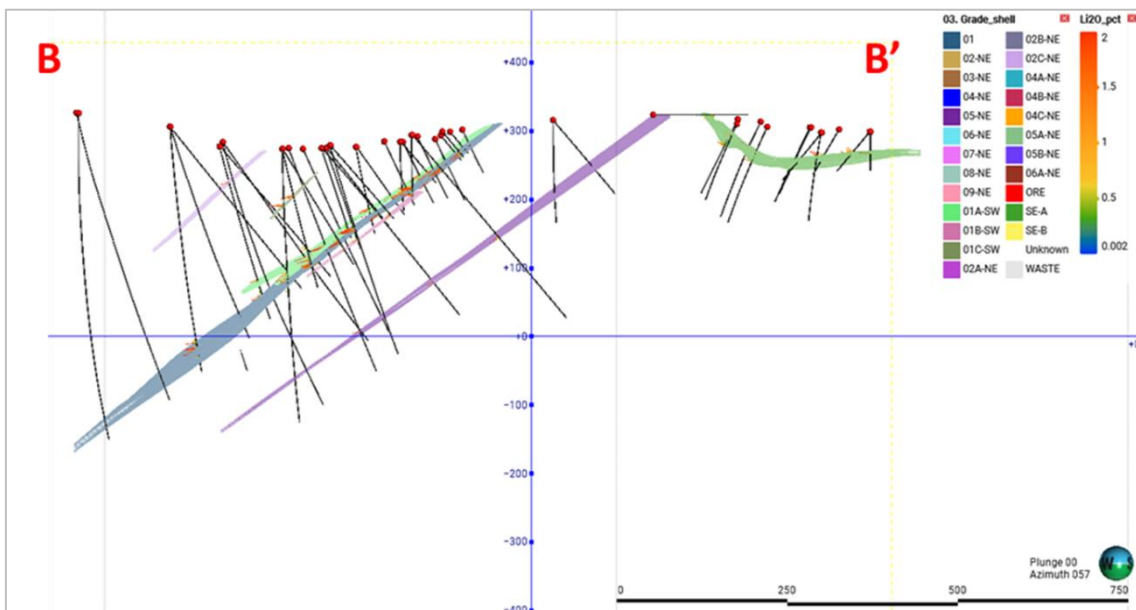


Figure 14.5: Spodumene grades shells model - assays composites Li₂O > 0.3 % - section view.

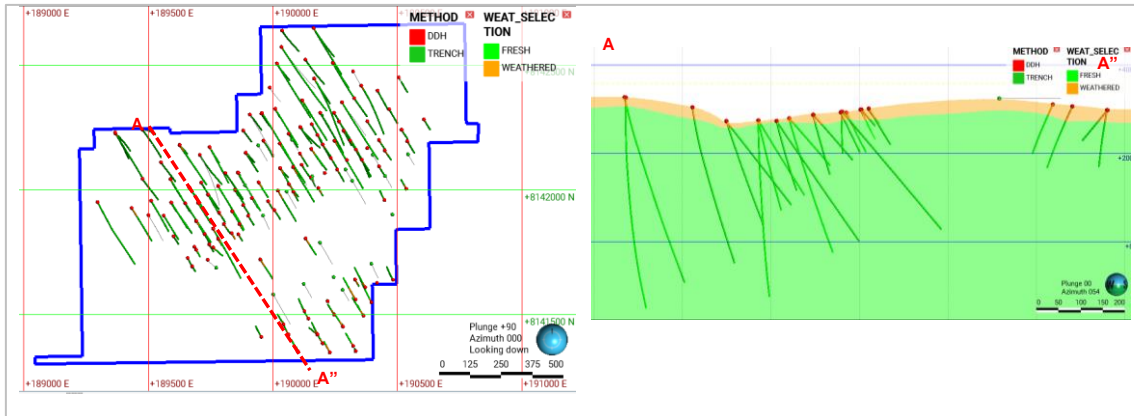


Figure 14.6: Weathering zone model - horizontal view plan (left side) and section view (right view plan).

14.1 Geostatistical Structural Analysis

14.1.1 Regularization of samples

The analysis of the sample support showed that more than 95% of the drilling samples have a length equal to 1 meter. GE21 performed the regularization of samples in 1 meter for the complementary studies of statistics and geostatistics (Figure 14.7).

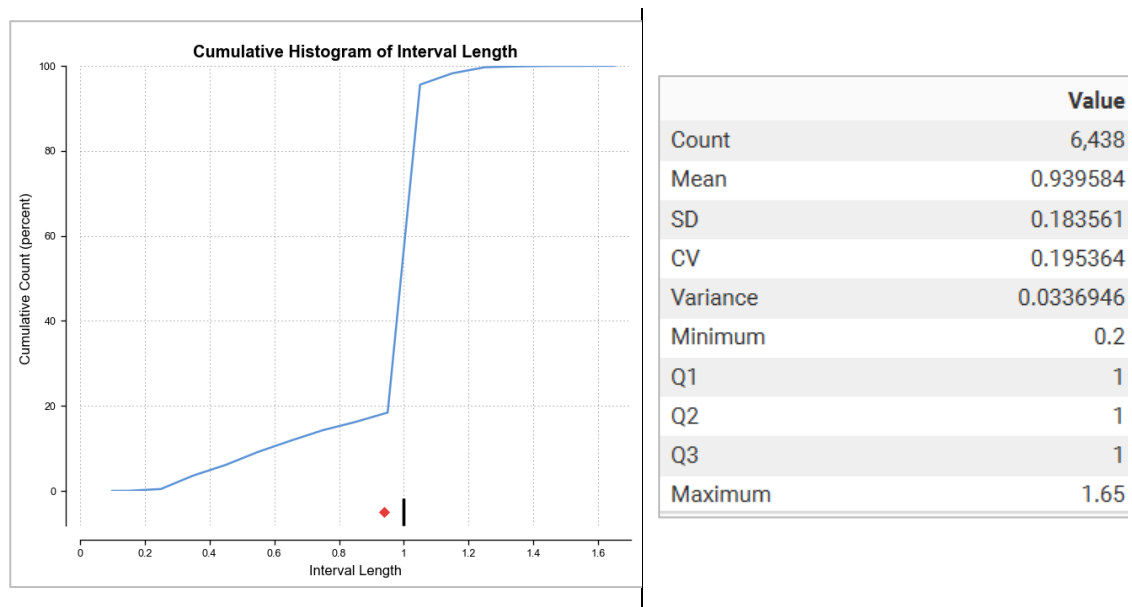


Figure 14.7: Bandeira Assays Interval Length Statistics.

14.1.2 Exploratory Data Analysis (EDA)

Statistical analysis on composited drilling samples was performed for the Li₂O% variable inside each modelled typology. Figure 14.8 shows the statistics for pegmatite veins.

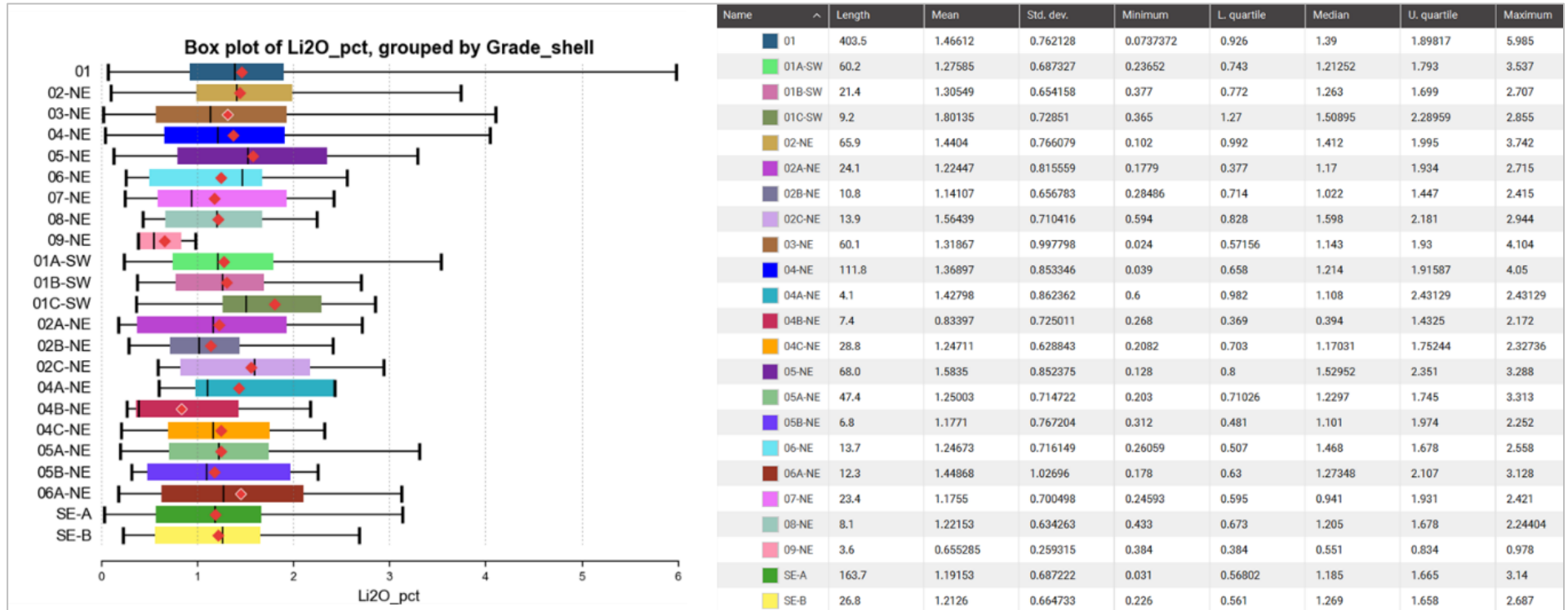


Figure 14.8: Li2O (%) Spodumene Pegmatites Veins Model Statistics – Boxplots (left side) and Statistics Table (right side).

14.1.3 Variographic Analysis

The structural analysis of the domains was conducted to determine the variographic parameters, which are essential for determining the spatial continuity model of the grade variables and for the grade estimate.

Variograms were generated explicitly for Li₂O% within the spodumene veins suite. This approach considered the geological similarity among them, enhancing the robustness of the variograms. Two distinct sets of veins were considered:

- NW Veins Suite.
- SE Veins Suite.

The variographic analysis was executed using Leapfrog Edge software. Figure 14.9 to Figure 14.12 show the variograms for the Li₂O% variable for each set of vein domains. Additionally, Table 14.1 presents the variographic parameters obtained from all conducted analyses. These parameters were applied in the process of grade estimation.

Table 14.1: Variographic Parameters.

| Variogram Name | Variance | Nugget | Normalised Nugget | Structures | Sill | Normalised sill | Structure | Major | Semi major | Minor | Dip | Dip Azi. | Pitch |
|----------------|----------|--------|-------------------|-------------|------|-----------------|-----------|-------|------------|-------|-----|----------|-------|
| NW | 0.58 | 0.25 | 0.43 | Structure 1 | 0.22 | 0.38 | Spherical | 137 | 136 | 3 | 36 | 323 | 40 |
| | | | | Structure 2 | 0.11 | 0.20 | Spherical | 298 | 247 | 3 | 36 | 323 | 40 |
| SE | 0.46 | 0.18 | 0.40 | Structure 1 | 0.22 | 0.48 | Spherical | 100 | 20 | 2 | 65 | 160 | 170 |
| | | | | Structure 2 | 0.05 | 0.12 | Spherical | 100 | 70 | 3 | 65 | 160 | 170 |

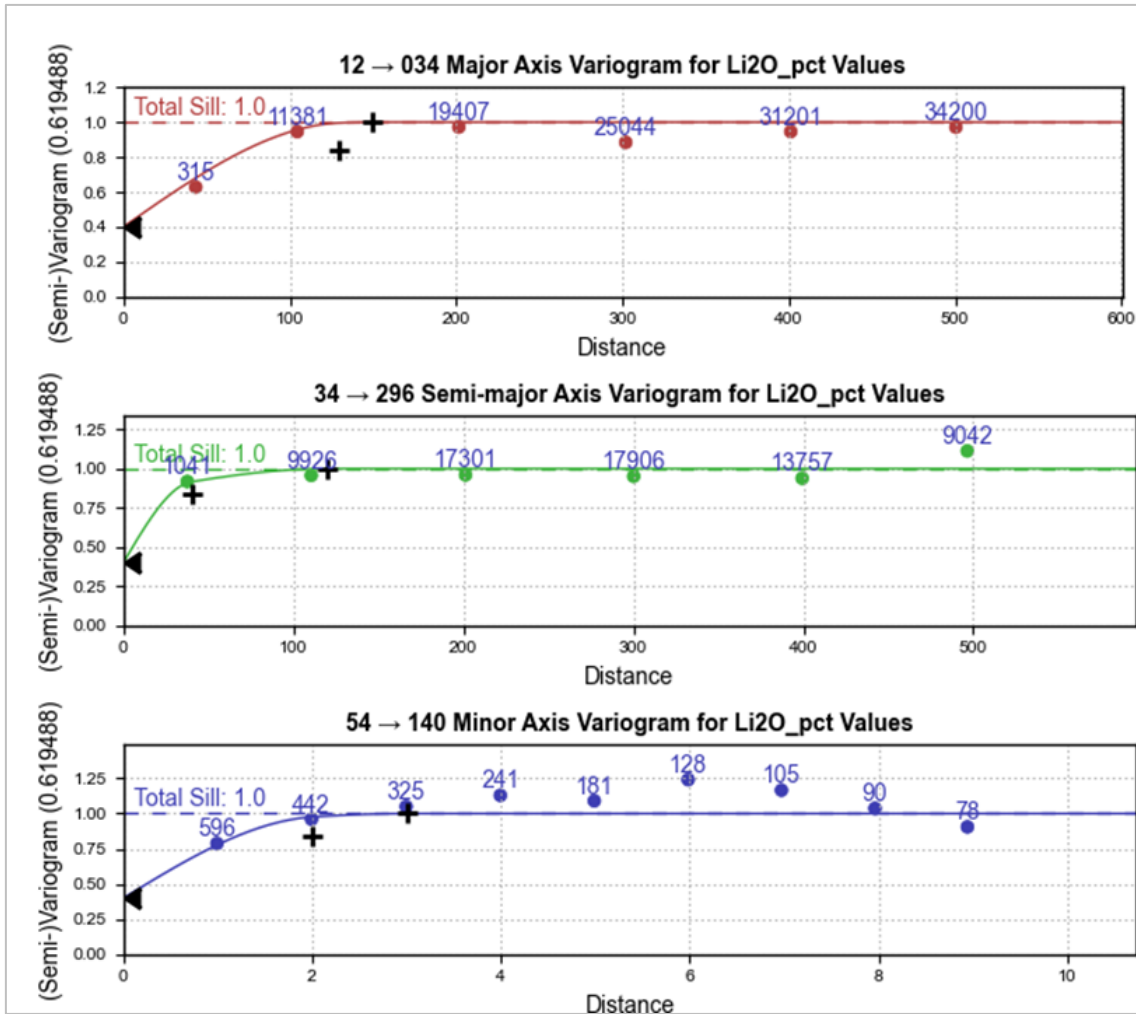


Figure 14.9: Variographic Model – Domains Set NW.

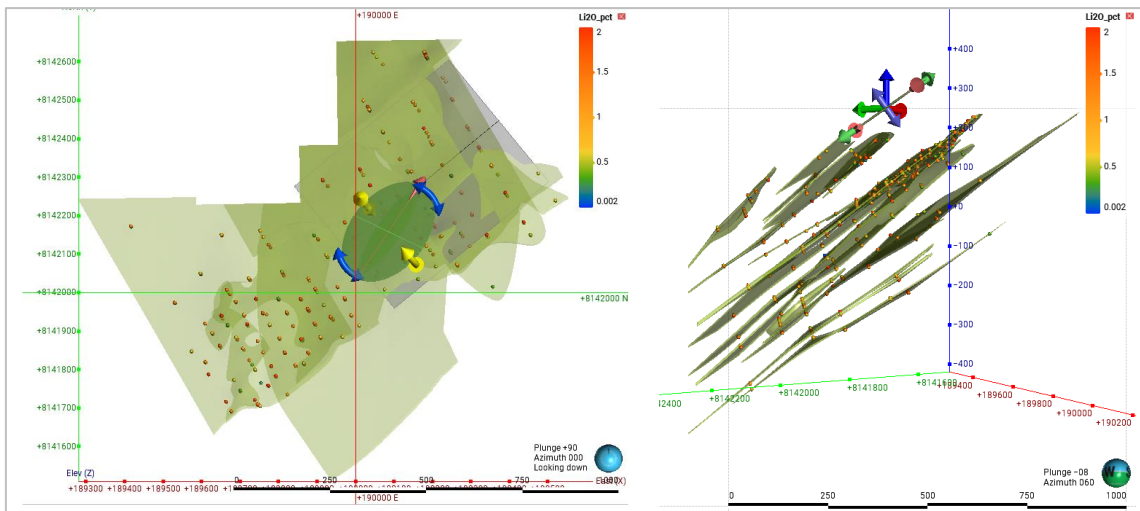


Figure 14.10: Variographic Ellipsoid – Domains Set NW.

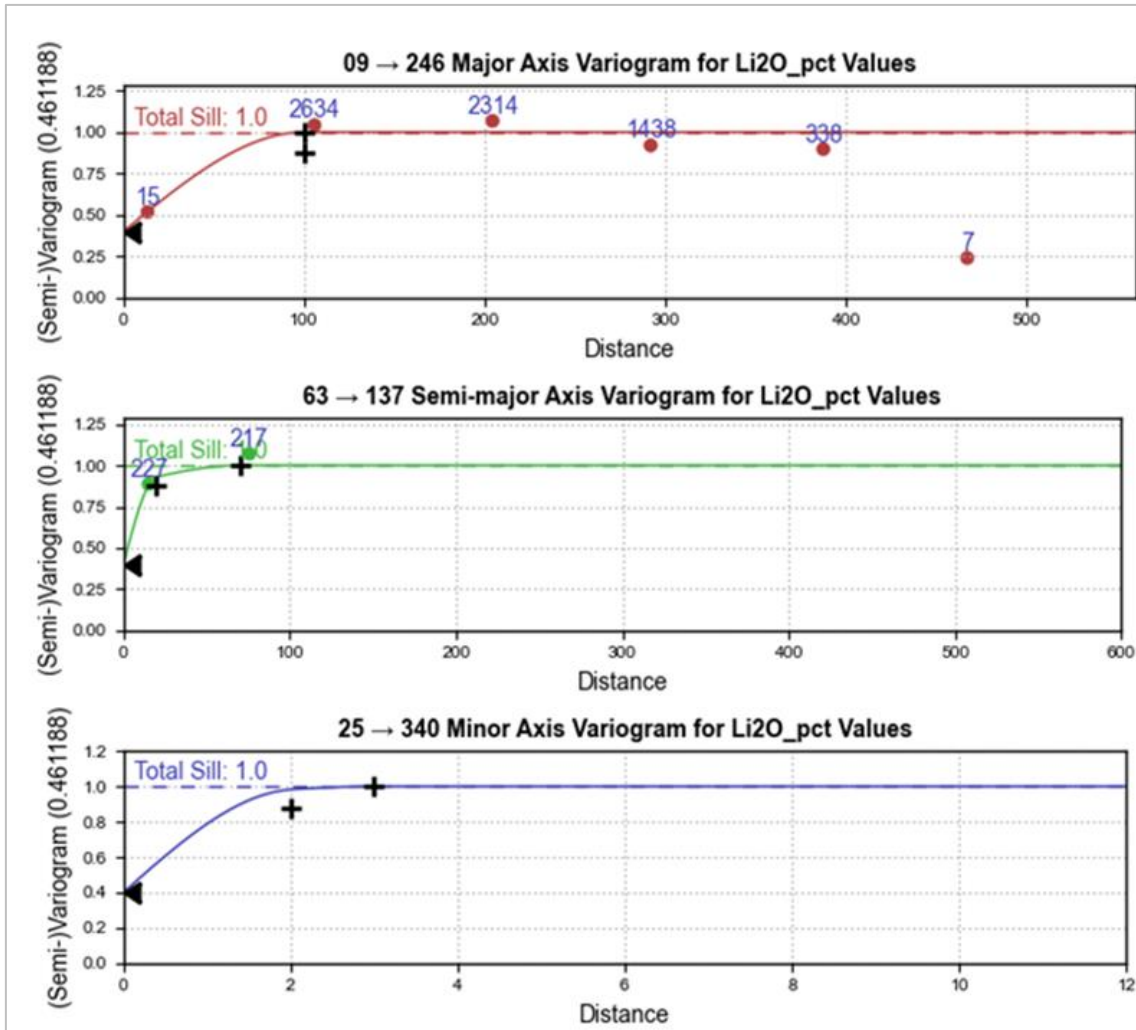


Figure 14.11: Variographic Model – Domains Set SE.

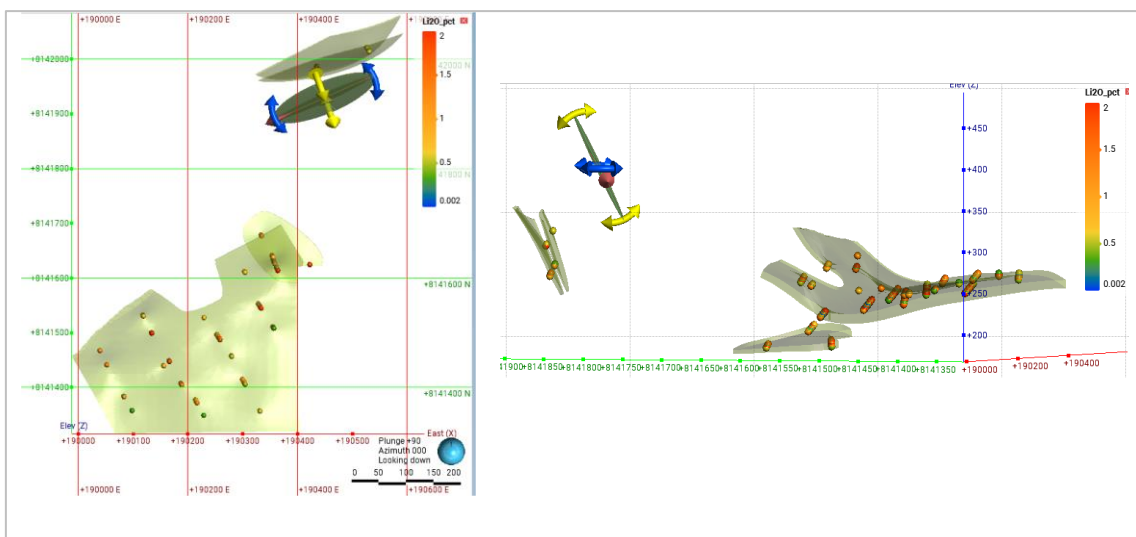


Figure 14.12: Variographic Ellipsoid – Domains set SE.

14.2 Block Model

A block model was built to carry out the grade estimation. The model's dimensions (12m x 12m x 4m) were defined based on the minimum spacing of the drilling grid. The sub-blocks model was set in 3m x 3m x 1m size to ensure the geometric adherence of the modelled bodies.

The dimensions of the block models and the attributes are shown in Table 14.2 and Table 14.3.

Table 14.2: Block Model Dimensions.

| | X | Y | Z |
|--|------------|--------------|--------|
| Minimum Coordinates (m) | 190,212.84 | 8,139,649.34 | -37.15 |
| Maximum Coordinates (m) | 189,831.38 | 8,144,016.02 | 69.73 |
| Number of nodes | 210 | 224 | 598 |
| Origin (Center) (m) | 190,213.66 | 8,139,657.71 | -39.48 |
| Origin (Corner) (m) | 189,830.56 | 8,144,016.02 | 67.40 |
| Block size (m) | 12 | 12 | 4 |
| Sub-Block | 3 | 3 | 1 |
| azimuth: 320 degrees (rotate clockwise around the Z axis when looking down) dip: 40 degrees (then rotate around the X' axis down from the horizontal plane) pitch: 0 degrees (then rotate clockwise around the Z'' axis when looking down) | | | |

Table 14.3: Block Model Variables Summary.

| Attribute Name | Type | Deals | Background | Description |
|----------------|-----------|-------|------------|------------------------|
| GM_weat | Character | - | | Weathering Model |
| GM_grad | Character | - | | Spodumene Veins Model |
| Class | Character | - | | Mineral Classification |
| Density | Real | 4 | -99 | Density Values |
| GM_miner | Character | - | | Bandeira Mineral Right |
| Li2O_ok | Real | 4 | -99 | Li2O OK estimation |

14.3 Grade Estimation

The Ordinary Kriging (OK) was carried out in the Leapfrog Edge software and was used on the Li2O% and Density% variables estimation, based on the structural analysis results described in this work.

Each mineralized vein was estimated independently, in a hard boundary strategy, ensuring that samples from one domain did not influence neighboring domains. The variograms were initially modelled considering the structural continuity across the entire set of domains, followed by an adjustment for honoring the specific behavior for each domain. Table 14.4 shows the main parameters of the Kriging strategy applied in the grade estimation.

Table 14.4: Kriging Parameters.

| Type | Steps | Ellipsoid Ranges | | | Number of Samples | |
|--|--------|------------------|--------------|---------|-------------------|---------|
| | | Maximum | Intermediate | Minimum | Minimum | Maximum |
| LiO2 | Step 1 | 50 | 50 | 3 | 5 | 12 |
| | Step 2 | 100 | 100 | 6 | 5 | 12 |
| | Step 3 | 150 | 150 | 12 | 5 | 12 |
| | Step 4 | 1500 | 1500 | 300 | 5 | 12 |
| Density | Step 1 | 50 | 50 | 3 | 5 | 12 |
| | Step 2 | 100 | 100 | 6 | 5 | 12 |
| | Step 3 | 150 | 150 | 12 | 5 | 12 |
| | Step 4 | 1500 | 1500 | 300 | 5 | 12 |
| Dynamic Variable Orientation for Estimation was applied to each domain in Leapfrog software. | | | | | | |
| Moving neighbourhood from ellipsoid, Dip = 36° Dip Azimuth = 320° Pitch = 160° (NW Veins) | | | | | | |
| Moving neighbourhood from ellipsoid, Dip = 65° Dip Azimuth = 160° Pitch = 170° (SE Veins) | | | | | | |
| Maximum number of samples per Drill = 2 | | | | | | |

14.4 Estimation Validation

The QP carried out the validation of the estimate through visual verification and by the Global and Local bias verification.

Both, Global and Local bias checks used The Nearest Neighbour as the comparison estimate.

NN-Checks plots, Figure 14.13 and Figure 14.14 show the results for global bias analysis of the estimated Li2O% and density variables, it allowed verifying the occurrence of expected smoothing of the estimation by Ordinary Kriging within the acceptance limits. The comparison showed that Ordinary Kriging globally respected the average grades, and the global bias in the estimated grades is within the limits of acceptance.

The local bias assessment by the Swath-Plot method aims to analyze the occurrence of local bias by comparing the average grades for the model through Ordinary Kriging and the Nearest Neighbour method in swath coordinates intervals graphs along the X, Y, and Z axes. Figure 14.15 and Figure 14.16 show the validation results of the Li2O% and Density swath plots.

The results from the grade estimate validation by Ordinary Kriging show that the smoothing effect or local and global bias are inside acceptance limits for the Mineral Resource estimate purposes.

14.5 Density

The density in the spodumene pegmatites was estimated by Ordinary Kriging. The schists density was defined as the mean of the 2297 samples from the Lithium Ionic database. The weathered zone doesn't have measurements, and GE21 has adopted the value 1.8g/cm³ for this domain, a common value used by other companies in the Jequitinhonha Valley region. GE21 recommends that additional density tests be carried out in weathered zones.

Table 14.5 shows the average kriged densities of each estimated pegmatite domain and the adopted densities of the host rocks.

Table 14.5: Density Values.

| Spodumene Veins | Density |
|-----------------|-------------------|
| | g/cm ³ |
| 01 | 2.67 |
| 02-NE | 2.67 |
| 03-NE | 2.68 |
| 04-NE | 2.66 |
| 05-NE | 2.65 |
| 06-NE | 2.68 |
| 07-NE | 2.70 |
| 08-NE | 2.43 |
| 09-NE | 2.36 |
| 01A-SW | 2.67 |
| 01B-SW | 2.70 |
| 01C-SW | 2.66 |

| Spodumene Veins | Density |
|-----------------|-------------------|
| | g/cm ³ |
| 02A-NE | 2.47 |
| 02B-NE | 2.73 |
| 02C-NE | 2.63 |
| 04A-NE | 2.51 |
| 04B-NE | 2.51 |
| 04C-NE | 2.72 |
| 05A-NE | 2.65 |
| 05B-NE | 2.69 |
| 06A-NE | 2.66 |
| SE-A | 2.60 |
| SE-B | 2.73 |
| | |

| Domains | Density |
|----------------|-------------------|
| | g/cm ³ |
| Shists Rocks | 2.76 |
| Weathered Zone | 1.80 |

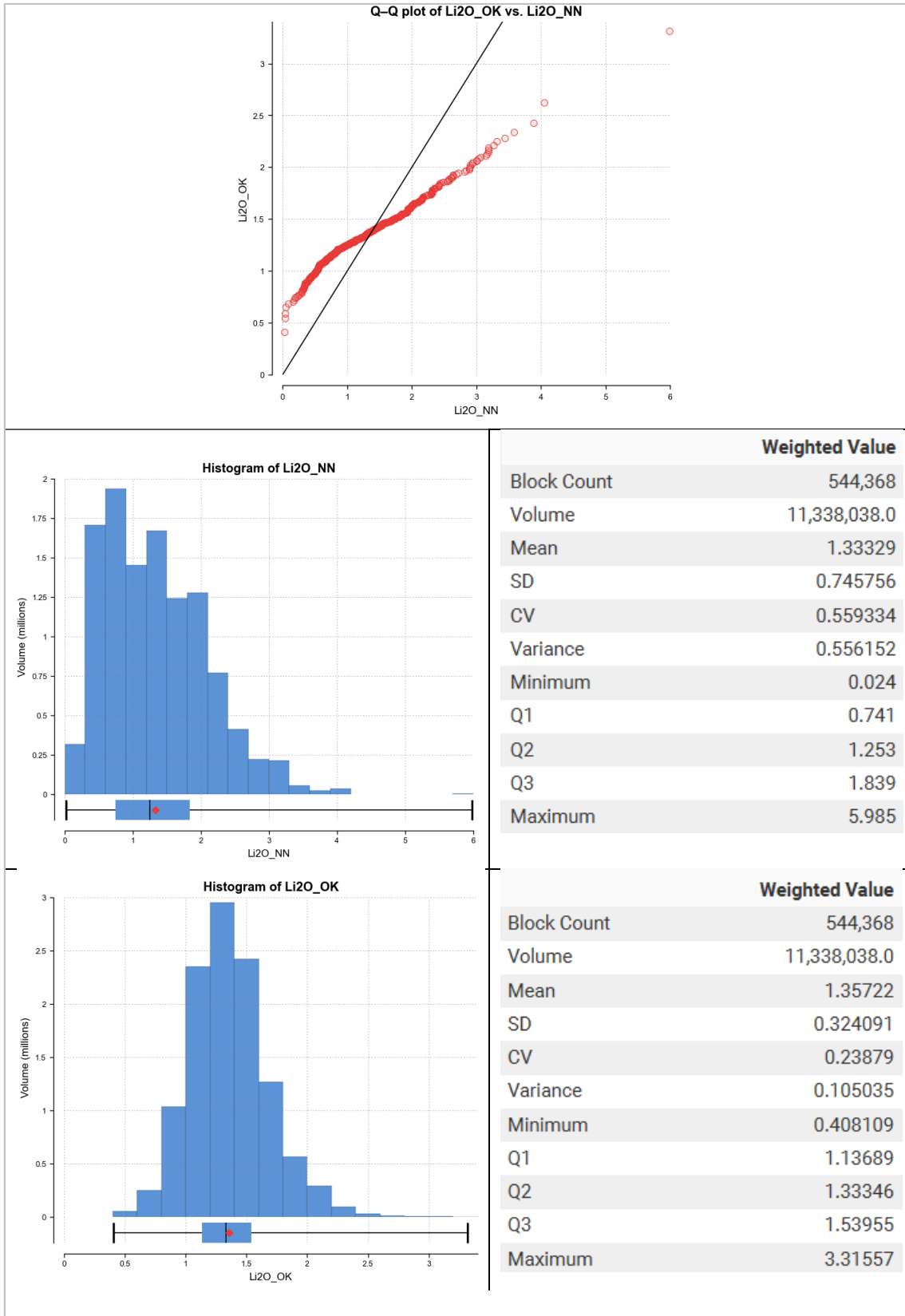


Figure 14.13: Estimation Validation - NN Check to Li2O.

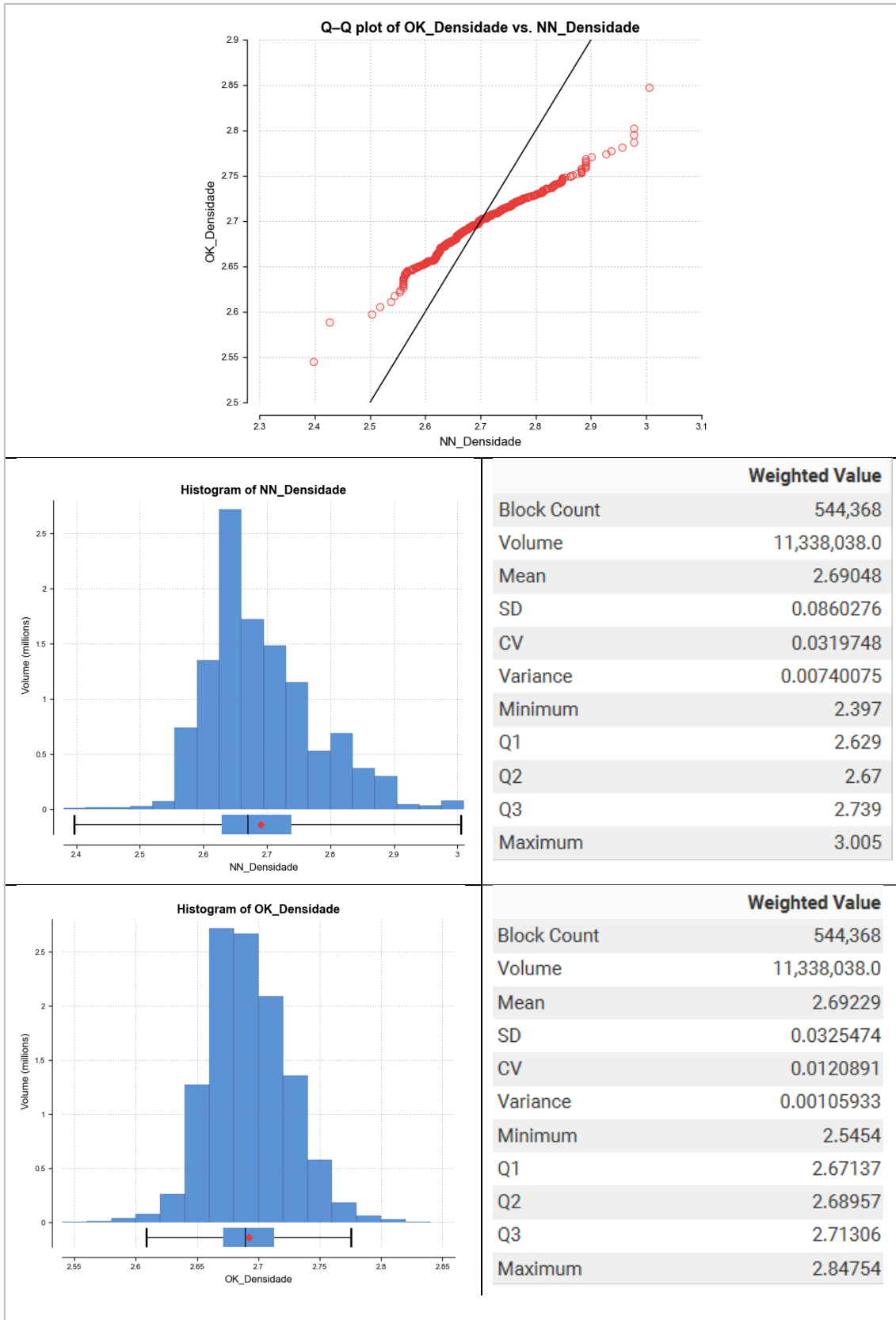


Figure 14.14: Estimation Validation - NN Check to Density.

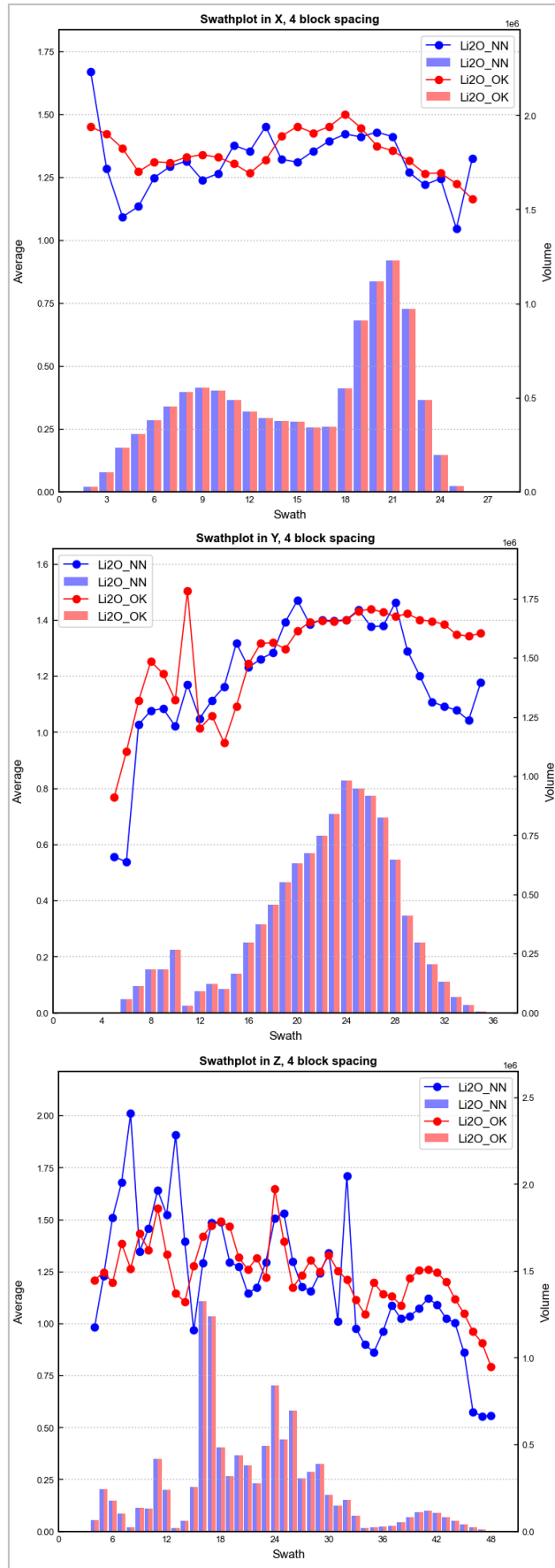


Figure 14.15: Estimation Validation - SwathPlot Li2O.

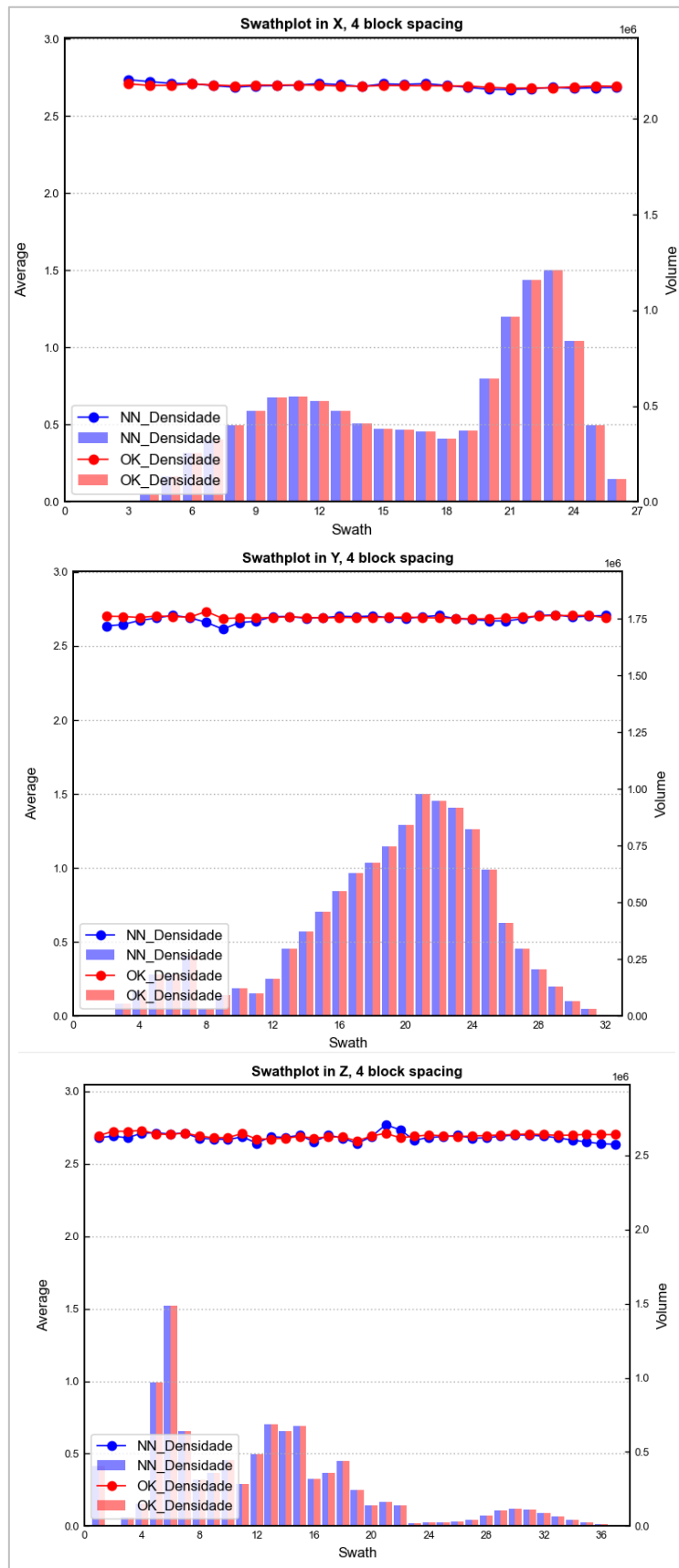


Figure 14.16: Estimation Validation - SwathPlot Denstiy.

14.6 Classification of Mineral Resources

The Mineral Resource was classified per CIM Standards and CIM Guidelines, utilizing geostatistical and classical methods, along with economically and mining-appropriate parameters relevant to the deposit type.

The Resource definitions by CIM are transcribed below:

- A Mineral Resource is a concentration or occurrence of diamonds, a natural solid inorganic material or natural fossilized solid organic material, including base and precious metals, coal and industrial minerals in the earth's crust or in the earth's crust in such form and quantity and of such grade or quality that allows reasonable prospects of economic extraction. The location, quantity, level, geological characteristics, and continuity of a Mineral Resource are known, estimated or interpreted from specific geological evidence and knowledge.
- An "Inferred Mineral Resource" is that part of a Mineral Resource for which the quantity and level or quality can be estimated on the basis of geological evidence and limited sampling and reasonably presumed but not verified geological and grade continuity. The estimation is based on limited information and sampling collected using appropriate techniques from locations such as outcrops, trenches, wells, and drill holes.
- An "Indicated Mineral Resource" is that part of a Mineral Resource for which quantity, grade or quality, densities, shape and physical characteristics can be estimated with a level of confidence sufficient to allow the appropriate application of technical and economic parameters, to support mine planning and assessment of the deposit's economic viability. The estimation is based on thorough and reliable exploration and testing information gathered using appropriate techniques from locations such as outcrops, trenches, wells, works, and drill holes spaced far enough apart for geological and level continuity to be reasonably assumed.
- A "Measured Mineral Resource" is that part of a Mineral Resource for which quantity, level or quality, densities, shape, and physical characteristics are so well established that they can be estimated with sufficient confidence to allow the appropriate application of technical and economic parameters, to support production planning and assessment of the deposit's economic viability. The estimation is based on thorough and reliable exploration, sampling, and analysis information gathered using appropriate techniques from locations such as outcrops, trenches, wells, works, and drill holes spaced far enough apart to confirm geological and level continuity.

The classification boundaries made by GE21 for the Measured, Indicated, and Inferred categories were established through an approach that considered a comprehensive set of factors.

These factors included the sampling procedure analysis, the sample grid spacing, the survey methodology, and the quality of assay data.

Additionally, drilling spacing and the progressive expansion of the search radius during grade estimation stages were also considered, as well as the average anisotropic distance of the samples and the continuity of pegmatite mineralization.

This multi-faceted approach ensured the robustness and accuracy of the classification process.

- The Measured Mineral Resource classification had as a reference the 50 meters of the Average Euclidean distance to sample (AvgD) used in ordinary

kriging estimation with a minimum of five composites in at least three different drill holes.

- The Indicated Mineral Resource classification had as a reference the 100 meters of the Average Euclidean distance to sample (AvgD) used in ordinary kriging with a minimum of five composites in at least three different drill holes.
- The Inferred Mineral Resource classification is all remaining estimated blocks.
- The total Mineral Resources were limited to the Mining Rights boundaries.

The resource classification was supported by a grade shell representing the underground mining appliance (Reasonable Prospect for Eventual Economic Extraction - RPEEE), performed through a restricted model which limits the blocks classified as resource generated from an economic and geometric function.

Resources were restricted to a 0.5% Li₂O grade shell and the results are shown in the Table 14.6, Figure 14.17 and Figure 14.18.

Table 14.6: Bandeira Mineral Resource Estimates (base case cut-off grade of 0.5 % Li₂O) – October 11, 2023.

| Category | Resource (Mt) | Grade (% Li ₂ O) | Contained LCE (t) |
|-----------------------------|---------------|-----------------------------|-------------------|
| Measured | 2.00 | 1.40 | 69,226 |
| Indicated | 11.72 | 1.40 | 405,666 |
| Measured + Indicated | 13.72 | 1.40 | 474,892 |
| Inferred | 15.79 | 1.34 | 523,118 |

Notes related to the Mineral Resource Estimate:

1. The spodumene pegmatite domains were modeled using composites with Li₂O grades greater than 0.3%
2. The mineral resource estimates were prepared in accordance with the CIM Standards, and the CIM Guidelines, using geostatistical and/or classical methods, plus economic and mining parameters appropriate to the deposit.
3. Mineral Resources are not ore reserves and are not demonstrably economically recoverable.
4. Grades reported using dry density.
5. The effective date of the MRE was October 11, 2023.
6. The QP responsible for the Mineral Resources is geologist Carlos José Evangelista da Silva (MAIG #7868).
7. The MRE numbers provided have been rounded to the estimate relative precision. Values cannot be added due to rounding.
8. The MRE is delimited by Lithium Ionic Bandeira Target Claims (ANM).
9. The MRE was estimated using ordinary kriging in 12m x 12m x 4m blocks.
10. The MRE report table was produced in Leapfrog Geo software.
11. The reported MRE only contains fresh rock domains.
12. The MRE was restricted by grade shell using 0.5% Li₂O cut-off.

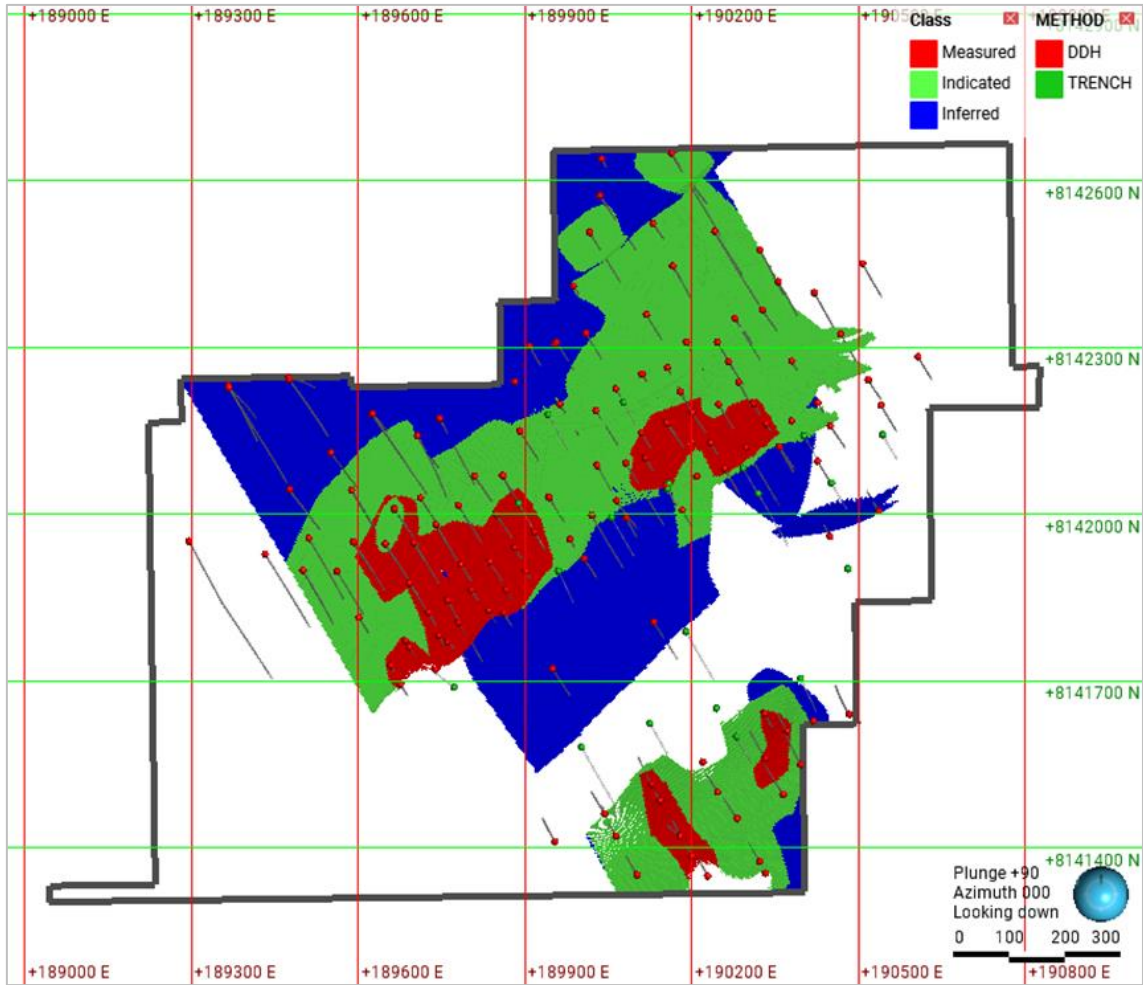


Figure 14.17: Resource Classification with RPEE – Horizontal view.

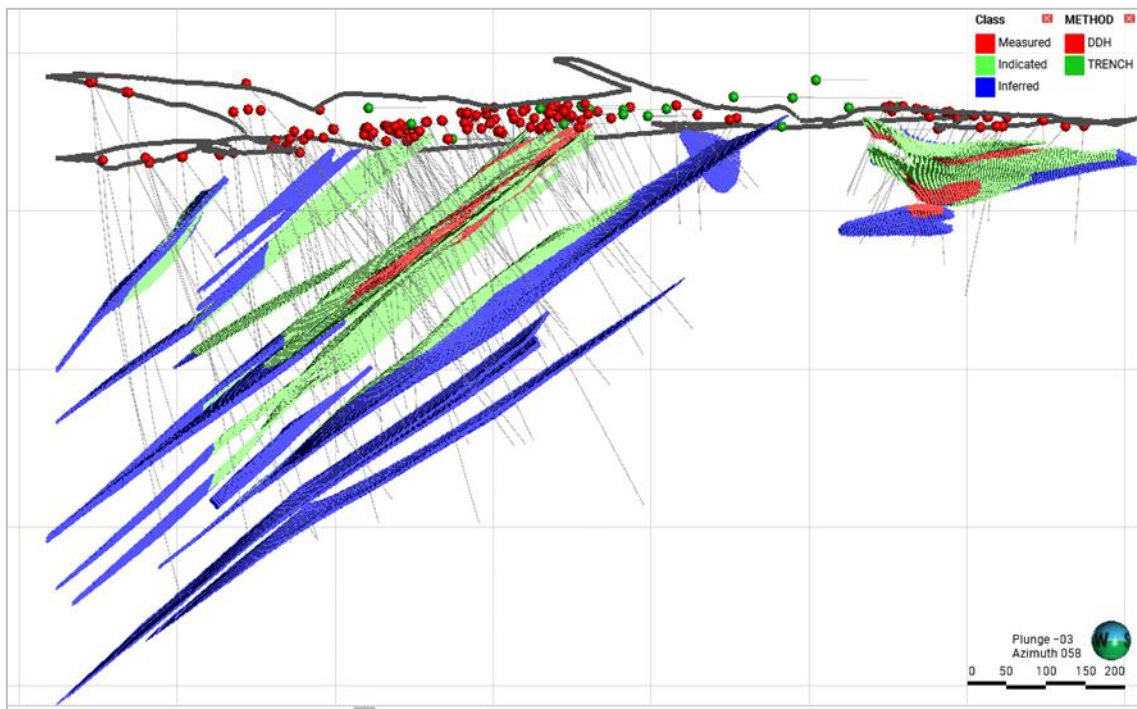


Figure 14.18: Resource Classification with RPEE – Oblique view.

15 MINERAL RESERVES ESTIMATES

A "Preliminary Economic Assessment" (PEA) means a preliminary study that is not a pre-feasibility or feasibility study. This preliminary study includes an economic analysis of the feasibility of the potential of the Mineral Resource. The PEA is a study with an insufficient level of accuracy to establish Mineral Reserves.

Mineral Reserves were not estimated for the Bandeira Project.

16 MINING METHODS

GE21 prepared a Preliminary Economic Assessment (“PEA”) to provide an economic analysis of the potential viability of the Underground Mining Project of the Bandeira Mine, based on the Mineral Resource Estimate presented in item 14.

A PEA is preliminary in nature and, in that sense, includes Inferred Mineral Resources. Materials classified as Inferred are considered too speculative geologically to have the economic considerations applied, that would enable their categorization as Mineral Reserves. There are no guarantees that results presented in this PEA will be implemented. The economic analysis was based on potentially mineable Resources. Mineable Resources are an estimate of the grade and tonnage in which the production plan was developed. Mineral Resources that are not Mineral Reserves do not have demonstrated economic viability.

16.1 Mine Design

The Bandeira Project design contemplates dual underground mining operations. The primary orebodies, accounting for approximately 90% of the deposit, are proposed to be extracted using a bottom-up “sublevel stoping” method (Bandeira Sublevel Mine, “BSL mine”). Simultaneously, the secondary southeast orebody, comprising approximately 1.8 Mt, is expected to be mined using “room-and-pillar” method (Bandeira Room and Pillar, “BRP mine”).

The BSL mine has been planned with two declines, extending along a NE/SW mineralized trend spanning 1.0 km. It is divided into 12 panels, each measuring 55 meters. (Figure 16.1).

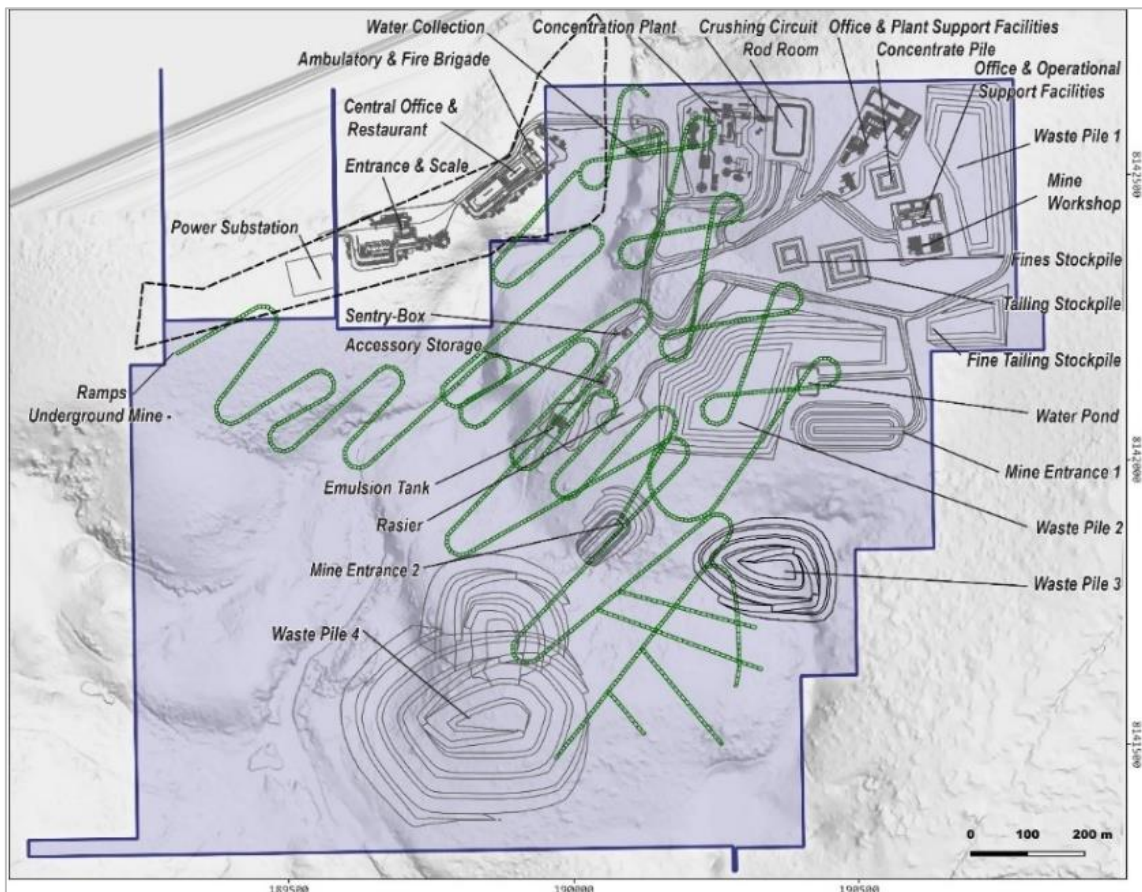


Figure 16.1: Proposed Project Layout and Infrastructure.

The BRP mine features a single panel with approximate dimensions of 380 meters in length, 330 meters in width, and 10 meters in height. Access to the mineralized zone was made through five

cross-cuts originating from the southern access ramp. Once fully operational, the BSL and BRP mines are expected to achieve a combined production of approximately 1.3 Mt per annum.

16.1.1 Mining Method Selection

The mine was divided into two types of mining methods, considering the dip of the lenses present in the ore body - one being more horizontally oriented, and the other more vertically oriented.

In the more horizontally oriented lens, the room and pillar mining method were selected to optimize the extraction of material and ensure the stability of the area where the operations were conducted. The Room and Pillar Method is an underground mining method which aim extracting the maximum amount of ROM possible while leaving rock pillars in place to support the mine's roof and walls (Table 16.1).

Table 16.1: Dimensions of pillar - room and pillar.

| Bandeira | Room and Pillar |
|---------------|-----------------|
| Domain | Fresh Rock |
| Crown pillar | 10,0 m |
| Pillar width | 4,0 m |
| Pillar length | 4,0 m |

For the more vertically inclined lens, the Sublevel Stopping method was chosen, considering the rock competency, the behavior of the ore body, and preliminary analyses based on projects with similar characteristics.

The mine design includes the layout of an operational mine featuring decline, cross-cuts, ore-drives, mucking bays, waste connect (between ore-drives), secondary decline, passing bay, and sumps along the lithium mineralized body down to an elevation of -380 meters.

For sublevel stopping, the ROM starts to be mined at an elevation of 250 meters, under a 10-meter crown pillar that serves as the upper structural element. Each panel is 55 meters long vertically (Z direction) and is separated by 4-meter-wide pillars. These panels are segmented into three stopes measuring 20, 15 and 20 meters, respectively, making a total vertical length of 55 meters. Each of these stopes corresponds to an individual mining level; the cross-cutting and ROM conduction structures intersect each of these levels. In total, the Sublevel Stopping method incorporates 12 panels and 36 mining levels (Table 16.2).

Table 16.2: Dimensions of panels and columns - Sublevel Stopping.

| BANDEIRA | | | | |
|---------------------|---------------|------------------|-------|-----------|
| PANEL | Mining Method | Panel roof/floor | Z (m) | H (m) |
| CROWN PILLAR | | | | 10 |
| 1 | Open Stope | Panel roof | 250 | 55 |
| | | Panel floor | 195 | |
| PILLAR | | | 191 | 4 |
| 2 | Open Stope | Panel roof | 191 | 55 |
| | | Panel floor | 136 | |
| PILLAR | | | 132 | 4 |
| 3 | Open Stope | Panel roof | 132 | 55 |
| | | Panel floor | 77 | |
| PILLAR | | | 73 | 4 |
| 4 | Open Stope | Panel roof | 73 | 55 |
| | | Panel floor | 18 | |
| PILLAR | | | 14 | 4 |
| 5 | Open Stope | Panel roof | 14 | 55 |
| | | Panel floor | -41 | |
| PILLAR | | | -45 | 4 |
| 6 | Open Stope | Panel roof | -45 | 55 |
| | | Panel floor | -100 | |
| PILLAR | | | -104 | 4 |
| 7 | Open Stope | Panel roof | -104 | 55 |
| | | Panel floor | -159 | |
| PILLAR | | | -163 | 4 |
| 8 | Open Stope | Panel roof | -163 | 55 |
| | | Panel floor | -218 | |
| PILLAR | | | -222 | 4 |
| 9 | Open Stope | Panel roof | -222 | 55 |
| | | Panel floor | -277 | |
| PILLAR | | | -281 | 4 |
| 10 | Open Stope | Panel roof | -281 | 55 |
| | | Panel floor | -336 | |
| PILLAR | | | -340 | 4 |
| 11 | Open Stope | Panel roof | -340 | 55 |
| | | Panel floor | -395 | |
| PILLAR | | | -399 | 4 |
| 12 | Open Stope | Panel roof | -399 | 21 |
| | | Panel floor | -420 | |

The dimensions of the Stopes' cross-sections are illustrated in Figure 16.2.

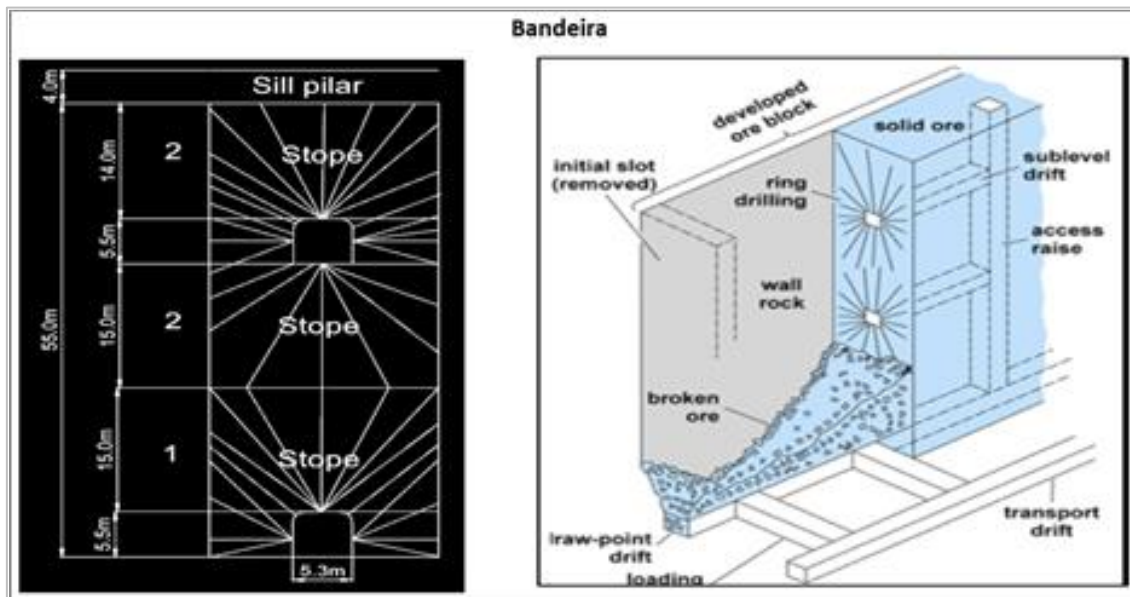


Figure 16.2: Dimensions of the Stopes cross-sections.

16.1.2 Geotechnical Analysis

A geotechnical study, analysis and design was performed by MGLIT in collaboration with the MLF Geomecnica (RELATÓRIO TÉCNICO – RECOMENDAÇÕES PRELIMINARES DE GEOTECNIA) to provide key underground design parameters for the Bandeira Project.

It is important to note that these studies are of a preliminary nature, as geotechnical and rock mechanics studies for the geomechanical characterization of rock masses in the mining areas are still under development.

16.1.2.1 Geotechnical Aspects

Geological and geotechnical / rock mechanics information was obtained from existing data, through works developed for mines in regions near MGLIT targets. This information was provided by the technical team of the Company, as well as those made a preliminary available, based on description of drill cores.

16.1.2.2 Preliminary Geomechanical Characterization of the Rock Mass

The lithological predominance in the mining implementation areas is essentially schists (host rock) and pegmatites (ROM). Based on observations of discontinuities and anisotropies through the geotechnical descriptions of drill cores, the presence of at least two families of discontinuities has been identified. Generally, these structures have limited apertures and lack soft infill material. Schists typically exhibit rough or irregular and flat discontinuity surfaces, whereas pegmatites feature rough surfaces. Structural conditions should be further investigated through geotechnical mapping surveys of the development drifts upon their implementation. This is to better understand the behavior of these structures in the rock mass concerning the excavation openings and slope stability. However, the information gathered from the drill core descriptions is deemed sufficient for defining preliminary geotechnical parameters and information that will facilitate the development of mine design work.

Geomechanical domains were delineated based on the geotechnical descriptions of core samples, which facilitated the determination of fracturing patterns, Rock Quality Designation (RQD) indices, degrees of alteration, and discontinuity apertures. These factors were associated with specific intervals and segregated according to their anticipated load-bearing capacities and expected behavior within the defined rock mass domains.

16.1.2.3 QP Opinion

Bandeira’s stability design is considered inside mining industry standards. However, the deepening of underground below the current operations have no updated stability studies to preview stability conditions.

The current mining plan at depth zones are designed for lateral extensions of the mineralization zones, but it’s recommended a new stability study for underground mining operations at project scale.

16.1.3 Underground Stope Optimization

The stope design optimization was conducted using the Mineable Stope Optimization (MSO). This allowed for the creation of stopes based on preset dimensions, achieving cut-off values selected based on economic parameters. This software, such as MSO Version 4.3.11.0 integrated with Datamine Studio UG, was used to determine the economic division of the mineral deposit.

The algorithms consider financial parameters, geological/geotechnical factors, and operational constraints for the optimal design of stopes throughout the ore body, encompassing elevations from 260 m to -420 m. Due to the complexity of the ore body along the azimuth and the number of present lenses, a methodology of creating multiple frameworks was adopted for stope optimization. Each lens was optimized in a configuration that best respected the dip angle of the material and its irregular behavior along the azimuth.

The stopes were optimized following operational and technical parameters, resulting in an estimated mine life of 20 years. In the Sublevel Stopping Method, the scenarios were configured to result in solids divided into dimensions of (20x15x20) m in height, totaling 55 m, and a minimum thickness of 2 m in accordance with the Figure 16.2.

About the rooms and pillars, chambers measuring (10x10) m and internal pillars measuring (4x4) m were created, in accordance with the Figure 16.3.

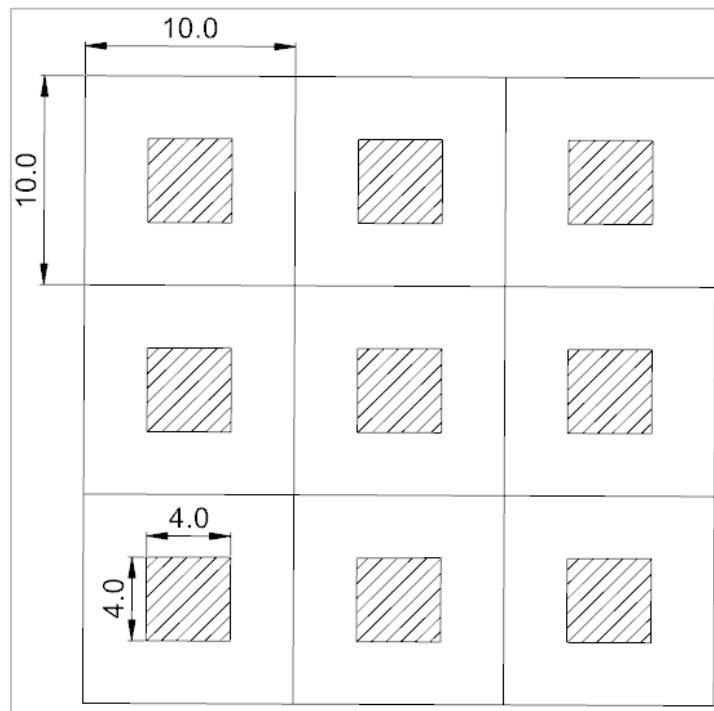


Figure 16.3: Schematic drawing of the room-and-pillar mining method.

The Table 16.3 presents the parameters used for optimization as well as for mining scheduling.

Table 16.3: MSO Parameters.

| Parameters | |
|-----------------------|-------------------|
| Optimized Grade | Li ₂ O |
| Cutoff | 0.50% |
| Minimum mining width | 2 m |
| Panel sublevel Height | 55 m |
| Stope Sublevel Height | (20/15/20) m |
| Stope Sublevel With | 10 m |
| Sill Pillar | 4 m |
| Dip | By lens |
| Azimuth | By lens |
| Room | (10x10) m |
| Pillar | (4x4) m |

As a result, two solids were generated representing the area of the room-and-pillar (Figure 16.4) and the sublevel stoping (Figure 16.5).

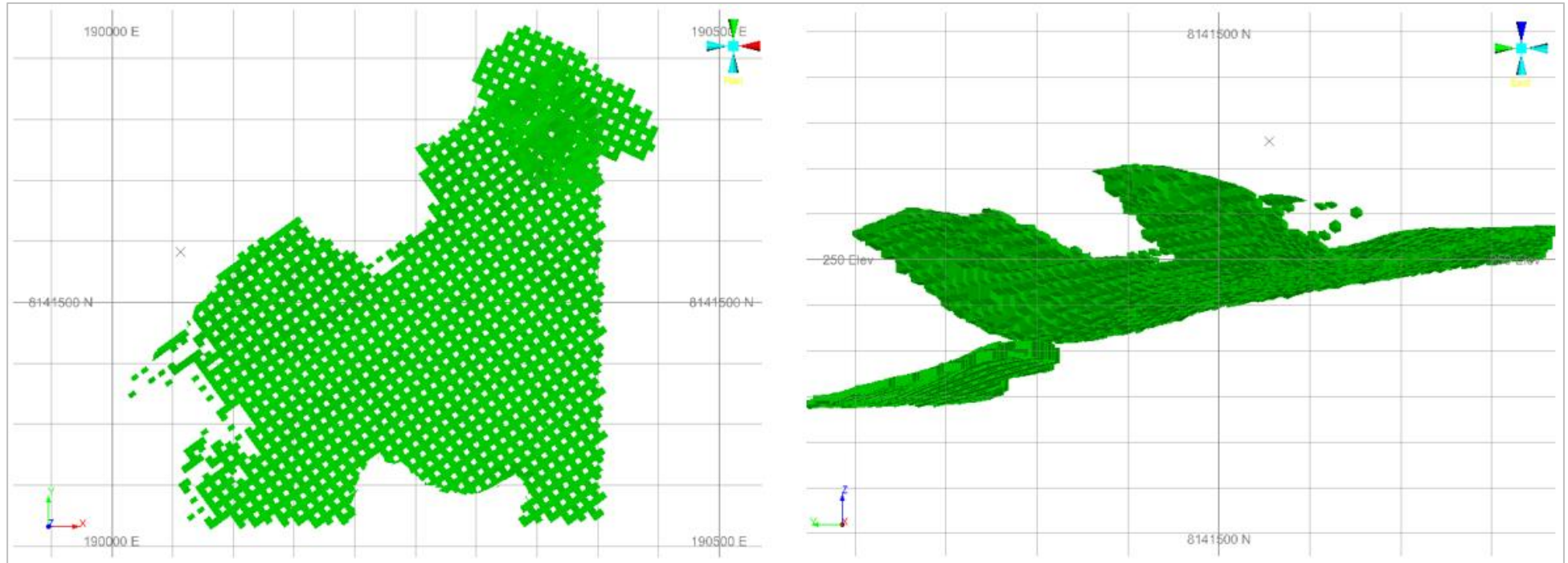


Figure 16.4: Room and Pillar solids generated.

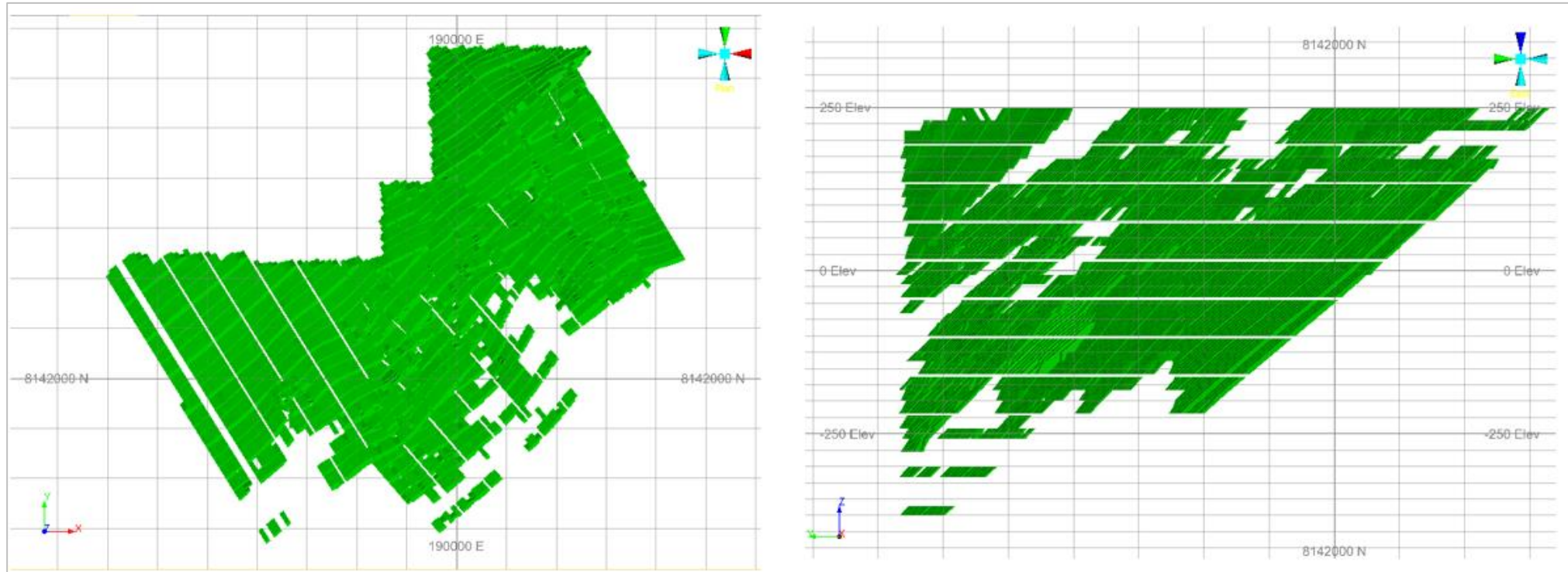


Figure 16.5: Sublevel Stopping solids generated.

The room and pillar optimization results presents a ROM mass of 1.8 Mt 1.05% Li₂O and for sublevel stoping a ROM mass of 21.1 Mt 1.25% Li₂O.

From the mining solids, access structures to the stopes were created, including cross-cuts, ore drives, declines, waste connects, passing bays, mucking bays, and ventilation drives. The primary and secondary development drifts, including the decline, have dimensions of (5.5 x 5.3) m with an arch radius of 1.25 m. Ventilation raises have a diameter of 2.1 m.

The Figure 16.6 illustrates the mine design structures and the Figure 16.7 shows how these structures integrate with the stopes from different views. Regarding development, the advancement for each structure can be observed in Table 16.4.

In Figure 16.7, it is possible to observe how the structures adapt to the ore body for the room-and-pillar method. The same can be observed in Figure 16.8 for for the sublevel stoping method.

Table 16.4: Advancement meterage for each structure.

| Development structures | |
|------------------------|---------------|
| Structure | Dimension (m) |
| Declines | 10.572 |
| Sump | 762 |
| Mucking bay | 3.429 |
| Cross-cut | 6.534 |
| Waste connect | 6.511 |
| Ore Drive | 36.960 |
| Ventilation drive | 13.383 |
| Raise | 3.876 |

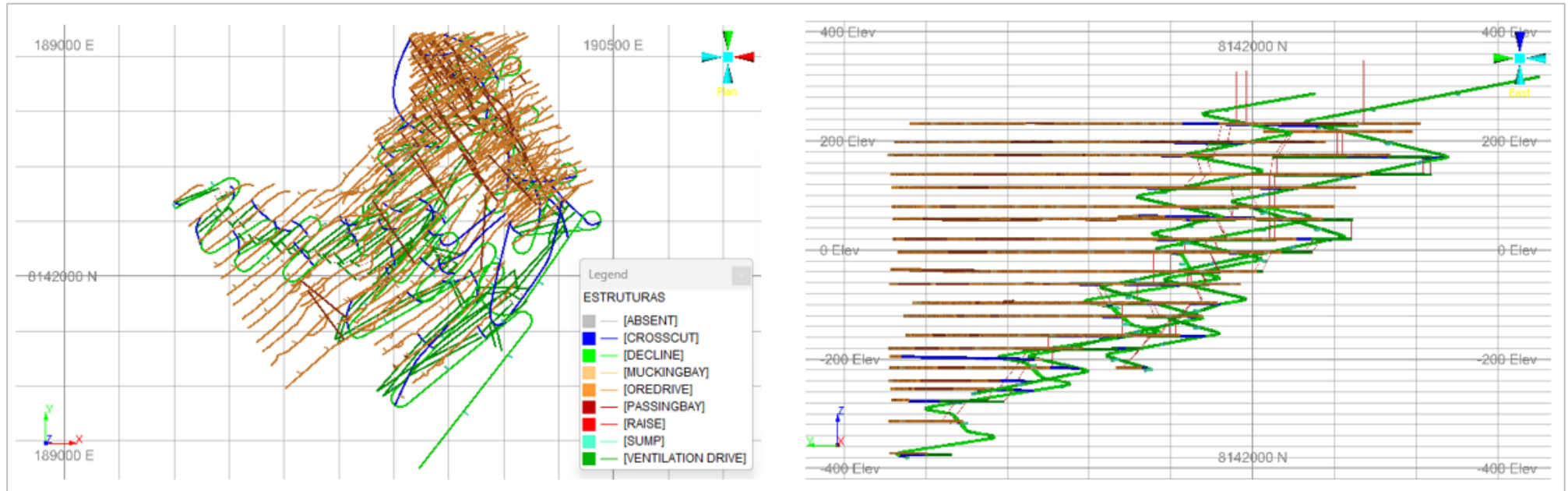


Figure 16.6: Mine design with all the development structures

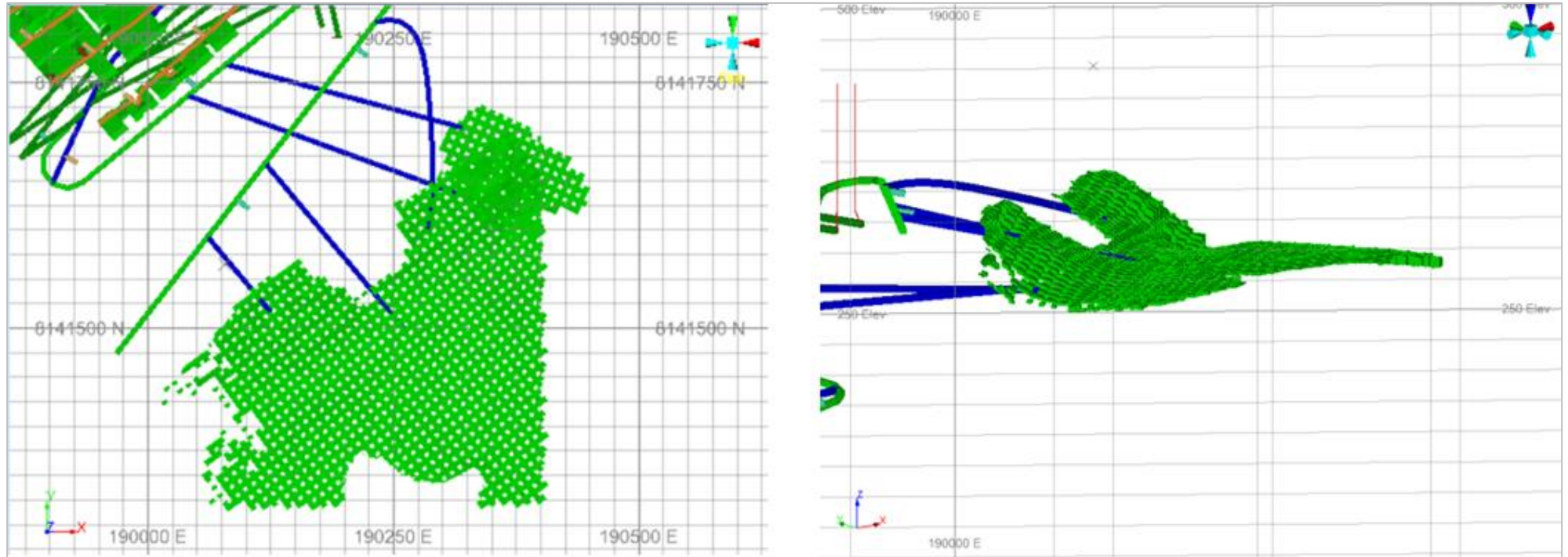


Figure 16.7: The mineralized body is fixed to the development structures - Room and pillar.

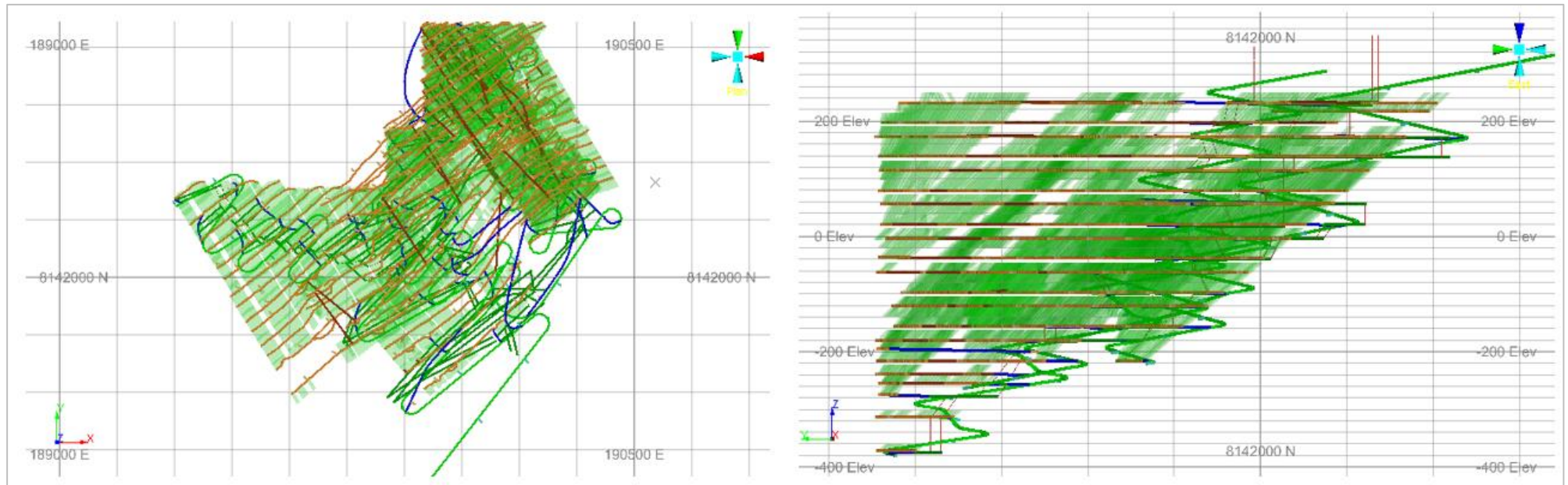


Figure 16.8: The mineralized body is fixed to the development structures - Sublevel Stopping.

The Table 16.5 present the First Pass Parameters used in the Stope Optimization.

Table 16.5: First Pass Parameters.

| Financial | | |
|----------------------------|--------------|--------------|
| Item | Unit | Value |
| Concentrate Selling Price | \$/t product | 1,900.00 |
| Selling Cost (CIF China) | \$/t product | 70.00 |
| Process Cost | \$/t ROM | 11.00 |
| G&A | \$/t ROM | 4.00 |
| Mine Cost Sublevel | \$/t | 35.00 |
| Mine Cost Room and Pillars | \$/t | 42.00 |
| Mine Development | \$/t | 5.25 |
| Cost Decline | \$/m | 5,000.00 |
| Cost Lateral Development | \$/m | 4,000.00 |
| Cost Raise Borer Machine | \$/m | 10,000/5,000 |
| CFEM | \$/t product | 0.02 |
| Metallurgical Recovery | % | 67.0 |
| Mass Recovery | % | Calculated |
| Concentrate Grade | % | 5.5 |

For the UG project, an average ROM metallurgical recovery of 67% and a mining dilution rate of 16.8% are assumed; however, further detailed analysis must be performed as the project matures to refine these assumptions.

The Table 16.6 present de Bandeira's Production Profile.

Table 16.6: Production Profile.

| | |
|---|---------------------------------------|
| Total Project Life (LOM) | 20 years |
| Room and Pilar LOM Production (Diluted) | 1.8 Mt @ 1.05% Li ₂ O |
| Sub Level LOM Production (Diluted) | 21.1 Mt @ 1.25% Li ₂ O |
| Total LOM Production (Diluted) | 22.9 Mt @ 1,23%Li₂O |
| Nominal Plant Capacity | 1.3 Mtpa |
| Average Plant Throughput | 1.26 Mtpa |
| Run-of-Mine Underground Mining Dilution | 16.8% |
| Waste Generation Average from Year 0 to 20 | 439 ktpa |
| SPO average Annual Production @ 5,5% Li ₂ O from Years 1 to 18 | 187 ktpa |

| | |
|--|----------|
| SPO average Annual Production @ 3,0% Li ₂ O from Years 1 to 18 | 56 ktpa |
| SPO average Annual Production @ 5.5% Li ₂ O Equivalent from Years 1 to 18 | 218 ktpa |
| SPO 5,5% Li ₂ O Metallurgical Recovery | 67.0% |
| SPO 3,0% Li ₂ O Metallurgical Recovery | 10.7% |
| SPO 5,5% Li ₂ O Mass Recovery | 15.2% |
| SPO 3,0% Li ₂ O Mass Recovery | 4.5% |

16.2 Mining Operation

The operational design for the BRP mine includes elements such as slopes and cross-sections. For the BSL mine, in addition to the designs contained in BRP, the ore channels, mucking bays, waste connections between the ore channels, a secondary slope, passage bays and sumps were included.

For the Bandeira Project, two declines were developed. The first decline starts at elevation 313 and end at elevation -380 in the Z-axis. The second decline begins at elevation 280 and ends at elevation -220. Both have a 15% gradient, a minimum radius of 25 m, and footwall access. Safety measures include having 20-meter pillars between the stope on the footwall and 4-meter pillars between galleries.

Sumps developed in cross-cuts are 12 m long, with the first 3 m having a 0% gradient, and the remaining 9 m having a -15% gradient. Sumps developed in the declines have the first 3 meters at a 0% gradient, and the following 12 m have a -15% gradient. Sumps were created every 200 meters of decline development.

Cross-cuts were developed from elevation 295 to 195 for Room and Pillar, and from 230 to -375 for Sublevel Stopping as needed for access. For the Room and Pillar method, 5 cross-cuts were developed from the southern access ramp, providing access to the two ore bodies, with 3 being developed for the main body (larger mass) and 2 for the secondary body (smaller mass). For the Sublevel, each panel has two accesses to the stopes: one in the upper sublevel and another in the lower sublevel. This setup ensures the drilling of both ascending holes (from the lower sublevel) and holes going both up and down (from the higher sublevel), allowing for mining of the entire 55-meter panel. All cross-cuts are at least 15 m long starting from the decline, with a gradient close to 1%, preventing water accumulation.

Ore Drives were developed from cross-cuts along the stopes. In sublevels where multiple stopes were generated in different lenses, waste connections are present, allowing mining of stopes in multiple lenses. Similar to the cross-cuts, Ore Drives have 15-meter Mucking Bays, but they are positioned every 100 m of Ore Drive development to meet maneuvering needs.

Ventilation raises extend from the surface level down to the lowest elevation of the decline. They are connected to the mine through ventilation galleries, adopting the same development configuration as the cross-cuts and Ore Drives, and subsequently connecting to the ventilation raises. These raises have a minimum incline of 45%, a diameter of 2.1 m, and are separated by a minimum 7-meter pillar from nearby excavations. The total length of each development structure in meters is presented in Table 16.7.

Table 16.7: Development structures metrics.

| Development structures | |
|------------------------|---------------|
| Structure | Dimension (m) |
| Declines | 10,572 |
| Mucking Bay | 3,309 |
| Cross-cut | 6,534 |
| Ore Drive | 36,112 |
| Sump | 762 |
| Waste Connect | 6,511 |
| Ventilation Gallery | 13,383 |
| Raise | 3,876 |
| Total | 81,059 |

16.3 Mining Scheduling

In this section, the term “ROM Stopes” is used to differentiate the mineralized material produced in the stopes and the term “Productive ROM” is used for the mineralized material produced in development. The term “ROM” refers to the sum of the ROM Stopes and ROM Productive materials, that have been sent to the plant stockpile. The waste material removed from development was hauled to the waste dump. For the Project, part of the waste material produced was used as rockfill in the stopes (around 80%), aiming to ensure the stability of empty areas and reducing the amount of material movement to the surface.

The mining scheduling was carried out using EPS. The mining was conducted in retreat, with the complete opening of Ore Drives at each advance before starting the stope mining.

The mining scheduling was performed using EPS software version 3.1.80. The mining scheduling involved retreat at the end of each level's Ore Drive development. With the software, targets were set for decline development, lateral gallery development, and mass movement.

For decline development, monthly values were defined, ranging from 80 to 90 m/month for the first three months, 175 to 180 m/month by the end of year 0, and a stabilization of 90 to 100 m/month from year 1 onwards. Lateral development aimed for an advance rate of 400 to 450 m/month, which held until 2031 when it decreased to a range of 350 to 400 m/month.

For mass movement targets, the mining scheduling was determined to achieve a plant feed close to 1.3 Mt of ROM. Separate targets were set for the room and pillar and sublevel stope methods to achieve the required ROM movement. This value was reached from year 2 and remained consistent until year 17, when the mine's resources began to deplete. The parameters used in EPS can be seen in Table 16.8.

Table 16.8: Bandeira Mining Assumptions EPS – Reference.

| Type | ITEM | Unity | Value |
|-----------------------|-----------------|---------|-------|
| Sublevel Stoping | Production Rate | ROM t/d | 300 |
| Sublevel Stoping | Mining Recovery | % | 90 |
| Sublevel Stoping | Op. Dilution | % | 16.8 |
| Room and Pillar | Production Rate | ROM t/d | 137 |
| Room and Pillar | Mining Recovery | % | 100 |
| Room and Pillar | Op. Dilution | % | 15 |
| Development All | Mining Recovery | % | 100 |
| Development All | Op. Dilution | % | 20 |
| Headings Development | Rate | m/mo | 40 |
| Lateral Dev. Priority | Rate | m/mo | 50 |
| Raise Borer | Rate | m/mo | 100 |
| Slot Raise | Rate | m/mo | 20 |

The Figure 16.9 to Figure 16.15 and the Table 16.9 present the mining scheduling results for sublevel stope mining.

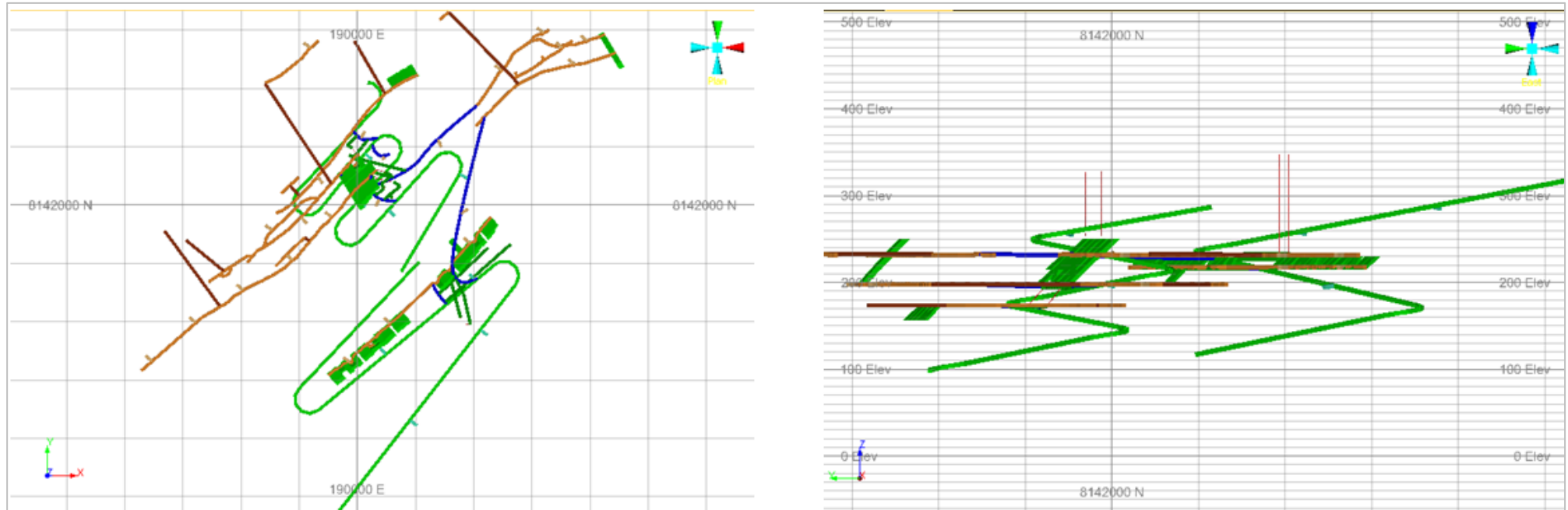


Figure 16.10: Plan view (left) and cross-sectional view (right) of the mining scheduling for year 2.

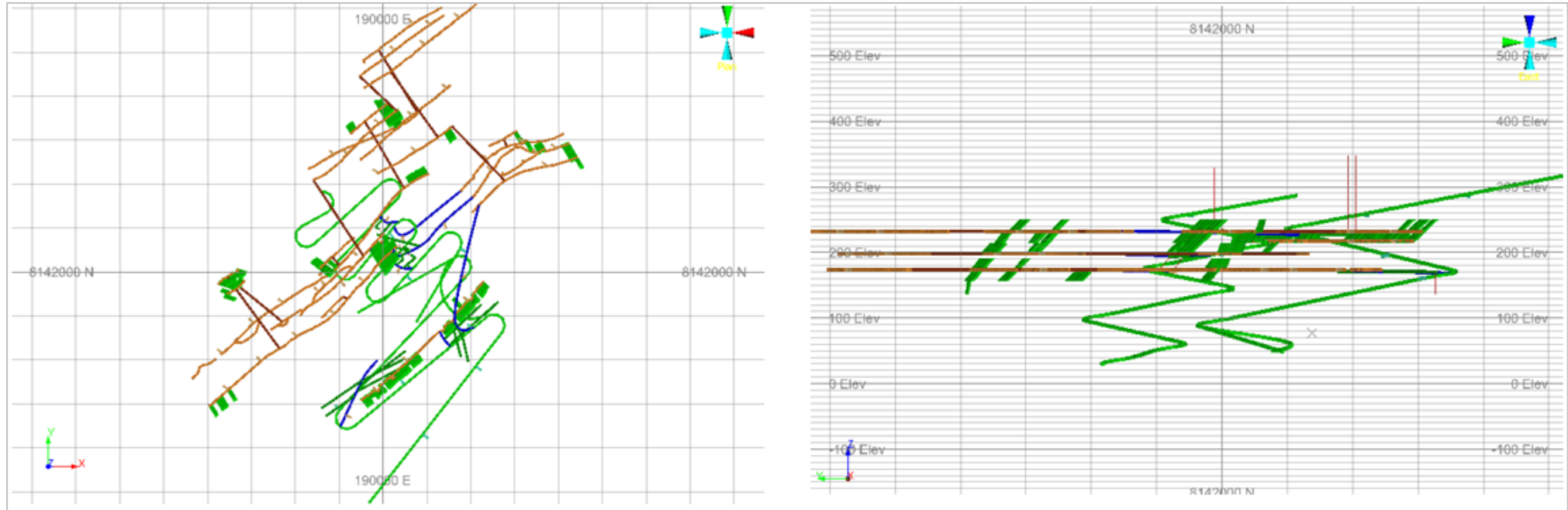


Figure 16.11: Plan view (left) and cross-sectional view (right) of the mining scheduling for year 3.

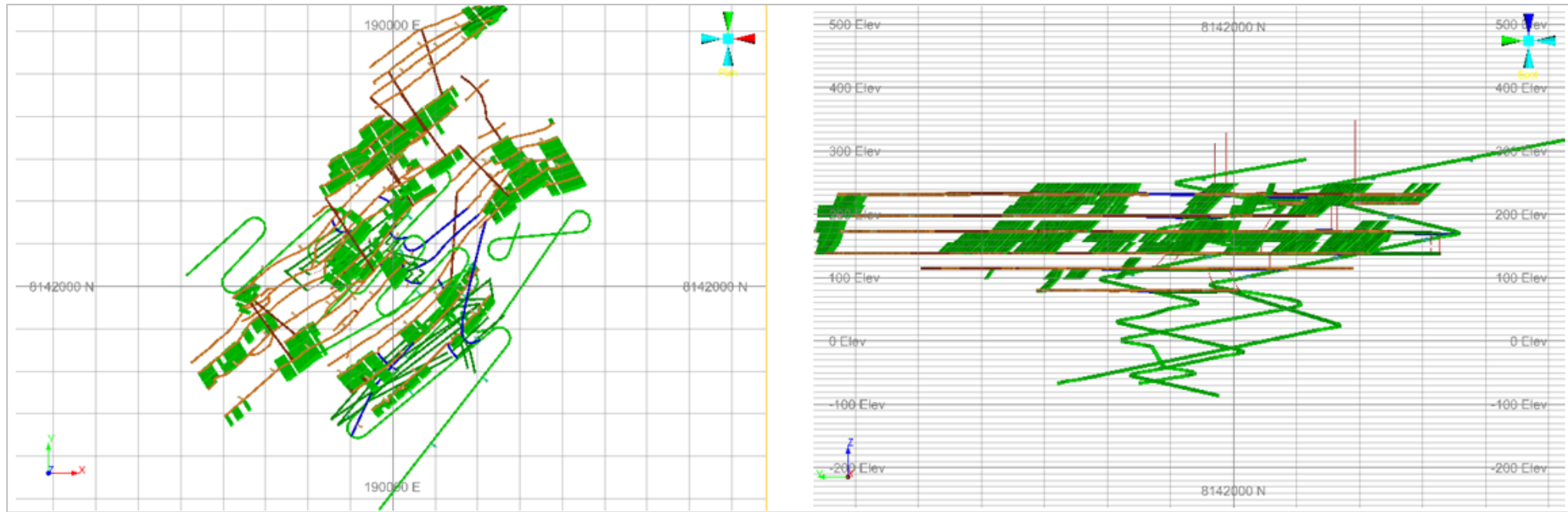


Figure 16.12: Plan view (left) and cross-sectional view (right) of the mining scheduling for year 5.

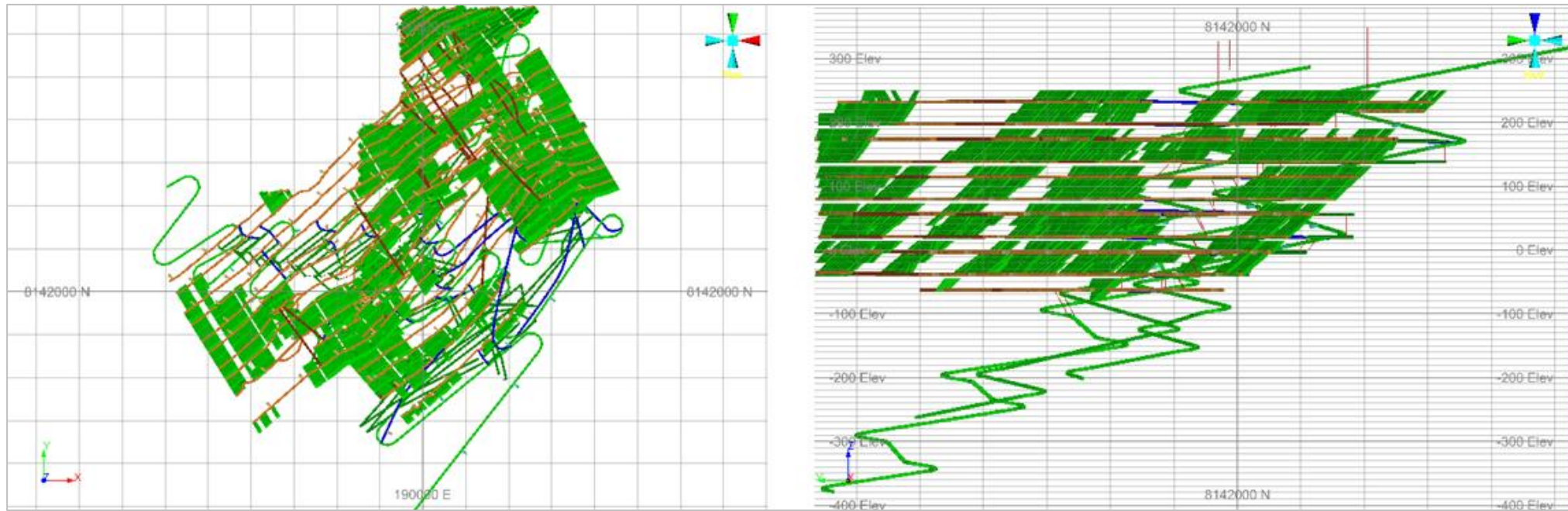


Figure 16.13: Plan view (left) and cross-sectional view (right) of the mining scheduling for year 10.

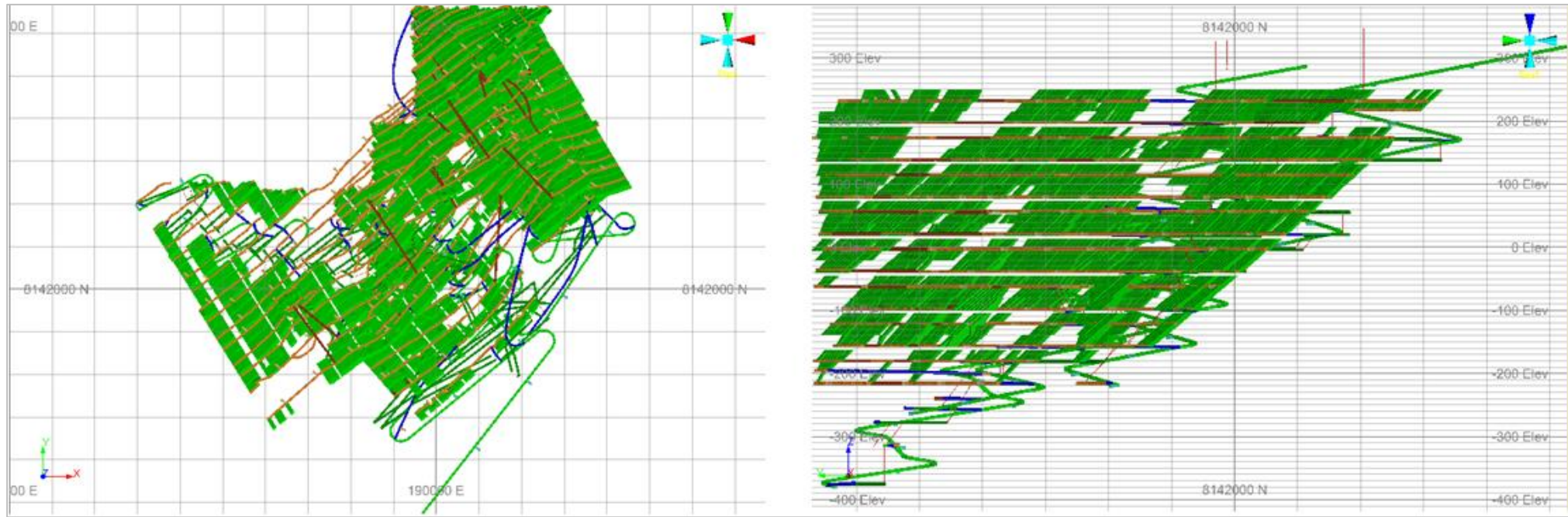


Figure 16.14: Plan view (left) and cross-sectional view (right) of the mining scheduling for year 15.

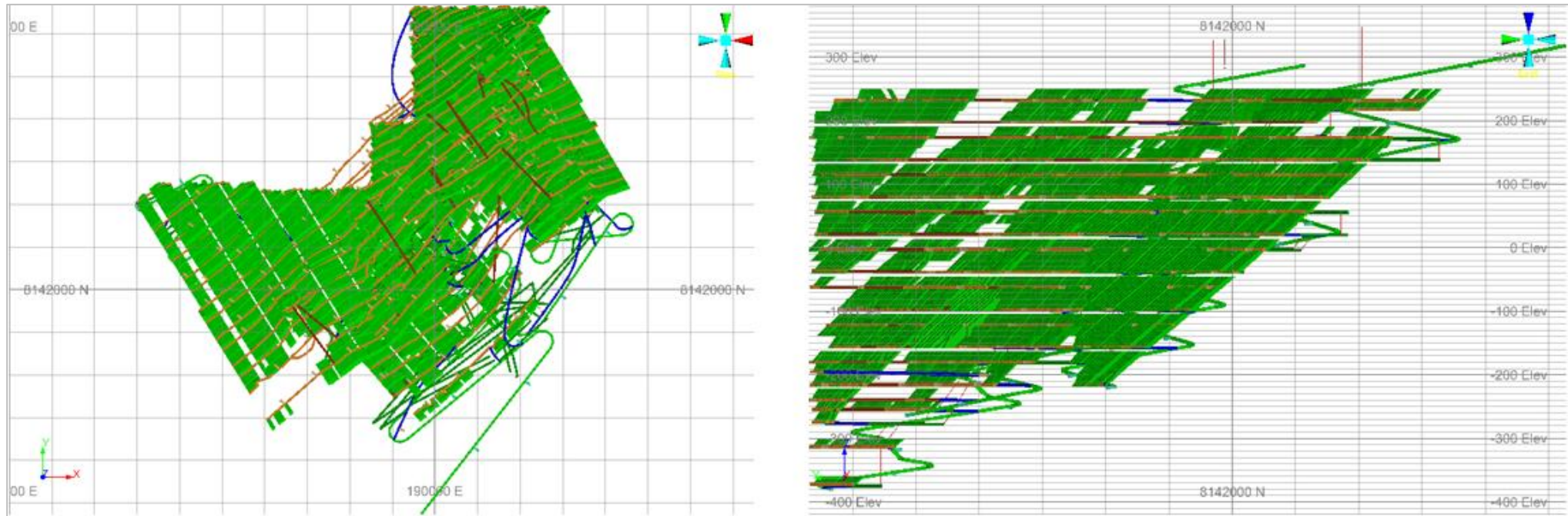


Figure 16.15: Plan view (left) and cross-sectional view (right) of the mining scheduling for year 20.

Table 16.9: Mining Scheduling Results.

| Year | 0 | 1 | 2 | 3 | 4 | 5 | 6 | 7 | 8 | 9 | 10 | 11 | 12 | 13 | 14 | 15 | 16 | 17 | 18 | 19 | 20 | 21 |
|-----------------------------------|---------|---------|---------|---------|---------|---------|---------|---------|---------|---------|---------|---------|---------|---------|---------|---------|---------|---------|---------|-------|-------|-------|
| PRODUCTION | | | | | | | | | | | | | | | | | | | | | | |
| TOTAL ROM MASS (Kt) | 1.3 | 998.0 | 1,246.0 | 1,312.4 | 1,271.2 | 1,276.2 | 1,274.1 | 1,263.3 | 1,288.2 | 1,293.5 | 1,298.2 | 1,254.9 | 1,259.6 | 1,224.5 | 1,284.1 | 1,284.1 | 1,294.5 | 1,289.2 | 1,078.0 | 281.5 | 109.8 | 25.6 |
| TOTAL ROM Li ₂ O (g/t) | 1.01 | 1.03 | 1.07 | 1.07 | 1.01 | 1.25 | 1.26 | 1.26 | 1.23 | 1.23 | 1.23 | 1.28 | 1.25 | 1.27 | 1.26 | 1.25 | 1.26 | 1.28 | 1.27 | 1.27 | 1.28 | 1.30 |
| REC MASS ROM (%) | 12.14 | 14.02 | 14.66 | 14.74 | 13.97 | 15.04 | 15.17 | 15.11 | 14.73 | 14.72 | 14.77 | 15.34 | 15.05 | 15.18 | 15.16 | 14.95 | 15.16 | 15.34 | 15.28 | 15.25 | 15.35 | 15.58 |
| CONCENTRATE MASS (kt) | 0.2 | 0.1 | 0.2 | 0.2 | 0.2 | 192.0 | 193.3 | 190.9 | 189.7 | 190.4 | 191.7 | 192.5 | 189.6 | 185.9 | 194.7 | 191.9 | 196.3 | 197.8 | 164.7 | 42.9 | 16.9 | 4.0 |
| WASTE MASS (kt) | 183.4 | 1,247.3 | 1,516.2 | 871.3 | 832.9 | 611.0 | 609.2 | 560.1 | 501.9 | 455.0 | 444.8 | 423.2 | 460.7 | 244.2 | 80.8 | 101.3 | 67.8 | 11.4 | - | - | - | - |
| BACKFILL MASS (kt) | - | 308.2 | 441.4 | 490.3 | 431.2 | 436.0 | 440.7 | 449.4 | 466.0 | 454.3 | 472.2 | 447.9 | 507.0 | 508.6 | 570.6 | 559.8 | 582.2 | 590.9 | 497.0 | 129.5 | 50.5 | 11.7 |
| DETAILED PRODUCTION | | | | | | | | | | | | | | | | | | | | | | |
| ROM MASS STOPE (kt) | - | 669.1 | 957.4 | 1,061.7 | 934.9 | 946.4 | 957.2 | 973.7 | 1,010.0 | 981.5 | 1,022.7 | 969.9 | 1,098.0 | 1,100.8 | 1,234.6 | 1,210.9 | 1,259.7 | 1,278.6 | 1,078.0 | 281.5 | 109.8 | 25.6 |
| Li ₂ O STOPE (%) | - | 1.04 | 1.07 | 1.07 | 1.01 | 1.26 | 1.28 | 1.28 | 1.24 | 1.24 | 1.23 | 1.27 | 1.25 | 1.27 | 1.27 | 1.25 | 1.27 | 1.28 | 1.27 | 1.27 | 1.28 | 1.30 |
| ROM MASS DEV (kt) | 1.3 | 328.9 | 288.6 | 250.7 | 336.3 | 329.7 | 316.9 | 289.6 | 278.2 | 311.9 | 275.5 | 285.0 | 161.6 | 123.7 | 49.5 | 73.2 | 34.7 | 10.6 | - | - | - | - |
| Li ₂ O DEV (%) | 1.01 | 0.84 | 1.12 | 0.00 | 0.00 | 1.24 | 1.22 | 1.20 | 1.18 | 1.19 | 1.24 | 1.31 | 1.26 | 1.25 | 1.22 | 1.19 | 1.15 | 1.13 | - | - | - | - |
| DEVELOPMENT | | | | | | | | | | | | | | | | | | | | | | |
| DEV PRIMARIO (m) | 1,973.2 | 612.9 | 510.8 | 3.9 | 2.5 | 2,793.0 | 2,863.7 | 2,747.7 | 2,100.0 | 1,545.1 | 1,462.2 | 1,467.5 | 2,990.9 | 1,258.5 | 157.6 | 63.9 | 417.2 | 17.0 | - | - | - | - |
| DEV SECUNDARY (m) | - | 613.7 | 512.0 | 2.6 | 4.0 | 3,731.3 | 3,646.0 | 3,146.0 | 3,263.7 | 3,342.1 | 3,300.8 | 2,990.0 | 1,910.3 | 1,333.8 | 705.4 | 1,020.2 | 304.5 | 105.6 | - | - | - | - |
| DEV LAT (m) | 469.7 | 5.3 | 4.7 | 5.4 | 5.4 | 5,358.6 | 5,359.3 | 4,758.6 | 4,762.5 | 4,760.5 | 4,762.9 | 4,457.5 | 4,783.3 | 2,521.7 | 863.0 | 1,084.1 | 628.0 | 122.7 | - | - | - | - |
| DEV RP (m) | 1,503.5 | 1.1 | 1.2 | 1.2 | 1.2 | 1,165.6 | 1,150.4 | 1,135.1 | 601.3 | 126.7 | - | - | 118.0 | 70.5 | - | - | 93.7 | - | - | - | - | - |
| DEV RAISE (m) | 99.7 | 0.5 | 0.03 | 0.5 | 0.1 | 107.8 | 168.5 | 574.9 | 122.5 | 335.3 | 338.7 | 48.1 | 466.8 | 452.9 | - | - | 31.2 | - | - | - | - | - |

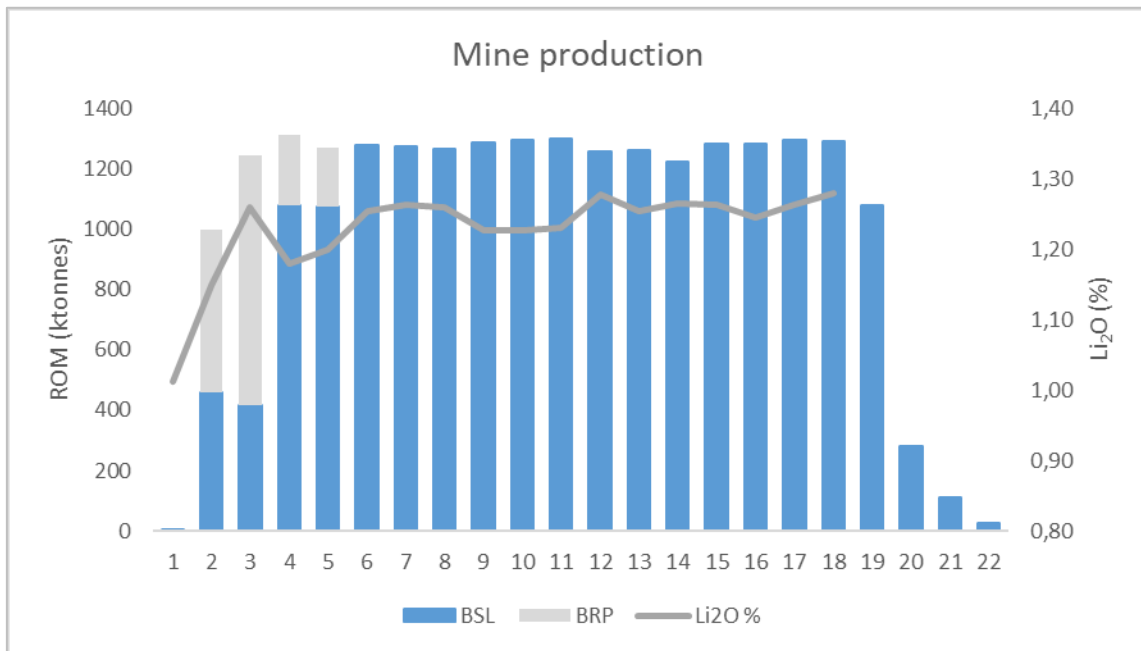


Figure 16.16: Mine Plan and Schedule with Li₂O%.

16.4 Mining Equipment

The Bandeira underground mining project was designed to employ own its fleet for ROM handling and the development of underground access galleries within the sublevel stope mining section. Equipment sizing has been planned, taking into consideration annual material removal volumes, ROM/stope tunnel specifications, and the planned production rates for these activities.

The ROM stopes will be drilled, blasted, loaded, and hauled by trucks to a stockpile, which, in turn, supplied the plant. As for the room and pillar method, the project utilizes a third-party fleet, which is stipulated based on the equipment used for mining the stopes.

The main underground mining activities will be:

- Drilling and rock blasting to advance the development tunnel through waste rock to the orebody.
- Ventilation of gallery.
- Drilling and rock blasting of the orebody.
- Loading, hauling and dumping of ROM and waste.
- Disposal of ROM in the stockpile and waste in the waste dump.
- Use of part of waste to rockfill.
- Construction and maintenance of accesses.
- Maintenance of the floor, drainage, coating and signaling of all access roads used in the operation.
- Implementation and maintenance of the mine's surface and underground drainage systems at access points to the mining operation, waste dump, ROM stockpile and other areas linked to mining operations.
- Mine infrastructure services, such as: construction and maintenance of accesses to the mining areas, crusher, waste dump, workshops, and offices, mine drainage, road signaling, mine dewatering etc.

- Production estimated at approximately 1.3 Mt of ROM per annum.
- Build and maintain the operation's support facilities: offices, workshops, cafeteria, living quarters, warehouses, changing rooms, ablution facilities, septic tanks, environmental, health and safety emergency, explosive magazine, electrical and hydraulic installations, and others, in strict accordance with the Brazilian environmental standards and labor laws.

16.4.1 Rock Types Properties

Rock properties are important, influencing the equipment fleet requirements, as well as the waste dump and stockpile design capacities.

The average in-situ dry density (in-site underground) used for fleet sizing is 2.70 t/m³ and 2.19 t/m³ for wet basis. An average swelling factor of 30% was estimated for ROM and waste.

A moisture content of 5% was estimated for ROM and waste. The mining equipment was sized according to the volumes of material to be removed each year.

16.4.2 Assumptions

Fleet sizing was based on the following assumptions and elements:

- End of Period (EOP) designs.
- Topography and location of the plant, stockpile, and waste dump.
- Project work regime: 364 days per year, with three 6-hour shifts per day and 4 rotating crews.
- Main fleet parameters by equipment: utilization, availability, and performance.
- Capacities and cycle times of main equipment.

Table 16.10: Equipment Utilization, Availability, and Performance Factors.

| Material | Utilization | | | Availability | | | Performance | | |
|-----------|-------------|-----|----------|--------------|-----|----------|-------------|-----|----------|
| | Truck | LHD | Fandrill | Truck | LHD | Fandrill | Truck | LHD | Fandrill |
| Waste | 50% | 50% | 70% | 75% | 75% | 80% | 83% | 83% | 83% |
| Stope ROM | 50% | 50% | 70% | 75% | 75% | 80% | 83% | 83% | 83% |

The quantity of available equipment for each year, based on the mining scheduling parameters, can be seen in the Table 16.11 for Room and Pillar and in Table 16.12: Schedule of Primary Equipment for Sublevel stope.

Table 16.11: Schedule of Primary Equipment for Room and Pillar.

| Mine Equipment | Reference Model | Year | | | | |
|----------------|----------------------|----------|-----------|-----------|----------|----------|
| | | 0 | 1 | 2 | 3 | 4 |
| Truck | Sandvik TH545i | 1 | 5 | 9 | 3 | 3 |
| LHD | Sandvik LH515i | 1 | 3 | 5 | 2 | 1 |
| Jumbo 2 Boom | Sandvik DD321 | 1 | 1 | 1 | 0 | 0 |
| Cable Bolter | Sandvik DS421 | 1 | 1 | 1 | 1 | 1 |
| Scaler | Normet Scamec 2000 S | 1 | 1 | 2 | 2 | 2 |
| Total | | 5 | 11 | 18 | 8 | 7 |

Table 16.12: Schedule of Primary Equipment for Sublevel Stopping.

| Mine Equipment | Reference Model | Year | | | | | | | | | | | | | | | | | | | | | |
|-----------------------|---|-----------|-----------|-----------|-----------|-----------|-----------|-----------|-----------|-----------|-----------|------------|-----------|------------|-----------|------------|-----------|-----------|-----------|-----------|-----------|-----------|-----------|
| | | 0 | 1 | 2 | 3 | 4 | 5 | 6 | 7 | 8 | 9 | 10 | 11 | 12 | 13 | 14 | 15 | 16 | 17 | 18 | 19 | 20 | 21 |
| Truck | Sandvik TH545i | 2 | 8 | 9 | 15 | 16 | 20 | 20 | 21 | 25 | 25 | 27 | 23 | 29 | 28 | 31 | 30 | 26 | 23 | 17 | 4 | 1 | 1 |
| LHD | Sandvik LH515i | 1 | 4 | 4 | 6 | 6 | 7 | 7 | 6 | 6 | 6 | 6 | 6 | 6 | 5 | 4 | 4 | 4 | 4 | 4 | 1 | 1 | 1 |
| Longhole Drill | Sandvik DL421 | 0 | 1 | 1 | 3 | 3 | 4 | 4 | 4 | 4 | 4 | 4 | 4 | 4 | 4 | 5 | 5 | 5 | 5 | 4 | 1 | 1 | 1 |
| Jumbo 2 Boom | Sandvik DD321 | 2 | 5 | 4 | 5 | 5 | 5 | 5 | 4 | 4 | 3 | 3 | 3 | 3 | 2 | 1 | 0 | 0 | 0 | 0 | 0 | 0 | 0 |
| Cable Bolter | Sandvik DS421 | 1 | 1 | 1 | 2 | 2 | 2 | 2 | 2 | 2 | 2 | 2 | 2 | 2 | 2 | 2 | 2 | 2 | 2 | 1 | 1 | 1 | 1 |
| Scaler | Normet Scamec 2000 S | 1 | 1 | 2 | 2 | 2 | 2 | 2 | 2 | 2 | 2 | 2 | 2 | 2 | 2 | 2 | 2 | 2 | 2 | 2 | 2 | 2 | 2 |
| Explosive Truck | Normet Charmec MF050 D | 1 | 1 | 3 | 3 | 3 | 3 | 3 | 3 | 3 | 3 | 3 | 3 | 3 | 3 | 3 | 3 | 3 | 3 | 3 | 3 | 3 | 3 |
| Scissor Lift | Normet Utilift SF330 | 1 | 1 | 2 | 2 | 2 | 2 | 2 | 2 | 2 | 2 | 2 | 2 | 2 | 2 | 2 | 2 | 2 | 2 | 2 | 2 | 2 | 2 |
| Shotcrete Remix Truck | Normet Tornado S2 | 0 | 0 | 0 | 0 | 0 | 0 | 0 | 0 | 0 | 0 | 0 | 0 | 0 | 0 | 0 | 0 | 0 | 0 | 0 | 0 | 0 | 0 |
| Shotcrete Spray Truck | Normet Alpha 30 VC | 0 | 0 | 0 | 0 | 0 | 0 | 0 | 0 | 0 | 0 | 0 | 0 | 0 | 0 | 0 | 0 | 0 | 0 | 0 | 0 | 0 | 0 |
| Fuel & Lube Truck | Normet Multimec SF60 + C350 Cassete | 1 | 1 | 2 | 2 | 2 | 2 | 2 | 2 | 2 | 2 | 2 | 2 | 2 | 2 | 2 | 2 | 2 | 2 | 2 | 2 | 2 | 2 |
| Personnel Carrier | Normet Variomec XS 115 PER + C162 Cassete | 1 | 1 | 2 | 2 | 2 | 2 | 2 | 2 | 2 | 2 | 2 | 2 | 2 | 2 | 2 | 2 | 2 | 2 | 2 | 2 | 2 | 2 |
| Maintenance Truck | Normet Variomec XS 040 Mat + C125 Cassete | 1 | 1 | 2 | 2 | 2 | 2 | 2 | 2 | 2 | 2 | 2 | 2 | 2 | 2 | 2 | 2 | 2 | 2 | 2 | 2 | 2 | 2 |
| Jackleg Drill | Atlas Copco BBC 34W | 1 | 1 | 4 | 4 | 4 | 4 | 4 | 4 | 4 | 4 | 4 | 4 | 4 | 4 | 4 | 4 | 4 | 4 | 4 | 4 | 4 | 4 |
| Stoper Drill | Atlas Copco BBD46WS-8 | 1 | 1 | 2 | 2 | 2 | 2 | 2 | 2 | 2 | 2 | 2 | 2 | 2 | 2 | 2 | 2 | 2 | 2 | 2 | 2 | 2 | 2 |
| Air Compressor | Atlas Copco XATS 127 | 1 | 1 | 2 | 2 | 2 | 2 | 2 | 2 | 2 | 2 | 2 | 2 | 2 | 2 | 2 | 2 | 2 | 2 | 2 | 2 | 2 | 2 |
| Grader | Paus PG 10 HA | 1 | 1 | 2 | 2 | 2 | 2 | 2 | 2 | 2 | 2 | 2 | 2 | 2 | 2 | 2 | 2 | 2 | 2 | 2 | 2 | 2 | 2 |
| Ventilation Fan | 93 kW | 2 | 2 | 12 | 12 | 12 | 12 | 12 | 12 | 12 | 12 | 12 | 12 | 12 | 12 | 12 | 12 | 12 | 12 | 12 | 12 | 12 | 12 |
| Exhauster | | 2 | 2 | 12 | 12 | 12 | 12 | 12 | 12 | 12 | 12 | 12 | 12 | 12 | 12 | 12 | 12 | 12 | 12 | 12 | 12 | 12 | 12 |
| Dewatering Pump | Flygt 1325 | 1 | 1 | 3 | 3 | 3 | 3 | 3 | 3 | 3 | 3 | 3 | 3 | 3 | 3 | 3 | 3 | 3 | 3 | 3 | 3 | 3 | 3 |
| Diesel Generator | Cummins C70D5P | 1 | 1 | 2 | 2 | 2 | 2 | 2 | 2 | 2 | 2 | 2 | 2 | 2 | 2 | 2 | 2 | 2 | 2 | 2 | 2 | 2 | 2 |
| Utility Vehicle | Toyota Land Cruiser | 4 | 4 | 6 | 6 | 6 | 6 | 6 | 6 | 6 | 6 | 6 | 6 | 6 | 6 | 6 | 6 | 6 | 6 | 6 | 6 | 6 | 6 |
| Total | | 26 | 39 | 77 | 89 | 90 | 96 | 96 | 95 | 99 | 98 | 100 | 96 | 102 | 99 | 101 | 99 | 95 | 92 | 84 | 65 | 62 | 62 |

16.4.3 Operations

The underground mine development operations will start with the construction of two declines extending along a NE/SW mineralized trend spanning 1.0 km. The first decline starts at the 320-meter level, and the second at the 286-meter level. This configuration is necessary due to the complexity of the ore body, facilitating access to different material lenses and ensuring the efficiency of the mining process.

Lithium Ionic Corp. will be responsible for the development of the sublevel section, while a third party undertook the development of the room and pillar section. This operation included opening and developing declines, Ore Drives, passing bays, cross-cuts, sumps, and stabilizing the galleries. Techniques such as rock bolting and mesh installation will be used to ensure safe access, in addition to the installation of electrical systems and ventilation.

The development operations will commence with drilling activities using drill Jumbos. Following drilling, blasting, and ventilation activities, a Scaler will inspect and remove any loose rock pieces from the roof and walls of the tunnels. LHDs (Load-Haul-Dump machines) will be utilized for material loading, and trucks will transport the material to the stockpile and waste dump areas.

Mining operations will commence after the completion of the last segment of the ore drive in the lowest sublevel of each panel, following the bottom-up method. The drilling of the stopes was conducted in fan patterns with a diameter of 3.5 inches and an average height of 13.75 m. This operation will be carried out by a long-hole fandrill.

After the drilling and blasting operations, the remaining ore and stopes ROM material will be loaded by LHDs with a bucket capacity of 6.3 m³ and transported to the stockpile by underground haulage trucks with a capacity of 43.7 t.

The Average Haulage Distances (AHDs) were estimated based on the quantities of each material mined and destinations defined by designed mining scheduling. The necessary amount of mine equipment was determined by integrating AHDs and mine fleet parameters, taking into consideration that 80% of waste material will not be transported and will be used as rockfill.

A wheel loader with a bucket capacity of up to 6.3 m³ was used to feed the plant at a rate of 231 t per hour (tph), operating 18 hours a day, 7 days a week.

Ventilation Fans with 93 kW have been positioned at each underground mining face to ensure proper ventilation for mining operations.

16.4.4 Work Shifts

The Bandeira mine will be mined using the underground Sublevel Stoping method with 4 teams that alternated in 3 shifts and 1 resting, operating 18 hours a day, 364 days a year. The mining scheduling were designed to produce enough ROM to feed a material processing plant with a nominal capacity of 1.3 Mtpy (Metric tons per year) and had a LOM of 22 years, with concentrate production having started in year 1.

16.4.5 Opening and Maintenance of Roads and Accesses

Roads and accesses will require the following items to be carried out:

- Opening and adjustment of accesses.
- Longitudinal and transverse drainage for water flow.
- Development of tunnels with a minimum slope of 1%.

16.4.6 Drilling and Blasting

The geology and rock types at the Bandeira Mine are crucial for defining drilling and blasting parameters, which relates to mining recovery.

It is important to define the boundaries of the orebody to minimize dilution and losses. MGlit will employ a geologist as a member of its technical staff who will collaborate directly with the drilling, blasting, and loading teams.

Previous studies (pre-blast surveys) will be developed before the first blasting to establish the minimum distances between pre-existing structures that will be kept and the blasted benches. As a result, restrictions or opportunities regarding to the maximum load per drill hole will be indicated, whit indicated the maximum blasthole diameter, as well as the type of accessories used.

Table 16.13 and Figure 16.17 shows the preliminary underground blasting plan considering development advances (Cross-cuts, Oredrives, Declines, Waste Conects, Ventilation Galleries, Sumps and Mucking Bays).

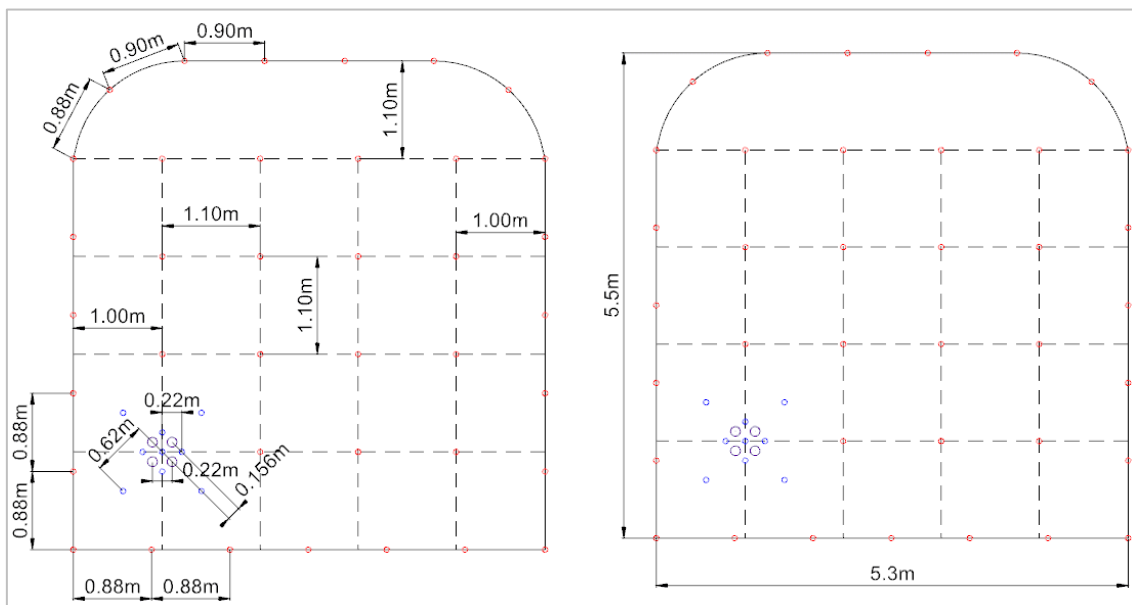


Figure 16.17: Blasting holes per cross-sectional area of each development activity.

Table 16.13: Preliminary plan for underground gallery development blasting.

| Item | # | Unit |
|------------------------------|------|------------------|
| Area | 28.5 | m ² |
| Width | 5.3 | m |
| Height | 5.5 | m |
| Arch Radius | 1.25 | m |
| Perimeter | 20.5 | m |
| Diameter of loaded holes | 51 | mm |
| Total number of holes | 51 | holes |
| Number of loaded holes | 47 | holes |
| Diameter of enlarged holes | 102 | mm |
| Number of empty holes | 4 | holes |
| Length of holes | 3.7 | m |
| Drilled size | 189 | m |
| Overbreak | 10 | % |
| Expected average advance 90% | 3.33 | m |
| Rock density | 2.8 | t/m ³ |
| Volume/fire | 104 | m ³ |
| Tonnage /fire | 292 | t |

Table 16.14: Drilling productivity data for development.

| Item | # | Unit |
|---------------------------|--------|------------------|
| Total length for advance. | 188.70 | m |
| Plane drilling index. | 1.55 | t/m |
| Plane drilling index. | 1.81 | m/m ³ |
| Advance drilling index | 56.67 | m/m |
| Ton/h | 123.92 | t/h |
| Productivity | 80.00 | m/h |
| Productivity | 21.6 | holes /h |
| Reference productivity. | 22.5 | holes /h |

Table 16.15: Data for hole properties and charge per hole.

| Item | # | Unit |
|---------------------------------|-------|-------------------|
| Plug | 0,5 | m |
| Loaded holes | 47 | holes |
| Contour holes | 10 | holes |
| Floor holes | 7 | holes |
| Center holes | 30 | holes |
| 1 hole volume | 7.558 | cm ³ |
| 1 hole volume with plug | 6.537 | cm ³ |
| Subtek Orica Emulsion Density | 1.00 | g/cm ³ |
| Emulsion putty pumped into hole | 6,54 | kg/ holes |
| Subtek Orica Anfo Density | 0,82 | g/cm ³ |
| Anfo putty for 1 hole | 5,36 | kg/ holes |

Table 16.16: Table of explosives used for detonations.

| Explosives | |
|------------|-------------------|
| Cartridge | Senatel Magnafrag |
| Anfo | Amex |
| Pumped | Subtek Charge |

In the excavation of the contour of the cross-section of the galleries, the explosive NP60 will be used. Meanwhile, for the excavation of the floor and other holes, both emulsion explosives and ANFO type explosives will be utilized. The explosive specifications for each of these activities can be found in the Table 16.17 to Table 16.19.

Table 16.17: Explosive charge used for advance blasting.

| Contour | | |
|--|-------|----|
| 1 cartridge of 1'1/2"x16" (0.532)kg + 3.9m of NP60 | | |
| For 10 holes | 5.32 | kg |
| | 39 | m |
| Floor | | |
| 1 BOOSTER 30 g + Emulsion | | |
| For 7 emulsion holes; Stopper = 0.50 m | 45.76 | kg |
| 1 booster 30 g + 5,8 kg of ANFO per hole | | |
| For 7 ANFO holes | 37.52 | kg |
| Remaining holes | | |
| 1 booster of 30 g+ 6kg of Emulsion per hole | | |
| For 43 holes; Stopper = 0.80 metros | 196.1 | kg |
| 1 booster 30 g + 5,8 kg de ANFO per hole | | |
| For 34 holes; Stopper = 0.80 metros | 160.8 | kg |

Table 16.18: Characteristics of hole loading by explosive

| Emulsion | | |
|------------------------|-------|------------------|
| Emulsion charge ratio | 0.85 | g/t |
| Charge ratio per meter | 74.23 | kg/m |
| Volumetric ratio | 2.37 | g/m ³ |
| ANFO | | |
| ANFO charge ratio | 0.70 | g/t |
| Charge ratio per meter | 61.16 | kg/m |
| Volumetric ratio | 1.95 | g/m ³ |

Table 16.19: Development blasting productivity.

| | | |
|-----------------------------|--------|------------------|
| Total length for an advance | 188.7 | m |
| Plane drilling index | 1.55 | t/m |
| Plane drilling index | 1.81 | m/m ³ |
| Drilling advance index | 56.67 | m/m |
| Ton/h index | 123.92 | t/h |
| Productivity | 80 | m/h |
| Productivity | 21.62 | holes/h |
| Reference productivity | 22.5 | holes/h |

For the development of stopes, Figure 16.18 illustrates the drilling plan for both ascending and descending holes. Table 16.20 presents data for fan drilling, including the number of holes, hole length, density, fan mass, and other factors considered in the blasting planning. All parameters were estimated to meet the production target of 1.3 million tons of ROM per year.

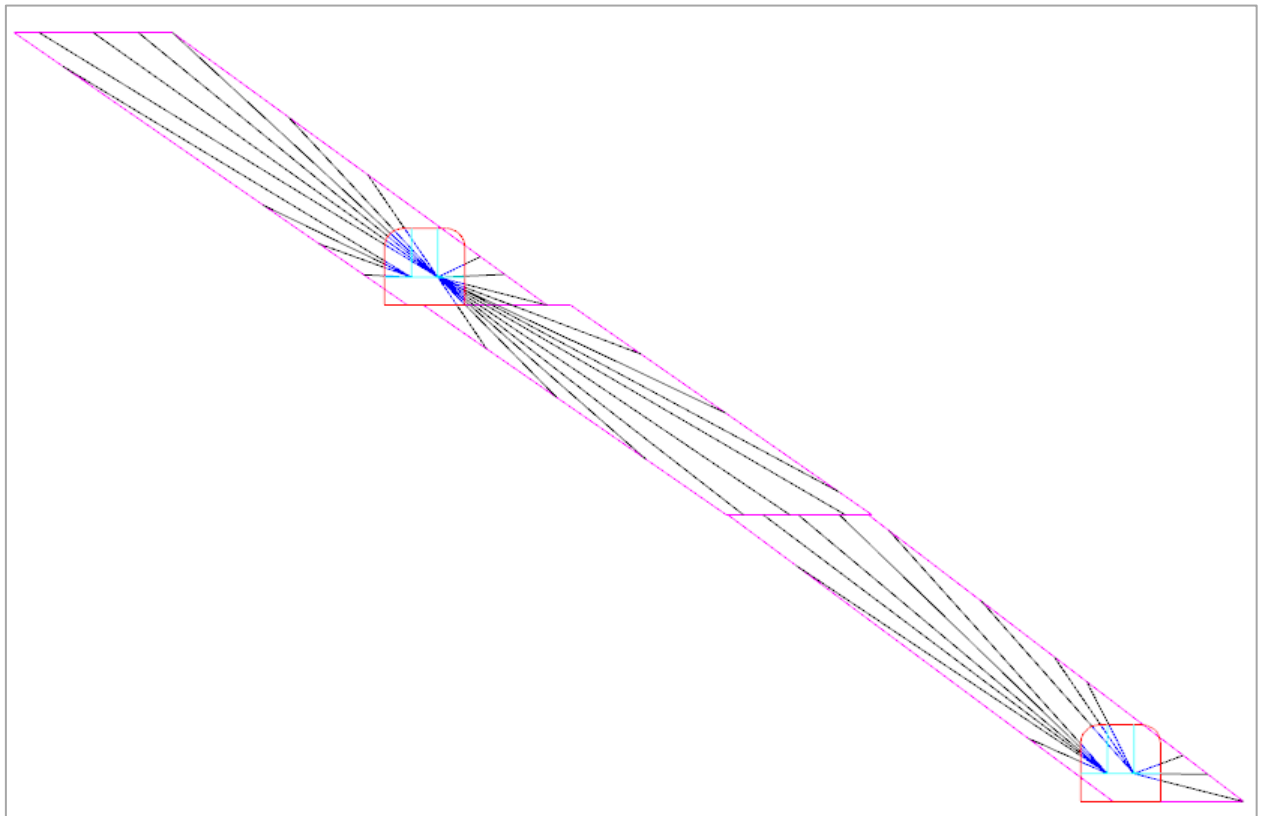


Figure 16.18: Scheme of fan drilling, both ascending and descending, in the stopes.

Table 16.20: Development blasting productivity.

| Specific Fan Drilling. | | |
|-------------------------------|-------------------|--------------|
| Item | Unit | Value |
| Drills | No | 36 |
| Total Length | m | 495 |
| Average hole length | m | 13.75 |
| Solid volume | m ³ | 1953 |
| ROM density | m ³ /t | 2.7 |
| Fan mass | t | 5273.1 |
| Spacing | m | 2 |
| Specific drilling | t/m | 5.33 |
| Charge ratio | | 4.93 kg/m |

16.4.7 Explosives Supply

The provision of explosives and the execution of blasting will be carried out by a specialized subcontractor, under the guidance of the mining contractor.

It is foreseen that Bandeira Mine will use pumped explosives, booster, and non-electrical accessories.

16.4.8 Labour Mining

Over the 22 years of Bandeira mine operation, MGLit will have a management team composed of a manager, engineers, geologists, technicians, surveyors, controller, and supervisors.

17 RECOVERY METHODS

17.1 Process Description

Preliminary metallurgical tests using dense media were carried out by SGS Geosol in Vespasiano and Sepro Minerals in Vancouver, Canada. In addition, ore sorter tests were conducted by TOMRA in Germany. Flotation tests were also carried out at SGS Geosol in Vespasiano.

The results of the separation in dense media and ore sorter were satisfactory, and these unit operations were included in the process route. The dense medium separation tests were carried out by particle size range and the overall result indicated a recovery of 74.8% to obtain a concentrate with 5.50% Li₂O. With regard to the ore sorter test, it was possible to enrich the grade of the dense medium feed by between 25 and 26%, recovering 91 to 94% of the lithium.

Preliminary flotation tests were carried out on the bench in an open circuit, with 62% recovery and 4.69% Li₂O grade. However, tests will be carried out to assess the behavior of the sample in a closed circuit. Flotation is being considered as a future stage for processing the fines, which will first be stored.

The results did not indicate the need to include the magnetic separation stage in the flowsheet, since the concentrate met the iron specification.

17.1.1 Description of the Processing Plant

The Bandeira Project aims to process 1.3 Mt of ore per year. The beneficiation plant includes the following unit operations: crushing, pre-concentration (ore sorter), DMS, filter circuit.

The reserve has spodumene as its main mineral of interest. The mineralogical composition expected for ROM is shown in Table 17.1.

Table 17.1: Lithium minerals found in pegmatite rocks.

| Mineral | Chemical formula | Density | Hardness | % Li ₂ O |
|--------------|---|-----------|-----------|---------------------|
| Ambligonite | LiAl(PO ₄)F | 3,0 - 3,1 | 5,5 - 6,0 | 11,90 |
| Eucryptite | LiAlSiO ₄ | 2,66 | 6,5 | 11,90 |
| Lepidolite | K(Li,Al ₃)(Si,Al)O ₄₁₀ (F,OH) ₂ | 2,8 - 2,9 | 2,5 - 3,5 | 3,3 - 7,8 |
| Montebrasite | LiAl(PO ₄)(OH) | 3,0 | 5,5 - 6,0 | 7,00 |
| Petalite | LiAlSiO ₄₁₀ | 2,4 | 6,5 | 4,90 |
| Spodumenio | LiAlSiO ₂₆ | 3,1 - 3,2 | 6,5 - 7,0 | 8,00 |
| Zinnwaldita | KLiFe ²⁺ Al(AISiO ₃₁₀)(F,OH) ₂ | 2,9 - 3,0 | 2,5 - 4,0 | 5,60 |
| Hectorite | Na _{0,3} (Mg,Li) ₃ (SiO ₄₁₀)(F,OH) ₂ | 2,3 | 1,0 - 2,0 | 1,22 |
| Triphyllite | LiFe ²⁺ PO ₄ | 3,4 - 3,6 | 4 | 9,47 |
| Zabuyelite | Li ₂ CO ₃ | 2,09 | 3 | 40,44 |

The plant's operating regime is 6,132 hours per year. The expected average feed content is 1.41% Li₂O, with a mass recovery of 16% and metallurgical recovery of 63%, producing 208 Ktpa of concentrate for export.

It is estimated that 204 Ktpa of tailings will be generated from the ore sorter pre-concentration process and 570 Ktpa of tailings from the DMS circuits. The fine material (<0.85 mm) and the average concentrate from the DMS fines that will be stockpiled represent 314 Ktpa.

The simplified process flowchart is shown in Figure 17.1.

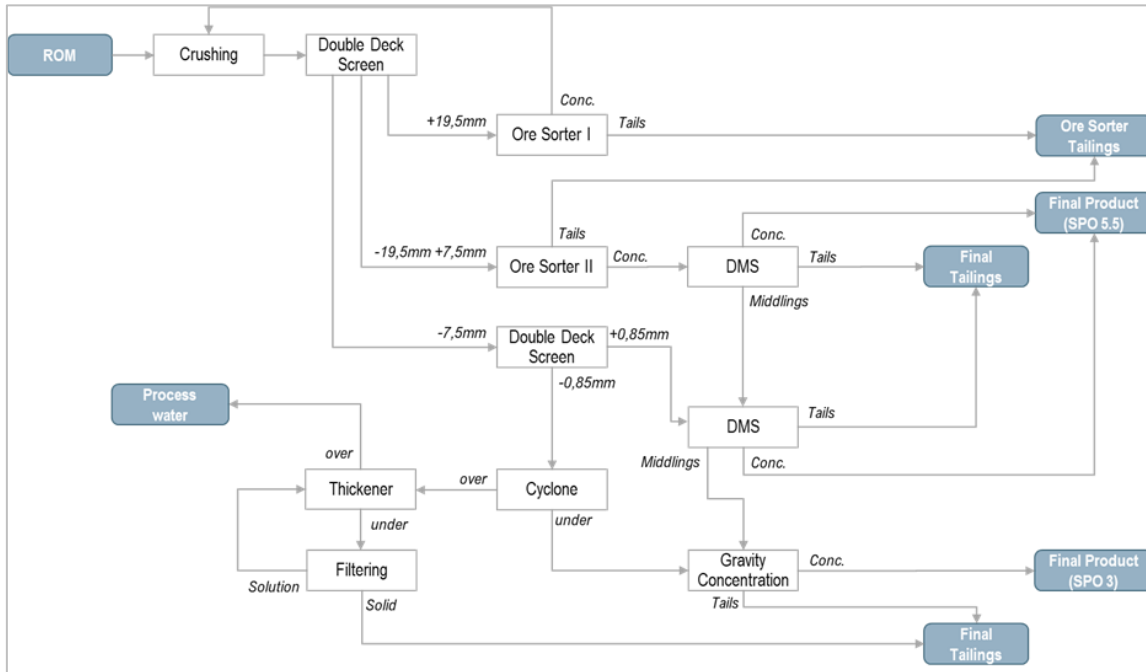


Figure 17.1: Process flowchart.

The material extracted from the underground mine (ROM, top size 420 mm, d50 close to 100 mm) will be stockpiled in a pile with an autonomy of 24 hours of operation and, using wheel loaders, the ROM will be fed into the primary crushing hopper (jaw crusher, APF 80 mm). The crushed material will be directed to the scrap extraction and detection, sampling and weighing system and then on to the 19 mm classification stage (primary screening).

The material that passes through (-19 mm) goes on to be screened on a double deck screen. The retained material (+19 mm) goes via belt conveyors to feed the secondary crushing (cone crusher, 20 mm APF). The crushed material joins the material passing through the primary screen to feed the secondary screening to be carried out on a double-deck screen (19 and 7.5 mm cut). A metal detector and extractor are planned to protect the cone crusher.

The material retained in the 19 mm secondary screening (material between 43 and 12 mm), before returning to the secondary crusher, will feed the plant's first ore sorter, the purpose of which is to remove shale (around 20% of the mass), which will then be conveyed to form a shale pile. The product from the ore sorter will be conveyed to close the circuit and feed the secondary crusher.

The material retained on the 2nd deck (-19 + 7.5 mm) will be sent to the second ore sorter system to also remove shale (around 20% of the mass), which will be conveyed to form the shale pile, together with the shale removed in the first ore sorter. The product from the ore sorter will be conveyed to the feed silo for the coarse DMS circuit.

The material that passes through the 2nd deck (-7.5 mm) will go to the wet screening (cut-off at 0.85 mm) to remove the fines (below 0.85 mm) from the dense media concentration (DMS) circuit. The fraction retained in the wet screening (-7.5 + 0.85 mm) will go to the storage silo to feed the Fines DMS circuit (-7.5 + 0.85 mm).

The material will be extracted by belt feeders and followed by conveyors to feed horizontal protection screens (with a spray system) whose purpose is to remove fine ore adhered to the surface of the particles to be processed. Those passing through the screens will be pumped to the thickener to recover fines and water. The retained ore will be sent through chutes to feed the solid/dense medium mixing boxes, which also receive the dense medium (suspension of water and FeSi).

The suspension of ore and dense medium will be pumped to feed the rougher stage to be carried out in dense medium cyclones. The density will be controlled and monitored using density meters.

The sunken fractions (higher density) from the rougher stages will come out through the cyclone underflow as the final concentrate from the dense medium circuits. The underflow from the cyclones will be conveyed to dewatering screens to remove the dense medium.

The dewatered concentrates will be conveyed to belt conveyors and stacked with a moisture content of 3% for the coarse concentrate and 6% for the fine concentrate.

The overflow from the dense medium cyclones of the rougher stages will contain the floated material (lower density) and will go on to static screens and then dewatering screens. The dewatered materials will then be sent to the mixing boxes with the dense medium to be pumped to feed the scavenger stages.

The underflow from the scavenger cyclones will be the middle of the circuits. They will also be dewatered by dewatering screens and FeSi will be recovered. The medium from the coarse circuit with a moisture content of 3% and a content of 1.63% Li_2O and 0.77% Fe_2O_3 will be reprocessed in secondary crushing in order to improve liberation. The middle of the fines circuit with a moisture content of 6% and a content of 1.65% Li_2O and 0.79% Fe_2O_3 will be stacked for future use through other concentration processes such as flotation.

The overflow from the scavenger cyclones will be the final rejects from the DMS circuits. They will also pass through DSM static screens and dewatering screens. The FeSi will be recovered for the dense medium scavenger system. The tailings will be stacked with a moisture content of 6% (coarse DMS tailings) and 3% (fine DMS tailings) in piles.

The material that passes wet screening will be pumped to feed the densification cyclone. The underflow from the cyclone will be fed to the filtering feed tank. The overflow from the cyclone will feed the thickener (\varnothing 18 m). The underflow from the thickener will be pumped to the filter feed tank to be filtered together with the underflow from the thickening cyclone. The overflow from the thickener will be pumped to the process water tank.

18 PROJECT INFRASTRUCTURE

18.1 Site Facilities

The location alternatives for the installation of the spodumene mineral concentration unit are closely tied to the mineral deposit location. The structures required for mineral beneficiation should be installed adjacent to the mining areas, increasing the synergy between mine and plant operations.

The administrative facilities (gatehouse, cafeteria, central office, infirmary, and firehouse) will be located on the left bank of the Piauí River, while the operational area (crushing unit, ore sorter, DMS, laboratory, maintenance, mine office) will be on the right side. The project layout is illustrated in Figure 18.1.

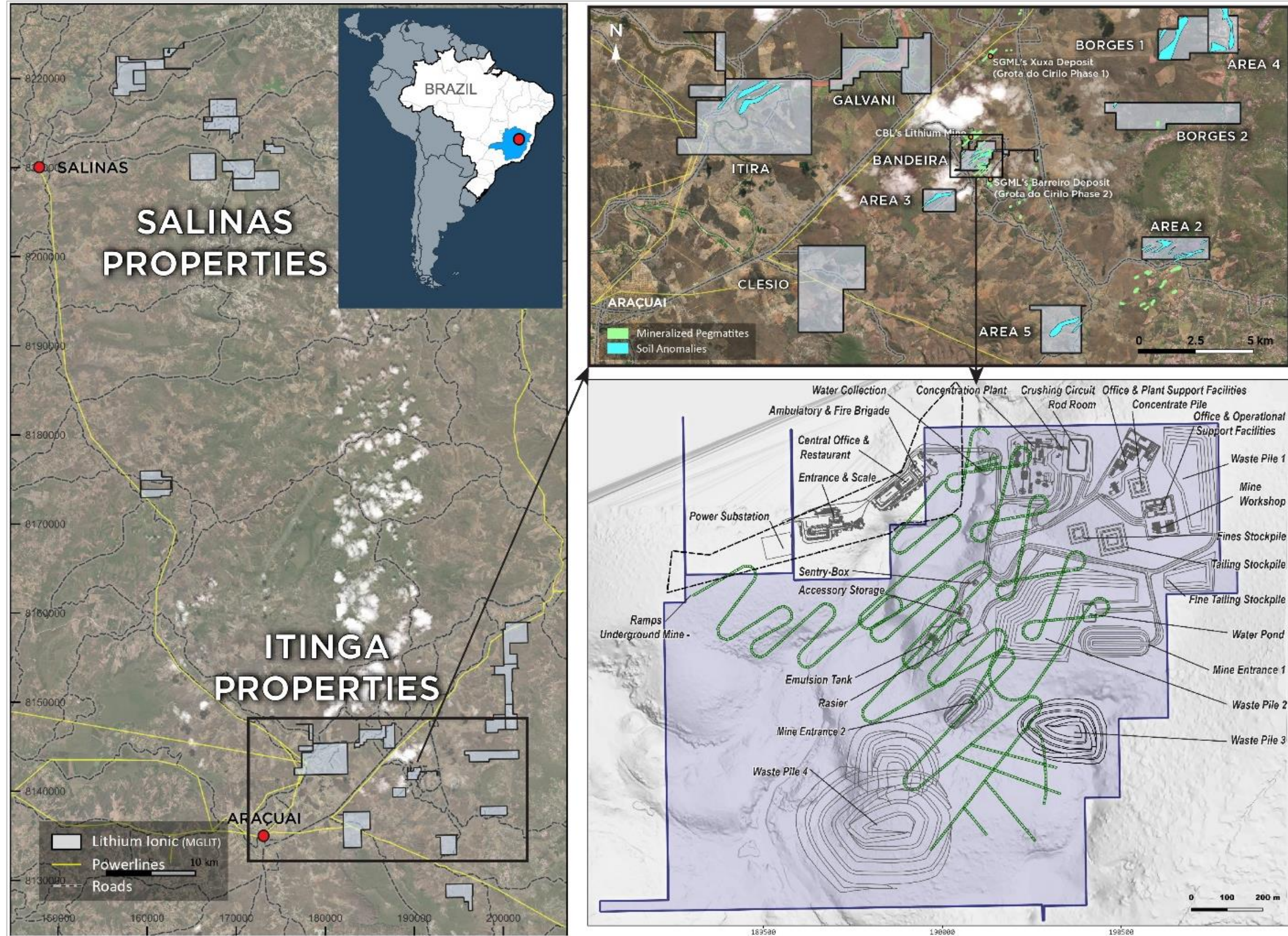


Figure 18.1: Bandeira Project Location.

Source: Lithium Ionic

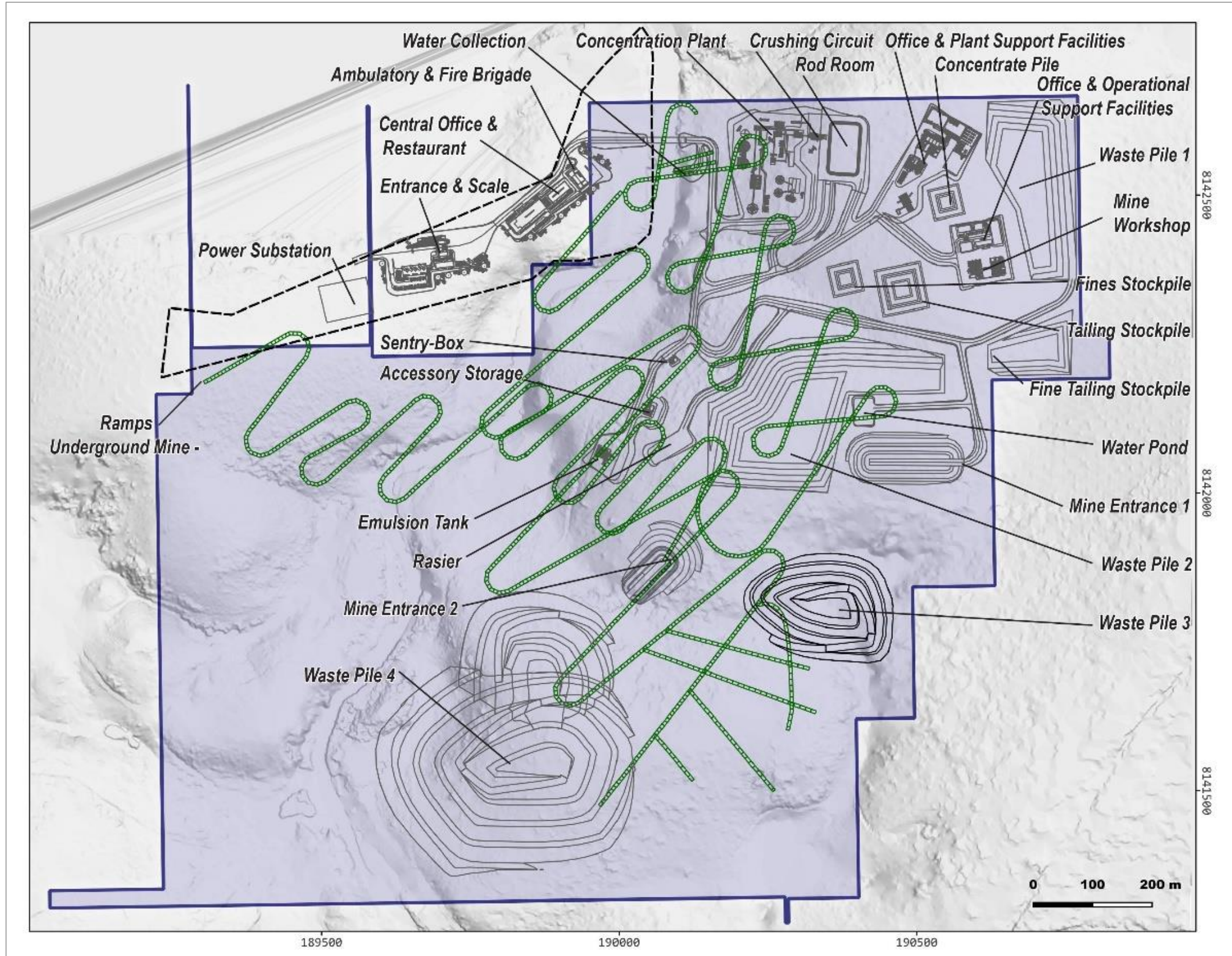


Figure 18.2: Proposed Project Layout and Infrastructure.

Source: Lithium Ionic

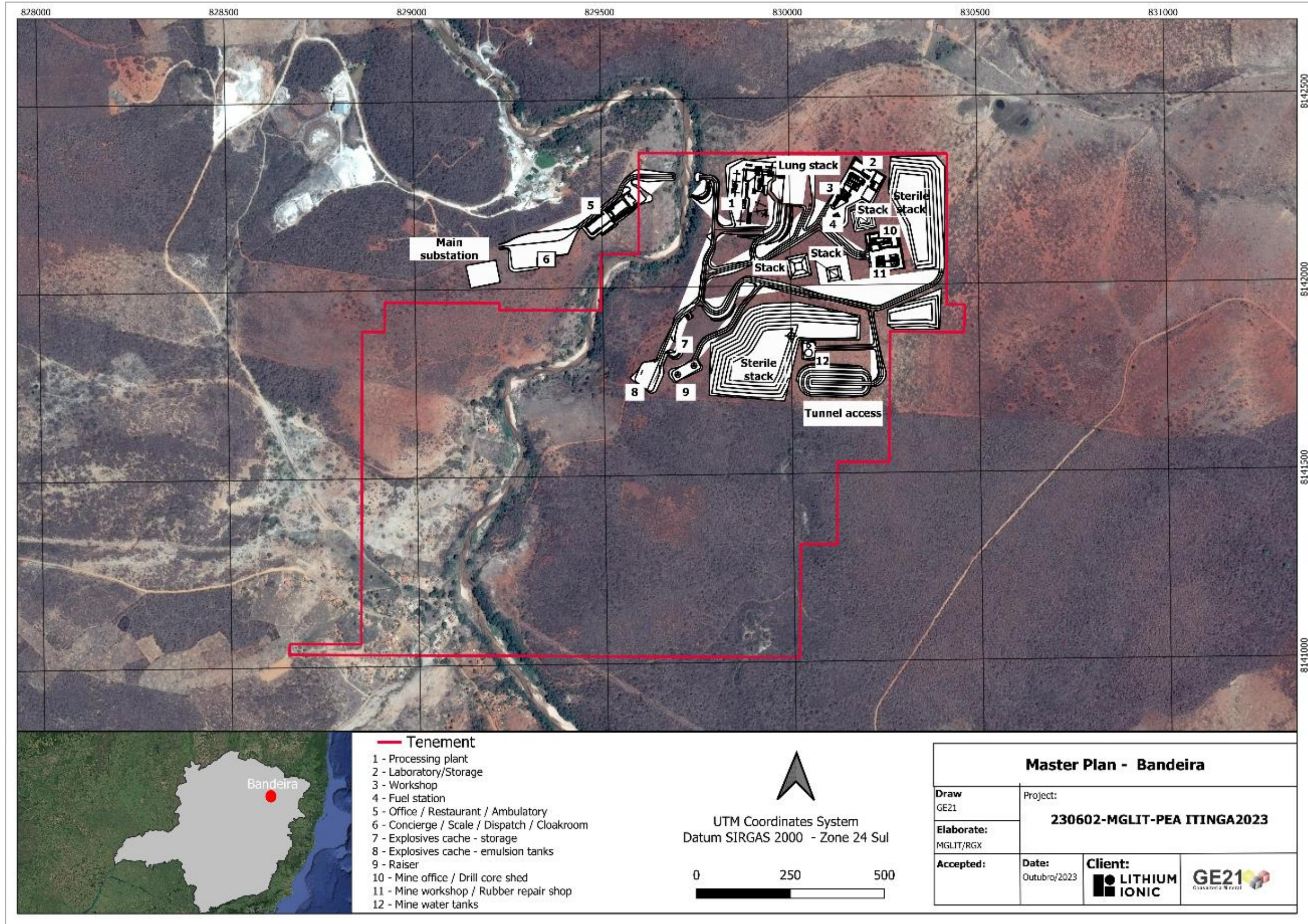


Figure 18.3 Master Plan - Bandeira Project

The master plan was selected as a good option for the industrial plant installation. The Piauí River divides the property into a left bank and a right bank. In the upper portion of the figure, the location of the bridge that will connect the two parts of the plant can be observed.

The beneficiation plant, which includes the unit operations of crushing, pre-concentration, dense medium separation, filtration, and thickening, is indicated in item 1. Areas 2, 3, and 4 are designated for the construction of the laboratory, intermediate waste storage (I.W.S.), warehouse, vehicle wash station, vehicle workshop, tire repair shop, industrial workshop, mine office, I.W.S., and fuel station.

The Project includes the implementation of a parking lot, gatehouse, scale, dispatch, and locker room in Area 6. The restaurant, central office, medical center, and fire brigade are positioned in Area 5.

Areas 7 and 8 are reserved for the explosive's magazine, with Area 7 for accessory storage and Area 8 for emulsion tanks. The raisers, responsible for the mine's exhaust system, are positioned at indicator 9. Points 10 and 11 include the mine office, the dispatch and communication system, locker rooms, core shed, battery room, I.W.S., vehicle wash station, mine workshop, tire repair shop, and office. Lastly, the mine water reservoir is located at point 12.

In the industrial area, two spaces have been allocated for waste stockpiles, one with a volume of 310,000 m³ and another with a volume of 190,000 m³.

The main items comprising the support infrastructure are:

- Locker Rooms.
- Restaurant.
- Office and Laboratory.
- Medical Center / Fire Brigade.
- Gatehouse / Scale / Bus Stop.
- Intermediate Waste Storage (I.W.S).
- Area Restrooms.
- Explosives Magazine.

18.2 Waste Dump

It was estimated that 80% of the waste rock will remain within the mined areas and the remaining 20%, around 1.5 Mm³, will be deposited in waste dumps.

18.3 Tailings Dump

The Bandeira Project will generate multiple tailings and two products, spodumene concentrates. All tailings will have a definitive end-use, but they will be temporarily stored at the industrial plant and a longer-term storage location.

All waste generated by the processing plant will be donated to the community of Itinga and Araçuaí for use in the maintenance of unpaved roads in the region.

18.4 Electrical Power Supply

The electrical power supply for the project will serve the ROM extraction process, electrical equipment, and automation systems of the processing plant, as well as generators, pumps, and

other operational equipment. A substation will be constructed, located approximately 3 km from the power line, and energy will be supplied by CEMIG.

18.5 Water Supply

Water will be sourced from the Piauí River to supply the industrial unit. A permit was requested for a flow rate of 100 m³/h, although normal operations are planned to require 40 m³/h.

The main water consumption will be for wet screening, dense medium separation, and seal water. Other services were also considered, such as cooling systems, potable water, and general utilities.

18.6 Security

The processing plant, the mine, as well as other infrastructure components of the project, such as the dam, will be surrounded by security fences to restrict access. The main entrance will have a manned gatehouse, and the security team will ensure the safety of the site, the explosive and accessory depots, as well as provide protection during the stages of lithium extraction.

19 MARKET STUDIES AND CONTRACTS

Since the Stockholm Conference in June 1972, the world has been calling for greater attention to environmental issues. However, at that time, there were no efficient tools to address the growth of the global industry and the negative impact of greenhouse gas emissions, particularly carbon dioxide. In 1979, academic research at the University of Oxford, led by Prof. John B. Goodenough, along with Stanley Whittingham and Akira Yoshino, resulted in the development of the first rechargeable lithium-ion battery (LCO).

International pressures have intensified throughout the Rio-92 Climate Conference, the Kyoto Convention in 1997, and the Paris Agreement in 2015. On July 27, 2023, the UN Secretary-General, Mr. António Guterres, declared that *"the era of global warming has come to an end, and the era of global consequences is here"*.

A quiet industrial revolution is unfolding globally to confront climate changes that are raising the planet's average temperature. Lithium has emerged as a valuable resource in this paradigm shift of global society concerning our daily lives. This metal plays a role far closer and more significant in our lives than we typically realize. It is an essential component in devices such as cell phones, laptops, computers, vehicles, public transportation, the financial sector, wireless communication, and even in the way we work and interact with others.

19.1 Projected Demand for Lithium Compounds (LCE)

Lithium, once considered a metal of scarce economic interest with limited industrial applications, recorded a global production of only 28,100 tons in 2010, equivalent to approximately 147,800 tons of lithium carbonate. In 2022, it recorded a production of 130,000 tons, an increase of 4.6 times.

In the automotive sector, the introduction of electric batteries began in 1994 in China, with the company BYD (Build Your Dreams), and in 2003 in the United States of America, through Tesla, a pioneering company in this field.

Australia, paying attention to global movements in the mining sector, saw its almost insignificant production in 2007 transform. In 2018, the country emerged as the world's leading producer of spodumene, a mineral used to supply lithium compound conversion facilities in China, reaching over 50% of global production in 2021, which corresponds to 55,400 tons. Argentina and Chile, important producers since before, also chose to position themselves in this promising market.

This scenario has led to the development of various lithium extraction projects from brines and rock deposits. However, it is estimated that the startup of a new mining project can take between 6 and 15 years, resulting in a lithium shortage in the market in the coming years. Figure 19.1 presents a map indicating countries with the largest resources of lithium-bearing rock ores and lithium brines worldwide.

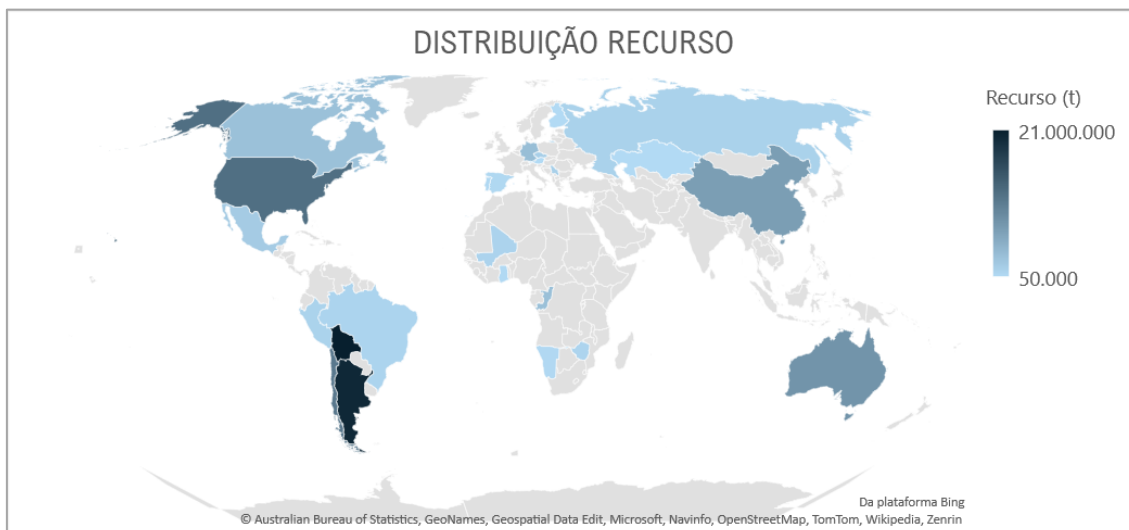


Figure 19.1 Map indicating countries with the largest resources.

Lithium-bearing brines, originating from the evaporation of accumulated waters in continental basins linked to volcanic systems (e.g., Andes), offer economically valuable content of sodium, potassium, lithium, and magnesium, primarily in the form of chloride. However, the combined concentration of lithium chloride is relatively low, ranging from 0.01 to 0.20 g/L. Economic viability for its extraction is only achieved after concentration, which is conducted through solar evaporation or forced processes utilizing fuels.

A novel and recent process known as DLE (Direct Lithium Extraction), initially developed by the American company Lilac Solutions, emerges as a true revolution in extracting this metal from brine, using ion-exchange resins. Projects based on this method are already under construction in both Argentina and the United States of America.

Lithium minerals extracted from hard rock deposits exhibit lithium oxide concentrations ranging between 1% and 3%. These deposits occur in granitic rocks, primarily in pegmatites rich in spodumene, originating from orogenic systems of various geological ages. The process of obtaining lithium carbonate from minerals like spodumene, lepidolite, petalite, and amblygonite is based on unit operations such as dense medium separation, calcination, and chemical precipitation.

The Figure 19.2 below outlines the lithium production chain from obtaining the chemical industry feedstock to the end consumer, who may be in the electric vehicle sector, electronics, or even electrical energy storage units.

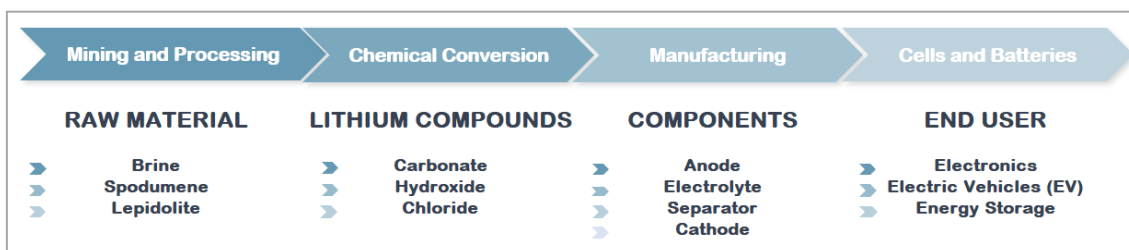


Figure 19.2 Lithium supply chain from mineral resource to product.

In the past five years, the demand for lithium has experienced a steep growth, particularly in China, which hosts over a dozen mineral conversion units for lithium chemical compounds. Notable companies with conversion units in China include Albemarle, Ganfeng, Tianqi, General, BYD, and Guangxi. Additionally, four new conversion units are under construction to process spodumene and lepidolite, belonging to Ganfeng, BYD, and Albemarle.

The expectation for increased production of lithium carbonate equivalent, predominantly in the form of lithium hydroxide, is significant, with a forecast to reach 2.4 million tonnes by 2030. In contrast, this number was 680,000 tonnes in 2022, according to Benchmark Source estimates. To meet this ambitious target, that is, to increase production by 3.6 times, several conversion units are being planned and are in various stages of development, as indicated in Table 19.1.

Table 19.1 Conversion Units at Different Stages of Development

| Company | Contry | State/region | City | Raw materials | Production LCE (tpa) | Stage |
|-------------------|-------------|----------------------|--------------------|---------------|----------------------|--------------|
| AMG | Brazil | Minas Gerais | São João Del Rey | Spodumene | 25.000 | Viability |
| Tesla | EUA | Texas | Corpus Christi | Spodumene | 30.000 | Viability |
| Albermarle | EUA | North Carolina | Kings Mountain | Brine | 30.000 | Construction |
| Albermarle | China | Sichuan | Pengshan | Brine | 88.000 | Construction |
| Ganfeng | China | Sichuan | Dazhou | Spodumene | 25.000 | Construction |
| Ganfeng | China | Jiangxi | Fengcheng | Spodumene | 25.000 | Construction |
| Eramet | Argentina | Salta | Centenario Ratones | Brine | 24.000 | Construction |
| Rock Tech Lithium | Germany | Brandenburg | Guben | Spodumene | 30.000 | Concept |
| Leverton Helm | Germany | Schleswig - Holstein | Hamburg | Spodumene | 20.000 | Concept |
| Green Lithium | England | North Yorkshire | Teeside | Spodumene | 50.000 | Concept |
| Nemaska | Canada | Quebec | Becancour | Spodumene | 30.000 | Viability |
| Posco | South Korea | South Jeolla | Gwangyang | Brine | 25.000 | Viability |
| Keliber | Finland | Kokkola | Kokkola | Spodumene | 30.000 | Concept |

Source: Company Websites and Online Disclosures.

According to the International Energy Agency (IEA), global electric vehicle sales reached 6.6 million units in 2021 and continued to rise significantly, hitting 10.5 million in 2022. China leads the production and consumption market for electric vehicles with over 50%, due to supportive government policies and public spending on subsidies and incentives. According to a report by Grand View Research, the battery market is expected to reach a market value of \$180 billion by 2030.

The lithium-ion battery market is anticipated to grow at a Compound Annual Growth Rate (CAGR) of 18.1% from 2022 to 2030. According to SNE Research, a South Korean market research institution, the total battery energy demand for electric vehicles (EVs) reached 202 GWh in the year 2022. Among the suppliers, Contemporary Amperex Technology Co., Ltd. (CATL) was the leading global supplier, with a total capacity of 69 GWh, or a market share of 34.8%. BYD also surpassed South Korean LG as the second-largest global battery producer for EVs, with a market share of 11.9%.

Installed production capacities for cells and batteries are shown in Figure 19.3, which indicates that most major factories have a clear strategic plan for significant growth over the next five years.

China, South Korea, and Japan are the most developed countries in this segment, with CATL, LG, and Panasonic leading the rankings.

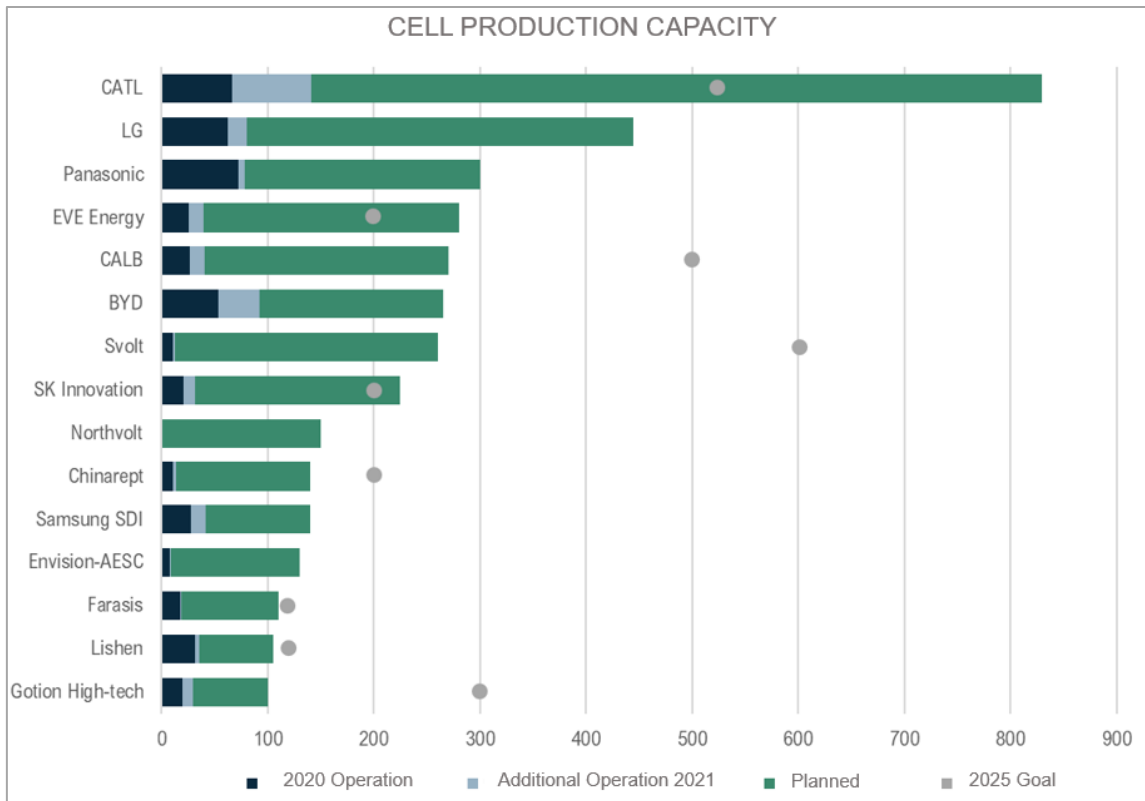


Figure 19.3 Strategic Growth Plan for Cell and Battery Manufacturing Companies

Some companies do not define projected production capacity for the year 2025

***Source: Wood Mackenzie, March 22, 2022 – Global lithium-ion battery capacity to rise five-fold by 2030*

The batteries most produced by China and commonly used in the electronics, electric vehicle, and energy storage industries are shown in Table 19.2, where the advantages and disadvantages of each set are also cited.

Sectors that consume batteries prefer sets that contain nickel and cobalt, such as NCA and NCM. However, the most widely used battery in recent years is LFP, which has lower production costs and ease in obtaining raw materials.

Table 19.2 Presents the Main Batteries Available in the Market for Different Sectors.

| Name | Chemical formula | Abbreviation | Voltage (V) | Advantages | Disadvantages | Application |
|---------------------------------------|---|--------------|-------------|--|---|---|
| Lithium Cobalt Oxide | LiCoO ₂ | LCO | 3.6 | High energy density | Price, lifespan, and thermal stability | Cell phones, cameras, and laptops |
| Lithium Iron Phosphate | LiFePO ₄ | LIP | 3.2 | Long cycles, withstands high temperatures, and is non-polluting | Low energy density, self-discharge | Power stations, EV (Electric Vehicles), and the medical field |
| Lithium Manganese Oxide | LiMn ₂ O ₄ | LMO | 3.7 | Low cost, low toxicity, and stable at high temperatures | Low energy density | Power stations, EV, and the medical field |
| Lithium Nickel Cobalt Aluminium Oxide | LiNiCoAlO ₂ | NCA | 3.6 | Long cycles and low specific density | Low safety and low performance at high temperatures | Energy storage systems and EV |
| Lithium Nickel Manganese Cobalt Oxide | LiNiMnCo ₂ | NMC | 3.6 | Chemical composition flexibility; Greater success in the industry; Several possible uses | High cost | Power stations, EV, and the medical field |
| Lithium Titanium Oxide | Li ₄ Ti ₅ O ₁₂ | LTO | 2.4 | Long cycles, high safety, fast charging, and excellent performance | Low specific voltage and low energy density | Energy storage systems and EV |

Source: TechSci Research, Chuancai Securities, Acclime Insights.

Bloomberg NEF ranks China as the global leader in this segment in raw materials, cells, and components, as well as in the demand for the lithium-ion battery supply chain for three consecutive years since 2020. Not just in terms of lithium, but China also controls over 50% of the refining capacity for battery-grade metals across all key materials, and Chinese companies such as Jiangxi Ganfeng Lithium Co. and Tianqi Lithium Co. have heavily invested in global mining assets.

The Chinese company Ganfeng Lithium established Ganfeng Recycle in 2016 for the dismantling of deactivated lithium batteries and comprehensive recycling of metals. This unit reached a recycling capacity of 34,000 tons in 2020, with a lithium recovery rate of over 90% and a total recovery rate of nickel-cobalt-manganese of 98%. The average lithium consumption per electric vehicle produced is estimated at about 7kg, while graphite, copper, and manganese lead these demands at approximately 70kg, 50kg, and 30kg, respectively. There are also needs for other elements such as nickel, cobalt, zinc, and rare earths.

19.2 Projected Supply of Lithium Compounds (LCE)

The production and supply of Lithium Carbonate Equivalent (LCE) have increased over the last three years at an annual rate exceeding 25%. The supply of spodumene concentrate recorded a lower offer than the demand in the years 2021 and 2022. This fact is substantiated by China's initiation of imports of fine ore, a fraction smaller than 0.5mm, which is rejected at the DMS unit. The supply of spodumene is expected to increase by approximately 250,000 tons in 2023 with the start-up of concentration units in Brazil, Zimbabwe, and Australia.

Figure 19.4 presents the lithium mineral asset transactions that occurred from 2012 to 2022, indicating a pressure on supply with the potential for an excess of lithium compounds within a 5 to 10-year timeframe.

| Buyer | Seller | Property | Negotiation value (\$M) |
|--|--|--------------------------------|-------------------------|
| Chengdu Tianqi Industry Group Co. Ltd. | SQM Chile SA | Salar de Atacama, Mt Holland | 4066,2 |
| Rio Tinto Group | Sentient Equity Partners | Rincon Mining Pty Ltd. | 825,0 |
| Chengdu Tianqi Industry Group Co. Ltd. | Greenbushes Lithium | Greenbushes | 803,3 |
| Zijin Mining Goup Co. Ltd. | Neo Lithium Corp. | Neo Lithium Corp. | 765,3 |
| Zijin Mining Group Co. Ltd. | Neo Lithium Corp. | Tres Quebradas | 765,0 |
| Zijin Mining Goup Co. Ltd. | Dunan Holding Group Co. Ltd. | Lakkor Tso Salt Lake | 741,1 |
| Sibanye Stillwater Ltd. | ioneer Ltd. | Rhyolite Ridge | 490,0 |
| Lithium Americas Corp. | Millennial Lithium Corp. | Millennial Lithium Corp. | 400,0 |
| Zhejiang Huayou Cobalt Co. Ltd. | Prospect Resources Ltd. | Arcadia | 342,9 |
| Contemporary Ampere Technology Ltd. | Millennial Lithium Corp. | Cauchari East, Pastos Grandes | 298,2 |
| Ganfeng Lithium Co. Ltd. | Bacanora Lithium Plc | Sonora and Zinnwald | 259,3 |
| Suzhou CATH Energy Technologies Ltd. | AVZ Minerals Ltd. | Manono | 240,0 |
| Sinomine Resource Group Co. Ltd. | Undisclosed sellers | Bikita Minerals Ltd. | 192,4 |
| Sayona Mining Ltd. | Lithium Royalty Corp.; GUOAO Lithium Ltd. | Moblan | 87,5 |
| Zhejiang Huayou Cobalt Co. Ltd. | Private investors | Arcadia | 44,2 |
| Lithium Power Intrnational Ltd. | Minera Salar Blanco SPA | Minera Salar Blanco SPA | 41,2 |
| Jiangxi Ganfeng Lithium Co. Ltd. | Reed Industrial Minerals Pty Ltd | Mount Marion | 27,2 |
| Jilin Jien Nickel Industry Co. Ltd. | Quebec Lithium Mine | Quebec | 23,6 |
| Lithium Ionic | Diversos | Diversos | 23,0 |
| Lithium Power Intrnational Ltd. | Bearing Lithium Corp. | Bearing Lithium Corp. | 20,1 |
| Jiangxi Ganfeng Lithium Co. Ltd. | Reed Industrial Minerals Pty Ltd | Mount Marion | 19,5 |
| Ganfeng Lithium Corp. | International Lithium Corp. | Mariana project | 13,2 |
| American Lithium Corp. | Undisclosed sellers | Crescent Dunes | 5,4 |
| Kodal Minerals PLC | Gorutumu Mining SARL; Triumvirat Mining Co. SARL | Bougouni | 1,2 |
| Spearmint Resources Inc. | Undisclosed sellers | Green Clay | 0,4 |
| Mineral Resources Ltd. | New Age Metals Inc. | Lithium Project | 0,3 |
| Jiangxi Ganfeng Lithium Co. Ltd. | International Lithium Corp. | Mavis | 0,2 |
| Green Technology Metals Ltd. | Solstice Gold Corp. | Lithium exploration properties | 0,1 |
| Mineral Resources Ltd. | Albemarle Corp. | Wodgina | N.A. |

Figure 19.4 Lithium Asset Transactions from 2012 to 2022.

Source: S&P Global Market Intelligence.

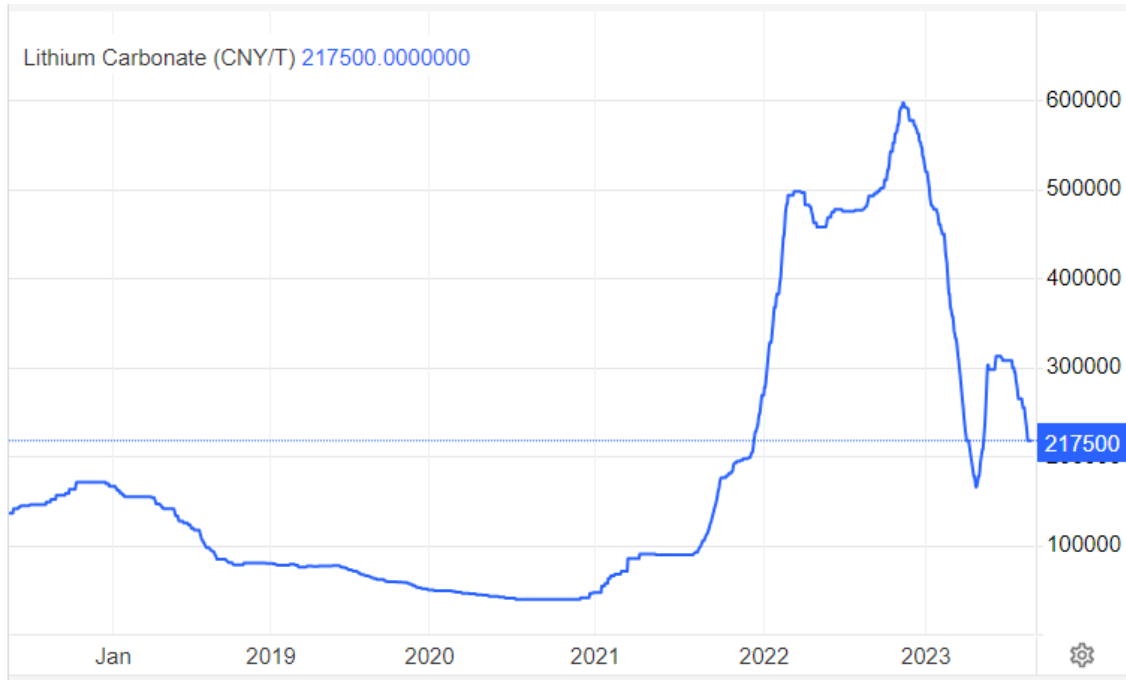
Energy Trend forecasts an excess supply of LCE around 85,000 tons in 2023. This trend is expected to persist in the coming years to accommodate the production expansion of Sigma Lithium in Brazil, with a production forecast of 760,000 tons of concentrate starting from 2025. From 2027 onwards, the market should again return to a balance in the supply and demand for spodumene and LCE.

New conversion units expected to come online in Europe and North America do not have guaranteed feedstock contracts, which could also be a lever for imbalance.

19.3 Projected Price of LCE and Spodumene

Due to the scarcity of raw material for lithium conversion units in China, the price of spodumene concentrate reached its peak in November 2022, hitting a maximum value of \$9,000/t. During this period, China built spodumene and lepidolite mineral concentration units and began importing raw ore from Australia, African countries, and Brazil. This practice continues.

Figure 19.5 shows the variation in the price of lithium carbonate in China over the last 05 years (2018 – 2023)



Source: tradingeconomics.com/commodities.

Figure 19.5 Lithium carbonate price curve in China over the last five years; value of CNY 217,500/t of Li₂CO₃ = US\$ 29,795/t of Li₂CO₃ on August 28, 2023.

The appreciation of lithium compounds observed from mid-2021 and continuing until November 2022, reached a record value of US\$87,795/t. From there, largely explained by the reduction in tax incentives and subsidies in China, the price of lithium carbonate experienced a drop almost in proportion to its rise but stabilizing in the range of US\$ 25,000 to 30,000 per ton.

In this report the selling price used for SPO 5.5% was based on a projection based on price history of Li₂O, in accordance with market practices. It predicts an oscillation of the price during the next 10 years, stabilizing at the current price level. Figure 19.6 – Li₂O SPO 5.5% Price Curve during the next 30 years shows the SPO 5.5% price curve for the next 30 years.

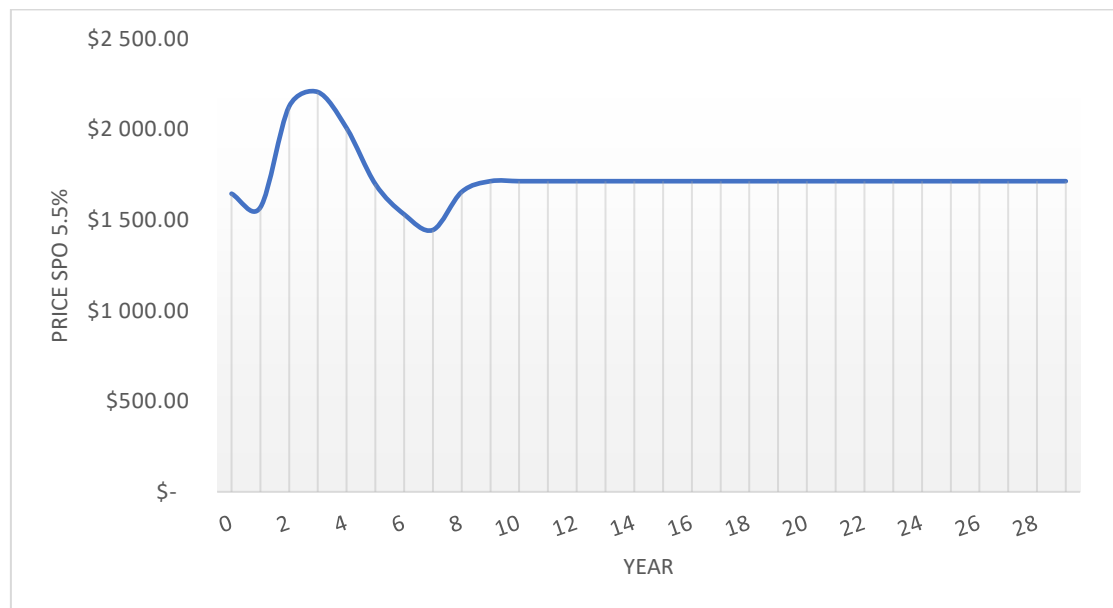


Figure 19.6 – Li₂O SPO 5.5% Price Curve during the next 30 years

The same method was applied for the projection of SPO 3% which was based on price history of Li₂O 3%, in accordance with market practices. It predicts an oscillation of the price during the next 10 years, stabilizing at the current price level. Figure 19-7 shows the SPO 3% price curve for the next 30 years.

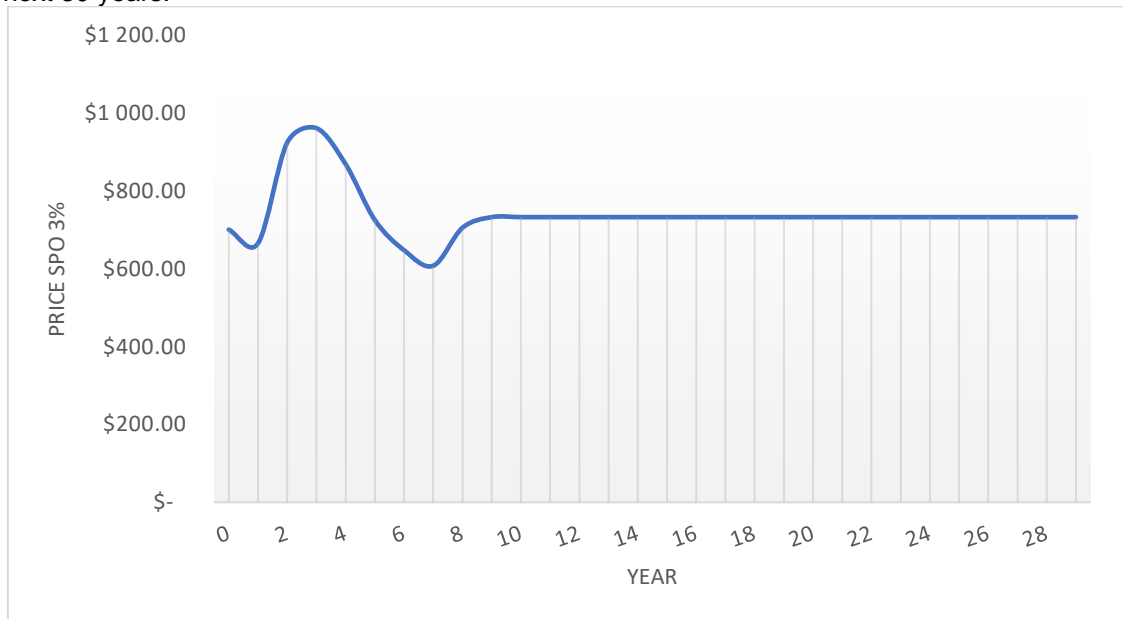


Figure 19.7 – Li₂O SPO 3% Price Curve during the next 30 years

19.4 Contracts

MGLIT and Lithium Ionic Corp. have not yet signed contracts for the sale of spodumene concentrate or even contracts for the construction of the Project. It's important to mention that various companies involved in the lithium supply chain have been visiting the projects currently under development with the aim of establishing agreements and purchase contracts for spodumene. The company's strategy has been to wait for Project approval before moving on to the next phase of basic and detailed engineering for engagement with other companies.

20 ENVIRONMENTAL STUDIES, PERMITS, AND SOCIAL OR COMMUNITY IMPACTS

For mineral extraction activities environmental studies, permits, and social or community impacts it is mandatory in Brazil and must be carried out in accordance with Federal Decree No. 99,274/90, which regulates Federal Law No. 6,938/81, which, in turn, establishes the National Environmental Policy.

Within the scope of environmental licensing, in addition to complying with applicable legislation at the Federal, State and Municipal levels, relevant environmental aspects are analyzed — such as water and effluents, flora and fauna, noise, natural, cultural, historical and archaeological heritage, environment, education, indigenous lands and quilombola and traditional populations —, and also analyzed the manifestations of the intervening bodies, including the City Hall, attesting to the project's compliance with municipal legislation on land use and occupation.

For mining activities, it is also necessary for the entrepreneur to prove that he holds the right to explore the intended mineral substance, which is granted by the National Mining Agency, considering that the mineral resources are property of the Union under the terms of art. 20, IX of the Federal Constitution of 1988.

The National Environmental Council through resolution CONAMA 237/97 has established a three-stage licensing process for mining projects in Brazil:

Issuance of a Preliminary License (LP) at the planning stage of development. Obtaining an LP requires approval by the relevant Environmental Authority of the project Environment Impact Assessment and Report (EIA-RIMA) and plan for the recovery of degraded areas (PRAD).

Issuance of an Installation License (LI), which authorizes construction according to specifications contained in the approved Environmental Impact Assessment (EIA) or Environmental Assessment (EA), as well as the Environmental Control Plan (PCA).

Issuance of the Operation License (LO). The LO is required to mine, process, and sell mineral substances, and is granted once the Environmental Authority has inspected the site and verified that construction was completed in keeping with all the requirements of the LI, and that the environmental control measures and other conditions of the LI have been satisfactorily implemented.

In Minas Gerais State the environmental licensing or permitting is responsibility of Secretaria de Estado de Meio-Ambiente e Desenv. Sustentável - SEMAD. Which is the institution that regulates, approves, and issues environmental licenses (LP, LI and LO).

All licenses are required before production can begin.

21 CAPITAL AND OPERATING COSTS

The Project costs include the initial capital expenditures (CAPEX) and the operational expenditures (OPEX). All costs are expressed in US Dollars and the exchange rate used is USD1.00 = R\$5.00.

The Capital Cost of Mining (CAPEX) and Operating Costs (OPEX) figures shown below are the result of similar mining project with similar characteristics.

21.1 Capital Costs

The Capital Expenses estimated for the Bandeira Project is based on the design of the engineering project, which contemplates an underground mining operation operated by MGLIT itself.

Bandeira Project mining costs consist of acquisition of equipment's, pre-production investments and the first year of the underground project development. The Total Mining Capex estimated is US\$ 72.5M.

The mineral processing is based on the quotation of fixed plant, structured around a two-stage crushing circuit, ore size classification, the implementation of an ore sorter for coarse and medium materials, and the utilization of DMS (Dense Media Separation) for coarse and medium materials. The capacity is based on a production of 1.3Mt of Li₂O. The Total Plant Capex estimated is US\$ 80.5M.

The Economic Assessment Estimates a Capital Sustaining of US\$ 118M applied from the third year of the Project.

The Capital Expenses forecast other costs such as engineering, environmental and infrastructures resulting in a Total Capex estimated is about US\$ 351M. The detailed pricing is presented on the Table 21.1 below:

Table 21.1 Total CAPEX Estimated.

| Description | Total (US\$ M) |
|------------------------------------|----------------|
| Mining – Total | 72.5 |
| Plant | 80.5 |
| Environmental | 2.9 |
| Engineering Services | 20.0 |
| General Infrastructures & Others | 10.3 |
| Initial Capex | 186.3 |
| Contingency (25%) | 46.6 |
| Initial Capex + Contingency | 232.8 |
| Sustaining | 118.0 |
| Total Capex | 350.8 |

This CAPEX was estimated in similar projects and GE21 database.

21.2 Operating Costs

The mining OPEX estimation is based on similar projects and GE21 database. Table 21.2 summarize the OPEX mining unitary costs.

Table 21.2 OPEX Mining Unitary Costs.

| Unitary Cost | | |
|---------------------|------------|----------|
| Description | | Cost |
| Decline Development | US\$/m | 5,000.00 |
| Raise | US\$/m | 5,000.00 |
| Development | US\$/m | 4,000.00 |
| Haulage | US\$/t ROM | 5.25 |
| Stoping | US\$/t ROM | 35.00 |
| Room and Pillar | US\$/t ROM | 41.96 |

Therefore, after processing data, it results the mining costs. The mining cost unitary per mined tonnes obtained for the Bandeira's Project is US\$ 45.03/t.

Processing costs are defined as US\$ 11.86/t per underground mined tonnes, experienced by GE21 for similar projects such as Bandeira's.

Sales and G&A (General and Administrative) costs were estimated based on similar projects such as Bandeira's and defined as US\$ 4.00/t per underground mined tonnes.

The annual total OPEX includes the costs related to mining, development, processing, sales, and general and administration costs (G&A), as summarized in Table 21.3.

Table 21.3 Summary Project OPEX

| Total Costs | |
|--------------|-----------------|
| Description | M US\$ |
| Mining | 1,041.54 |
| Process | 271.65 |
| SG&A | 91.63 |
| Total | 1,404.81 |

22 ECONOMIC ANALYSIS

22.1 Taxes

The taxes for the Bandeira Project were estimated account for current tax laws applied to the forecasted revenues.

CFEM – Financial Compensation for the Exploitation of Mineral Resources:

Financial Compensation for the Exploration of Mineral Resources (CFEM) is the consideration paid to the Government of Brazil for the extraction and economic exploration of Brazilian mineral resources.

The CFEM rate for this Project is 2% over Gross Revenue.

IR – Income Tax:

A tax rate of 15% is applied to pre-tax profit (EBIT) over the first R\$ 240,000, and after a 25% over the profits surpassing the R\$ 240,000. This value has a 75% discount due to the tax incentive offered by the Superintendência do Desenvolvimento do Nordeste (SUDENE), the Northeast Development Superintendence.

Social Contribution:

The social contribution tax is 9% calculated based on EBIT.

PIS and COFINS were not applied in this analysis because all production is directed for exportation, in this scenario.

Royalties:

Royalties is a fee paid for the right to use, exploit, or trade an asset. The Royalties rate used for this Project is 3%, 50% over CFEM estimated.

ICMS (Tax on Circulation of Goods and Provision of Transport and Communication Services) was not applied in the discounted cash flow since, considering the product will be shipped abroad, for which ICMS is not applied. This tax is usually not accounted for in PEA's, however it could be estimated in future analysis when the logistics are defined.

22.1.1 Discounted Cash Flow

A Discounted Cash Flow (DCF) analysis was developed to assess the Bandeira Mining Project based on the economic-financial parameters presented, the results of the mine scheduling and the premises of only evaluating the material mined presented on Section 16.

The Project base case estimates a Net Present Value of US\$ 1.6 billion post-tax, at a Discount Rate of 8% per year. The Table 22.1 and Table 22.2 presents the Discounted Cash Flow for the Project.

Table 22.1 Discounted Cash Flow for the Project – Page 1

| Year | Total | 0 | 1 | 2 | 3 | 4 | 5 | 6 | 7 | 8 | 9 | 10 |
|-----------------------------------|--------------|-----------|-----------|-----------|-----------|-----------|-----------|-------------|-------------|-------------|-------------|-------------|
| Total | 32.131 | 185,67 | 2.245,34 | 2.762,11 | 2.183,71 | 2.104,05 | 1.887,20 | 1.883,26 | 1.823,41 | 1.790,10 | 1.748,46 | 1.743,01 |
| ROM (kt) | 22.908 | 1,30 | 998,00 | 1.245,96 | 1.312,40 | 1.271,15 | 1.276,18 | 1.274,11 | 1.263,31 | 1.288,18 | 1.293,48 | 1.298,22 |
| Waste (kt) | 9.223 | 184,36 | 1.247,34 | 1.516,15 | 871,31 | 832,90 | 611,03 | 609,15 | 560,10 | 501,92 | 454,99 | 444,79 |
| Strip Ratio | 0,40 | 141,28 | 1,25 | 1,22 | 0,66 | 0,66 | 0,48 | 0,48 | 0,44 | 0,39 | 0,35 | 0,34 |
| Metalurgic Recovery (%) | 67,0% | 67% | 67% | 67% | 67% | 67% | 67% | 67% | 67% | 67% | 67% | 67% |
| LiO2% | 1,23 | 1,01 | 1,09 | 1,13 | 1,16 | 1,17 | 1,25 | 1,26 | 1,26 | 1,23 | 1,23 | 1,23 |
| Recup Mass (%) | 14,85 | 12,14 | 13,90 | 14,80 | 14,26 | 14,32 | 15,04 | 15,17 | 15,11 | 14,73 | 14,72 | 14,77 |
| Li2O 5,5% Product (kt) | 3.435 | 0,16 | 131,90 | 171,53 | 185,33 | 181,01 | 194,78 | 196,08 | 193,72 | 192,46 | 193,21 | 194,49 |
| SPO 3% Product(kt) | 1.024 | 0,06 | 44,61 | 55,70 | 58,67 | 56,83 | 57,05 | 56,96 | 56,48 | 57,59 | 57,82 | 58,04 |
| Gross Revenue (M US\$) | \$ 6.746,61 | \$ 0,31 | \$ 236,67 | \$ 416,18 | \$ 465,29 | \$ 412,71 | \$ 372,15 | \$ 337,12 | \$ 314,27 | \$ 359,17 | \$ 373,57 | \$ 375,91 |
| Mining Costs (M US\$) | \$ 1.031,59 | \$ - | \$ 60,68 | \$ 67,69 | \$ 69,85 | \$ 63,75 | \$ 62,66 | \$ 63,20 | \$ 63,18 | \$ 59,48 | \$ 57,34 | \$ 57,99 |
| Process Costs (M US\$) | \$ 271,65 | \$ - | \$ 10,85 | \$ 19,61 | \$ 23,58 | \$ 16,54 | \$ 16,23 | \$ 14,02 | \$ 13,90 | \$ 14,17 | \$ 14,23 | \$ 14,28 |
| Gross Profit (M US\$) | \$ 5.443,36 | \$ 0,31 | \$ 165,13 | \$ 328,88 | \$ 371,87 | \$ 332,42 | \$ 293,26 | \$ 259,91 | \$ 237,19 | \$ 285,53 | \$ 302,00 | \$ 303,65 |
| SG&A (M US\$) | \$ 91,63 | \$ - | \$ 1,83 | \$ 3,82 | \$ 7,64 | \$ 5,22 | \$ 5,90 | \$ 5,10 | \$ 5,05 | \$ 5,15 | \$ 5,17 | \$ 5,19 |
| Royalties (M US\$) | \$ 67,47 | \$ 0,00 | \$ 2,37 | \$ 4,16 | \$ 4,65 | \$ 4,13 | \$ 3,72 | \$ 3,37 | \$ 3,14 | \$ 3,59 | \$ 3,74 | \$ 3,76 |
| CFEM (M US\$) | \$ 134,93 | \$ 0,01 | \$ 4,73 | \$ 8,32 | \$ 9,31 | \$ 8,25 | \$ 7,44 | \$ 6,74 | \$ 6,29 | \$ 7,18 | \$ 7,47 | \$ 7,52 |
| TFRM (M US\$) | \$ 8,98 | \$ 0,00 | \$ 0,36 | \$ 0,46 | \$ 0,49 | \$ 0,48 | \$ 0,51 | \$ 0,51 | \$ 0,50 | \$ 0,50 | \$ 0,51 | \$ 0,51 |
| Depreciation (M US\$) | \$ 296,56 | \$ - | \$ 37,77 | \$ 46,85 | \$ 47,16 | \$ 47,85 | \$ 32,74 | \$ 13,93 | \$ 7,11 | \$ 8,74 | \$ 10,51 | \$ 8,67 |
| EBIT (US\$) | \$ 4.843,79 | \$ 0,30 | \$ 118,07 | \$ 265,26 | \$ 302,62 | \$ 266,49 | \$ 242,95 | \$ 230,26 | \$ 215,09 | \$ 260,36 | \$ 274,60 | \$ 278,00 |
| Income Tax (M US\$) | \$ 1.686,65 | \$ 0,08 | \$ 59,17 | \$ 104,05 | \$ 116,32 | \$ 103,18 | \$ 93,04 | \$ 84,28 | \$ 78,57 | \$ 89,79 | \$ 93,39 | \$ 93,98 |
| Social Contribution (M US\$) | \$ 607,19 | \$ 0,03 | \$ 21,30 | \$ 37,46 | \$ 41,88 | \$ 37,14 | \$ 33,49 | \$ 30,34 | \$ 28,28 | \$ 32,33 | \$ 33,62 | \$ 33,83 |
| SUDENE tax incentive (M US\$) | \$ -686,82 | \$ - | \$ -44,37 | \$ -78,03 | \$ -87,24 | \$ -77,38 | \$ -69,78 | \$ -63,21 | \$ -58,93 | \$ -67,35 | \$ -70,04 | \$ -70,48 |
| Operational Profit(M US\$) | \$ 3.236,77 | \$ 0,19 | \$ 81,98 | \$ 201,79 | \$ 231,66 | \$ 203,55 | \$ 186,20 | \$ 178,85 | \$ 167,17 | \$ 205,58 | \$ 217,64 | \$ 220,67 |
| EBIT | \$ 4.843,79 | \$ 0,30 | \$ 118,07 | \$ 265,26 | \$ 302,62 | \$ 266,49 | \$ 242,95 | \$ 230,26 | \$ 215,09 | \$ 260,36 | \$ 274,60 | \$ 278,00 |
| (+) Depreciation | \$ 296,56 | \$ - | \$ 37,77 | \$ 46,85 | \$ 47,16 | \$ 47,85 | \$ 32,74 | \$ 13,93 | \$ 7,11 | \$ 8,74 | \$ 10,51 | \$ 8,67 |
| (-) EBTIDA | \$ 5.140,36 | \$ 0,30 | \$ 155,84 | \$ 312,12 | \$ 349,78 | \$ 314,34 | \$ 275,69 | \$ 244,19 | \$ 222,21 | \$ 269,09 | \$ 285,11 | \$ 286,67 |
| (-) Capex | \$ 350,81 | \$ 68,57 | \$ 123,89 | \$ 40,37 | \$ 21,44 | \$ 3,50 | \$ 13,12 | \$ 1,52 | \$ 3,46 | \$ 10,69 | \$ 8,58 | \$ 11,32 |
| (+) Working Capital | \$ 0,00 | \$ 0,02 | \$ 26,04 | \$ 13,22 | \$ 3,38 | \$ -4,40 | \$ -3,00 | \$ -2,23 | \$ -1,55 | \$ 2,43 | \$ 0,62 | \$ 0,27 |
| (-) IR | \$ 1.607,02 | \$ 0,10 | \$ 36,09 | \$ 63,47 | \$ 70,96 | \$ 62,94 | \$ 56,75 | \$ 51,41 | \$ 47,93 | \$ 54,77 | \$ 56,97 | \$ 57,33 |
| (+) Residual Capex | \$ - | \$ - | \$ - | \$ - | \$ - | \$ - | \$ - | \$ - | \$ - | \$ - | \$ - | \$ - |
| (=) Discount Cash Flow | \$ 3.178,66 | \$ -68,39 | \$ -30,18 | \$ 195,05 | \$ 254,00 | \$ 252,29 | \$ 208,82 | \$ 193,50 | \$ 172,38 | \$ 201,19 | \$ 218,94 | \$ 217,76 |
| (=) Acumulated Discount Cash Flow | \$ 41.630,40 | \$ -68,39 | \$ -98,57 | \$ 96,48 | \$ 350,48 | \$ 602,77 | \$ 811,59 | \$ 1.005,08 | \$ 1.177,46 | \$ 1.378,66 | \$ 1.597,60 | \$ 1.815,35 |

Table 22.2 Discounted Cash Flow for the Project – Page 2

| Year | Total | 11 | 12 | 13 | 14 | 15 | 16 | 17 | 18 | 19 | 20 | 21 |
|---|--------------|-------------|-------------|-------------|-------------|-------------|-------------|-------------|-------------|-------------|-------------|-------------|
| Total | 32.131 | 1.678,15 | 1.720,28 | 1.468,66 | 1.364,83 | 1.385,46 | 1.362,21 | 1.300,67 | 1.077,96 | 281,46 | 109,80 | 25,55 |
| ROM (kt) | 22.908 | 1.254,90 | 1.259,63 | 1.224,50 | 1.284,05 | 1.284,11 | 1.294,46 | 1.289,23 | 1.077,96 | 281,46 | 109,80 | 25,55 |
| Waste (kt) | 9.223 | 423,24 | 460,65 | 244,17 | 80,78 | 101,35 | 67,76 | 11,44 | - | - | - | - |
| Strip Ratio | 0,40 | 0,34 | 0,37 | 0,20 | 0,06 | 0,08 | 0,05 | 0,01 | - | - | - | - |
| Metalurgic Recovery (%) | 67,0% | 67% | 67% | 67% | 67% | 67% | 67% | 67% | 67% | 67% | 67% | 67% |
| LiO2% | 1,23 | 1,28 | 1,25 | 1,27 | 1,26 | 1,25 | 1,26 | 1,28 | 1,27 | 1,27 | 1,28 | 1,30 |
| Recup Mass (%) | 14,85 | 15,34 | 15,05 | 15,18 | 15,16 | 14,95 | 15,16 | 15,34 | 15,28 | 15,25 | 15,35 | 15,58 |
| Li2O 5,5% Product (kt) | 3.435 | 195,29 | 192,39 | 188,61 | 197,56 | 194,73 | 199,17 | 200,72 | 167,07 | 43,54 | 17,10 | 4,04 |
| SPO 3% Product(kt) | 1.024 | 56,10 | 56,31 | 54,74 | 57,40 | 57,41 | 57,87 | 57,63 | 48,19 | 12,58 | 4,91 | 1,14 |
| Gross Revenue (M US\$) | \$ 6.746,61 | \$ 375,87 | \$ 371,05 | \$ 363,43 | \$ 380,71 | \$ 375,87 | \$ 383,81 | \$ 386,30 | \$ 321,69 | \$ 83,85 | \$ 32,91 | \$ 7,76 |
| Mining Costs(M US\$) | \$ 1.031,59 | \$ 53,51 | \$ 61,34 | \$ 51,88 | \$ 46,92 | \$ 47,10 | \$ 47,41 | \$ 45,30 | \$ 37,73 | \$ 9,85 | \$ 3,84 | \$ 0,89 |
| Process Costs (M US\$) | \$ 271,65 | \$ 13,80 | \$ 13,86 | \$ 13,47 | \$ 14,12 | \$ 14,13 | \$ 14,24 | \$ 14,18 | \$ 11,86 | \$ 3,10 | \$ 1,21 | \$ 0,28 |
| Gross Profit (M US\$) | \$ 5.443,36 | \$ 308,55 | \$ 295,86 | \$ 298,08 | \$ 319,66 | \$ 314,64 | \$ 322,16 | \$ 326,82 | \$ 272,11 | \$ 70,90 | \$ 27,86 | \$ 6,58 |
| SG&A (M US\$) | \$ 91,63 | \$ 5,02 | \$ 5,04 | \$ 4,90 | \$ 5,14 | \$ 5,14 | \$ 5,18 | \$ 5,16 | \$ 4,31 | \$ 1,13 | \$ 0,44 | \$ 0,10 |
| Royalties (M US\$) | \$ 67,47 | \$ 3,76 | \$ 3,71 | \$ 3,63 | \$ 3,81 | \$ 3,76 | \$ 3,84 | \$ 3,86 | \$ 3,22 | \$ 0,84 | \$ 0,33 | \$ 0,08 |
| CFEM (M US\$) | \$ 134,93 | \$ 7,52 | \$ 7,42 | \$ 7,27 | \$ 7,61 | \$ 7,52 | \$ 7,68 | \$ 7,73 | \$ 6,43 | \$ 1,68 | \$ 0,66 | \$ 0,16 |
| TFRM (M US\$) | \$ 8,98 | \$ 0,51 | \$ 0,50 | \$ 0,49 | \$ 0,51 | \$ 0,51 | \$ 0,52 | \$ 0,52 | \$ 0,43 | \$ 0,11 | \$ 0,04 | \$ 0,01 |
| Depreciation (M US\$) | \$ 296,56 | \$ 8,64 | \$ 6,68 | \$ 5,05 | \$ 2,89 | \$ 2,89 | \$ 1,52 | \$ 1,52 | \$ 1,52 | \$ 1,59 | \$ 1,28 | \$ 0,98 |
| EBIT (US\$) | \$ 4.843,79 | \$ 283,11 | \$ 272,51 | \$ 276,74 | \$ 299,70 | \$ 294,83 | \$ 303,43 | \$ 308,04 | \$ 256,20 | \$ 65,56 | \$ 25,11 | \$ 5,26 |
| Income Tax (M US\$) | \$ 1.686,65 | \$ 93,97 | \$ 92,76 | \$ 90,86 | \$ 95,18 | \$ 93,97 | \$ 95,95 | \$ 96,57 | \$ 80,42 | \$ 20,96 | \$ 8,23 | \$ 1,94 |
| Social Contribution (M US\$) | \$ 607,19 | \$ 33,83 | \$ 33,39 | \$ 32,71 | \$ 34,26 | \$ 33,83 | \$ 34,54 | \$ 34,77 | \$ 28,95 | \$ 7,55 | \$ 2,96 | \$ 0,70 |
| SUDENE tax incentive (M US\$) | \$ -686,82 | | | | | | | | | | | |
| Operational Profit(M US\$) | \$ 3.236,77 | \$ 155,32 | \$ 146,35 | \$ 153,17 | \$ 170,25 | \$ 167,03 | \$ 172,94 | \$ 176,70 | \$ 146,82 | \$ 37,05 | \$ 13,92 | \$ 2,62 |
| EBIT | \$ 4.843,79 | \$ 283,11 | \$ 272,51 | \$ 276,74 | \$ 299,70 | \$ 294,83 | \$ 303,43 | \$ 308,04 | \$ 256,20 | \$ 65,56 | \$ 25,11 | \$ 5,26 |
| (+) Depreciation | \$ 296,56 | \$ 8,64 | \$ 6,68 | \$ 5,05 | \$ 2,89 | \$ 2,89 | \$ 1,52 | \$ 1,52 | \$ 1,52 | \$ 1,59 | \$ 1,28 | \$ 0,98 |
| (=) EBTIDA | \$ 5.140,36 | \$ 291,75 | \$ 279,18 | \$ 281,79 | \$ 302,59 | \$ 297,72 | \$ 304,95 | \$ 309,55 | \$ 257,71 | \$ 67,15 | \$ 26,39 | \$ 6,24 |
| (-) Capex | \$ 350,81 | \$ 9,63 | \$ 12,30 | \$ 1,52 | \$ 8,41 | \$ 1,52 | \$ 1,52 | \$ 1,52 | \$ 1,52 | \$ 1,52 | \$ 1,52 | \$ 1,52 |
| (+/-) Working Capital | \$ 0,00 | \$ -6,61 | \$ 1,05 | \$ -1,96 | \$ 0,06 | \$ -0,22 | \$ 0,46 | \$ -0,22 | \$ -4,58 | \$ -16,84 | \$ -3,61 | \$ -1,78 |
| (-) IR | \$ 1.607,02 | \$ 127,80 | \$ 126,16 | \$ 123,57 | \$ 129,44 | \$ 127,79 | \$ 130,49 | \$ 131,34 | \$ 109,38 | \$ 28,51 | \$ 11,19 | \$ 2,64 |
| (+) Residual Capex | \$ - | | | | | | | | | | | |
| (=) Discount Cash Flow | \$ 3.178,66 | \$ 160,93 | \$ 139,68 | \$ 158,67 | \$ 164,68 | \$ 168,63 | \$ 172,47 | \$ 176,92 | \$ 151,40 | \$ 53,96 | \$ 17,30 | |
| (=) Acumulated Discount Cash Flow | \$ 41.630,40 | \$ 1.976,28 | \$ 2.115,96 | \$ 2.274,63 | \$ 2.439,30 | \$ 2.607,94 | \$ 2.780,41 | \$ 2.957,33 | \$ 3.108,72 | \$ 3.162,69 | \$ 3.179,99 | \$ 3.179,99 |
| (=) Discount Cash Flow pre tax | \$ 4.785,68 | \$ 288,72 | \$ 265,84 | \$ 282,23 | \$ 294,12 | \$ 296,43 | \$ 302,97 | \$ 308,26 | \$ 260,77 | \$ 82,47 | \$ 28,49 | \$ 2,64 |
| (=) Acumulated Discount Cash flow pre tax | \$ 60.146,93 | \$ 2.662,79 | \$ 2.928,63 | \$ 3.210,87 | \$ 3.504,98 | \$ 3.801,41 | \$ 4.104,38 | \$ 4.412,64 | \$ 4.673,41 | \$ 4.755,88 | \$ 4.784,37 | \$ 4.787,01 |

The discounted cash flow analysis results are summarized in Table 22.3.

Table 22.3: Simplified Discounted Cash Flow Results (Post-Tax)

| Summary | |
|-----------------------|-----------------|
| Sale Price(\$/t) | 1,859.25 |
| CAPEX (\$ M) | 350.80 |
| NPV (\$ M) | 1,585.74 |
| IRR (%) | 120% |
| NPVi (\$ M) | 3.50 |
| NPV/NPVi | 2.24 |
| OPEX (\$/t ROM) | 25.57 |
| Payback time (months) | 14 |

22.2 Sensitivity Analysis

A sensitivity analysis was undertaken to evaluate the impact of the resulting economic indicators for the following parameters, within the cash flow:

- Price.
- OPEX.
- CAPEX.

The Underground Mining Project Expansion of the Bandeira Mine NPV was evaluated by varying each of the parameter’s values from -40% to +40% and the results are presented on the sensitivity analysis graph on Figure 22.1.

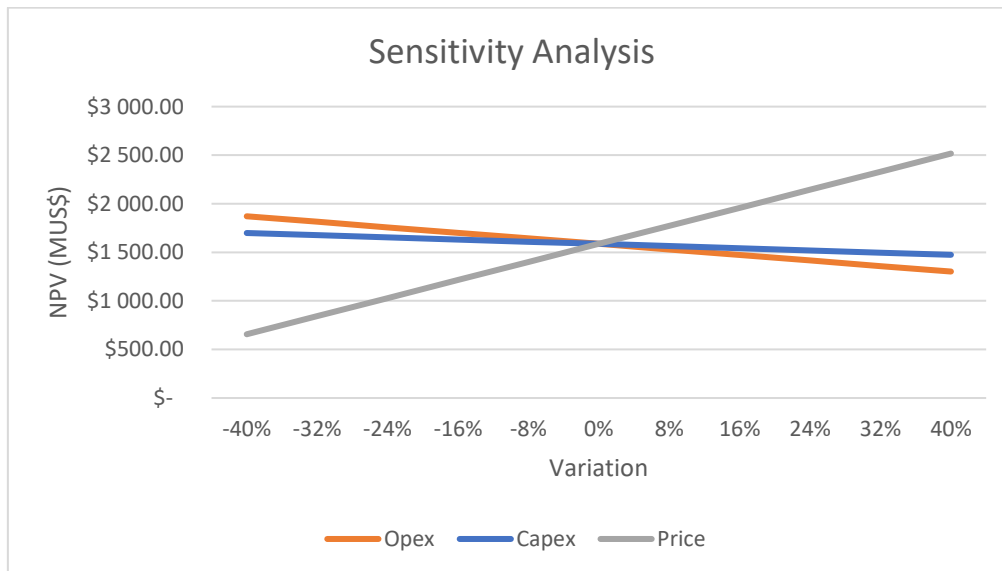


Figure 22.1 Sensitivity Analysis

Prices have major influence on the NPV results of the economic analysis.

23 ADJACENT PROPERTIES

The Araçuaí Pegmatitic District, situated in the northeastern sector of Brazil's Eastern Pegmatitic Province, encompasses the region bounded by Salinas, Araçuaí, and Capelinha to the west, and Itinga and Carai to the east. In this district, Brazil's is a lithium producer, including lithium-bearing pegmatites, gemological pegmatites, and pegmatites that produce ceramic minerals and ornamental rocks. Many of these have been exploited by mineral exploration and mining companies, as well as by artisanal miners, for over a century.

The lithium-bearing pegmatites in the Araçuaí Pegmatitic District include complex zoned bodies with highly diverse mineralogy type, as well as simply to complexly zoned pegmatites rich in disseminated spodumene within a quartz-feldspar matrix that is rich in albite and relatively poor in accessory minerals. Current lithium exploration focuses on spodumene, which typically makes up deposits that can exhibit ore mass volumes of 5 to 30 million tons, with economic grades of lithium oxide.

The Araçuaí Pegmatitic District, particularly the Itinga Pegmatitic Field, is of extreme importance for prospecting projects, considering its production history and its geological and metallogenetic characteristics in this district, in terms of history and prospects for spodumene production, are the Brazilian Lithium Company (CBL) and the Sigma Lithium Corporation (successor to Arqueana de Minérios e Metais Ltda).

The Bandeira lithium ore deposit, registered under ANM 832439/2009, is located adjacent to the mineralized areas of spodumene-bearing pegmatites, which include the Cachoeira deposits of the Companhia Brasileira de Lítio (CBL) and the Barreiro, Murial, and Lavra do Meio deposits of Sigma Lithium Corporation.

Figure 23.1 shows the locations of the mineral rights of CBL and Sigma Lithium surrounding the mining right 832.439/2009.

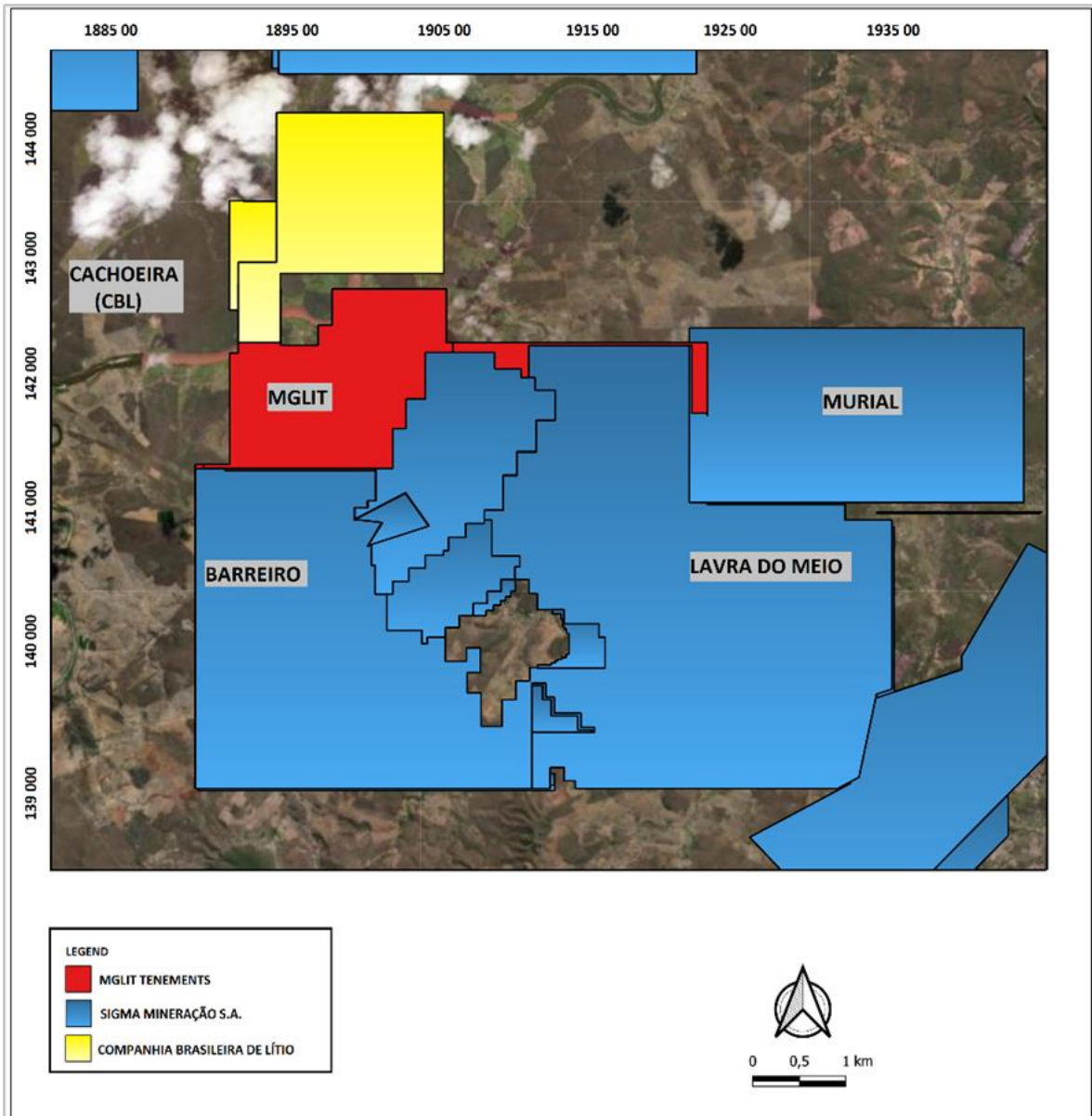


Figure 23.1 Mining Right MGLIT 832.439/2009 (in red) and in the Surrounding Areas CBL and Sigma.

24 OTHER RELEVANT DATA AND INFORMATION

There is no relevant information which affect the opinions offered in this Report.

25 INTERPRETATION AND CONCLUSIONS

25.1 Geology and Mineral Resources

Mineral Resources were estimated and limited to the areas outlined using the Mining Rights polygonal that comprise the Bandeira Property and the Reasonable Prospect for Eventual Economic Extraction - RPEEE.

The Bandeira database contains 4,876 assay intervals covering 4,592 meters, comprising 164 assays from trenches totaling 157 meters and 4,712 assay intervals from drill holes totaling 4,434 meters.

A set of solid grade shells for estimation domains was created using a 0.3% Li₂O (%) threshold. These interpretations were then transformed into a series of implicit 3D models, aligned with the dominant strike directions of 235° and 140°. Additionally, weathering modeling was performed, taking into account the information provided in the logs. The model was built from implicit modelling using the Leapfrog 2023.1 software.

The Ordinary Kriging (OK) estimation method was used on the Li₂O% and Density variables based on results of a structural analysis.

The mathematical/geostatistical criterion for classifying the resource was based on:

- The Measured Mineral Resource classification had as a reference the 50 meters of the Average Euclidean distance to sample (AvgD) used in ordinary kriging estimation with a minimum of five composites in at least three different drill holes.
- The Indicated Mineral Resource classification had as a reference the 100 meters of the Average Euclidean distance to sample (AvgD) used in ordinary kriging with a minimum of five composites in at least three different drill holes.
- The Inferred Mineral Resource classification is all remaining estimated blocks.

The Bandeira Mineral Resources are summarized in Table 25.1.

Table 25.1: Bandeira Mineral Resource Estimates (base case cut-off grade of 0.5 % Li₂O)

| Category | Resource (Mt) | Grade (% Li ₂ O) | Contained LCE (t) |
|-----------------------------|---------------|-----------------------------|-------------------|
| Measured | 2.00 | 1.40 | 69,226 |
| Indicated | 11.72 | 1.40 | 405,666 |
| Measured + Indicated | 13.72 | 1.40 | 474,892 |
| Inferred | 15.79 | 1.34 | 523,118 |

Notes related to the Mineral Resource Estimate:

1. The spodumene pegmatite domains were modeled using composites with Li₂O grades greater than 0.3%.
2. The Mineral Resource Estimates were prepared in accordance with the CIM Standards, and the CIM Guidelines, using geostatistical and/or classical methods, plus economic and mining parameters appropriate to the deposit.
3. Mineral Resources are not Ore Reserves and are not demonstrably economically recoverable.
4. Grades reported using Dry Density.
5. The effective date of the MRE was October 11, 2023.

6. The QP responsible for the Mineral Resources is geologist Carlos José Evangelista da Silva (MAIG #7868).
7. The MRE numbers provided have been rounded to the estimate relative precision. Values cannot be added due to rounding.
8. The MRE is delimited by Lithium Ionic Bandeira Target Claims (ANM).
9. The MRE was estimated using ordinary kriging in 12m x 12m x 4m blocks.
10. The MRE Report Table was produced in Leapfrog Geo software.
11. The reported MRE only contains Fresh Rock Domains.
12. The MRE was restricted by Grade Shell using 0.5% Li₂O cut-off.

25.2 Mining Study

The Bandeira Project have dual underground mining operations. The primary orebodies, accounting for approximately 90% of the deposit, are proposed to be extracted using a bottom-up “sublevel stoping” method (Bandeira Sublevel Mine, “BSL mine”) comprising approximately 21.1Mt@1.25%Li₂O. Simultaneously, the secondary southeast orebody, comprising approximately 1.8Mt@1.05Li₂O, is expected to be mined using “room-and-pillar” technique (Bandeira Room and Pillar, “BRP mine”).

The BSL mine has been planned with two declines, extending along a NE/SW mineralized trend spanning 1.0 km. It is divided into 12 panels, each measuring 55 meters, and consists of two sublevels.

The BRP mine features a single panel with approximate dimensions of 380 meters in length, 330 meters in width, and 10 meters in height. Access to the ore chamber will be provided through five cross-cuts originating from the southern decline.

The mineral processing is based on the fixed plant, structured around a two-stage crushing circuit, ore size classification, the implementation of an ore sorter for coarse and medium materials, and the utilization of DMS (Dense Media Separation) for coarse and medium materials.

The PEA Study resulted in an underground mine scenario processing 1.3Mtpa of ore over a 20 year mine life, with an average LOM annual production of 217,700t of high-quality spodumene concentrate at 5.5% Li₂O (“SC5.5”) equivalent (187,230 tpa SC5.5, in addition to 56,860 tpa of spodumene tails concentrate at 3% Li₂O, or “SC3”) after ramp up in the year 3.

The economics results of Bandeira PEA present Post-tax Net Present Value (“NPV”) 8% of \$1.6 billion, Post-tax Internal Rate of Return (“IRR”) of 121% and After-tax payback of 14 months. The Total capital expenditure (“CAPEX”) of \$233 million (including a 25% contingency), Pre-tax annual average free cash flow of \$243 million.

Mineral Resources that are not Mineral Reserves do not have demonstrated economic viability. The estimate of Mineral Resources may be materially affected by environmental, permitting, legal, title, socio-political, marketing or other relevant issues.

26 RECOMMENDATIONS

Based on the positive nature of this PEA the primary recommendation is to continue the development of the Project through additional detailed investigations and higher confidence engineering studies. The aim being to complete a higher confidence engineering study as the next major project milestone.

The following recommendations are made with respect to future work on the Property. This work will be required for upgrading Bandeira's Resources to Indicated and Measured category, and to advance next stage detailed engineering and economic studies. These are listed as separate phases, as increasing the confidence of the Resources to Indicated or Measured category will be required prior to economic studies.

26.1 Work Required to Increase Confidence in the Resource

26.1.1 Geology and Mineral Resource Estimate

GE21 proposes the following recommendations for the continuous improvement of the Mineral Resource estimate:

- A 50x50m infill drilling program in domain of the indicate resource classification where will focus on resource delineation improvement.
- A 100x100m infill drilling program in domain of the inferred resource classification where will focus on resource delineation improvement.
- A density campaign to measure the density of drill holes cores by drying the samples in an oven, as well as waterproofing them. Compare the results with the methodology used in the current project procedure to check whether there is a bias in the results.
- Conduct an on-site density survey in the weathered zone.
- An updated mineral resource assessment is currently underway through the ongoing infill drilling program.
- Detail Geotechnical analysis including a geotechnical oriented diamond drilling campaign and logging, including sampling collecting for tensile, compressive and shear strength tests.
- Perform supplementary geotechnical investigations of planned infrastructure sites including at waste pile areas; supplementary geochemical tests (ARD); large-scale waste rock and tailings co-disposal stockpile field test.
- To implement the hydrological and hydrogeological studies for the next phases of the project.

26.1.2 Mining and Infrastructure Studies

For the next stage, GE21 recommends the following trade-offs to be undertaken:

- It is suggested to conduct an underground dilution study to verify the suitability of the assumed dilution rate.
- Study the depth-specific moisture content of the material to ensure compliance with standards.
- Carry out a ventilation system study within the underground mining to ensure compliance with required standards for air quality, temperature, and airflow.

- To conduct a quotation for mining equipment including a full services contract for corrective and preventive maintenance services, including the supply of parts.

26.1.3 Environmental Studies, Permitting and Social/Community Impact

MGLit needs to initiate the EIA process, by engaging with the appropriate federal and provincial authorities and engage in the process. Commencement and completion of the required permitting process will be dependent on timing and outcome of the EIA.

The Table 26.1 present the estimate a budget for the implementation of the recommendations.

Table 26.1 Planned Budget recommendations.

| Recommended work | | Details | Estimated cost (US\$) |
|---|--|--|-----------------------|
| Additional work to upgrade to Indicated and Measured category | A 50x50m infill drilling program | | ~\$50,000 |
| | A 100x100m infill drilling program in domain of the inferred resource classification | | ~\$3,000,000 |
| | A density campaign | | ~\$15,000 |
| | on-site density survey | | ~\$15,000 |
| | Updated mineral resources | Interpretation modelling reporting | ~\$60,000 |
| | Total estimated costs | | |
| Work to advance next stage higher level engineering study | Detail Geotechnical analysis | | ~\$500,000 |
| | Perform supplementary geotechnical investigations | | ~\$350,000 |
| | Environmental studies | Commence baseline studies, stakeholder engagement, preliminary work for ESIA | ~\$500,000 |
| | Geotechnical study | Drilling, sampling, analysis and reporting | ~\$300,000 |
| | Hydrogeology and hydrology studies | Drilling, data gathering, modelling | ~\$1,000,000 |
| | Mining Studies (PFS) | | ~\$450,000 |
| | Infrastructure studies | | ~\$160,000 |
| | Total estimated costs | | |
| GRAND TOTAL | | | ~\$6,400,000 |

27 REFERENCES

- Afgouni, K. and Sá, J.H.S., 1978. Lithium Ore in Brazil. *Energy*, 3, 247-253.
- Afgouni, K., and Marques, F. F., 1997. Depósitos de lítio, berílio e céσιο de Araçuaí/Itinga, Minas Gerais. In: Schobbenhaus, C., Queiroz, E. T., & Coelho, C. E. S. (Coords.). 1997. Principais Depósitos Minerai s do Brasil. Brasília: DNPM/CPRM. v. 4B. p. 373-388.
- Alkmim, F. F., Marshak, S., Pedrosa-Soares, A. C., Peres, G. G., Cruz, S. C. P., Whittington, A., 2006. Kinematic evolution of the Araçuaí-West Congo orogen in Brazil and Africa: Nutcracker tectonics during the Neoproterozoic assembly of Gondwana. *Precambrian Research*, 149, 43–64.
- Cerný, P., 1991. Rare-element granite pegmatites. Part I: anatomy and internal evolution of pegmatite deposits. Part II: regional to global relationships and petrogenesis. *Geoscience Canada* 18: 49-81
- Cerný, P. and Ercit, T., 2005. The classification of granitic pegmatites revisited. *The Canadian Mineralogist*, 43, 2005-2026.
- Cerný, P., London, D., Novak, M., 2012. Granitic pegmatites as reflections of their sources. *Elements*, 8, 289-294.
- Chaves, M. L. S. C., Dias, C. H., Cardoso, D. K., 2018. Lítio. In: Pedrosa-Soares, A. C, Voll, E., & Cunha, E. C. (orgs.). *Recursos Minerai s de Minas Gerais*. Belo Horizonte: Companhia de Desenvolvimento de Minas Gerais (Codemge). p. 1-21. <http://recursomineralmg.codemge.com.br>
- Correia-Neves, J.M., Pedrosa-Soares, A.C., Marciano, V.R., 1986). A Província Pegmatítica Oriental do Brasil à luz dos conhecimentos atuais. *Revista Brasileira de Geociências*, 16(1), 106-118.
- Costa, A. G., Neves, J. M. C., & Mueller, G. (1984). Feições polimetamórficas de metapelitos da região de Itinga (Minas Gerais, Médio Jequitinhonha). In: Congresso Brasileiro de Geologia, 33, Rio de Janeiro, Anais, 6. Sociedade Brasileira de Geologia, 3166–3180.
- Costa, A. G., 1989. Evolução petrológica para uma sequência de rochas metamórficas regionais do tipo baixa pressão, Itinga, NE de MG. *Revista Brasileira de Geociências*, 19, 440–448.
- Delboni Jr., H., Laporte, M-A, Quinn, J., Rodriguez, P.C., O'Brien, N., 2023. Grotta do Cirilo Lithium Project, Araçuaí and Itinga regions, Minas Gerais, Brazil, Updated Technical Report (<https://www.sigmalithiumresources.com>)
- Dias, C. H., 2015. Mineralogia, tipologia e causas de cor de espodumênios da Província Pegmatítica Oriental do Bra-sil e química mineral de Nb-tantalatos da mina da Ca-choeira (Minas Gerais). Belo Horizonte, IGC- UFMG. (Dissert. Mestrado). URL: <https://repositorio.ufmg.br/handle/1843/BUBD-9ZWPNA>.
- London, D., 2008. Pegmatites. *Canadian Mineralogist Special Publication*, 10, 347 pp.
- Luiz, C.R., 2023. Como garantir segurança geotécnica em minas subterrâneas: O exemplo da Mina da Cachoeira da Companhia Brasileira de Lítio. Invited lecture in Lithium Business 2023,

Vale do Jequitinhonha, Araçuaí, Brazil. Video available in YouTube (<https://www.youtube.com/watch?v=5QKjPYJtV8k>).

Paes, V. J. C., Heineck, C. A., and Drumond, J. B. V. (2010). Folha SE.24-V-A-IV Itaobim. Belo Horizonte: CPRM, Programa Geologia do Brasil, 1:100000.

Paes, V.J.C., Santos, L.D., Tedeschi, M; F., 2016. Avaliação do Potencial do Lítio no Brasil: Área do Médio Rio Jequitinhonha, Nordeste de Minas Gerais. Programa Geologia do Brasil. CPRM, Belo Horizonte, 276p.

Paiva, G. (1946). Províncias Pegmatíticas do Brasil. Bo-letim DNPM/DFPM, 78, 13-21.

Pedrosa-Soares, A. C., Leonardos, O. H., Correia-Neves, J. M., 1984. Aspectos metamórficos de seqüências supracrustais da Faixa Araçuaí em Minas Gerais. In: Congresso Brasileiro de Geologia, 33, Rio de Janeiro, Anais, 6. Sociedade Brasileira de Geologia, 3056–3065.

Pedrosa-Soares, A.C., Monteiro, R., Correia-Neves, J.M., Leonardos, O.H., Fuzikawa, K. 1987. Metasomatic evolution of granites, Northeast Minas Gerais, Brazil. Revista Brasileira de Geociências, 17, 512-518.

Pedrosa-Soares A.C., Correia-Neves J.M., Leonardos O.H., 1990. Tipologia dos pegmatitos de Coronel Murta – Virgem da Lapa, Médio Jequitinhonha, MG. Revista Escola de Minas: 44-54.

Pedrosa-Soares, A.C.; Baars, F.J.; Lobato, L.M.; Magni, M.C.V.; Faria, L.F. 1993. Arquitetura tectono-metamórfica do setor central da Faixa Araçuaí e suas relações com o Complexo Guanhães. In: 4 Simpósio Nacional de Estudos Tectônicos, Belo Horizonte. Anais: SBG Núcleo MG, p. 176-182.

Pedrosa-Soares, A.C.; Leonardos, O.H.; Ferreira, J.C.H.; Reis, L.B. 1996. Duplo Regime Metamórfico na Faixa Araçuaí: Uma reinterpretacao à luz de novos dados. In: 39 CONGRESSO BRASILEIRO DE GEOLOGIA, 1996, Salvador. Anais. Salvador: SBG Núcleo Bahia-Sergipe, v. 6. p. 5-8.

Pedrosa-Soares, A. C. (1997). Mapa Geológico da Folha Araçuaí, Minas Gerais, Brasil. Belo Horizonte, Pro-jeto Espinhaço, 1:100.000. Mapa e relatório, CODEMIG, <http://www.portalgeologia.com.br/index.php/mapa>

Pedrosa-Soares, A.C.; Romeiro, J.C.P.; Castañeda, C. 1997. Papel do Controle Estrutural de Pegmatitos Graníticos em suas Mineralizações. In: VI Simpósio Nacional de Estudos Tectônicos, 1997, Pirenópolis. Anais. SBG-Núcleo Brasília, 1997. p. 357-359.

Pedrosa-Soares, A.C.; Pinto, C. P.; Custódio Netto; Araújo, M. C.; Castañeda, C.; Achtschin, A.B.; Basilio, M. S. 2001. A Província Gemológica Oriental do Brasil. In: Cristiane Castañeda; João Eduardo Addad; Antônio Liccardo (Org.). Gemas de Minas Gerais. 1ed. Belo Horizonte: Sociedade Brasileira de Geologia-Núcleo Minas Gerais, v. único, p. 16-33.

Pedrosa-Soares, A.C.; Chaves, M.; Scholz, R. 2009. Eastern Brazilian Pegmatite Province. PEG 2009, Fieldtrip Guide: https://www.researchgate.net/publication/234037120_Eastern_Brazilian_Pegmatite_Province

Pedrosa-Soares, A.C., De Campos, C.P., Noce, C.M., Silva, L.C., Novo, T., Roncato, J., Medeiros, S., Castañeda, C., Queiroga, G., Dantas, E., Dussin, I., Alkmim, F., 2011. Late Neoproterozoic-Cambrian Granitic Magmatism in the Araçuaí Orogen (Brazil), the Eastern Brazilian Pegmatite Province and Related Mineral Resources. In: Sial, A.N., Bettencourt, J.S., De Campos, C.P., Ferreira, V.P. (Eds.), Granite-Related Ore Deposits. London, Geological Society of London, Special Publication 350, 25–51.

Pedrosa-Soares, A.C., Deluca, C., Araujo, C.S., Gradim, C.S., Lana, C.C., Dussin, I., Silva, L.C., Babinski, M. 2020. Capítulo 11: O Orógeno Araçuaí à luz da Geocronologia: um tributo a Umberto Cordani. In: Bartorelli, A., Teixeira, W., Brito Neves B.B. Geocronologia e evolução

tectônica do Continente Sul-Americano: a contribuição de Umberto Giuseppe Cordani. – 1. ed. – São Paulo: Solaris Edições Culturais, p. 250-272.

Pedrosa-Soares, A.C., Diniz, H.B., Costa, C.H.C., Guimarães, A., Costa, R., 2023. Lithium ore in the Eastern Brazilian Pegmatite Province: a review and new discoveries of spodumene-rich pegmatites. (Article to be submitted).

Peixoto, E.; Alkmim, F.F.; Pedrosa-Soares, A.; Lana, C.; Chaves, A.O. 2017. Metamorphic record of collision and collapse in the Ediacaran-Cambrian Araçuaí orogen, SE-Brazil: Insights from P-T pseudosections and monazite dating. *Journal of Metamorphic Geology*, p. 1-26.

Quéméneur, J. and Lagache, L., 1999. Comparative study of two pegmatitic fields from Minas Gerais, Brazil, using the Rb and Cs contents of micas and feldspars. *Revista Brasileira de Geociências*, 29(1): 27-32.

Romeiro, J. C. P. (1998). Controle da mineralização de lítio em pegmatitos da Mina da Cachoeira, Companhia Brasileira de Lítio, Araçuaí, MG. Belo Horizonte: Instituto de Geociências, UFMG. (Dissertação de Mestrado).

Romeiro, J. C., Pedrosa-Soares, A.C., 2005. Controle do minério de espodumênio em pegmatitos da Mina da Cachoeira, Araçuaí, MG. *Geonomos*, 13, 75-85.

Saadi, A., Pedrosa-Soares, A.C., 1990. Um graben cenozóico no Médio Jequitinhonha, Minas Gerais. In: *Workshop sobre Neotectônica e Sedimentação Cenozoica Continental no Sudeste Brasileiro*. Belo Horizonte: SBG-MG. Bol. 11, p. 101-124,

Santos, R. F., Alkmim, F. F., Pedrosa-Soares, A. C., 2009. A Formação Salinas, Orógeno Araçuaí, MG: História deformacional e significado tectônico. *Revista Brasileira de Geociências*, 39, 81–100.

231017_Lithium Ionic_Bandeira PEA Results_181023.pdf (Lithium Ionic Announces PEA and Expanded Mineral Resource Estimate for Bandeira; Post-tax NPV8% US\$1.6 Billion & IRR of 121%)

MLF-MGLIT001-2023 (003).docx (Relatório Técnico de Recomendações de Geotecnia Para Desenvolvimento dos Projetos de Mina – Alvos Bandeira e Outro Lado)

BAN-2000-45D1-10000_RevD.pdf (Projeto Conceitual Geral – Plano Diretor)

APPENDIX A

Technical Report QP Certificates

QP CERTIFICATE OF CARLOS JOSÉ EVANGELISTA DA SILVA

- a) I, Carlos José Evangelista da Silva, am a Geologist for GE21 Consultoria Mineral, located at Avenida Afonso Pena, 3130 – 12º andar, Belo Horizonte, MG, Brazil, CEP 30.130-910.
- b) This certificate applies to the Technical Report entitled “Preliminary Economic Assessment for the Bandeira Lithium Project, Minas Gerais State, Brazil” with an effective date of August 30th, 2023.
- c) I hold the following academic qualifications:
 - d) a B.A.Sc. in Geology from the Federal University of Minas Gerais, in Belo Horizonte, Brazil,
 - e) a master’s degree in engineering in Mineral Technology from the Postgraduate Program in Mining, Metallurgical and Materials Engineering (PPGE3M) at the Federal University of Rio Grande do Sul, Brazil,
- f) I am a professional Geologist with more than 17 years of experience in the mining industry. My relevant experience for this Technical Report includes:
 - I have 12 years of experience as a Specialist Geologist on Mineral Exploration:
 - i. 2006 to 2011 – Geologist in Coffey Mining Brazil, which provides advice, assistance, and audits for the mineral exploration, project development, geological assessments, for JORC and NI 43-101.
 - ii. 2011 to 2014 – Geologist in Colossus Minerals, Serra Pelada - Gold Project in Curionópolis – Pará – Brasil. Which provides assistance in brown field exploration projects.
 - iii. 2014 to 2016 - Geologist in SMCA - Sociedade Mineira de Cobre de Angola, Mavio Copper Project – Maquela do Zombo – Uige - Angola, which provides mineral resource management.
 - I have 6 years of experience in Consultancy Companies as Specialist in Resource Estimate and Geostatistics:
 - i. 2018 to present – Resource Geologist of GE21 Consultoria Mineral, which provides advice, assistance, and audits for the Mineral Resource Estimation and Mineral Exploration, for JORC and NI 43-101 Reports.
- g) I am a Member of the Australian Institute of Geoscientists (#7868).
- h) I meet all the education, work experience, and professional registration requirements of a “Qualified Person” as defined in Section 1.1 of National Instrument 43-101.
- i) I inspected between 13th and 14th of September 2023 the property that is the subject of this Technical Report.
- j) I am jointly responsible for Sections 5, 6, 7, 8, 9, 10, 11 and 14, and jointly responsible for Sections through 1 and 25 of this Technical Report.
- k) I am independent of the Issuer, Lithium Ionic Corp.
- l) I have read National Instrument 43-101 and the parts of the Technical Report for which I am responsible have been prepared in compliance with this Instrument, including the CIM Definition Standards on Mineral Resources and Mineral Reserves.

- m) At the effective date of the Technical Report, and at the date, it was filed, to the best of my knowledge, information, and belief, the parts of the Technical Report for which I am responsible contain all scientific and technical information that is required to be disclosed to make the Technical Report not misleading.

Original document signed and sealed.

Carlos José Evangelista da Silva.

Belo Horizonte, Brazil, on November 30th, 2023.

QP CERTIFICATE OF GUILHERME GOMIDES FERREIRA

- a) I, Guilherme Gomides Ferreira, am a Mining Engineer for GE21 Consultoria Mineral, located at Avenida Afonso Pena, 3130 – 12º andar, Belo Horizonte, MG, Brazil, CEP 30.130-910.
- b) This certificate applies to the Technical Report entitled “Preliminary Economic Assessment for the Bandeira Lithium Project, Minas Gerais State, Brazil” with an effective date of August 30th, 2023.
- c) I hold the following academic qualifications: a B.A.Sc. in Mining Engineering from the Federal University of Minas Gerais, in Belo Horizonte, Brazil.
- d) I am a professional Mining Engineer, with more than 16 years of experience in the mining industry. My relevant experience for the purpose of this Technical Report includes:
 - 2006 to 2017– Mining Engineer at mining companies, developing technical studies of Mineral Reserves, mine planning, pit optimization, and economic analysis as well as producing iron ore and gold mine.
 - 2017 to present – Manager of GE21 Consultoria Mineral, which provides advice, assistance, and audits for the entire mining cycle, from defining strategies, generating, and selecting targets and investments, mineral exploration, project development, geological assessments, resource reserve estimation for JORC and NI 43-101 reports, conceptual technical and economic studies, and economic feasibility.
- e) I am a Member of the Australian Institute of Geoscientists (#7586).
- f) I meet all the education, work experience, and professional registration requirements of a “Qualified Person” as defined in Section 1.1 of National Instrument 43-101.
- g) I am responsible for Technical Report sections 15,16,18,19, 21, 22, 23, 24 and jointly responsible for Sections through 1, 25, 26 and 27 of this Technical Report.
- h) I am independent of the Issuer, Lithium Ionic Corp.
- i) I have read National Instrument 43-101 and the parts of the Technical Report for which I am responsible have been prepared in compliance with this Instrument, including the CIM Definition Standards on Mineral Resources and Mineral Reserves.
- j) At the effective date of the Technical Report, and at the date it was filed, to the best of my knowledge, information, and belief, the parts of the Technical Report for which I am responsible contain all scientific and technical information that is required to be disclosed to make the Technical Report not misleading.

Original document signed and sealed.

Guilherme Gomides Ferreira.

Belo Horizonte, Brazil, on November 30th, 2023.

QP CERTIFICATE OF BRANCA HORTA DE ALMEIDA ABRANTES

- a) I, Branca Horta de Almeida Abrantes, am a Environmental Specialist for GE21 Consultoria Mineral, located at Avenida Afonso Pena, 3130 – 12º andar, Belo Horizonte, MG, Brazil, CEP 30.130-910.
- b) This certificate applies to the Technical Report entitled “Preliminary Economic Assessment for the Bandeira Lithium Project, Minas Gerais State, Brazil” with an effective date of August 30th, 2023.
- c) I hold the following academic qualifications: a B.A.Sc. in Geography from the Federal University of Minas Gerais, in Belo Horizonte, Brazil.
- d) I am a professional Environmental Specialist, with more than 19 years of experience in the environmental sector. My relevant experience for the purpose of this Technical Report includes:
 - I work in the Environment area, from participating in the preparation of environmental studies to environmental management, as well as strategic studies.
 - Throughout my professional career, I had acquired experience in the industrial, mining, energy, and sanitation sectors.
- e) I am a Member of the Australian Institute of Geoscientists (#8145).
- f) I meet all the education, work experience, and professional registration requirements of a “Qualified Person” as defined in Section 1.1 of National Instrument 43-101.
- g) I am responsible for Section 20 of this Technical Report.
- h) I am independent of the Issuer, Lithium Ionic Corp.
- i) I have read National Instrument 43-101 and the parts of the Technical Report for which I am responsible have been prepared in compliance with this Instrument, including the CIM Definition Standards on Mineral Resources and Mineral Reserves.
- j) At the effective date of the Technical Report, and at the date, it was filed, to the best of my knowledge, information, and belief, the parts of the Technical Report for which I am responsible contain all scientific and technical information that is required to be disclosed to make the Technical Report not misleading.

Original document signed and sealed.

Branca Horta de Almeida Abrantes.

Belo Horizonte, Brazil, on November 30th, 2023.

QP CERTIFICATE OF PAULO BERGMAN

- a) I, Paulo Bergman, am a Mining Engineer associated to GE21 Consultoria Mineral, located at Avenida Afonso Pena, 3130 – 12º andar, Belo Horizonte, MG, Brazil, CEP 30.130-910.
- b) This certificate applies to the Technical Report entitled “Preliminary Economic Assessment for the Bandeira Lithium Project, Minas Gerais State, Brazil” with an effective date of August 30th, 2023.
- c) I hold the following academic qualifications: a B.A.Sc. in Mining Engineering from the Federal University of Minas Gerais, in Belo Horizonte, Minas Gerais, Brazil.
- d) I am a professional Mining Engineer, with more than 40 years of experience in the mining industry. My relevant experience for the purpose of this Technical Report includes:
 - 30 years in mining and plant operation management, including AngloGold, Yamana, Jaguar Mining and Buritirama Mineração.
 - 10 years as engineering development and consultancy in the mining industry, including gold, iron, manganese, rare earth elements and others.
- e) I am a Member of the Australasian Institute of Mining and Metallurgy (#333121).
- f) I meet all the education, work experience, and professional registration requirements of a “Qualified Person” as defined in Section 1.1 of National Instrument 43-101.
- g) I am responsible for Technical Report sections 13,17, and jointly responsible for Sections through 1, 25 and 26 of this Technical Report.
- h) I am independent of the Issuer, Lithium Ionic Corp.
- i) I have read National Instrument 43-101 and the parts of the Technical Report for which I am responsible have been prepared in compliance with this Instrument, including the CIM Definition Standards on Mineral Resources and Mineral Reserves.
- j) At the effective date of the Technical Report, and at the date it was filed, to the best of my knowledge, information, and belief, the parts of the Technical Report for which I am responsible contain all scientific and technical information that is required to be disclosed to make the Technical Report not misleading.

Original document signed and sealed.

Paulo Bergman.

Belo Horizonte, Brazil, on November 30th, 2023.